INFORMATION TO USERS

This manuscript has been reproduced from the microfilm master. UMI films the text directly from the original or copy submitted. Thus, some thesis and dissertation copies are in typewriter face, while others may be from any type of computer printer.

The quality of this reproduction is dependent upon the quality of the copy submitted. Broken or indistinct print, colored or poor quality illustrations and photographs, print bleedthrough, substandard margins, and improper alignment can adversely affect reproduction.

In the unlikely event that the author did not send UMI a complete manuscript and there are missing pages, these will be noted. Also, if unauthorized copyright material had to be removed, a note will indicate the deletion.

Oversize materials (e.g., maps, drawings, charts) are reproduced by sectioning the original, beginning at the upper left-hand corner and continuing from left to right in equal sections with small overlaps.

Photographs included in the original manuscript have been reproduced xerographically in this copy. Higher quality 6" x 9" black and white photographic prints are available for any photographs or illustrations appearing in this copy for an additional charge. Contact UMI directly to order.

ProQuest Information and Learning
300 North Zeeb Road, Ann Arbor, MI 48106-1346 USA
800-521-0600

UMI®

LATE HOLOCENE CLIMATE CHANGE AND CALVING GLACIER FLUCTUATIONS ALONG THE SOUTHWESTERN MARGIN OF THE STIKINE ICEFIELD, ALASKA

by

Robert Joseph Viens

A dissertation submitted in partial fulfillment of the
requirements for the degree of

Doctor of Philosophy

University of Washington

2001

Program Authorized to Offer Degree:
Earth and Space Sciences

ProQuest Information and Learning Company
300 North Zeeb Road
P.O. Box 1346
Ann Arbor, MI 48106-1346

Doctoral Dissertation

In presenting this dissertation in partial fulfillment of the requirements for the Doctoral degree at the University of Washington, I agree that the Library shall make its copies freely available for inspection. I further agree that extensive copying of the dissertation is allowable only for scholarly purposes, consistent with "fair use" as prescribed in the U.S. Copyright Law. Requests for copying or reproduction of this dissertation may be referred to Bell and Howell Information and Learning, 300 North Zeeb Road, P.O. Box 1346, Ann Arbor, MI 48106-1346, to whom the author has granted "the right to reproduce and sell (a) copies of the manuscript in microform and/or (b) printed copies of the manuscript made from microform."

Signature ____________

Date 17 December 2001

University of Washington
Graduate School

This is to certify that I have examined this copy of a doctoral dissertation by

Robert Joseph Viens

and have found that it is complete and satisfactory in all respects, and that any and all revisions required by the final examining committee have been made.

Chair of Supervisory Committee: Stephen C. Porter

Reading Committee: Stephen C. Porter

Charles F. Raymond

Charles F. Raymond

Linda B. Brubaker

Date: 17 December 2001

University of Washington

Abstract

LATE HOLOCENE CLIMATE CHANGE AND CALVING GLACIER FLUCTUATIONS ALONG THE SOUTHWESTERN MARGIN OF THE STIKINE ICEFIELD, ALASKA

by Robert Joseph Viens

Chairperson of the Supervisory Committee:
Professor Stephen C. Porter
Department of Earth and Space Sciences

The retreat of large tidewater- and lake-calving glaciers, as well as nearby land-based glaciers, in southeastern Alaska during the middle to late Holocene was primarily triggered by increases in summer temperature. Shakes, LeConte, Patterson, and Baird glaciers, located along the southwestern margin of the Stikine Icefield in southeastern Alaska, experienced two or three major periods of advance and retreat during this period. Historical, stratigraphic, and dendrochronological evidence suggests that these periods of advance culminated approximately 3,500-3,300, 2,700-2,200, 1,100-900, and 220-110 years ago in the study area. Comparison with previously published regional records from glaciers located along the coast of northwestern North America suggests a general synchrony in the timing of ice advance across the region. Regional intervals of ice maxima date approximately 3,000-1,900, 1,500-900, and 250-100 years ago, and encompass three of the main periods of advance represented in the study area.

To determine a regional cause of glacier synchrony, glacier chronologies were compared to local and regional climate and climate proxies. Summer temperature fluctuations in the study area for the past four centuries were derived from tree-ring-width time-series from Crystal Mountain near Petersburg. Previously published precipitation and summer temperature values, inferred from palynological studies, provide a record of climate change for the last 10,000 years. Throughout southeastern Alaska, periods of glacier retreat for both calving glaciers and land-based glaciers tend to correlate with periods of warming summer temperature.

The collective data imply that the geologic record left by calving glaciers, like that left by land-based glaciers, has the potential to serve as an important climate-proxy record in a region where few such records have been studied. Furthermore, such a relationship helps further to quantify calving glacier dynamics and improve prediction of calving-glacier response to human-induced global warming.

TABLE OF CONTENTS

Table of Contents i
List of Figures iv
List of Tables x
Chapter 1: Introduction 1
  Objectives 3
  Significance 3
  Setting 4
  Local Geology 5
Chapter 2: Holocene Climate History in the region of the Stikine Icefield Based on Tree-rings and Historical records 13
  General Introduction 13
  Modern Conditions 14
    Modern Climate 14
    Modern Vegetation 15
  Late Quaternary Climate from Palynology 16
  Methods 18
    Historical Records 18
    Tree rings 20
    Correlation of Historical Climate Records and Tree rings 22
  Results and Discussion: Climate Records 23
    Historical Records 23
    Tree ring Records 23
    Comparison with other regional records 24
  Summary 25
Chapter 3: Stikine Glacier Chronologies 38
  Introduction: Historical Observations and previous work 38
  Methods 40
    Mapping Holocene Ice Margins 41
    Dating Methods 41
      Dendrochronology 41

Radiocarbon Dating 42
Cosmogenic Isotope Surface–Exposure Dating 43
Late Pleistocene Deglaciation 45
Neoglacial Chronologies 47
Shakes Glacier 48
Early to Middle Neoglaciation 48
Late Neoglaciation: Little Ice Age 49
LeConte Glacier 50
Early to Middle Neoglaciation 50
Late Neoglaciation: Little Ice Age 53
Patterson Glacier 55
Early to Middle Neoglaciation 55
Late Neoglaciation: Little Ice Age 55
Baird Glacier 57
Early to Middle Neoglaciation 57
Late Neoglaciation: Little Ice Age 58
Summary 59
Other Neoglacial Coastal glacier fluctuations along the Northwestern margin of North America 59
Stikine and Juneau Icefields 59
Glacier Bay and the St. Elias Mountains: 60
Western Gulf of Alaska 61
Southern British Columbia 62
Comparison of Regional Glacial Chronologies 62
Chapter 4: Tidewater Glaciers and Climate Change 108
Background - Calving Theory 108
Response of Stikine Glaciers to Climate Change 111
Early to middle Neoglaciation 111
Late Neoglaciation: Little Ice Age 112
Implications for Calving Theory 113
Calving Theory, Reconstructions, and Heinrich Events 113
Predictions 115
Shakes Glacier 115

LeConte Glacier 116
Patterson Glacier 116
Baird Glacier 116
Future work 116
Bibliography 121
Appendix A: Climate Data For Southeastern Alaskan Weather Stations 130
Appendix B: Tree Ring Data 147

LIST OF FIGURES

Number *Page*

Figure 1.1 – Variations in the Earth's surface temperature for the last (a) 140 years and (b) 1,000 years (from Houghton et al., 2001). The 95% confidence range is represented by error bars (a) and light-grey shaded area (b). 7

Figure 1.2 – Map of (a) southeastern Alaska and (b) close up of study area, showing location of the major geographic features discussed in the text. [1 – Dawes Glacier; 2,3 – Sawyer and South Sawyer glaciers; 4 – Baird Glacier; 5 – Patterson Glacier; 6 – Muddy Glaicer; 7 – LeConte Glacier; 8 – Shakes Glacier; 9 – Great Glacier; 10 – Mud Glacier; 11 – Flood Glacier] 8

Figure 1.3 – Geologic map of southeastern Alaska, showing the boundaries of the major terranes and/or lithic assemblages (modified from Gehrels and Berg, 1994). The study area includes the Coast Mountains batholith (shaded black), the Taku Terrane (T), the Gravina belt (G), and late Cretaceous granodirite and diorite intrusions in the Gravina belt (cross-hatched shading). 10

Figure 1.4 – Low-angle aerial photograph of LeConte Bay (U.S. Geological Survey #77R1, 8-30-77). The dashed line marks the contact between the more resistant Coast Mountains batholith and the Taku terrane. 11

Figure 1.5 – Glacial map of Alaska showing Late Wisconsin and earlier extent of glaciers (modified from Hamilton, 1994). 12

Figure 2.1 – Map of southeastern Alaska and northwestern British Columba showing location of late-Pleistocene/Holocene pollen cores. [(1) Langara Island, B.C. (Heusser, 1995), (2) Montana Creek ((Heusser, 1960) adapted in Ager, 1983), (3) Pleasant Island (Hansen and Engstrom, 1996), (4) Muskeg Cirque (Mann, 1983), and (5) Munday Creek (Heusser et al., 1985).] 26

Figure 2.2 – Late Pleistocene/Holocene average July temperature and annual precipitation at Munday Creek derived from transfer function applied to pollen core (modified from Heusser et al. (1985)). Triangles represent

radiocarbon dates. Selected calibrated radiocarbon ages are shown on the left. 27

Figure 2.3 – Map showing location of individual weather stations used to create the regional temperature and precipitation composites (Figure 2.6 and Appendix A) and collection site for Crystal Mountain tree-ring samples. 28

Figure 2.4 – Crystal Mountain Chronology (CMC) of standardized tree-ring widths from 14 tree cores (Appendix B). 29

Figure 2.5 – Summer temperature "index" determined by fitting a 10-year running mean to the Crystal Mountain Chronology. 30

Figure 2.6 – Instrumental records for the 20th century showing (a) average annual temperature and (b) annual precipitation for southeast Alaska. 31

Figure 2.7 – Annual and summer temperature reconstructions based on dendrochronology (ring width and late wood density). Reconstructions are for (a) Crystal Mountain (this study), (b) the northern hemisphere (Briffa et al., 1998), (c) northern North America (D'Arrigo and Jacoby, 1993), (d) the Pacific Northwest (Wiles et al., 1996) (e) south-central Alaska (Wiles et al., 1996), and (f) Vancouver, British Columbia (Dobry and Klinka, 1998). 33

Figure 3.1 – Terminus of LeConte Glacier in 1993. 65

Figure 3.2 – Patterson Glacier in 1994. 66

Figure 3.3 – 1897 photograph of the U.S. Coast and Geodetic Survey Steamer *Patterson* in Chatham Straight, southeast Alaska (NOAA Photo Library, NOAA Central Library; NOAA Office of Coast Survey, Hydrographic Descriptive Report 2333). 66

Figure 3.4 – Baird Glacier terminus in 1995. 67

Figure 3.5 – Shakes Glacier in 1995. 67

Figure 3.6 – Regional map of the southeastern part of the Stikine Icefield showing the location of regional glacier maps (Figures 3.13, 3.18, 3.28 and 3.34). 68

Figure 3.7 – Cross dating sub-fossil wood samples, from Stokes and Smiley (1968). 69

Figure 3.8 – (a) Photograph and (b) cross section of late Pleistocene and Holocene sediments exposed in the *Scandia House* parking lot, downtown Petersburg. Statigraphic section shows unit descriptions and interpretations as well as the location of radiocarbon-dated sample SCAN-3 (Table 3.5). Terry Swanson (University of Washington) is shown for scale. 70

Figure 3.9 – Late Pleistocene glacialmarine drift from lower Spurt Lake Creek in Thomas Bay (Figure 3.34) where TBS-95 was collected. 72
Figure 3.10 – Treeline at the top of Crystal Mountain where rock samples were collected for ^{36}Cl dating and tree cores were collected for CMC (Table 3.6 and Chapter 2). 72
Figure 3.11 – Late Pleistocene deglaciation dates from southeastern Alaska. All dates are reported as 10^3 calibrated years B.P. and shell samples reflect a marine reservoir correction of 925 years (see text and Table 3.4 for details). 73
Figure 3.12 – Post glacial rise in global sea level as recorded in corals collected off the coast of Barbados (from Bard et al., 1990). Samples are thought to have grown within a few meters of sea level. Differences in radiocarbon and uranium thorium ages reflect lack of calibration of the radiocarbon dates. 74
Figure 3.13 – Regional map of Shakes Glacier and vicinity showing the location of mapped and reconstructed termini positions, radiocarbon samples, and significant tree-ring ages. Radiocarbon ages are calibrated and all dates are reported in calendar years A.D. Calibrated radiocarbon ages are shown as a 1σ range and tree-ring ages are reported as the initiation of growth ±5 years. 75
Figure 3.14 – (a) U.S. Geological Survey topographic map and (b) aerial photo (U.S. Geological Survey #6642, Aug 79) of the Shakes Glacier moraine complex at the confluence of Shakes Slough and the Stikine River. The map shows the position of an outwash channel formed by the inpoundment of a side valley. 76
Figure 3.15 – International Boundary Commission Map (International Boundary Commission, 1952) showing the position of Shakes and LeConte glacier as surveyed between 1904 and 1909. 77
Figure 3.16 – Aerial photograph of the floating terminus of Shakes Glacier in 1977 (U.S. Geological Survey #77V2-9, 8-30-77). 78
Figure 3.17 – Retreat of the Shakes Glacier terminus since the 18th century. When the terminus receded past the constriction in the valley, the retreat rate increased from 14 m/yr to 137 m/yr. 79
Figure 3.18 – (a) Regional map of LeConte Glacier and vicinity and (b) inset of the area around the Little Ice Age maximum showing the location of mapped and

reconstructed termini positions, radiocarbon samples, and significant tree-ring ages. Radiocarbon ages are calibrated and all dates younger than 1200 A.D. are reported in calendar years A.D. Radiocarbon ages older than 1200 A.D. are reported as calibrated years B.P. (refer to appropriate figures for stratigraphic relationships). Calibrated radiocarbon ages are shown as a 1σ range and tree-ring ages are reported as the initiation of growth ±5 years...... 80
Figure 3.19 – Stratigraphic section of the exposure along the west fork of Cabin Creek, showing unit descriptions and interpretations as well as the location of radiocarbon-dated sample CC-4 (Table 3.5)...... 82
Figure 3.20 – Stratigraphic section of the exposure along the east fork of Cabin Creek, showing unit descriptions and interpretations as well as the location of radiocarbon-dated sample CC-15 (Table 3.5)...... 83
Figure 3.21 – Southern stratigraphic section of the exposure along lower Cabin Creek, showing unit descriptions and interpretations as well as the location of radiocarbon-dated sample CC-7 (Table 3.5)...... 84
Figure 3.22 – Northern stratigraphic section of the exposure along lower Cabin Creek, showing unit descriptions and interpretations as well as the location of radiocarbon-dated sample CC-11 (Table 3.5)...... 85
Figure 3.23 – Stratigraphic correlation between Cabin Creek sections (Figures 3.19-3.22)...... 86
Figure 3.24 – Bathymetry of LeConte Bay (modified from Post and Motyka, 1995)...... 87
Figure 3.25 – Coast and Geodetic Survey map (U.S. Coast and Geodetic Survey, 1895) showing the position of LeConte, Patterson and Baird glaciers as surveyed in 1887...... 88
Figure 3.26 – Photograph of the 1995 terminus of LeConte Glacier. High ice flux at the glacier terminus led to initiation of rapid retreat in 1995...... 89
Figure 3.27 – Retreat of the LeConte Glacier terminus since the 18th century...... 90
Figure 3.28 – Regional map of Patterson Glacier and vicinity showing the location of mapped and reconstructed termini positions, radiocarbon samples, and significant tree-ring ages. Radiocarbon ages are calibrated and all dates younger than 1200 A.D. are reported in calendar years A.D. Radiocarbon ages older than 1200 A.D. are reported as calibrated years B.P. Calibrated

radiocarbon ages are shown as a 1σ range and tree-ring ages are reported as the initiation of growth ±5 years. 91

Figure 3.29 – (a) Exposure of two layers of glacial drift near the mouth of Garnet Creek and (b) Tree stumps rooted in the lower till near the mouth of Garnet Creek. The log from the lower exposure (GCW-1; Table 3.5) was dated at 3,341 (3,255) 3,168 calibrated years B.P. 92

Figure 3.30 – (a) Historical photograph of the terminus of Patterson Glacier taken in the 1890's (source unknown) compared with (b) a 1995 photograph taken from the same location. These photographs show the Little Ice Age maximum position of Patterson Glacier. 93

Figure 3.31 –International Boundary Commission map (International Boundary Commission, 1952) showing the position of Patterson and Baird glaciers, as surveyed between 1904 and 1909. 94

Figure 3.32 – Trees of the "buried forest" eroding out of outwash ca. 2.4 km in front of the 1995 terminus position of Patterson Glacier. Sample BF-3 (Table 3.5) from the buried forest was radiocarbon dated and cross dated with the CMC. It likely died ca. 1792 A.D. during the Little Ice Age advance of Patterson Glacier. 95

Figure 3.33 – Retreat of the Patterson Glacier terminus since the 19th century. Once the glacier formed a lake at it terminus in ca. 1965, retreat rates increased from 25 m/yr to 74 m/yr. 96

Figure 3.34 – Regional map of Baird Glacier and vicinity showing the location of mapped and reconstructed termini positions, radiocarbon samples, and ^{36}Cl samples. Radiocarbon ages are calibrated and all dates are reported as calibrated years B.P. Calibrated radiocarbon ages and ^{36}Cl exposure ages are shown as a 1σ range. 97

Figure 3.35 – Stratigraphic section of the exposure along Spurt Lake Creek, showing unit descriptions and interpretations as well as the location of radiocarbon-dated sample TBW-2 (Table 3.5). 98

Figure 3.36 – Brad Hunter (U.S. Forest Service, Petersburg) and Terry Swanson (University of Washington) sampling a granodiorite erratic (VAN-1; Table 3.6) on Vanderput Point, at the mouth of Thomas Bay. 99

Figure 3.37 – Outwash apron in front of Baird Glacier that has been growing since at least the mid-18th century (photo from 1992). 99
Figure 3.38 – Trimline above the 1995 terminus of Baird Glacier that may reflect an earlier calving margin of the glacier. 100
Figure 3.39 – Comparison of Neoglacial advances of glaciers located along the coast of northwestern North America. 101
Figure 4.1 – Tidewater calving glacier cycle (from Viens, 1995). 118
Figure 4.2 – Graph comparing 20-year running mean of summer temperature variations derived from tree rings (CMC; Figure 2.5) with the initiation of glacier retreat in southeastern Alaska. Boxes show retreat from the most extensive Little Ice Age moraine for calving glacier termini (grey) and land-based termini (white). Numbers correspond with glacier data listed on Table 4.1. 119

LIST OF TABLES

Number *Page*

Table 2.1 – Weather station histories for southeastern Alaska. 34

Table 2.2 – Correlation between temperature records from individual weather stations and the regional composite generated in this study.......... 35

Table 2.3 – Correlation coefficients (r values) between the Crystal Mountain tree-ring chronology and instrumental (a) temperature and (b) precipitation data from 1899 to 1995. Each ring-width was correlated with monthly data for an 18-month period starting with June of the previous year (T-1) and extending throughout the growth year of the ring (T).......... 36

Table 2.4 – Correlation equations between instrumental summer temperature values and CMC ring-width series for 1899-1947 and 1948-1995 and correlation coefficients between predicted and instrumental summer temperature values.. 37

Table 3.1 – Basic data for glaciers included in this study (1995 statistics). 102

Table 3.2 – Significant tree cores from the study area used limit the age of deglaciated surfaces.......... 103

Table 3.3 – Radiocarbon dates (calibrated from Southon et al., 1990) used to determine an average marine reservoir effect of 925 yr.......... 104

Table 3 4 – Calibrated radiocarbon ages for deglaciation in southeastern Alaska and adjacent regions.......... 105

Table 3.5 – Calibrated radiocarbon ages from the study area.......... 106

Table 3.6 – Cosmogenic ^{36}Cl samples discussed in this study. 107

Table 4.1 – Glaciers from southeastern Alaska that have known ages for retreat from their most extensive Little Ice Age position. 120

ACKNOWLEDGMENTS

This project has spanned a continent and lasted nearly a decade – 1/7 of the world's landmass and about the same portion of my life. A journey that covers that much time and space isn't possible without the assistance of hundreds of people. All of them are, in some way, part of the document before you. I thank everyone who has given me advice and support, shared stories and field rations, and made the journey more pleasant and enjoyable. Although I can't name everyone, I like to single out a few people who made this all possible.

Everywhere I went in the field I felt as if I was walking in the footsteps of two great glacial geologists – John Muir and Austin Post. John Muir made the first recorded observations of LeConte glacier. Austin introduced me to calving glaciers and the Stikine Icefield and has supported my work ever since. This project would not have been possible without his wisdom and encouragement.

I have the honor of being part of a distinguished "academic lineage" which stretches from T.C. Chamberlain, and includes Richard Foster Flint (my academic "grandfather") and my advisor Steve Porter. Steve is one of the great Quaternary geologists and I am ever humbled by his knowledge. He read several drafts of my dissertation, provided countless suggestions, and supported me through the "slow" times. Without Steve's support I would not be writing this document today.

Field work required significant logistical and financial support. Ryn Schneider, Jason Briner, and Jen Gibbs all lugged coring equipment, paddled kayaks, watched for bears, and survived weeks of rain as field assistants. I couldn't have survived (literally) without them. I would like to thank everyone in Petersburg and Wrangell for a warm welcome and immeasurable assistance. In particular, Brad Hunter, Dave Rak, Bob Zorich, Don Holms, and Doc and Karen Gohmert went out of their way to help me get settled in town and provided transportation to and from field sites. (This was not an easy task as it involved trucks, bicycles, motor boats, river rafts, kayaks, helicopters, airplanes, and ferries!) As well as field assistance, Ryn lent me the use of a kayak and a room in her house. Paul

Bowen of Petersburg High School "broke the ice" by surveying LeConte Glacier with his students beginning in the 1980s and shared all his results.

Financial support came in the form of grants from the University of Washington Geology Department Graduate Student Research Fund, Geological Society of America (GSA), GSA Quaternary Division (J. Hoover Mackin Scholarship), and Sigma Xi, and field support from U.S. Geological Survey and U.S. Forest Service. Andrew Fountain and Brad Hunter played a key role in obtaining funding and logistics from U.S. agencies.

Steve Porter, Charlie Raymond, Linda Brubaker, Terry Swanson, Diana Olson, and Mike Hanson all provided lab advice, suggestions, and manuscript reviews. Any errors that squeaked through are entirely my own. Terry Swanson was an invaluable resource in preparing and running cosmogenic ^{36}Cl samples. My colleagues at Bellevue Community College provided support and encouragement throughout the home stretch.

Finally, and most importantly, I would like to thank those close to me who have supported me, even when I didn't believe in myself. Friends – Tracy and Justine Furutani, Leon Sawyko, Carol Franck, Mike Harrell, Cynthia Graff, Morgan Daybell, Beth Crane – all gave me something to look forward to after long days in the lab and never asked if "I was done yet." My family – Charlie, Carol, Kristin, and Dan Viens, and Alex and Helen Federchuck – made my education possible and were always there for me with encouragement and a place to "get away from it all".

And, of course, I wouldn't be writing this today without the love and support of my wife, Gwyn Jones. Gwyn supported and assisted me during every day of this endeavor and reminded me of the light at the end of the tunnel when I was ready to call it all off (more than once). Gwyn sacrificed as much as, or more than, I did to see this project to the end and I will always be grateful for her patience, assistance, and encouragement.

CHAPTER 1: INTRODUCTION

As we begin the 21st century, it is increasingly clear that the Earth is experiencing a warming trend. Instrumental records indicate that global-average surface temperatures increased by 0.6 ± 0.2°C in the 20th century (Figure 1.1a; Houghton et al., 2001). Mann et al. (1998) report that the 1990's have been the warmest decade of the last millennium and 1998 the warmest year; the Intergovernmental Panel on Climate Change (IPCC) (Houghton et al., 2001) states that the rate of temperature increase is likely to be greater than for any century in the past 1,000 years (Figure 1.1b). These data have fueled a major debate centered on the role that fossil fuel emissions and changing land-use practices have played in increasing global temperature during the 20th century. Many scientists think that this increase in global temperature is largely anthropogenic and is the result of the documented 31% increase in atmospheric CO_2 since the beginning of the Industrial Revolution, about 1750 (Houghton et al., 2001). It is impossible to answer this question definitively until the natural and anthropogenic contributions to fluctuations in global temperature can be separated. Separation, in turn, requires the establishment of a baseline that reflects Earth's natural climate variation. Therefore, in order to understand fully the significance of anthropogenic effects on Earth's climate, a detailed understanding of regional and global Holocene climate history is essential.

In the western Cordillera and along the northwestern coast of North America, historical climate records are short. Instrumental records in the western United States and Canada span, at most, the last 200 years, and in Alaska, continuous records generally do not predate the beginning of the 20th century. Therefore, an understanding of Holocene climate change in the western Cordillera requires the use of climate proxies, such as glacial deposits (Porter, 1981), lacustrine deposits (Leonard, 1997; Leonard and Reasoner, 1999), palynological records (Ager, 1983; Barnosky et al., 1987; Heusser, 1985), and tree-ring records (Fritts, 1976; Jacoby and D'Arrigo, 1995; Luckman et al., 1997; Wiles et al., 1998). Two such proxies — high-altitude tree-ring records and land-based glacial deposits — have been used in this study to reconstruct the late Holocene climate history of southeastern Alaska.

Ring-width and ring-density measurements have been used by numerous researchers (e.g., Luckman et al., 1997; Schweingruber, 1996; Schweingruber et al., 1993; Wiles et al., 1998) to reconstruct paleotemperature and paleoprecipitation conditions throughout the temperate latitudes. Studies have shown that ecologically stressed trees, including those in areas prone to drought and temperature extremes, are the most reliable for providing climate-proxy information (Fritts, 1976). Furthermore, previous research in coastal Alaska, where precipitation is high, indicates that ring width in trees growing at treeline is strongly dependent on summer temperatures (Wiles et al., 1996; Wiles et al., 1998). Records such as these provide an annual record of summer temperature variation for 1000-2000 years if enough intact subfossil wood is obtained.

In contrast to dendrochronological data, glacial deposits record climate at a lower frequency, usually on a decadal to millennial time scale. It has long been known that the steady-state position of alpine glacier termini is directly related to climate. Therefore, accurate mapping of glacial deposits can provide a means of reconstructing low-frequency variations in summer temperature and winter precipitation — the climatic variables that most affect alpine glacier equilibrium. However, depending on the size and temperature of the glacier, there is a lag of the terminus response to mass-balance changes. Furthermore, the interpretation of deposits from tidewater calving glaciers can be problematic, as their advance/retreat behavior is a function of calving dynamics — controlled by water depth (Brown et al., 1982), fjord geometry (Mercer, 1961), and ice dynamics (van der Veen, 1996) — and has been inferred to be largely independent of climatic influences (Mann, 1986a). Regional analysis of tidewater glacier cycles (Viens, 1995) suggests, however, that climate change may induce the retreat of calving glaciers, and therefore act as a pacemaker for controlling a glacier's advance/retreat cycle. Therefore, although such glaciers are relatively insensitive to climate changes on a decadal scale, their major cyclic pattern — measured on a multicentury or millennial time scale — may be related to climatic changes on the time scale of the Little Ice Age (ca. 1250-1850 A.D.). By comparing the low-frequency fluctuations of calving glaciers with those of land-based glaciers that have experienced the same climatic variations, it should be possible to isolate the effect of climate change on calving glacier advance/retreat cycles.

OBJECTIVES

The southwestern margin of the Stikine Icefield, located in southeastern Alaska (Figure 1.2), provides an excellent opportunity to quantify the role of climate change in the behavior of tidewater-calving glaciers. Furthermore, the climate-proxy information derived from land-based and calving glacier deposits, examined in conjunction with high-altitude (ca. 1,000 m) tree-ring measurements, provides an excellent proxy for both low- and high-frequency changes in summer temperature and winter precipitation. The objectives of this study are (1) to use high-altitude ring-width records to reconstruct annual changes in summer temperature during the Little Ice Age, (2) to use climate reconstructions from tree rings and land-based glacier deposits to show that the sediments left by calving glaciers can be interpreted as representing changing climate, and (3) to use calving and non-calving glacier deposits to infer 100- to 1,000-year climate variations in southeastern Alaska during the late Holocene.

SIGNIFICANCE

The effect of climate change on the steady-state position of calving glaciers has implications for many aspects of glacial geology. In itself, this study contributes to a more complete theory of tidewater glacier dynamics than presently exists. Furthermore, freshwater-calving Shakes Glacier provides a unique opportunity to compare fluctuations of tidewater and freshwater calving glaciers.

If the fluctuations of calving glaciers are shown to reflect multicentury-scale climatic changes, then such fluctuations can be used as a proxy for low-frequency Holocene climate change in the Gulf of Alaska. Such a relationship also increases the predictability of future glacier fluctuations, which might affect local human settlements.

Tidewater calving margins existed intermittently throughout the Pleistocene along Hudson Strait, and the bergs they generated periodically deposited ice-rafted debris layers across the North Atlantic Ocean (Heinrich, 1988). Because these "Heinrich events" are postulated to have been climatically driven (Broecker et al., 1992), understanding the influence of climate on tidal glacier fluctuations may play an important role in the interpretation of these events.

Assessment of ice sheet behavior during the last ice age requires a better understanding of calving glacier dynamics than now exists. At the glacial maximum, many marginal sectors of the major ice sheets terminated in the sea, and presumably had calving margins (Denton and Hughes, 1981). As they receded, other sectors of the ice sheets calved into freshwater lakes, which surrounded the retreating terminus. Therefore, much of the last deglaciation was controlled not only by climatic change, but also by calving dynamics.

Finally, the low-resolution Holocene climate variation recorded in glacial deposits and high-resolution summer temperature proxy found in tree rings provide an excellent record of summer temperatures through the Little Ice Age. These climate proxies provide a record of climate change in a region of North America where few data now exist and help establish a baseline for climate change studies. This addresses one of the major future goals of the IPCC (Houghton et al., 2001) — to "enhance the development of reconstructions of past climate periods".

SETTING

The Stikine Icefield is located in the Coast Mountains of southeastern Alaska and northwestern British Columbia between Juneau and Wrangell (Figure 1.2). The icefield is bordered on the north by the Taku River, on the east and south by the Stikine River, and on the west by the Pacific Ocean. Within a few kilometers of the ocean, peaks of the Coast Mountains reach 1,500-3,100 m altitude and intercept moisture-laden clouds moving inland off the Gulf of Alaska. At these altitudes, precipitation falls as snow and accumulates to form the icefield, which covers the range with more than 3,400 km^2 of ice. Large outlet glaciers originating in the Stikine Icefield include Dawes Glacier (653 km^2), Sawyer Glacier (399 km^2), South Sawyer Glacier (683 km^2), Baird Glacier (784 km^2), Patterson Glacier (64 km^2), Muddy Glacier (unofficial name; 15 km^2), LeConte Glacier (472 km^2), and Shakes Glacier (80 km^2) on the coastal (Alaska) side of the Coast Mountains (Viens, 1995), and Great Glacier (176 km^2), Flood Glacier (37 km^2), and Mud Glacier (ca. 45 km^2) on the continental (British Columbia) side (Field, 1975). Many of the large westward-flowing glaciers terminate in deep, sinuous fjords, carved during successive Pleistocene glaciations. The largest glaciers in the region terminate in the ocean and lose tremendous volumes of ice to calving. LeConte Glacier is the southernmost tidewater-calving glacier in the northern hemisphere. To the south and east (in British Columbia), many of the glaciers terminate in moraine-dammed lakes.

LOCAL GEOLOGY

The bedrock geology of southeastern Alaska consists of a complex of microterranes that were accreted onto North America during the late Mesozoic. These terranes are bounded by strike-slip faults and intruded by granitic plutons (Gehrels and Berg, 1994). The study area is underlain by three major microterranes and lithic assemblages (Figure 1.3).

To the east of Frederick Sound, and largely covered by the icefield, are the high-grade metamorphic and intrusive rocks of the Coast Mountains batholith. The Coast Mountains batholith formed during the late Cretaceous and early Tertiary periods, and primarily consists of hornblende-rich tonalites, quartz diorites, and granodiorites that intrude the surrounding medium- to high-grade metamorphic rocks. Metamorphic rocks in this region are dominated by schists and gneisses, but also include amphibolites, quartzites, marbles, and calc-silicates (Gehrels and Berg, 1994). Many of the glacial erratics sampled in this study for cosmogenic ^{36}Cl dating (Chapter 3) came from the Coast Mountains batholith.

To the west of the Coast Mountains batholith, the high-grade metamorphic rocks grade into the poorly understood, low- to medium-grade metasedimentary rocks of the Taku terrane. In the study area these rocks primarily include phyllites, garnet-schists, and limestones (Gehrels and Berg, 1994). The NW-SE foliation of the metamorphic rocks of the Taku terrane plays a major role in controlling the orientation of fjords and stream valleys in this region. The heads of fjords that intersect the Coast Mountains batholith tend to be steep-walled. Downvalley, where they cut into the Taku Terrane, fjords tend to be much broader and more densely forested (Figure 1.4).

A large part of Mitkov Island is underlain by the Gravina belt, which is thought to have been deposited on the Taku terrane in the east and the Alexander terrane in the west (McCelland and Gehrels, 1987). The rocks of the Gravina belt consist of marine argillites and greywackes that were exposed to low-grade metamorphism. In some areas, the metasedimentary rocks have been intruded by small quartz diorite and granodiorite intrusions. Samples from Crystal Mountain (Figure 1.2), collected for ^{36}Cl dating, came from granodiorite intrusives of the Gravina belt.

Several times during the Pleistocene, southeastern Alaska was covered by the Cordilleran Ice Sheet (Clague, 1989; Denton and Hughes, 1981); at the last glacial maximum the ice sheet reached a position on the continental shelf between 21,000 and 17,000 years ago (Hamilton, 1994; Mann, 1986b) (Figure 1.5). As the ice sheet retreated it deposited glacialmarine sediments that were later uplifted isostatically as much as 200 m above sea level (Clague, 1989; Mann, 1986b). Shells from these sediments were collected to date the timing of glacial retreat in the study area. During the Holocene, bedrock was covered by a veneer of Neoglacial drift (glacial lacustrine and glaciomarine deposits, till and outwash), colluvium, and Holocene peat. Determining the extent and age of these Holocene sediments provided a means of reconstructing the Holocene glacial history of the southwestern margin of the Stikine Icefield.

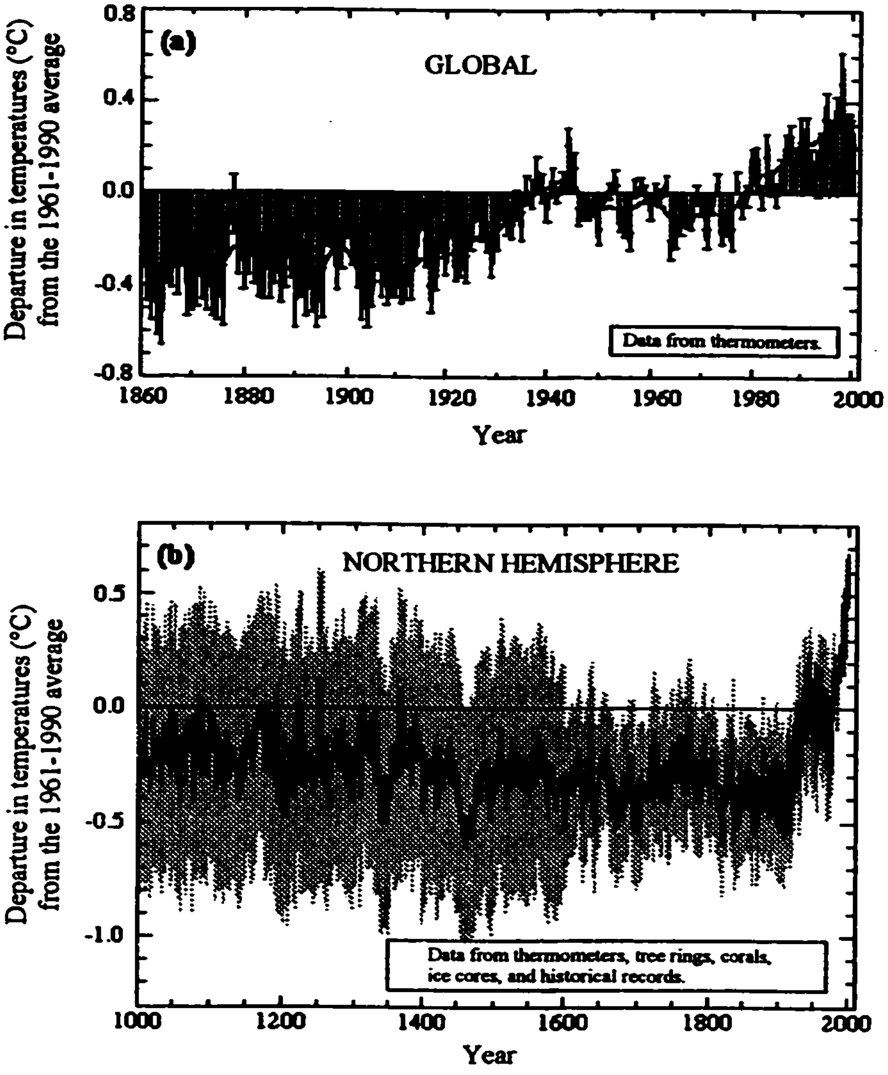

Figure 1.1 – Variations in the Earth's surface temperature for the last (a) 140 years and (b) 1,000 years (from Houghton et al., 2001). The 95% confidence range is represented by error bars (a) and light-grey shaded area (b).

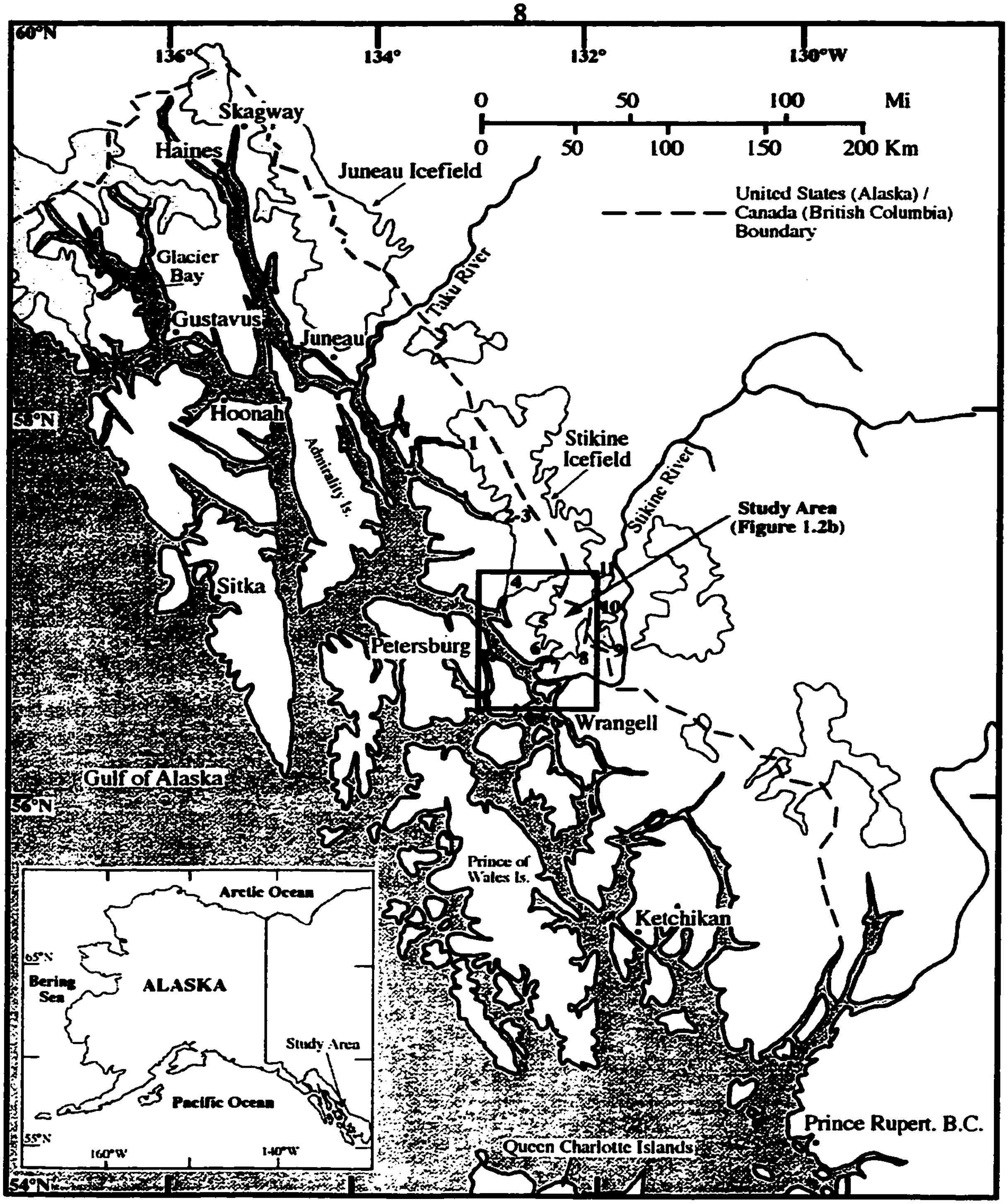

Figure 1.2 – (a) Map of southeastern Alaska showing location of the major geographic features discussed in the text. [1 – Dawes Glacier; 2,3 – Sawyer and South Sawyer glaciers; 4 – Baird Glacier; 5 – Patterson Glacier; 6 – Muddy Glaicer; 7 – LeConte Glacier; 8 – Shakes Glacier; 9 – Great Glacier; 10 – Mud Glacier; 11 – Flood Glacier]

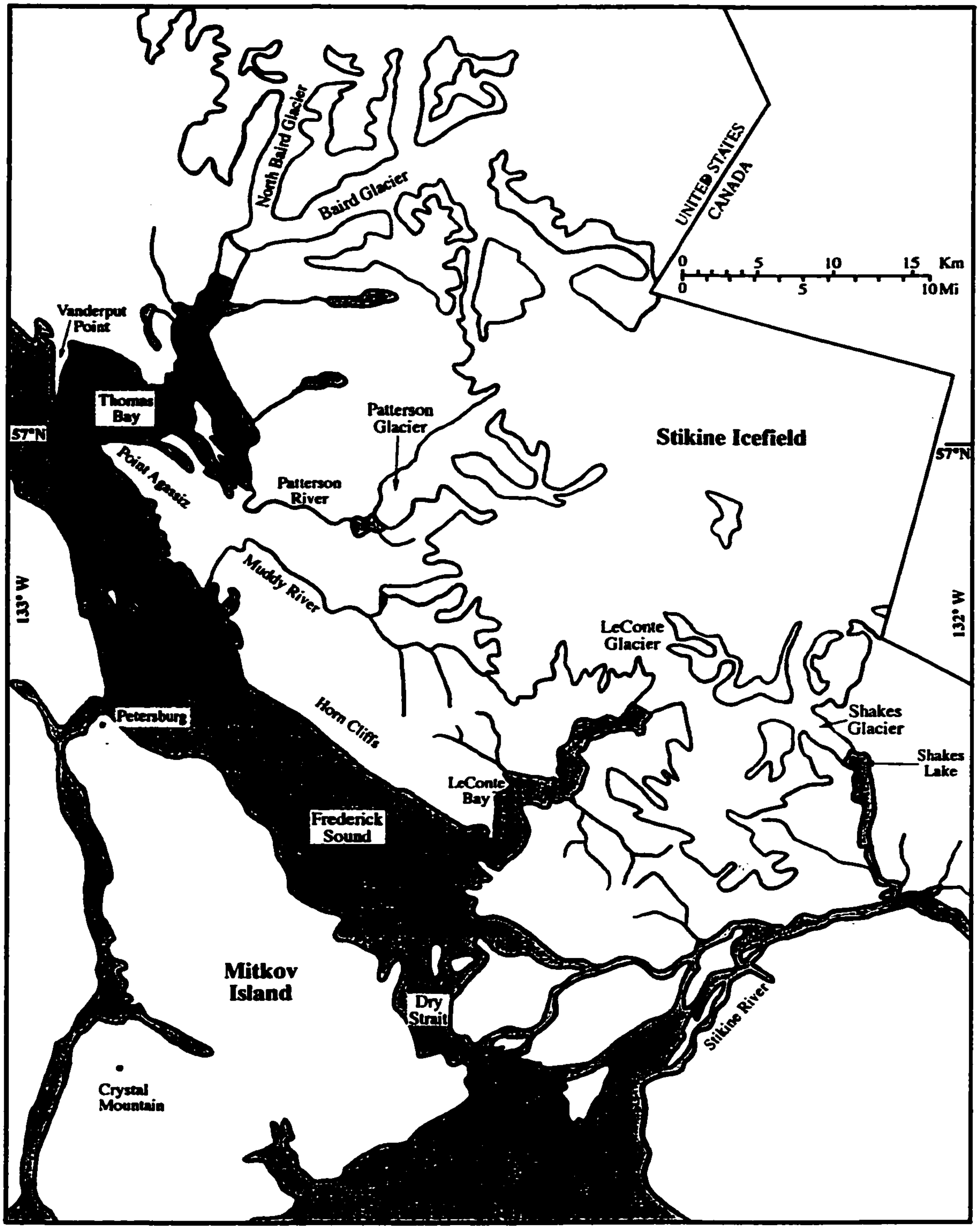

Figure 1.2 (cont.) – (b) Close up of study area, showing location of the major geographic features and glaciers discussed in the text.

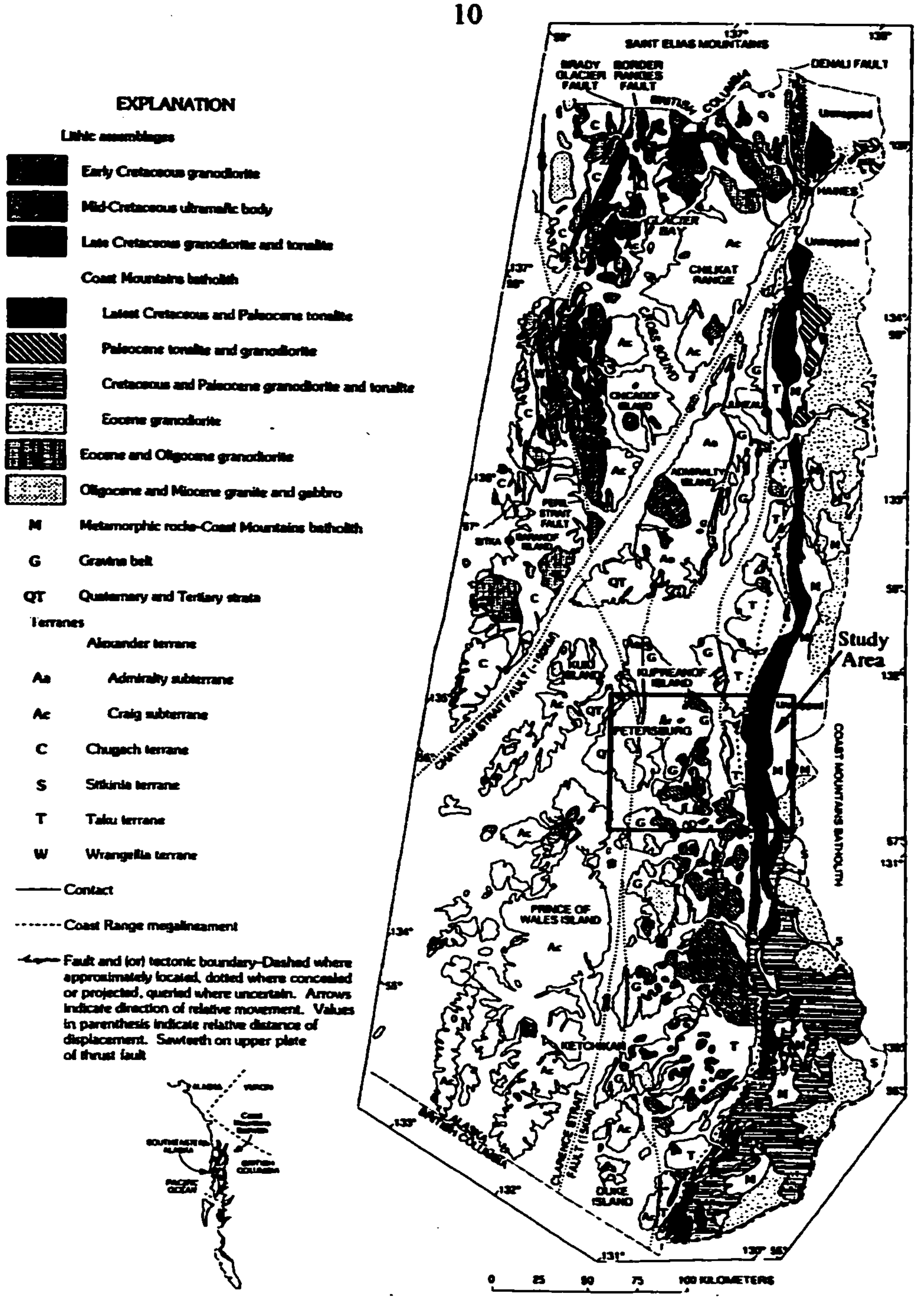

Figure 1.3 – Geologic map of southeastern Alaska, showing the boundaries of the major terranes and/or lithic assemblages (modified from Gehrels and Berg, 1994). The study area includes the Coast Mountains batholith (shaded black), the Taku Terrane (T), the Gravina belt (G), and late Cretaceous granodirite and diorite intrusions in the Gravina belt (cross-hatched shading).

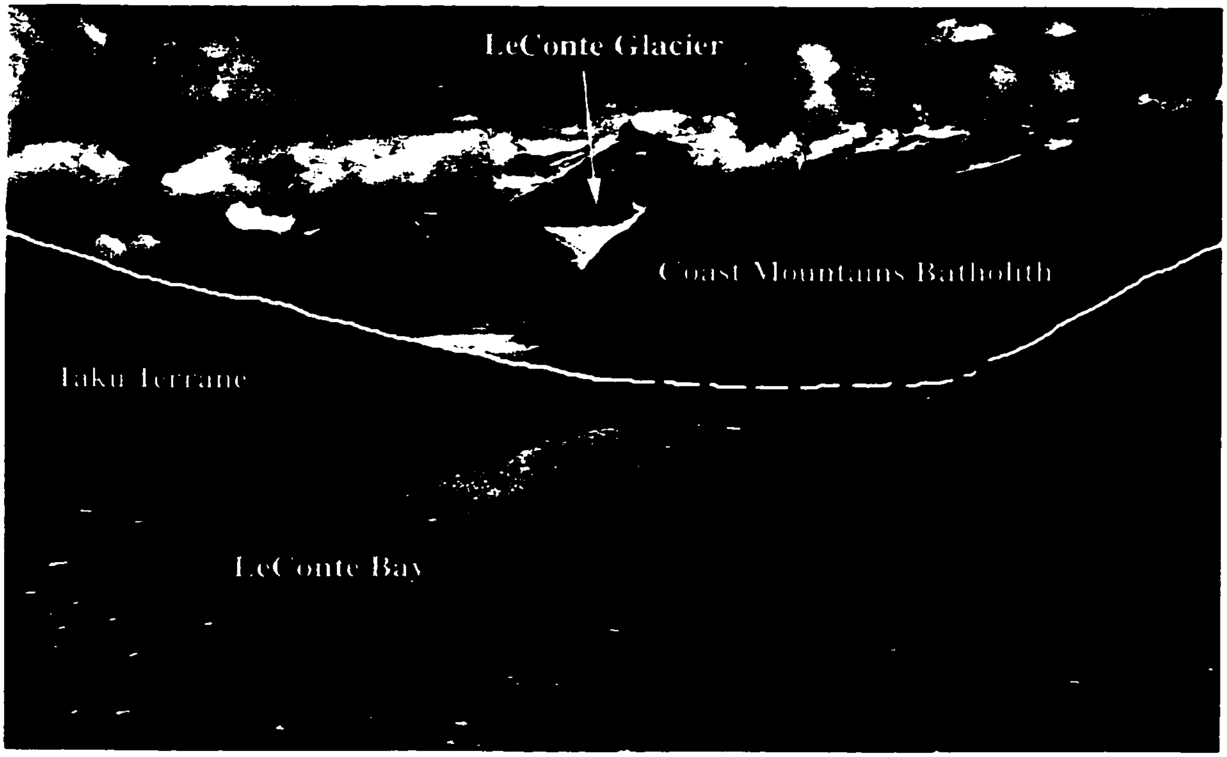

Figure 1.4 – Low-angle aerial photograph of LeConte Bay (U.S. Geological Survey #77R1, 8-30-77). The dashed line marks the contact between the more resistant Coast Mountains batholith and the Taku terrane.

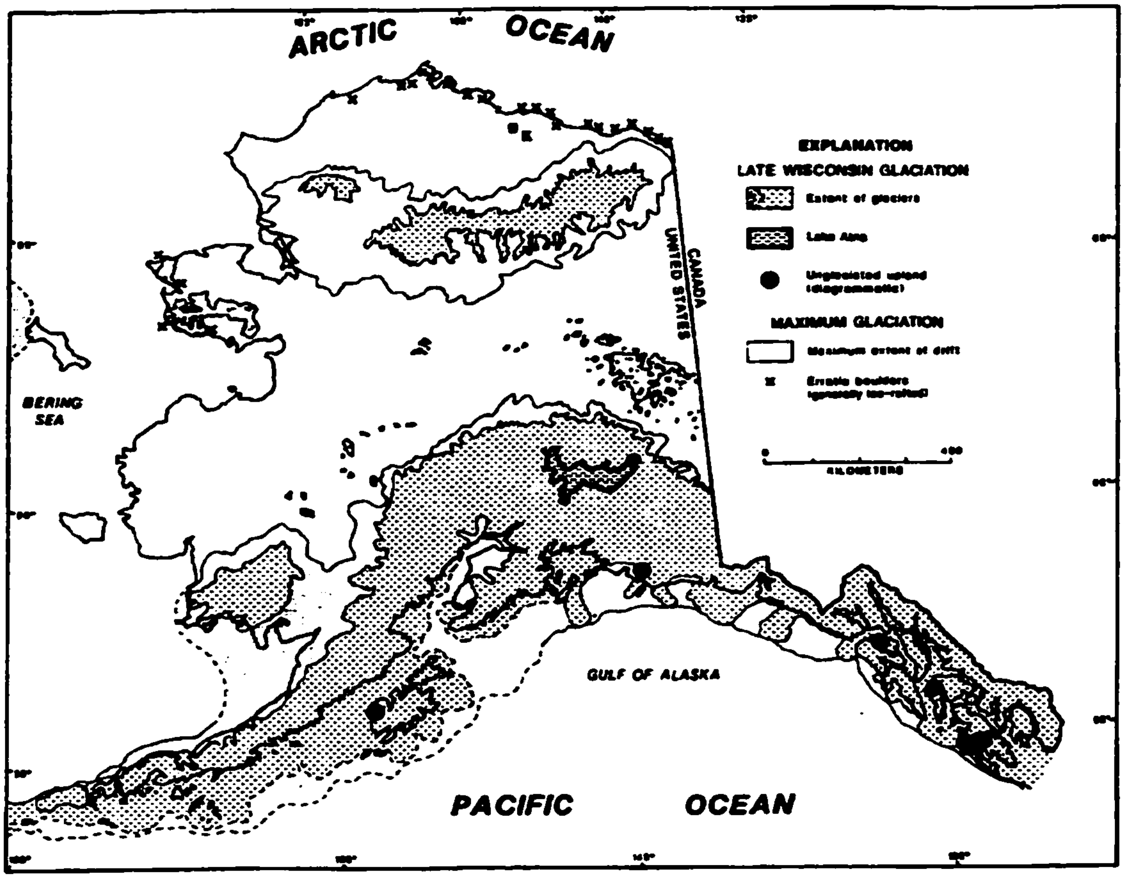

Figure 1.5 – Glacial map of Alaska showing Late Wisconsin and earlier extent of glaciers (modified from Hamilton, 1994).

CHAPTER 2: HOLOCENE CLIMATE HISTORY IN THE REGION OF THE STIKINE ICEFIELD BASED ON TREE-RINGS AND HISTORICAL RECORDS

GENERAL INTRODUCTION

A detailed, multicentury record of climate variation is required to understand tidewater glacier response to climate change. In southeastern Alaska, however, instrumental climate records have been kept continuously only since the early part of the 20th century. Furthermore, all these records are from weather stations within 100 m of sea level (see Table 2.1 for a summary of weather station histories for southeastern Alaska). Although a few weather stations exist at high-elevations in southeastern Alaska, no continuous records from these stations have been published. Therefore, climate data from high elevations must be obtained from U.S. Weather Service radiosonde measurements, or be extrapolated from stations at sea level (Tangborn, 1997); the resulting data are somewhat reliable for temperature, but tenuous for precipitation.

Ring-width indexes from trees growing at treeline provide a means of reconstructing relative temperature fluctuations through the Little Ice Age in southeastern Alaska. As shown locally by Jacoby and D'Arrigo (1995) in northern Alaska, Wiles et al. (1996) in south-central Alaska, Luckman et al. (1997) in the Canadian Rockies, and Dobry and Klinka (1998) in coastal British Columbia, high-altitude ring-width indices often reflect local summer temperature variations. The 425-yr tree ring record presented in this study provides a proxy for summer temperature fluctuations through the late Little Ice Age in a region where no instrumental records exist. Because the termini of alpine glaciers respond to changes in ablation-season temperature and accumulation-season precipitation, these records provide an important record for evaluating glacier behavior during the Little Ice Age.

MODERN CONDITIONS

MODERN CLIMATE

Mild winters, cool summers, and heavy rainfall are characteristic of the maritime climate of southeastern Alaska (see climate records, climatographs, and climate diagrams, Appendix A). Mean monthly temperatures along the coast average 6.2°C, with a range from -2.2°C in January to 14.5 °C in July. Located in a slightly more continental setting along Lynne Canal, Haines has a January mean of -5.1°C and annual mean of 4.9°C. Extreme monthly temperatures during the century have ranged from -12°C to 17.7°C. Coastal areas are not permanently frozen.

Although there are no weather monitoring stations at high elevations, radiosonde measurements recorded at the Annette Island Airport near Ketchikan (the closest regional radiosonde station) indicate that within a few thousand meters of the surface, average lapse rates are about 0.55°C/100 m [data synthesized from 1996 (National Climate Data Center (NCDC) and Environmental Research Laboratory (ERL), 1998)]. Assuming an adiabatic temperature drop of 0.55°C/100 m, mean annual temperatures at high altitudes (1,000-3,000 m) would range from about 1°C to -10°C. On average, treeline occurs at about 1,000 to 1,400 m where mean annual temperatures are about 1°C to -1°C, and tundra extends up to about 1,600 m (-2°C). The growing season at these altitudes is very short and above about 1,600 m vegetation is sparse. Where outlet glaciers reach sea level, temperatures are cooler than normal and alpine tundra vegetation is common.

Mean annual rainfall averages about 2,500 mm/year, and ranges from about 1,300 mm/year in Haines to nearly 4,000 mm/year in Ketchikan. In extremely wet years Ketchikan receives >5,000 mm of precipitation. Even in dry years most recording stations receive well over 1,000 mm of precipitation. Therefore, it is not surprising that the region is classified as very humid on the Thornthwait scale, with indices ranging from 485 in Ketchikan to 220 in Haines. High rainfall along the coast is primarily due to the orographic effect of the Coast Mountains. Precipitation is high on the west slope of the Coast Mountains as moist Pacific air rises up the west-southwest-facing slopes and cools. By the time the air mass reaches the 3,000-m-high crest of the range, it has lost most of it's moisture. This effect is evident when one compares rainfall data from Haines (1,300 mm/year), which is located in a deep inlet on the landward side of the St. Elias Mountains, with stations on the seaward side of the Coast Mountains. Rainfall is greatest in autumn, with the maximum occurring in October. Although June is the driest month, average monthly rainfall is still >100 mm. Cloudiness and relative humidity are high along the coast as well.

The region can be classified according to Koppen's system as a Cfc climatic regime. Warmth indices range from 32 to 43 month-°C (average 36 month-°C), and coldness indices from -11 to -37 month-°C (average -22 month-°C).

MODERN VEGETATION

The vegetation of the study region can be divided into four major classes: (1) coastal spruce-hemlock forests, (2) deciduous forests and shrub thickets, (3) muskegs or peat bogs, and (4) dry alpine tundras. Unless otherwise noted, the modern vegetation distribution is referenced from Viereck and Little (1972).

High rainfall along the coast supports dense, boreal, coniferous rainforests, which primarily consist of Sitka spruce (*Picea sitchensis*) and western hemlock (*Tsuga heterophylla*). Although they are not as common at sea level, mountain hemlock (*Tsuga mertensiana*) and Alaska yellow-cedar (*Chamaecyparis nootkatensis*) are found throughout the region. These forests are essentially an extension of the coastal forests of British Columbia and Washington. Western redcedar (*Thuja plicata*), Pacific yew (*Taxus brevifolia*), and Pacific silver fir (*Abies amabilis*) extend into the southern Panhandle of Alaska from British Columbia, although they are rare in Frederick Sound at the margin of their range. Near treeline there is an abundance of mountain hemlock and Alaska yellow-cedar, and one can also find some subalpine fir (*Abies lasiocarpa*). Common forest shrubs include blueberries and huckleberries (*Vaccinium* ssp.), devils club (*Oplopanax horridus*), and salal (*Gaultheria shallon*). To the east of the Coast Mountains, the coastal forests gradually merge with the spruce-birch forests of interior British Columbia.

Along river valleys, coastlines, avalanche scars, and the edge of the tundra one finds a variety of pioneer deciduous trees and shrub thickets. Most common are Sitka alder (*Alnus sinuata*), red alder (*Alnus rubra*), willow (*Salix* ssp.), luetkea (*Luetkea pectinata*), and currents (*Ribes* ssp.). Alder, black cottonwood (*Populus trichocarpa*) and balsam poplar (*Populus balsamifera*) are also common on floodplains and gravelly alluvial fans.

Muskegs, consisting predominantly of peat moss (Sphagnidae), develop at low altitudes where drainage is poor. Sedges (Cyperaceae), rushes (Juncaceae), low shrubs, and lichens are also common in these environments. Although usually treeless, bogs may contain isolated spruce, hemlock, and lodgepole pine (*Pinus contorta* var. *latifolia*). Common shrubs include bog-rosemary (*Andromeda polifolia*), common juniper (*Juniperus communis*), willow (*Salix* ssp.), bog cranberry (*Vaccinium oxycoccos*), and bog blueberry (*Vaccinium uliginosum*).

Above treeline in the Coast Mountains (1,000-1,400 m), heavy winter snowfall lasts late into the spring. It is in these regions, and at the heads of many fjords, amidst the barren rock and ice, where alpine tundra occurs. The alpine tundra is relatively dry and consists mainly of herbaceous species, grasses (Poaceae), and some small shrubs. The most common shrubs are blue mountain heath (*Phyllodoce coerulea*) and red mountain heath (*Phyllodoce empetriformis*).

LATE QUATERNARY CLIMATE FROM PALYNOLOGY

The little information that is currently known about late Pleistocene/Holocene climate in southern Alaska comes from palynological studies. Pollen data for the coastal region of southeastern Alaska record the succession of vegetation from surfaces deglaciated starting as early as 17,000 years ago[1] (see deglaciation summary in Chapter 3) to the present combination of coastal rainforests, muskegs, deciduous thickets, and alpine tundra. Changes in vegetation during the postglacial period represent changing temperature and precipitation conditions that led to the structure of the modern forest ecosystem.

Although there are no published pollen cores from the Petersburg area, several cores that extend back to the late Pleistocene have been obtained from southeast Alaska and the Queen Charlotte Islands in northern British Columbia. From south to north (Figure 2.1), these

---

[1] Throughout the paper radiocarbon dates were calibrated to calendar years using Calib 3.0.3 (Stuiver and Reimer, 1993) and are reported as calibrated years ("years") with a range of 1σ. Radiocarbon and calibrated ages for samples are summarized in Tables 3.3 - 3.6. Because the major boundaries in pollen cores are often based on extrapolation from one or two radiocarbon ages in the core, the dates in this section are reported as approximate calendar years and the published radiocarbon years ("^{14}C years") are also provided.

cores include, (1) Langara Island, B.C. (Heusser, 1995), (2) Montana Creek (Heusser, 1960; adapted in Ager, 1983), (3) Pleasant Island (Hansen and Engstrom, 1996), (4) Muskeg Cirque (Mann, 1983), and (5) Munday Creek (Heusser et al., 1985).

During the last glacial (ca. 17,000 years ago) almost all of southeastern Alaska was covered with an extensive ice sheet (Figure 1.5). Some coastal stretches, such as those near Lituya Bay (Mann, 1983), Prince of Wales Island (Heaton et al., 1996), and the Queen Charlotte Islands (Warner et al., 1982), may have been nonglaciated refugia for tundra species during the glacial maximum. However, it is unlikely that any arboreal species survived in the northern refugia (Mann and Hamilton, 1995). Interior Alaska, which was not ice-covered during full-glacial times, acted as a refugium for additional species, while others migrated up the coast of British Columbia from nonglaciated regions to the south (Heusser, 1983b).

The cores from southeastern Alaska and northwestern British Columbia (Figure 2.1) indicate that after the ice sheet retreated (ca. 16,000 to 12,000 years ago for the cited cores), herb and shrub tundra migrated north in front of the melting ice (colonization of recently deglaciated areas by the alpine tundra can be observed today at the heads of many fjords). Shortly afterwards, lodgepole pine, alder, and sedge were the dominant taxa. Although alder dominated the region until ca. 8,500 years ago (ca. 7,500 ^{14}C years), Sitka spruce and western hemlock first appeared about 10,500 years ago (ca. 9,500 ^{14}C years). Furthermore, abundant peat moss and skunk cabbage (*Lysichiton americanum*) in the Juneau area from 8,500 – 3,800 years ago (7,800 – 3,500 ^{14}C years) indicates warmer-than-present climates during the middle Holocene (Ager, 1983). Further west, in the Muskeg Cirque core near Lituya Bay, a decline in pine and an increase in spruce and alder occurred ca. 12,400 years ago (10,500 ^{14}C years; Mann, 1983). Western hemlock reached this region about 7,900 years ago (7,100 ^{14}C years) and mountain hemlock about 5,600 years ago (4,900 ^{14}C years).

Alder and lodgepole pine were well established on the Alaska Panhandle ca. 12,400 years ago (10,500 ^{14}C years). Rapid migration of the pioneering alder probably indicates optimum growing conditions at that time. Peteet (1986) suggested that increasing temperatures and decreasing precipitation in the early Holocene facilitated the rapid spread of alder in southern Alaska and supported these deciduous shrubs for the next 2,000 years.

The decline in alder, ca. 8,800 – 8,300 years ago (8,000 – 7,500 ^{14}C years), corresponds well with the invasion of spruce, which prefers a moister climate (Peteet, 1986).

The modern spruce-hemlock forests of southeastern Alaska represent the climax community for the region. The current combination of high precipitation, cool temperature during the growing season, and frequent frost-free days probably has played a role in regulating the distribution of vegetation in the coastal forests (Anderson, 1955).

Heusser et al. (1985) used a transfer function based on modern pollen data and the Munday Creek pollen core to reconstruct average summer temperature and average annual precipitation. Their results, shown in Figure 2.2, are supported by changing vegetation recorded in all the pollen cores from southeastern Alaska.

In summary, four major late Pleistocene/Holocene climatic periods are recorded in pollen records from southeastern Alaska. In general, these periods can be described chronologically as (1) cold and dry, (2) warm and dry, (3) warm and moist, and (4) cool and moist. Tundra and shrub forests of the late Pleistocene record a cool, dry period that lasted from as early as 16,000 years ago to ca. 12,500 years ago. Alder/pine forests record an early Holocene warm, dry period (ca. 12,500 to 9,000 years ago) that was followed by a warm, moist period between 8,800 – 6,800 years ago (recorded by skunk cabbage and an increase in spruce). By ca. 6,800 years ago summer temperatures were falling and precipitation was rising, leading to the development of modern coastal forests along the Alaskan coast. Heusser et al.'s (1985) climate reconstructions show that temperatures and precipitation reached modern levels about 4,500 years ago. This date corresponds to the establishment of modern Sitka spruce/western hemlock forests in all of the pollen cores. This climate regime has dominated the coast until the present.

METHODS

HISTORICAL RECORDS

Daily precipitation and temperature values have been recorded in the Stikine region almost continuously since the 1920's. Discontinuous record keeping at the Wrangell airport (Table 2-1; WRG) began in the late 1800's; however, nearly complete record keeping did not begin until after 1925. In Petersburg, reliable record keeping began in 1929 and includes a hiatus between 1933 and 1936. The Petersburg meteorological station was moved in 1980 from downtown Petersburg (Table 2-1; PTG) to the airport (Table 2-1; PTG2), located about 1.5 km inland. Because of the short length and incomplete nature of the two weather records closest to the study area, older and more-complete weather records were also used to create temperature and precipitation indices for southeastern Alaska. These stations include Sitka (SK), Juneau (JNU2), Haines (HNS), Petersburg (PTG/PTG2), Wrangell (WRG), and Ketchikan (KTH) (Table 2-1; Figure 2.3). Discontinuous records from Juneau and Sitka extend back to 1881 and 1828, respectively, and, in addition, represent two of the most complete records for southeastern Alaska in the 20th century. Because of their incomplete nature, the pre-1899 records were not used in this study. By integrating the data from all six stations it is possible to create a nearly complete record of temperature and precipitation that extends back into the late 19th century.

Monthly precipitation and temperature data, as well as yearly totals and averages were obtained from the Alaska/U.S. Weather Bureau's Climatological Data (Alaska/U.S. Department of Commerce - Weather Bureau, 1920-1995) for Petersburg and Wrangell and from the Alaska Climate Research Center internet page (http://climate.gi.alaska.edu/climatology/data.html; Alaska Climate Research Center, 2001) for Sitka, Juneau and Haines. Monthly and yearly averages, and maximum and minimum values, where calculated for all stations. Monthly temperature and precipitation data were normalized for each station using z-scores. Normalized data were averaged between the six stations (weighted equally) to create regional average temperature and precipitation records for southeastern Alaska. Only monthly data that included two or more stations were used for this study.

Normalized weather data from each station were compared to the five remaining stations, as well as to the composite data set for southeastern Alaska (Table 2.2). In general, correlation between individual stations and the composite chronology was good ($r > 0.88$, except for Ketchikan with $r = 0.79$). Therefore, because of it's completeness, the regional composite data were deemed more useful than that of any individual station for correlation with tree-ring indices.

TREE RINGS

Annual tree ring width is affected by numerous environmental factors, as well as by the age of the tree. These growth-dependent factors include the effect of the age of the tree (A), climatic variables (C), local disturbance to the tree (e.g., competition with other trees, broken tops; D_1), stand-level disturbance (e.g., fire, disease; D_2), and error associated with unpredictable variables (E) (Schweingruber, 1996). In combination these variables create ring-width patterns that can be unique to an individual tree (A, D_1, E), a local stand of trees (D_2), and/or an entire geographic region (C). In order to use trees to study climatic factors that affect a large geographic region and to use those records as a means of dating subfossil wood, it becomes necessary to remove the effects of the local or individual effects on ring width. This can be accomplished by standardizing ring-width indices to remove the growth effects (A) and creating composite chronologies from an entire stand of trees to remove the factors that affect individual trees (D_1, E). Regional factors (D_2), aside from climate, can be more difficult to remove, but can be ruled out as a major source of variation if multiple stands of trees show similar ring-width patterns.

For this study, tree rings were collected for three purposes: (1) to use as a proxy for climate change over the last 425 years, (2) to date the age of deglaciated surfaces recently colonized by vegetation, and (3) to develop a master tree-ring chronology for cross-dating subfossil wood. The general methodology for collection and preparation of tree rings, as well as the development of a climate proxy (1), will be discussed below. The use of tree rings for dating deglaciated surfaces (2) and subfossil wood (3) will be covered in the following chapter.

For (1) and (3), two cores were collected from each of 12 mountain hemlock trees growing at treeline (about 1000 m) at Crystal Mountain, Mitkov Island (about 20 km south of PRG2 and 45 km northwest of WRG; Figure 2.3). Cores for (2) were collected from Sitka spruce, western hemlock, and Alaska yellow cedar growing on deglaciated surfaces, former outwash plains, and from old trees outside the glacier limit. Slabs of subfossil wood (mostly Sitka spruce) were also collected from glacial sediments in order to determine the timing of glacier advance (Chapter 3). In all cases, trees were selected to give the strongest climate record, i.e., healthy trees that did not appear to be in close competition with their neighbors. Living trees were sampled at ca. 1 m using a increment borer. Two cores were collected from each tree used for constructing the Crystal Mountain climate chronology; multiple cross sections of sub-fossil trees were collected whenever possible. Appendix C lists the collection location and other relevant data for each tree sampled.

In the laboratory, cores were mounted and sanded using standard preparation procedures (Stokes and Smiley, 1968) and the rings were counted using a binocular microscope. Cores were then locally and regionally crossdated manually to minimize error due to false rings, missing rings, or human error. Ring widths were measured to the nearest 0.02 mm using a sliding stage micrometer with a digital encoder. Cores were further analyzed for measurement and crossdating errors using the program COFECHA (Holmes, 1983). Cores with crossdating errors flagged by COFECHA were reexamined and the missing rings were inserted where necessary. After crossdating was completed, intracorrelation between cores from the stand of trees on Crystal Mountain was high ($r = 0.65$) and deemed to be significant. (Raw and standardized ring-width chronologies for trees used to construct the Crystal Mountain master tree ring chronology are shown in Appendix C.)

Once accurately crossdated, 14 ring-width series (at least 1 from each of the 12 different trees) from Crystal Mountain were combined using the program ARSTAN (Cook, 1985; Cook and Holmes, 1984) to create a master ring-width chronology for the Crystal Mountain trees. The computer program ARSTAN was used to standardize each ring-width series by fitting each series to a curve and computing an index of ring width by dividing the measured value by the expected value. This produced a dimensionless tree-ring index that removes the growth trend of the tree and makes it possible to compare relative ring width patterns between several trees. Standard and residual ring-width chronologies were produced by detrending the ring-width series with a standard cubic-smoothing spline having a 50% frequency response cutoff of 256 years. This detrending curve was chosen in order to preserve as much of the low-frequency fluctuations in the ring-width series, without losing the high-frequency record — preserving 98% of the variance on a time scale of up to 102 years, and 80% of the variance on time scales of up to 18 years.

By averaging the ring-width indices for the trees on Crystal Mountain, ARSTAN created a master ring-width chronology. This record, which spans 425 years and begins in 1564, will hereafter be referred to as the Crystal Mountain Chronology (CMC) (Figure 2.4).

Standardization and the formation of the CMC eliminate the major ring-width variations caused by factors that affect individual trees (A, D_1, E). To rule out any major variations caused by non-climatic factors affecting the entire stand, the CMC was crossdated using COFECHA with a stand of eight trees sampled in the Shakes Lake valley (Figure 1.2; located ca. 50 km to the west of Crystal Mountain). Correlation between the trees from these two regions was high enough (r = 0.58) to indicate that the major ring-width signal remaining in the CMC is largely a regional climatic signal.

CORRELATION OF HISTORICAL CLIMATE RECORDS AND TREE RINGS

To determine which climatic variables best represent the ring-width record, the CMC was correlated with monthly temperature and precipitation data for an 18-month period starting with the June of the previous year (T-1) and extending throughout the growth year of the ring (T). The correlation coefficients for this time period are shown in Table 2.3. Correlation with precipitation was barely significant, with the largest correlation (r = -0.20) being for August precipitation of the previous year (T-1). Correlation with temperature during the summer of a ring's growing season was relatively high (r = 0.42 for June to September). Jacoby and D'Arrigo (1995) and D'Arrigo and Jacoby (1993) in northern Alaska, Wiles et al. (1996) in south-central Alaska, Luckman et. al (1997) in the Canadian Rockies, and Dobry and Klinka (1998) in coastal British Columbia also found that ring width correlated well with summer temperatures. Therefore, further analysis focused on the summer temperature record.

The CMC was correlated with summer temperature data using the methods outlined by Fritts (1976). First, the regional summer temperature dataset was divided into two subsets, each spanning half the total record (subset 1: 1899 – 1947, subset 2: 1948 - 1995). Summer temperatures from subset 1 were correlated with ring-width indices from the same time period, and a regression equation was obtained (Table 2.4). This equation and the standardized ring-width indices were used to predict independently the summer temperature values for the period spanning subset 2. The predicted data were then compared to the instrumental data. The same process was carried out for the subset 2 and its correlation equation (Table 2.4) and the standardized ring-width indices were used to predict the summer temperatures for period spanning subset 1. The correlation coefficients between the predicted and actual values (Table 2.4) were considered significant enough (r = 0.30 to 0.51) to indicate trends in summer temperature; however, they were not considered high enough to transfer actual temperature values to the tree-ring data. Therefore, general temperature trends where superimposed on the annual CMC by fitting a 10-year running mean to the data, resulting in a summer temperature "index" for Crystal Mountain that spans 425 years from 1564 to 1990 A.D. (Figure 2.5).

RESULTS AND DISCUSSION: CLIMATE RECORDS

HISTORICAL RECORDS

Twentieth century instrumental temperature records from southeastern Alaska show a general warming trend of about 0.3°C (Figure 2.6a), less than the 0.6°C-warming observed globally (Figure 1.1; Houghton et al., 2001). Decadal variations during the last 100 years, however, are consistent with general global trends. Whereas historic highs occurred in the 1920's, 1960's, and 1990's, lows occurred in the 1940's and 1970's. Annual precipitation fluctuated considerable during the 20th century, with a rapid rise in precipitation in the beginning of the century, followed be a gradual decline since ca. 1920 (Figure 2.6b). The driest year on record corresponds to the eruption of Katmai Volcano in 1911.

TREE RING RECORDS

The summer temperature record generated using the Crystal Mountain Chronology shows a great deal of high-frequency (annual to decadal) variation in summer temperature over the last 425 years. During this period, however, there was no low-frequency (multi-century) change in summer temperature, implying that (1) temperatures have not changed dramatically since the mid 16th century, (2) the trees did not record the change, or (3) the record was lost during the standardization process. Because the age-detrending process is required to remove the overall decrease in ring width during the lifespan of the tree, and because many of the trees are between 300 and 400 years old, some of the low-frequency record was likely lost during the detrending process (the smoothing spline only preserves 50% of the variability on time scales of 256 years). In fact, half of the trees sampled show a low frequency rise in ring width during the 19th and 20thcenturies which was removed by the age-detrending process. There is no reason to suspect that the trees did not record a long-term change, and it certainly seems likely that some change occurred during that time period, because many of the glaciers in the region were expanding or in an expanded state in the 16th through 19th centuries.

The remaining high-frequency record proves interesting (Figure 2.5). The first 47 years of record (1564 to 1611 A.D.) are only represented in one core and should be viewed with caution. Taken at face value, they imply a major cool period, that began in the mid-1500's with the warmest years of the record and culminated in the early 1600's with the coldest years on record (1603 being the coldest). Other major cold periods occurred in the late 1600's, mid-1700's, mid- to late-1800's, and the early 1900's. Periods of warmer-than-average summer temperatures occurred in the last half of the 1700's, early- to mid-1800's, and mid-1900's. The record shows no major warming trend during the 1980's. The largest and most abrupt periods of warming occurred from 1603 to 1635, 1754 to 1780, and 1910 to 1950.

Some of the largest volcanic eruptions of the last 400 years may also be recorded in the tree-ring record. When Briffa et al.(1998)averaged tree-ring density records in the northern hemisphere and compared them to volcanic eruptions, they found that rings with dense late-wood where typically produced in the year following a major eruption.. In the study area, unusually narrow rings follow by 1 to 3 years the eruptions of Hauynaputing, Peru (de Silva and Zielinski, 1998) in 1600 (narrow ring in 1603), Tambora, Indonesia in 1815 (narrow rings in 1817-19), Krakatoa, Indonesia in 1883 (narrow ring in 1886), and Katmai, Alaska in 1911 (narrow ring in 1912). A 2 to 3 year delay is apparent between eruptions in the tropics (e.g., Tambora) and the reduced ring width in southeastern Alaska, whereas local eruptions (e.g., Katmai) affect tree growth within a year. Understanding the discrepancy between the uniform delay (1 yr) published by Briffa et al.(1998) and the variable delay (1 to 3 yr) in the local study area will require more local data.

COMPARISON WITH OTHER REGIONAL RECORDS

Several studies have used tree-ring width and/or ring late-wood density to reconstruct summer temperatures for northwestern North America. Large-scale studies have concentrated on the broader changes recorded throughout the northern hemisphere (Briffa et al., 1998), across northern North America (D'Arrigo and Jacoby, 1993) or throughout the Pacific Northwest (Wiles et al., 1996) (Figure 2.7b,c,d). Closer to the study area, Wiles et al. (1996) reconstructed summer temperatures along the south-central Alaska coast (Figure 2.7e). To the south of the study area, in southern British Columbia (Dobry and Klinka, 1998), tree-ring width and late-wood density have also been used to reconstruct summer temperatures (Figure 2.7f). Figure 2.7 shows all five of these temperature reconstructions in conjunction with the CMC from this study.

Different studies have used different detrending methods to construct their tree-ring series. This means that some studies have removed the low-frequency (century-scale) trends in order to remove the age effects on ring width. Therefore, although it is possible to compare the high-frequency trends between studies, comparison of low-frequency fluctuations would be meaningless.

Nevertheless the general agreement appears to be quite good. Older, hemispheric records show a general warming trend in early 1600's, and Briffa et al. (1998) report that the coldest year in the last 600 years occurred in 1601. After a late 17th century cold period, most records show warming in the early 1700's and again in the mid- to late 1700's. All records agree that the early 19th century was a period of cooling; however, there was a fair degree of variation in the last half of the 19th century. Most records show a general warming trend in the early 20th century followed by significant cooling in the 1960's.

SUMMARY

Tree-ring chronologies from southeastern Alaska that span the last 425 years provide an important record of fluctuating summer temperatures for a region where such records have not existed. The general trends evident in the climate records are in good agreement with trends determined from other tree-ring chronologies in the Pacific Northwest. Furthermore, the tree-ring chronology generated in this study provides an excellent (and inexpensive) basis for dating glacial sediments and archeological sites in the region (Chapter 3). These techniques are used to interpret the glacial history of the Stikine region (Chapter 3) and the relationship between the temperature records and glacier fluctuations (Chapter 4).

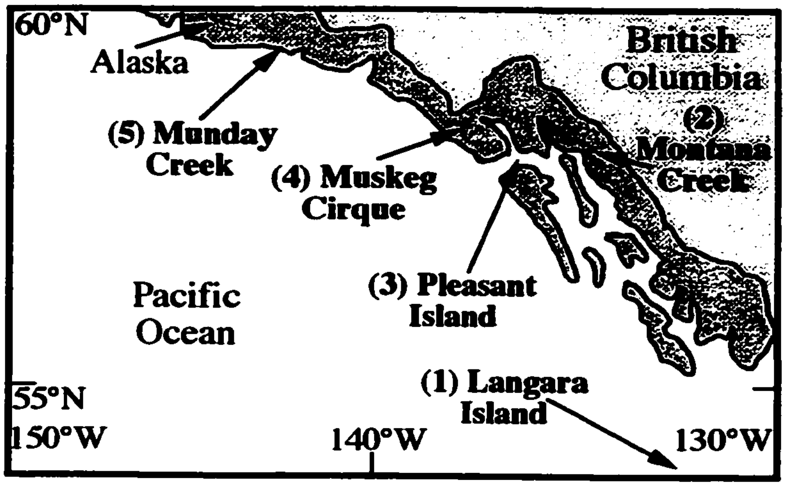

Figure 2.1 – Map of southeastern Alaska and northwestern British Columba showing location of late-Pleistocene/Holocene pollen cores. [(1) Langara Island, B.C. (Heusser, 1995), (2) Montana Creek ((Heusser, 1960) adapted in Ager, 1983), (3) Pleasant Island (Hansen and Engstrom, 1996), (4) Muskeg Cirque (Mann, 1983), and (5) Munday Creek (Heusser et al., 1985).]

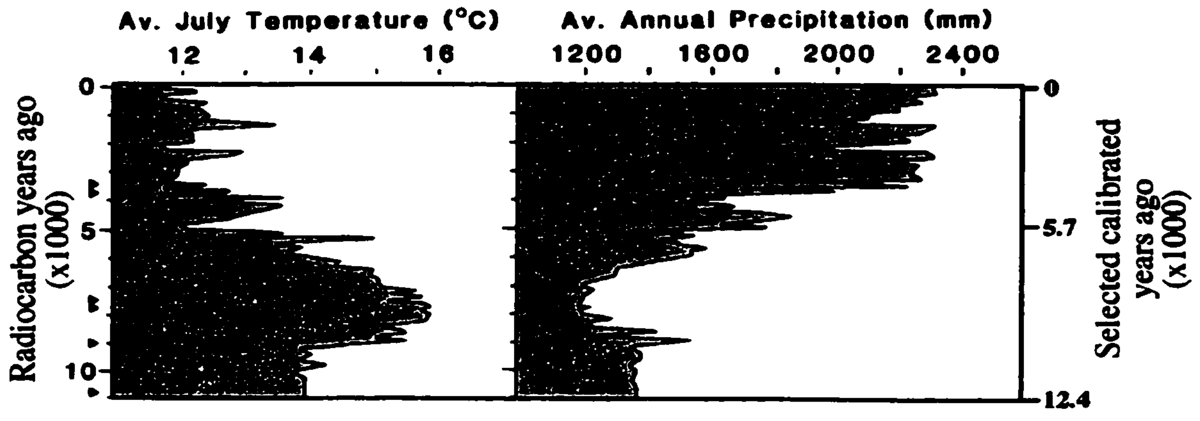

Figure 2.2 – Late Pleistocene/Holocene average July temperature and annual precipitation at Munday Creek derived from transfer function applied to pollen core (modified from Heusser et al. (1985)). Triangles represent radiocarbon dates. Selected calibrated radiocarbon ages are shown on the left.

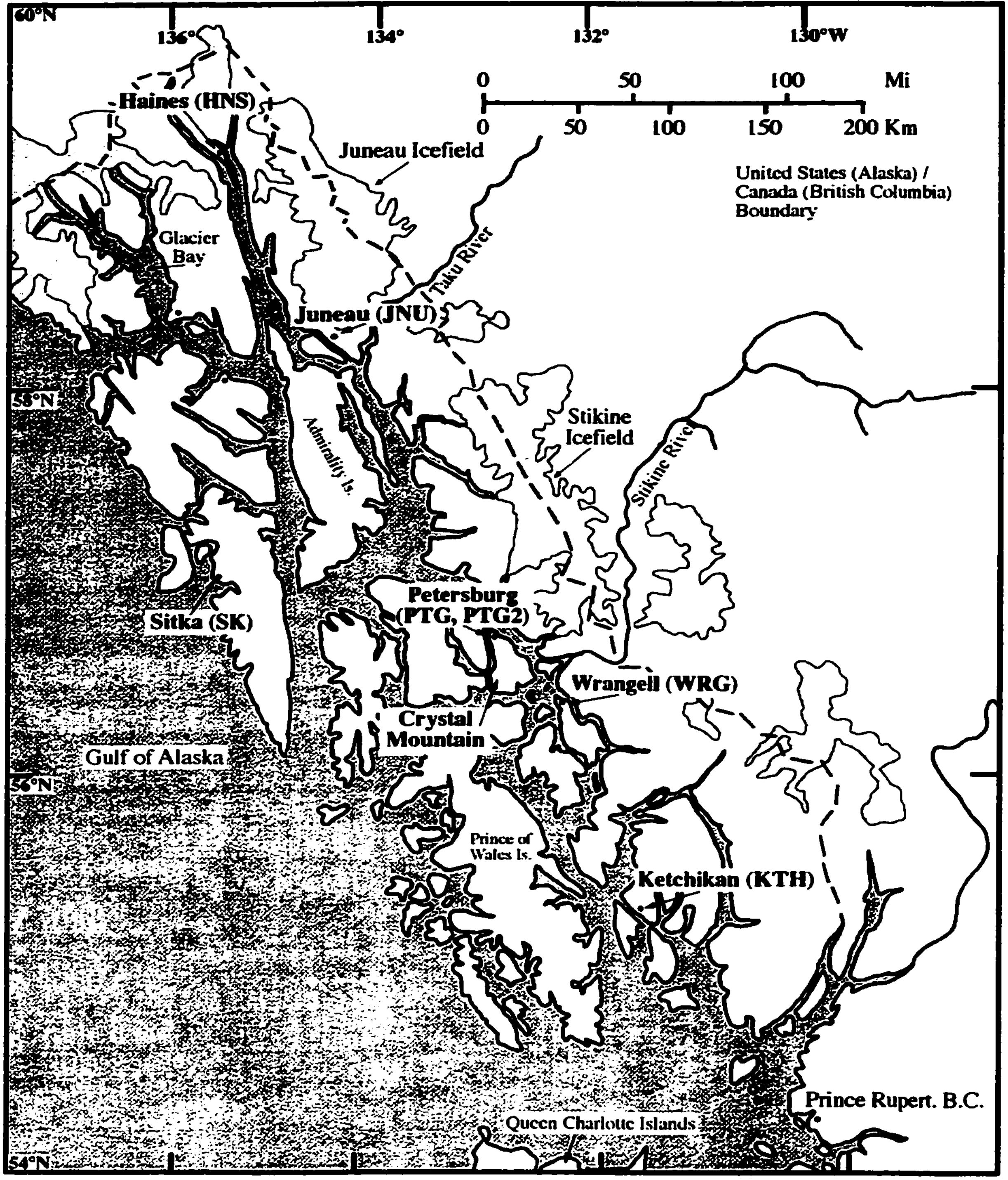

Figure 2.3 – Map showing location of individual weather stations used to create the regional temperature and precipitation composites (Figure 2.6 and Appendix A) and collection site for Crystal Mountain tree-ring samples.

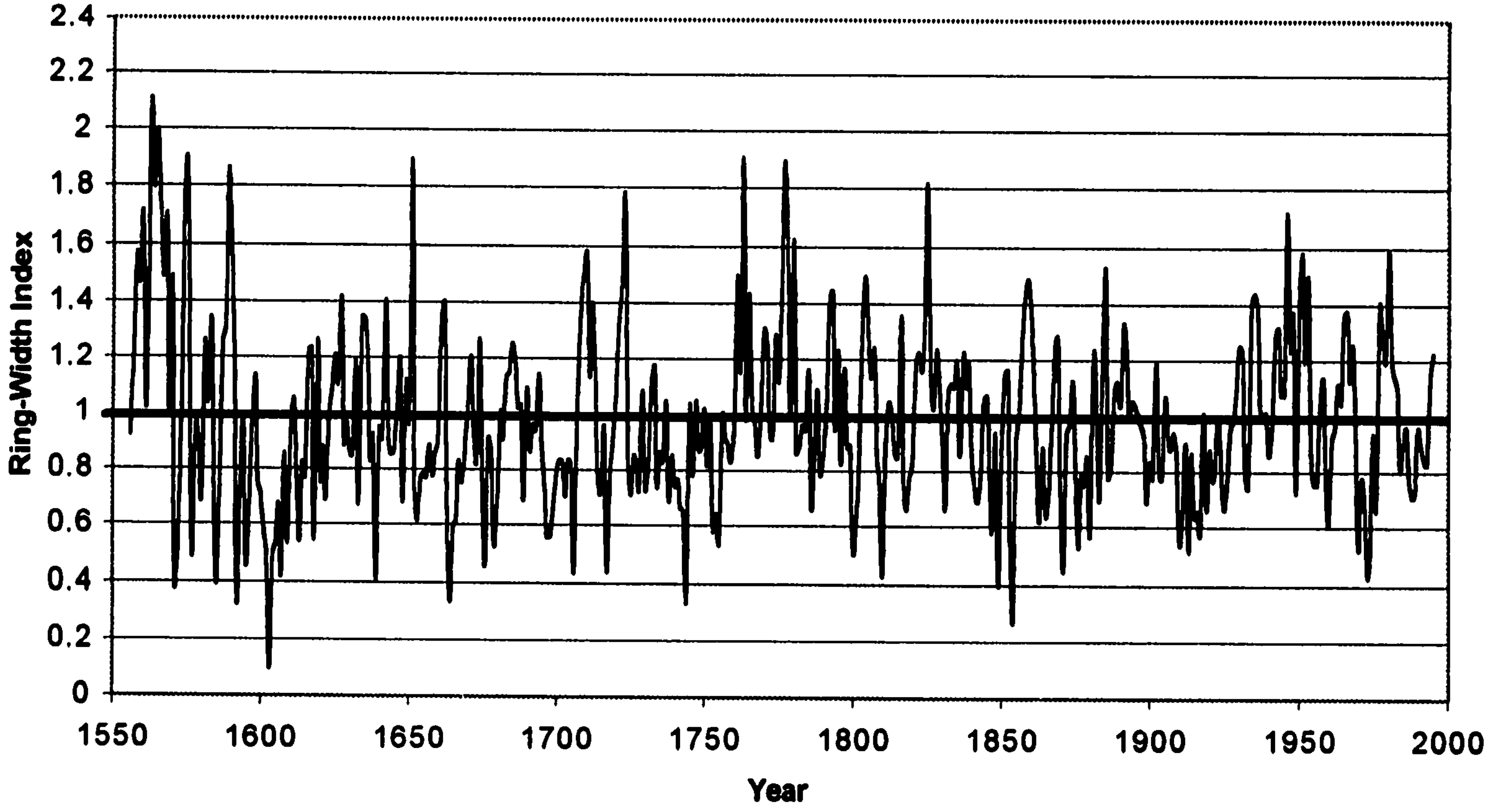

Figure 2.4 – Crystal Mountain Chronology (CMC) of standardized tree-ring widths from 14 tree cores (Appendix B).

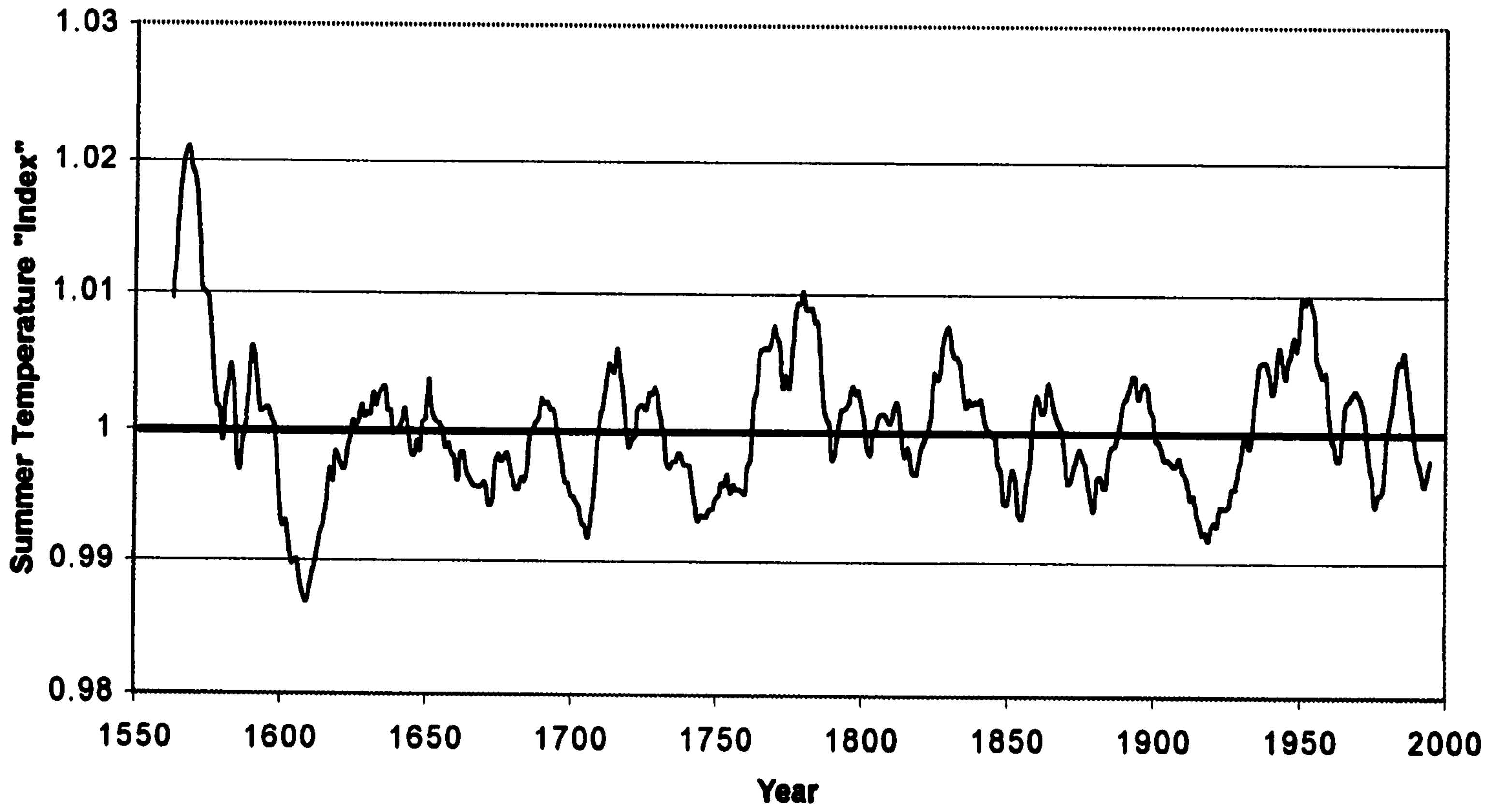

Figure 2.5 – Summer temperature "index" determined by fitting a 10-year running mean to the Crystal Mountain Chronology.

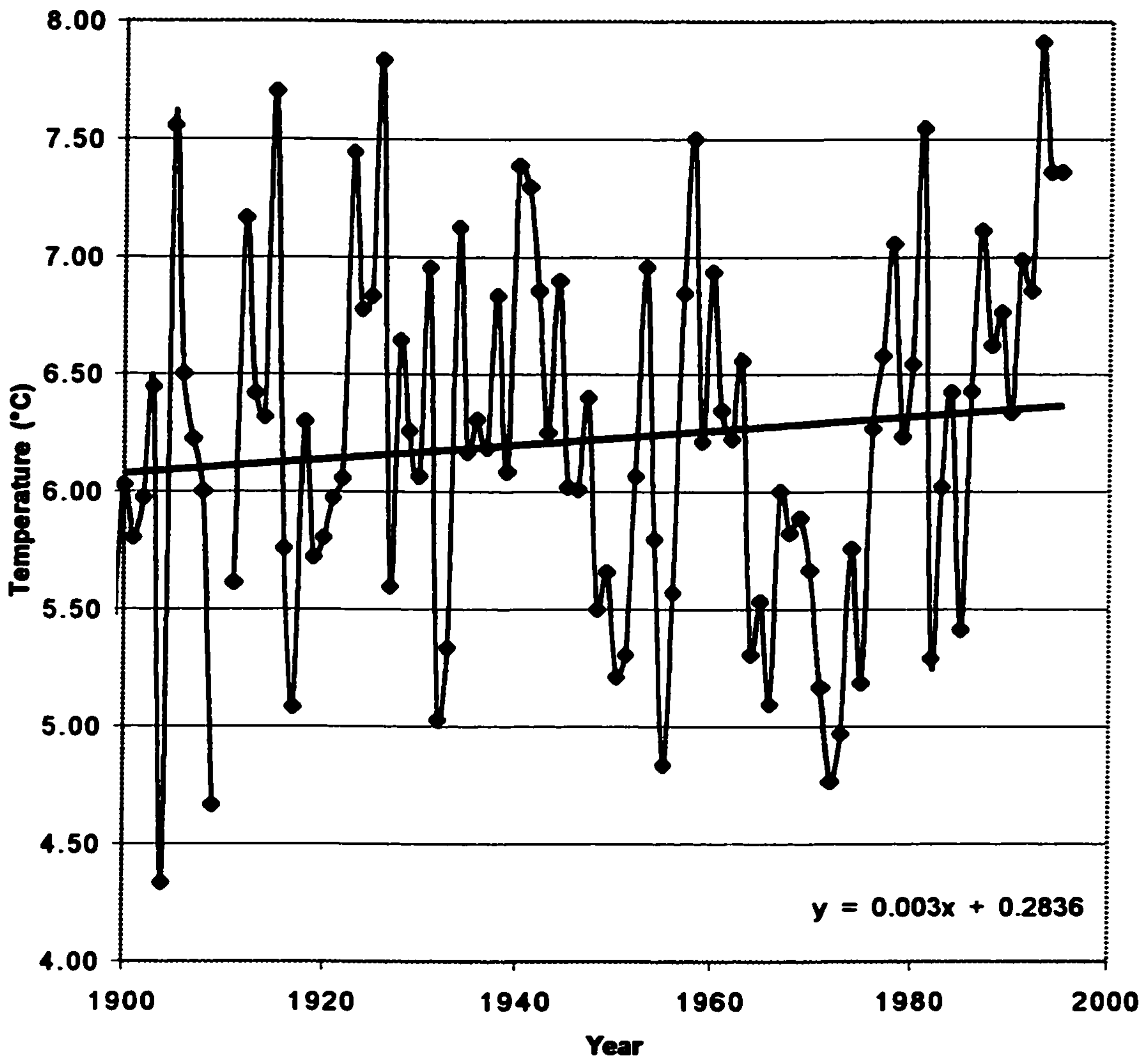

Figure 2.6 – (a) Instrumental records for the 20th century showing average annual temperature for southeast Alaska.

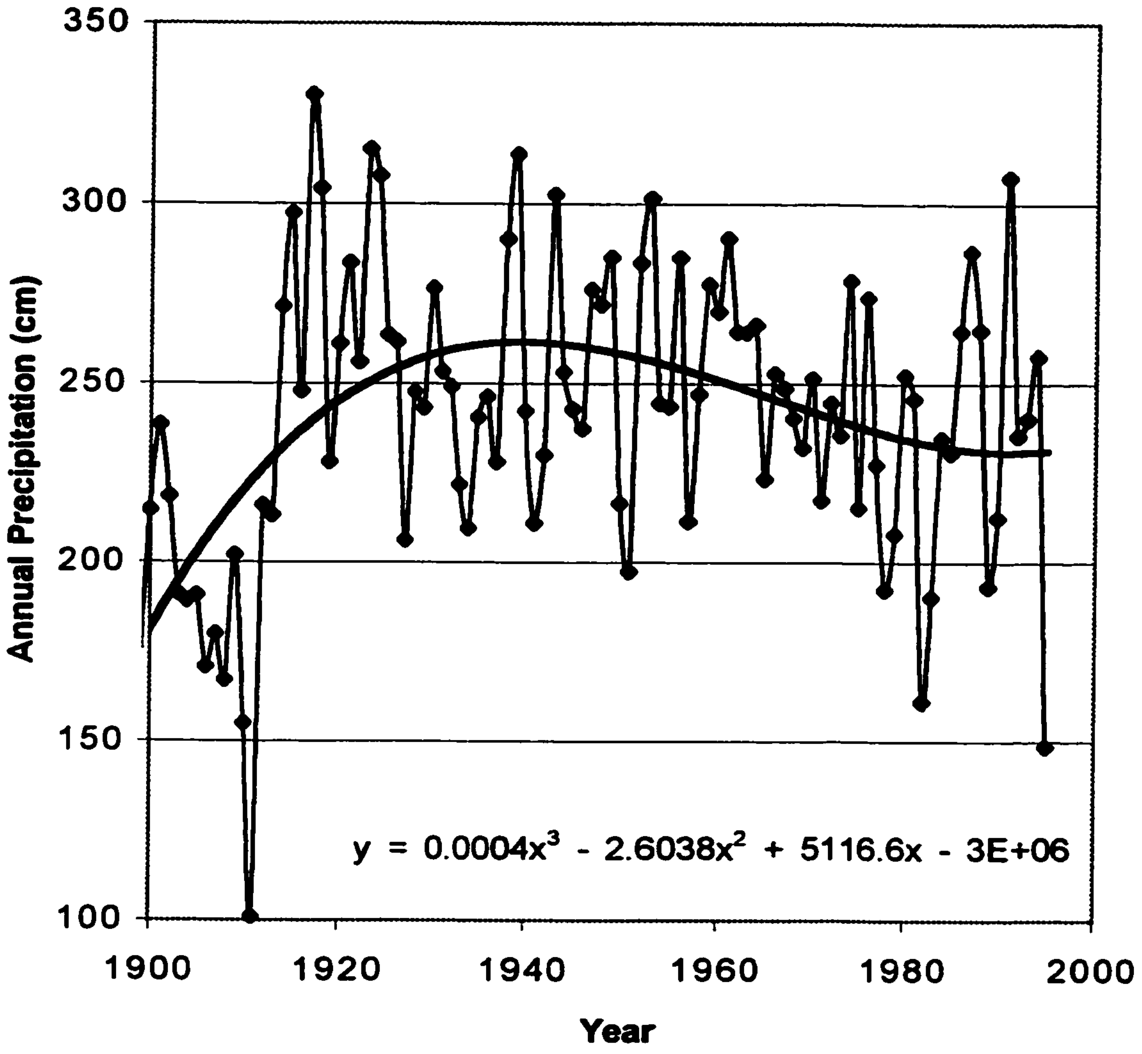

Figure 2.6 (cont.) – (b) Instrumental records for the 20th century showing annual precipitation for southeast Alaska.

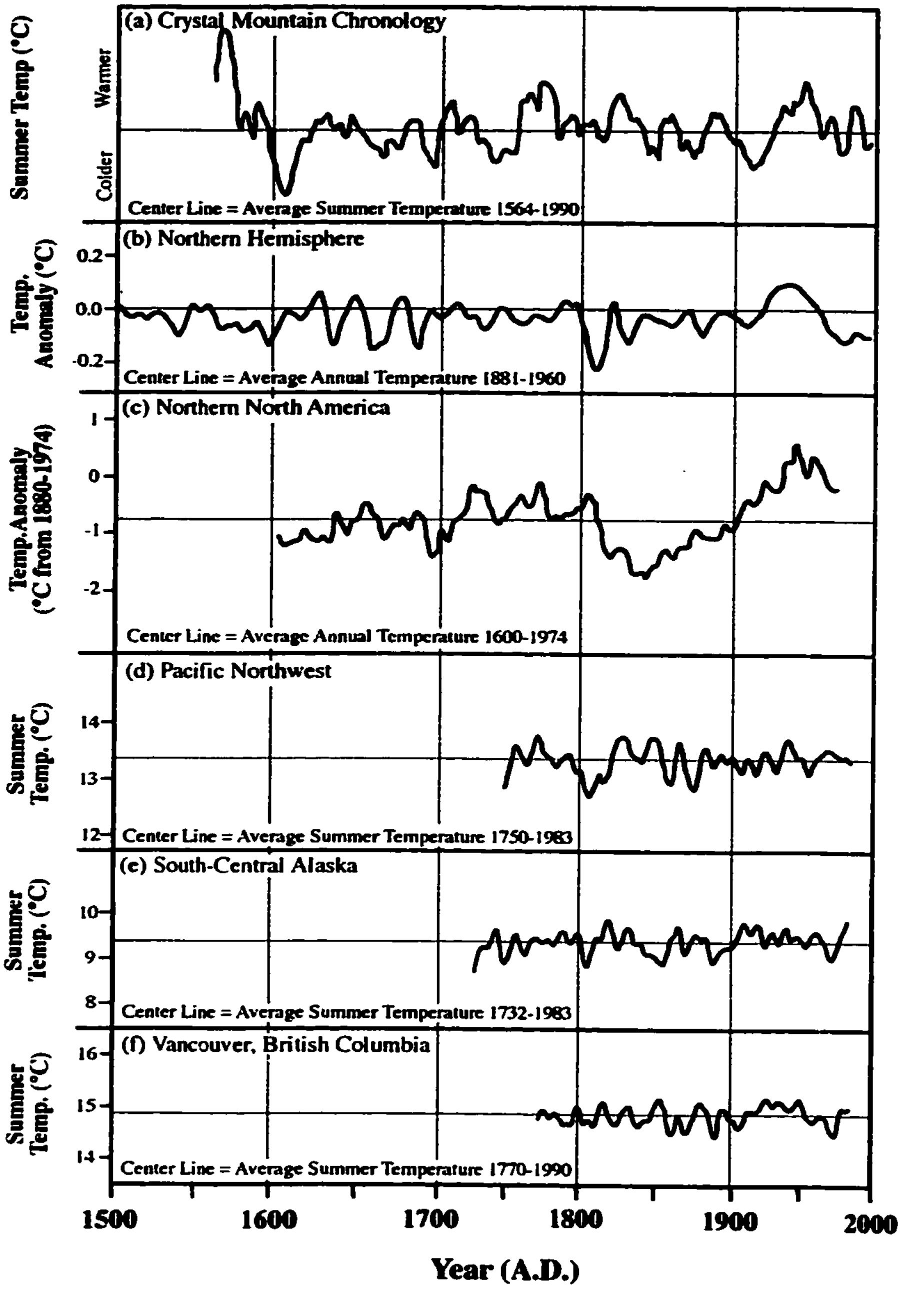

Figure 2.7 – Annual and summer temperature reconstructions based on dendrochronology (ring width and late wood density). Reconstructions are for (a) Crystal Mountain (this study), (b) the northern hemisphere (Briffa et al., 1998), (c) northern North America (D'Arrigo and Jacoby, 1993), (d) the Pacific Northwest (Wiles et al., 1996) (e) south-central Alaska (Wiles et al., 1996), and (f) Vancouver, British Columbia (Dobry and Klinka, 1998).

Table 2.1 – Weather station histories for southeastern Alaska.

City	Station ID	Latitude	Longitude	Elevation (m)	Oldest Records	Nearly continuous records since:
Ketchikan	KTH	55°22' N	131°43' W	23	1902	1910
Wrangell	WRG	56°29' N	132°22' W	13	1868	1917
Petersburg	PTG, PTG2	56°49' N	132°57' W	15	1925	1932
Sitka	SK	57°03' N	135°20' W	20	1828	1908
Juneau	JNU2	58°18' N	134°24' W	8	1888	1888
Haines	HNS	59°14' N	135°26' W	9	1925	1925

Table 2.2 – Correlation between temperature records from individual weather stations and the regional composite (SE Alaska) generated in this study.

	Wrangell	**Petersburg**	**Juneau**	**Ketchikan**	**Haines**	**Sitka**	**SE Alaska**
Wrangell	1	0.81	0.65	0.66	0.54	0.79	0.88
Petersburg		1	0.85	0.73	0.82	0.9	0.96
Juneau			1	0.67	0.86	0.74	0.91
Ketchikan				1	0.49	0.61	0.79
Haines					1	0.71	0.89
Sitka						1	0.91
SE Alaska							1

Table 2.3 – Correlation coefficients (r values) between the Crystal Mountain tree-ring chronology and instrumental (a) temperature and (b) precipitation data from 1899 to 1995. Each ring-width was correlated with monthly data for an 18-month period starting with June of the previous year (T-1) and extending throughout the growth year of the ring (T).

(a) Temperature vs. Ring Width

Correlation with:	Jan	Feb	Mar	Apr	May	Jun	Jul	Aug	Sep	Oct	Nov	Dec	Annual
Previous Year (T-1)						-0.01	-0.06	0.31	0.30	0.04	0.06	-0.07	
Growth Year (T)	0.04	0.18	0.05	0.10	0.23	0.44	0.19	0.21	0.20	0.06	-0.01	-0.06	0.22
Other Ranges	Jun-Sept 0.42		May-Sept 0.40		May-Aug 0.38		Jun-Aug 0.40		May-Jun 0.38		Jul-Sept 0.28		Feb-May 0.21

(b) Precipitation vs. Ring Width

Correlation with:	Jan	Feb	Mar	Apr	May	Jun	Jul	Aug	Sep	Oct	Nov	Dec	Annual
Previous Year (T-1)						0.15	0.02	-0.20	-0.11	0.14	0.01	-0.09	
Growth Year (T)	-0.10	0.01	0.04	0.07	-0.19	-0.18	-0.02	-0.04	-0.08	0.08	-0.03	-0.02	-0.05
Other Ranges	Jun-Sept -0.15		May-Sept -0.16		May-Aug -0.15		Jun-Aug -0.14						

Table 2.4 - Correlation equations between instrumental summer temperature values and CMC ring-width series for 1899-1947 and 1948-1995 and correlation coefficients between predicted and instrumental summer temperature values.

	Time Period		
	1899-1947	**1948-1995**	**1899-1995**
Regression Equation	(RW*1.021)+10.756	(RW*0.996)+10.875	(RW*1.012)+10.812
Based on data from:	1948-1995	1899-1947	1899-1995
r-value	0.51	0.30	0.42

RW = Normalized ring width from CMC

CHAPTER 3: STIKINE GLACIER CHRONOLOGIES

INTRODUCTION: HISTORICAL OBSERVATIONS AND PREVIOUS WORK

Although exploration of southeastern Alaska by Europeans was under way by the late 1700's, many of the early explorers did not successfully venture into the inlets of Frederick Sound. Therefore, records of exploration in the vicinity of the Stikine River are practically nonexistent until the mid- to late-1800's. In 1794, an exploring party from Vancouver's expedition, in search of the elusive Northwest Passage, approached the mouth of the Stikine River from the North. The ship's naturalist, Archibald Menzies, was one of the first Europeans to describe Frederick Sound;

> "Here they entered a spacious arm leading first eastward for a few leagues, and then winding to the southeast, and also becoming considerably contracted in its width and spacious appearance [Frederick Sound]. As they pursued their examination in this Arm against strong gales and unfavorable wet weather, its shores were found much indented with remarkable projecting points - bays and coves surrounded by a tract of low land forming a border of small extent, before a range of very lofty snowy mountain, which in one or two places approached the arm in overhanging precipices of vast height [Horn Cliffs], and when viewed from underneath of a singularly awful and terrific appearance, from the great quantity of ice and snow with which they were encumbered and which seemed to threaten instant destruction on those who approached the base of either of these precipices. After the party advanced in this arm about 10 or 11 leagues, they conceived it from all appearances to be closed up, at least so much so as not to merit any further examination; they therefore returned back along the opposite shore anxious now to make the best of their way for the Vessels." (Archibald Menzies from Olson and Thilenius (1993)[1])

Although Menzies did not mention the presence of glaciers in southern Frederick Sound, Lieutenant Joseph Whidbey of the same expedition observed LeConte Glacier before turning his longboat around and returning to the *Chatham* and *Discovery*. Vancouver

---

[1] Vancouver and Menzies, like many of the explorers who came after them, incorectly thought that south end of Frederick Sound was completely enclosed. However, this only appears to be the case due to the shallow Stikine River delta that nearly fills in the southern end of the sound. In fact there is a passage (Dry Straight) that connects Frederick Sound with Cross Sound to the south.)

(1798) summarized Whidbey's description, the first ever of LeConte Glacier, in the fourth volume of *A Voyage of Discovery* as follows:

> "Soon after passing this very remarkable promontory [Horn Cliffs], the arm of the sea over which it hangs appeared to be entirely closed by a beach, extending all round the head of it [Dry Straights]; at the south-east extremity was a large body of ice, formed in a gully between the mountains that approach the water-side, from whence, much broken ice seemed to have fallen, and had entirely covered the surface of the water in that direction. " (Vancouver, 1798).

The first detailed descriptions of Thomas Bay and LeConte Bay where recorded by John Muir (1893, 1915), during his 1869 and 1887 explorations of the glaciers of Alaska. Muir was the first to describe Baird Glacier and to illustrate the calving front of LeConte Glacier;

> "....after rounding a bluff cape opposite the mouth of the Wrangell Narrows, a fleet of icebergs came in sight, and of course I was eager to trace them to their source....The bergs were close packed almost throughout the whole extent of the fiord, but we managed to reach a point about two miles from the head - commanding a good view of the down-plunging lower end of the glacier and blue, jagged ice-wall. This was one of the most imposing first-class glaciers I had yet seen, and with its magnificent fiord formed a fine triumphant close for our season's ice work." (Muir, 1915)

Between 1886 and 1895, the U.S. Coast and Geodetic Survey (CDS, now NOAA) surveyed the coast of Alaska and made the first accurate maps of the coastline and glacier termini positions in Frederick Sound (U.S. Coast and Geodetic Survey, 1895). In 1887, Lieut. Commander Charles Mitchell Thomas, in command of the CGS Steamer *Patterson*, not only mapped the region but also left his mark by naming many of the geographic features. He officially recorded the name LeConte Glacier (Figure 3.1) after University of California geologist Joseph LeConte, replacing the native name, Hutli Glacier (meaning "The Thunder"), noted by Muir (1893, 1915) and Russell (1898).

Patterson Glacier (Figure 3.2) was named by W.H. Dall after the CDS survey ship (Figure 3.3), which in turn was named after Carlile Patterson, Superintendent of the Coast and Geodetic Survey from 1874 to 1881. (The CDS *Patterson* was built in 1882, and used for surveying Alaska waters from 1885 to 1917.) Baird Glacier (Figure 3.4) was named after Spencer Baird, former Secretary of the Smithsonian Museum and founder of the National Marine Fisheries Service.

Shakes Glacier (Figure 3.5) was mapped in 1893-4 (Field, 1975) and first appeared on the 1927 International Boundary Commission map (International Boundary Commission, 1952) incorrectly labeled as Popov Glacier. [Popov Glacier is a small hanging glacier located to the west of Shakes Glacier. Popov Glacier was first described, and named by a Russian Survey party exploring the Stikine River after their commanding officer, Admiral Popov of the imperial Russian navy (Blake, 1868).] Shakes Glacier is named after Chief Shakes, a prominent Tlingit chief who lived in Wrangell in the 19th century.

Preliminary research on Baird Glacier was conducted by Klotz (1895). Preliminary research on LeConte Glacier was conducted in the 1980's by Austin Post (personal communication, 1995), Paul Bowen of Petersberg Alaska (unpublished data), and a preliminary late Holocene history of LeConte Glacier was published by Post and Motyka (1995). In their recent studies, White et al. (1999), Motyka (1997), and Echelmeyer and Motyka (1997) concentrated on calving dynamics at the ice margin and the mass balance of LeConte Glacier. Patterson and Shakes glaciers were noted by Field (1975) but have not previously been studied in any detail. Basic information on the four major glaciers included in this study are summarized in Table 3.1.

METHODS

The terminus position of the outlet glaciers of the Stikine Icefield were poorly mapped until surveyed by the U.S. Coast and Geodetic Survey in 1887 (U.S. Coast and Geodetic Survey, 1895) and the International Boundary Commission in the early 20th century (International Boundary Commission, 1952). Therefore, understanding the extent and timing of glacier advance/retreat in the study area required detailed field mapping and high-precision dating of glacial sediments. The main glaciers included in this study are retreating (Patterson Glacier, Shakes Glacier, LeConte Glacier) or in a stable-extended position (Baird Glacier). Glacier retreat has recently exposed organic-rich sediments that were covered by ice for centuries, and bedrock, which, in most cases, has been rapidly colonized by vegetation (Figure 3.6). The former extent of the glaciers was determined by mapping terminal moraines, the extent of glacial sediments, and forest trimlines. Dendrochronology, radiocarbon dating, cosmogenic ^{36}Cl dating, and historical records were used to constrain the chronology of glacier advance throughout the middle to late Holocene.

Once determined, terminus fluctuations of land-based Patterson Glacier and ring-width records from high-altitude trees (Chapter 2) were used as a proxy for low-frequency late Holocene climatic variation, and compared to the advance/retreat history of LeConte Glacier, Baird Glacier, and Shakes Glacier during this time period (Chapter 4).

MAPPING HOLOCENE ICE MARGINS

Early– to middle–Neoglacial ice marginal positions were determined by mapping the distribution of ice-marginal sediments, end moraines, and submarine shoals. In addition, Little Ice Age maximum ice–marginal positions and 19th/20th century fluctuations were determined using trimlines and historical maps and photographs. The 1995 terminal positions are used as a reference point for all four glaciers because this is the last year in which they were accurately mapped in all glacier systems.

DATING METHODS

Dendrochronology

For the purpose of dating glacial deposits, tree cores were collected from more than 200 living and sub-fossil trees (collection, preparation, and analysis methods described in Chapter 2). Tree-ring ages described in the text are provided in Table 3.2.

Ring counts were from cores of living trees that were growing on recently deglaciated surfaces, and the oldest trees were used to estimate the timing of colonization. Previous research has shown that in temperate glacial environments it typically takes about 5 to 60 years for the first trees to colonize a deglaciated landscape and reach a coring height of 1 m (McCarthy and Luckman, 1993; Sigafoos and Hendricks, 1969), a period known as *ecesis*. Studies conducted by McCarty and Luckman (1993) on the best methods to identify ecesis concluded that 10 to 20 years was a good estimate for sites in the Canadian Rockies. This seems to be a reasonable estimate for southeastern Alaska as well, for excellent growing conditions facilitate the rapid growth of coastal rainforests. To confirm this ecesis period, trees growing in areas that where covered with ice this century were dated and compared to historical charts and photographs. The oldest trees growing near the Little Ice Age margin of Patterson Glacier (photographed in the 1890's) was dated at 1913 (Figure 3.28). On a rocky knob in front of LeConte Glacier, deglaciated between about 1930 and

1950, the oldest trees reached 1 m by 1953 (Figure 3.18). In both locations, the delay between late 19th– to 20th–century ice retreat and the appearance of trees occurred within one to two decades.

Two trees (a western hemlock and Sitka spruce) growing in a recent clear cut in Thomas Bay were slabbed and sampled at 30-cm intervals to test the ecesis period for the study region. By the time the trees started growing rings at coring height (1 m) they were 12 and 14 years old, respectively, supporting a minimum 10– to 20–year ecesis period. Therefore, 15 ± 5 years was added to deglaciation ages determined using ring counts from living trees.

The 425-yr tree-ring chronology established on Crystal Mountain and discussed in Chapter 2 (Figure 2.4) was also used to cross date sub-fossil tree samples from Patterson Glacier. Samples were cross dated using standard methods described by (Stokes and Smiley, 1968) and the analysis program COFETCHA (Holmes, 1983), as described in Chapter 2. This chronology was instrumental for understanding the glacial history of the Stikine area.

Radiocarbon Dating

Radiocarbon dating was used to date "sub-fossil" wood and shells derived from within and around glacial sediments, and for dating the basal organics of peat bogs established within the margins of the most extensive end moraines. These dates provide constraints on the timing of glacier advance and retreat in the four glacier systems for late Pleistocene time.

To ensure meaningful ages, only *in situ* samples were collected for radiocarbon analysis. Basal peat ages were obtained from peat bogs overlying glacial sediments and/or impounded by glacial landforms. Cores typically consisted of 0.5 to 2 m of peat deposited on organic-poor silty sands. Samples for radiocarbon dating consisted of wood fragments collected just above the lower silty-sandy layer at the base of the core. Conventional beta radiocarbon dating was conducted at the Quaternary Isotope Lab at the University of Washington. Accelerator mass spectrometry (AMS) dating of samples that were too small for conventional dating was completed at the Center for Accelerator Mass Spectrometry (CAMS) at Lawrence Livermore National Laboratory.

To compare accurately the ages derived using different dating methods, radiocarbon dates were calibrated to calendar years using Calib 3.0.3 (Stuiver and Reimer, 1993) and are reported as calibrated years ("years"). Tables 3.3 to 3.6 list ^{14}C and calibrated ages of samples referenced in the text, including previously published dates that were calibrated for use in this study. These ages are referred to as radiocarbon years ("^{14}C years") and reported in the text as calibrated years.

After calibration, radiocarbon dates of shells were corrected for the marine ^{14}C reservoir effect by subtracting 925 years from the calibrated ages. Southen et al. (1990) calculated a reservoir effect for the Queen Charlotte Islands of 800 ^{14}C years by radiocarbon dating more than 40 shell/wood pairs. It is here assumed that the ocean water in the Alaskan archipelago farther north is chemically similar to that in the Queen Charlotte's. To improve the accuracy of the reservoir correction for this study, Southen et al.'s (1990) radiocarbon ages were calibrated using Calib (Stuiver and Reimer, 1993) and the reservoir effect was recalculated to be 925 calendar years (Table 3.3). By applying the reservoir correction after the radiocarbon calibration, it is possible to derive a more accurate calendar age.

The reservoir effect for the waters around the Queen Charlotte Islands remained relatively constant throughout the Holocene (mean values from 775 to 1,032 years, a range of 257 years). Alternatively, Southen et al.'s (1990) uncalibrated correction spans a range of 508 ^{14}C years (from mean values of 671 ± 92 to 1,179 ± 113 ^{14}C years) for the same period of time.

Cosmogenic Isotope Surface–Exposure Dating

Cosmogenic ^{36}Cl surface-exposure dating was used to determine the deglaciation ages of exposed glacial erratics on Neoglacial end moraines and late Pleistocene bedrock surfaces. ^{36}Cl is produced in rocks near the Earth's surface by cosmic-ray-induced spallation reactions of ^{39}K and ^{40}Ca, neutron activation of ^{35}Cl, and muon capture by ^{40}Ca and ^{39}K. In terrestrial rocks exposed at the surface of the Earth, cosmic-ray-induced spallation and neutron activation reactions produce almost all of the ^{36}Cl. ^{36}Cl is radioactive and has a half-live of about 3.01 x 10^5 yr. Therefore, the presence of ^{36}Cl in terrestrial rocks is a function of its production and decay rate over the time in which the surface has been exposed to the cosmic flux. ^{36}Cl surface-exposure dating has been successfully used to date late Pleistocene and Holocene geomorphic surfaces exposed by glacier retreat (Briner and Swanson, 2001; Phillips et al., 1996; Swanson and Caffee, 2001).

Rock samples were collected from the upper 1 to 2 cm of boulders and bedrock surfaces in order to minimize scaling depth-dependencies associated with ^{36}Cl production (Liu et al., 1994). Sample sites were limited to relatively flat surfaces (dip angles < 10°), and to stable boulders with a diameter of ≥ 2 m in order to minimize the effects of cosmic ray shielding and boulder reorientation. It is assumed that bedrock surfaces have experienced little or no erosion since the time of original exposure during Late Pleistocene-Holocene time. This assumption is supported by the presence of polished and striated surfaces preserved in the sampling areas.

Standard X-Ray fluorescence (XRF) spectrometry was performed on rock samples by XRAL laboratories (Don Mills, Ontario, Canada). Major elemental analysis had an analytical uncertainty of < 2% and a detection limit of 0.01% (detection limit for boron, gadolinium, uranium, and thorium was 0.5 ppm). Total chlorine analysis was performed in the Quaternary Isotope Laboratory (University of Washington) using modified procedures discussed by Aruscavage and Campbell (1983). Three to six replicates of each sample were run to minimize analytical uncertainty (<5%). Chloride was extracted for accelerator mass spectrometry measurement in the Quaternary Isotope Laboratory (University of Washington) using methods described by Swanson (1994). Samples ^{36}Cl/Cl ratios were determined by accelerator mass spectrometry (AMS) in CAMS at Lawrence Livermore National Laboratory. AMS measurements of samples from late Pleistocene deglaciated surfaces typically have analytical uncertainties of 2 to 5%. Samples collected from Neoglacial moraines generally have large analytical uncertainties (10 to 20%) because of short exposure time and low ^{36}Cl concentrations. Despite the large error, these data are useful for discriminating late Holocene from late Pleistocene moraines and are consistent with radiocarbon ages that provide limiting ages for the glacial deposits.

^{36}Cl ages (Table 3.6) where calculated using the computer spreadsheet program CHLOE (Phillips and Plummer, 1996). The production rates of Swanson and Caffee (2001) were used to solve for ^{36}Cl ages because their production rates were calibrated at moderately high geomagnetic latitudes (48°N) on late-Pleistocene samples obtained near sea level. Because paleomagnetic field intensity scaling is minor for latitudes greater than 50°, it is expected that Swanson and Caffee's (2001) ^{36}Cl production rates should be similar to those in southeastern Alaska (latitudes ca. 58°N). Briner and Swanson (2001) used these rates to calculate surface exposure ages in southwestern Alaska and found them to be consistent with corresponding radiocarbon ages. Because snow cover can also effect the calculated exposure age of a rock surface, ^{36}Cl ages were calculated using a snow cover scaling factor that assumed samples were covered with 10 to 300 cm of snow from November to June. Errors were calculated from percent AMS analytical uncertainty.

Although striations and glacial polish are preserved on many surfaces, some erosion likely has occurred during the Holocene. Therefore, Table 3.6 lists calculated ages for 1 mm/ 10^3 yr of erosion, as well as for no erosion. Even when an erosion rate of 1 mm/10^3 yr is taken into account, age differences are typically very small (<2%). ^{36}Cl ages in the text are reported for erosion rates of 1.0 mm/yr.

LATE PLEISTOCENE DEGLACIATION

During the peak of the last glaciation (marine isotope stage (MIS) 2) along the western Cordillera (ca. 23,000-17,000 years ago; Figure 2.1), most of the coast of southeastern Alaska was covered by the Cordilleran Ice Sheet, which likely extended to the edge of the continental shelf. In the study area, the timing of late Pleistocene deglaciation is controlled by two radiocarbon ages and nine ^{36}Cl ages. A radiocarbon sample (SCAN-3), collected from an excavation in downtown Petersburg, ca. 10 m above high tide (Figure 3.6), consists of a complete mussel shell embedded in an uplifted glacialmarine silt, 135 cm below a gravel beach lag (Figure 3.8). A second sample (TBS-95), a small shell from an uplifted glacialmarine deposit excavated by Spurt Lake Creek in Thomas Bay, was found ca. 6 km in front of Baird Glacier (Figures 3.6 and 3.9). These samples have calibrated ages of 15,990-15,726 years (13,280 ± 60 ^{14}C years) and 15,083-14,715 years (12,670 ± 60 ^{14}C years), respectively (Table 3.4). After applying a marine reservoir correction of 925 years, these data suggest that the coast of southeastern Alaska was deglaciated by approximately 15,000 years ago and that Baird Glacier had retreated to within at least 6 km of its present position by 14,000 years ago (Table 3.4).

To constrain the age of deglaciation in the region further, rock samples were collected from abraded bedrock and two boulders near the summit of Crystal Mountain (at the southwestern end of Mitkov Island, about 800 m above sea level) for ^{36}Cl dating (Figure 3.6 and 3.10). These samples range in age from 14,510 to 8,390 years (Table 3.6; XTAL 1-7, SR 2-3), and have a mean age of 11,300 years. The two outlying dates are both for boulders, and if they are rejected, the exposure ages of the remaining samples fall between 13,200 and 9,300 years ago (Table 3.6) and have an average value around 11,300 years ago. These data suggest that highlands of Mitkov Island were free of ice by about 11,300 years ago. There is no geologic or historical evidence to suggest that any cirque glaciers existed on Crystal Mountain during the Holocene. According to Vancouver (1798), no large glaciers existed on the islands during the late phase of the Little Ice Age (late 18th century);

> "Mr. Whidbey observes, that in no one instance during his researches, either in the several branches of Prince William's sound, in those extending from Cross sound, or, in the course of his present excursion, did he find any immense bodies of ice on the islands; all those which he had seen on shore, were in the gullies or vallies of the connected chain of lofty mountains so frequently mentioned, and which chiefly constituted the continental shore from Cook's inlet to this station; though, in different places these mountains are at different distances from the sea side." (Vancouver, 1798 p. 1380)

Ages for deglaciation from this study are in good agreement with other ages for deglaciation of the Alaskan panhandle (Table 3.4; Figure 3.11). To the south, on Prince of Wales Island, the oldest dates for deglaciation are from bones of brown bear from Eldorado Cave dated at 14,586-14,165 years (Heaton et al., 1996). The oldest shells in the Gastineau Channel Formation, a glacialmarine unit near Juneau that is similar to glacialmarine drift in Frederick Sound, have ages of 14,390-11,916 years (Miller, 1973). Basal dates from pollen cores adjacent to Montana Creek and Lemon Creek suggest that the Juneau area was ice-free by 12,636-11,004 years ago (Heusser, 1960) and 12,826-10,952 years ago (Heusser and Marcus, 1964), respectively. McKenzie and Goldthwait (1971) report that glaciers in Glacier Bay were retreating by 16,251-15,360 years ago, at which time glacialmarine sediments were deposited. A log from a lateral moraine of Finger Glacier indicates that glaciers in the Lituya Bay area retreated sometime after 14,760-14,350 years ago (Mann, 1986b).

Farther west, Bering Glacier had retreated off the continental shelf by 17,320-15,287 years ago (Sirkin and Tuthill, 1971) and coastline in the Icy Bay area was free of ice by 13,151-12,292 years ago (Heusser, 1960). Basal peat ages indicate that the northern region of Prince William Sound was deglaciated by 11,850-11,002 years ago (Heusser, 1983a). Basal peat from near the bottom of a core on the Kenai Peninsula places the age of deglaciation before 16,625-16,293 years ago (Ager, 1983). Hamilton and Thorson's (1983) summary indicates that the Cook Inlet area was ice-free by ca. 16,000 (ca. 13,500 ^{14}C years ago).

The southwestern margin of the Cordilleran Ice Sheet, which was grounded below present sea level, was also retreating at that time. In Puget Sound, ice reached a maximum limit by 17,000 years ago and had retreated north of Seattle by 16,600 years ago (Porter and Swanson, 1998). Basal peat from the northeast end of Vancouver Island at Port Hardy indicates that the region was ice-free by 16,630-15,906 years ago (Hebda, 1983).

Deglaciation was approximately synchronous around the northwest coast of North America, with retreat off the shelf starting ca. 17,000-16,000 years ago and proceeding to uncover inlets and fjords by 15,000 to 14,000 years ago. Rapid and synchronous retreat of the ice margin at that time was in part the result of rising sea level, which would have increased the depth of tidewater at the ice margins and dramatically increased the rate of ice calving. Coral records from Barbados show that sea-level rose (Figure 3.12) rapidly between 16,000 and 14,000 years ago, rising more than 30 m between 15,000 and 14,000 years ago (Bard et al., 1990).

No evidence was found in the Petersburg area to suggest that a late-glacial readvance of coastal glaciers occurred after 15,000 years ago. However, such evidence could have been removed during more extensive Holocene glacier advances. Miller (1973) suggested that glaciers in the Juneau area may have readvanced sometime between 15,000 and 10,000 years ago.

NEOGLACIAL CHRONOLOGIES

Evidence for two to three Neoglacial advances exists along the southwestern margin of the Stikine Icefield. No evidence was found for early to middle Holocene advances. However, evidence for these earlier episodes may have been eroded or buried by more recent ice advances. The earliest Neoglacial advance for which there is evidence occurred between 4,000 and 3,000 years ago in at least two of the glacier systems. Advanced positions also were reached between 2,700 and 2,200 years ago, and 1,100 and 900 years ago. Evidence for the most recent advance, which occurred during the Little Ice Age, is found in three of the four glacier systems. To avoid confusion and make it easier to compare ^{14}C ages with tree ring ages (Table 3.2), radiocarbon ages are reported in calibrated radiocarbon years (Table 3.5).

SHAKES GLACIER

Early to Middle Neoglaciation

Evidence suggests that Shakes Glacier expanded two or three times during the late Holocene. Two large moraines (Figures 3.13 and 3.14) mark the furthest late Holocene extent of the glacier along the banks of the Stikine River. A third moraine, which dams the mouth of Shakes Lake, marks the Little Ice Age maximum of Shakes Glacier (Figure 3.13).

Tlinget oral tradition tells how the people came to the coast, from interior British Columbia, by traveling underneath a glacier that blocked the valley they had been following for a long time (Willard, 1995). Since the Stikine River is one of two or three major valleys that cross the Coast Mountains, and was used as a major highway by Tlinget people (Emmons, 1991), it is possible that the story originated when a glacier blocked the Stikine River. Although Shakes Glacier is one of the major glaciers near the mouth of the river, and the presence of moraines indicates that it has reached the Stikine River in the past, no physical evidence was found in the Stikine River valley to suggest that Shakes Glacier ever dammed the river. Such a damming likely would require a more positive mass balance than any glacier on the lower Stikine River has possessed during the Holocene in order to compensate for the volume of ice lost to undercutting and erosion by the rapidly flowing river. The Taku Glacier, flowing off the Juneau Ice field to the north, is known to have dammed the Taku River in the eighteenth century (Lawrence, 1950; Post and Motyka, 1995). However, the Taku River is smaller than the Stikine, and Taku Glacier has a much higher accumulation area ratio (AAR = 0.88) than the Shakes Glacier or any other glacier on the Stikine River (Viens, 1995).

The late Holocene maximum position of Shakes Glacier is marked by two moraines located at the confluence of Shakes Slough and the Stikine River. These moraines may represent two separate advances of Shakes Glacier or, if they are a single moraine complex, one advance. The oldest trees on the outermost moraine (SM-9 and SM-26; Table 3.2; Figure

3.13) started growing in 1689 ± 5 and 1698 ± 5 A.D. A peat core collected between the two moraines had a calibrated basal age of 1547-1663 A.D (sample SM-PB-80; Table 3.5). However, living trees cored upvalley from the moraine (Sk-6 and SL-16; Table 3.2; Figure 3.13) began growing by 1553 ± 5 and 1558 ± 5 A.D. These limiting ages restrict the formation of both moraines to the early 16th century or before. There are no data to provide a maximum limiting age on one or both moraines. Because evidence of early Little Ice Age advances (12th-16th centuries) has not been reported for other glaciers in this region and because they are found so far in advance of the 18th century moraines, these moraines are likely older than the early Little Ice Age. However, more fieldwork is required to constrain the age Shakes Glacier's late Holocene maximum more closely.

Late Neoglaciation: Little Ice Age

The late phase Little ice Age position of Shakes Glacier is marked by a terminal moraine located at the outlet of Shakes Lake, 7.3 km beyond the position of the 1995 glacier terminus (Figure 3.13). The moraine dams the lake and creates a hazard to boats navigating the lake outlet. The time of the Little Ice Age advance of Shakes Glacier is poorly known. A wood sample collected from outwash in a side valley 1.3 km beyond the 1995 ice margin dates between 1678 and 1950 A.D. (SL-3; Table 3.5; Figure 3.13). The oldest trees growing just inside the Little Ice Age moraine (SL-1, SK-2; Table 3.2; Figure 3.13) began growing in 1782 ± 5 and 1806 ± 5 A.D. These dates imply that the wood samples found 1.3 km from the ice front most likely died between 1678 and 1780 A.D. Furthermore, it probably would have taken a decade or more for the glacier to advance an additional 6 km to it's Little Ice Age maximum, so it is likely that the glacier advanced during the middle to late 17th century. This advance would require a minimum advance rate of ca. 60 m/yr, which is reasonable for a lake-calving glacier terminus (Viens, 1995).

Based on the dendrochronological evidence discussed above, the post-Little Ice Age retreat of Shakes Glacier began by ca. 1780 A.D. The glacier continued to retreat for the next two centuries at an average rate of 34 m/yr. Historical positions of the glacier front, however, show that the retreat of the terminus was not constant (Figures 3.13 and 3.17).

The first recorded position of the Shakes Glacier terminus appeared on the International Boundary Commission's 1927 map (International Boundary Commision, 1927), which was surveyed between 1904 and 1909 (Figure 3.15). This map shows the terminus 1.8

km upvalley from the Little Ice Age limit. There are no records that indicate the position of the terminus during the intervening time period; however, trees growing behind the moraine and within 500 m of it are 150 to 200 years old, indicating that the glacier did not readvance into this region. Furthermore, limited depth soundings in the lake (the bathymetry has never been mapped) do not indicate the presence of any significant shoals in the lake. Therefore, the glacier may have retreated slowly during the 19th century.

Continuous retreat of the glacier during the 20th century has been documented by aerial photographs dating to the late 1950's (Figure 3.13 and 3.16). The terminus continued to retreat slowly (average of 14 m/yr) until ca. 1960 when it entered a significantly wider section of Shakes Lake. Since that time, retreat has been rapid (average of 137 m/yr), and the terminus has retreated approximately 5 km upvalley, exposing upper Shakes Lake (Figure 3.17). Retreat during this period was intermittent, occurring mainly during years when massive tabular bergs calved off the terminus. Between years of significant retreat the terminus maintained a state of quasi-stability.

The gentle profile of the tongue of Shakes Glacier makes it appear as a floating "shelf" (Figure 3.16). Periodically enormous tabular bergs calve off the terminus, and in this manner the glacier seems to retreat in steps. The glacier has remained relatively stable for the last 5 years; however, there is no indication that the glacier front is approaching the head of the lake, and so retreat is expected to continue.

LECONTE GLACIER

Early to Middle Neoglaciation

LeConte Glacier terminates at the head of LeConte Bay, a 24-km long fjord with a large moraine complex at its mouth (Figure 3.18a). It is difficult to determine whether the morainal shoal is a single moraine or a compound moraine because it merges with the Stikine River delta, which fills Dry Strait and the southern part of Frederick Sound. Large boulders exposed at low tide, however, leave no doubt as to the glacial origin of the shallow shoal at the southern mouth of the LeConte Bay. Stratigraphic evidence, derived from the "Cabin Creek" valley (unofficial name), located ca. 9.5 km from the 1995 ice limit, indicates that LeConte Glacier blocked the valley at least three times during the middle to late Holocene. At least one advance is believed to have reached the fjord mouth. A second, middle- to late-Neoglacial advance reached the vicinity of Cabin Creek and fluctuated around this position, impounding Cabin Creek at least twice, before reaching its Little Ice Age maximum limit in the 18th century (Figure 3.18a).

The first Holocene advance of LeConte Glacier beyond Cabin Creek occurred between ca. 4,300 and 3,200 years ago and reached the mouth of LeConte Bay. These constraining dates are based on two stratigraphic sections exposed along the west and east forks of Cabin Creek. The exposure in the west fork of Cabin Creek (Figure 3.19) consists of till, overlain by clay and deltaic sand. A peat unit on top of the sand contains wood (CC-4) that is 3,320 (3,214) 3,167 years old (Table 3.5; Figure 3.18b). This outcrop likely represents a retreat sequence, which formed as a lobe of LeConte Glacier retreated from the valley leaving till, then impounded Cabin Creek to form an ice-marginal lake. The coarsening upwards sequence in the section represents shallowing of the lake and the influx of deltaic sands. Because it is found just above the post-retreat ice-marginal lake sediments, the wood places a minimum age limit on the damming of Cabin Creek by LeConte Glacier.

The section in the east fork of Cabin Creek (Figure 3.20) provides a maximum limiting age on the damming of Cabin Creek. This section apparently lacks a till, displaying only interbedded clay, peat and sand covered by coarse sand and gravel. Near the base of the section is a wood-bearing clayey peat that likely represents forest colluvium. The sediments above this unit are interpreted to be glacial lacustrine deposits formed by the inpoundment of Cabin Creek by LeConte Glacier. Approximately 15 cm above the peat unit is an 8-cm-diameter log dated at 4,343 (4,238) 4,155 years (CC-15; Table 3.5; Figure 3.18b). This site was likely covered by an ice-marginal lake in the middle Holocene and the alternating layers of clay, silt, and sand are interpreted to represent fluctuations in the level of the lake. After the lake drained the section was covered by postglacial stream gravels. The wood date from the base of the outcrop provides a maximum limiting age for inundation at ca. 4,300 years. A living tree cored near this outcrop began growing in 1341 A.D. (CC-26; Table 3.2 and Figure 3.18b) indicating that the valley has not been inundated since at least the 14th century. The glacial lacustrine sediments in the east fork of Cabin Creek are interpreted to be contemporary with the till in the west fork (Figure 3.23). The east fork outcrop is less than 50 m higher than the west fork outcrop, implying that the ice in Cabin Creek terminated at an elevation somewhere between those of the two localities.

Tidewater calving glaciers commonly advance on a morainal shoal that helps stabilize the glacier terminus. Once the retreat cycle of these glaciers begins, the shoal is abandoned and the ice retreats until ice flux reaches equilibrium with iceberg calving at the terminus. In order for ice to reach the west fork Cabin Creek site, LeConte Glacier must have advanced beyond the limit of the Thunder Point Moraine (described below). The only other shoal downvalley from this moraine is the one located at the entrance to LeConte Bay (Figure 3.18a). Therefore, it is likely that LeConte Glacier extended to the mouth of the bay sometime between the constraints set by the radiocarbon ages (ca. 4,300 and 3,200 years ago). Because the advance cycle of tidewater calving glaciers typically is an order of magnitude longer than the retreat cycle (Viens, 1995), it is likely that during much of the time Cabin Creek was inundated the glacier was in the advance stage of the tidewater calving glacier cycle. Once retreat off of the morainal shoal brgan, the retreat phase would have been rapid. If we assume an order-of-magnitude difference in the advance and retreat rate, and also consider the post-Little Ice Age retreat rate of 56 m/yr (described below), it is possible that retreat of LeConte Glacier from its late Holocene maximum position occurred about 3,500 to 3,300 years ago. No evidence was found to indicate how far the terminus retreated upvalley.

Based on the south and north sections of a cutbank exposed along the lower reaches of Cabin Creek (Figures 3.18b, 3.21 and 3.22), the second Holocene ice advance in LeConte Bay dammed Cabin Creek intermittently starting ca. 2,150 years ago. The basal unit in the south section (Figure 3.21) is likely old forest litter containing a log with a 2,147 (2,138) 2,117 yr-old date near its top (CC-7; Table 3.5; Figure 3.18b). Directly above this unit is glacial lacustrine silt capped with a second layer of colluvium. Above the second colluvial unit the sloping section was covered by modern colluvium for almost 2 m. The base of the northern section (Figure 3.22) also is covered by colluvium. It is interpreted that the two sections correlate with one another in this unexposed region, so that the northern section rests stratigraphically above the lower units of the southern section (Figure 3.23). The northern section consists of a 3-m-thick unit that grades up from sand to sand mixed with coarse gravel. In the middle of this unit (near the base of the gravel) is a log dated at 1,223 (1,161) 1,064 years old (CC-11, most likely Sitka spruce; Table 3.5; Figure 3.18b). This unit grades up into sands and is capped with silty clay. Silty clay is also found at the top of the southern section (Figure 3.23). These two sections together are interpreted as representing a time during which the terminus of LeConte Glacier fluctuated around the mouth of Cabin Creek. The lower wood provides a maximum limiting age of inpoundment of the valley; however, the wood is covered by a second colluvial layer, implying that the glacier front receded, exposing the valley. The ice again impounded the valley, this time reaching far enough upvalley to deposit outwash that coarsened as the ice front advanced. Radiocarbon sample CC-11 was found near the base of the coarsest outwash; therefore, it likely provides a close limiting age for an ice-maximum position about 1,100 years ago. Deltaic sands and silts above these gravels imply a receding ice front after this time.

Because no till is exposed in the lower Cabin Creek outcrops, and no stratigraphic evidence for these advances was found in the upper sections of Cabin Creek (Figures 3.19 and 3.20), LeConte Glacier likely did not extend far beyond the entrance to Cabin Creek during this phase of advance. Furthermore, the lack of another morainal shoal between the Little Ice Age maximum and the fjord mouth (Figure 3.24) implies that this advance did not extend beyond the Thunder Point Moraine. Therefore, it is inferred that LeConte Glacier terminated between the mouth of Cabin Creek and the Thunder Point Moraine.

Although a decrease in grain size near the top of the section implies that the Cabin Creek lobe of LeConte Glacier receded after 1,100 years ago, the ice margin apparently did not retreat far upvalley. In fact, LeConte Glacier likely remained in the vicinity of Cabin Creek until reaching its Little Ice Age maximum in the 18th century (described below).

Late Neoglaciation: Little Ice Age

The Little Ice Age maximum position of LeConte Glacier is marked by a shallow morainal shoal (50 m deep) located offshore from Thunder Point, 11 km in front of the 1995 terminus position (Figure 3.18). Post and Motyka (1995) refered to this shoal as the "Thunder Point Moraine" (TPM). The shoal separates the relatively shallow (ca. 130 m), sediment-laden outer bay from the much deeper (>300 m), relatively sediment-free inner bay (Post and Motyka, 1995; Figure 3.24). Radiocarbon and dendrochronological evidence suggests that LeConte Glacier reached the moraine by at least the 15th century and began to retreat by the mid-18th century.

Post and Motyka (1995) collected a wood sample from lower Cabin Creek that, once calibrated, limits the Little Ice Age maximum position to after 1262-1433 A.D. (GX-9387; Table 3.5; Figure 3.18b). This sample was collected 1 m below the top of a delta (6 m altitude) built in a ice-marginal lake that formed when LeConte Glacier dammed Cabin Creek (Austin Post, personal communication 1995). The mouth of Cabin Creek is located 1.5 km upvalley from the morainal shoal. Therefore, the glacier was back to within 1.5 km of its Little Ice Age limit by at least the early 15th century, and possibly by the 13th century.

The oldest tree growing behind the TPM (TP-5) began growing in 1786 ± 5 A.D. (the oldest trees just downvalley from the shoal are > 350 years old; MC-1 and BC-12). Based on this evidence, it is believed that LeConte Glacier began to retreat off its Little Ice Age moraine about 1780 A.D. Once the terminus retreated into water that deepened as the ice front receded, the glacier entered a calving-retreat phase. Based on a few tree cores from lower Cabin Creek and by extrapolating the 20th-century retreat rate back in time, Post and Motyka (1995) deduced that the glacier retreated off the TPM in ca. 1800 A.D., which is in good agreement with results from this study.

Dedrochronological evidence and historical maps and photographs document retreat since the late 18th century (Figure 3.18a). Initial tree growth near lower Cabin Creek placed the glacier 1.5 km from the TPM by 1800 A.D. (MC-13, CC-15, CC-21, WP-4). By 1887, when the glacier terminus was mapped by the Coast and Geodetic Survey (1895), the glacier was 5.5 km from the TPM (Figure 3.25). Between 1904 and 1913, when it was mapped by the International Boundary Commission (1952), the terminus was ca. 500 m farther upvalley (Figure 3.15). After retreating another 5.5 km, the glacier terminus stabilized in 1963 in water more than 100 m deep. The high AAR of the glacier (0.90 in 1995; Viens, 1995) allowed the glacier to maintain it's position, even though it was calving at an extremely rapid rate (often filling the bay with bergs). For the next 32 years the terminus fluctuated seasonally by ca. 500 m (Paul Bowen, unpublished data).

After remaining relatively stable for more than 32 years, LeConte Glacier again began to retreat in early 1995 (Figure 3.26). Between 1995 and 1999 the glacier receded an additional 1.5 km (White et al., 1999) and continues to retreat today. Echelmeyer and Motyka (1997) used airborne laser profiles and 1948 USGS topographic maps to determine the change in ice thickness along the entire length of LeConte Glacier. They attributed the latest retreat to an average thinning of 30 m over the entire accumulation area between 1948 and 1996.

The average retreat rate for LeConte Glacier between 1780 and 1963 A.D. was 56 m/yr (Figure 3.27), significantly slower than the average rate of tidewater glacier retreat (Viens, 1995). However, the high AAR of the glacier, as well as the narrow and sinuous nature of the fjord probably have allowed the glacier to maintain a high calving rate, and lateral constrictions have helped stabilize the terminus. These factors support a model of sporadic ice-front recession over the last two centuries, with periods of rapid retreat followed by intervals of relative stability.

PATTERSON GLACIER

Early to Middle Neoglaciation

Stratigraphic evidence indicates that Patterson Glacier advanced at least once before reaching its Little Ice Age maximum (Figure 3.28). Garnet Creek (unofficial name), which flows into Patterson Lake about 500 m from the 1995 limit of Patterson Glacier, has excavated a 12-m-high cutbank that exposes two layers of till (Figure 3.29a). The lower unit is a 7.5-m-thick compact basal till that contains large logs. One log was sampled (GCW-1) and outer rings dated at 3,341 (3,255) 3,168 years ago (Table 3.5; Figure 3.28). The upper till is believed to be an ablation till deposited during the LIA retreat. The log date provides a maximum limiting age for the pre-Little Ice Age advance of Patterson Glacier of ca. 3,250 years ago. No minimum limiting age is available for the lower till; however, an unconformity between the upper and lower tills in Garnet Creek is marked by a weak soil and >200-year-old tree stumps rooted in place (Figure 3.29b). These trees were not radiocarbon-dated, although they are thought to correlate with the buried forest 1 km down the Patterson River valley, which were killed in the 18th century by the Little Ice Age advance of the glacier. Because the soil here is poorly developed, Patterson Glacier likely remained beyond this position for most of the last 3,000 years, excluding the brief interval during the 16th to 18th centuries when the trees were growing.

Late Neoglaciation: Little Ice Age

The Little ice Age limit of Patterson Glacier is located 4.5 km beyond the 1995 limit of the glacier terminus (Figure 3.28). Although this limit is not marked by an obvious moraine, it was documented on a 1890's photograph (Figure 3.30), which shows the glacier terminus fronted by a mature forest.

The Little Ice Age advance of Patterson Glacier is dated by several *in situ* stumps that are now eroding out of drift. As discussed above, sheared stumps (most likely Sitka spruce) are rooted in till 500 m in front of the 1995 terminus (Figure 3.29b). These stumps were not dated; however, the paleosol below the stumps is not very well developed. An approximate ring count indicates that the stumps are >200 years old.

Similar stumps were found 2.4 km in front of the 1995 terminus eroding out of outwash (Figure 3.32). Although the stumps have been exposed for almost 40 years, it was possible to collect at least one intact cross section (sample BF-3). A radiocarbon date of the outer rings of this sample is equivalent to a calibrated age range of 1529 to 1950 A.D. (Table 3.2). To limit the time of death for the stump more closely, ring widths were measured and the sample was cross dated with the master tree-ring chronology established on Crystal Mountain (CMC). The CMC spans all but the first 25 years of the calibrated age of sample BF-1; thus although the correlation likely is meaningful, there is a small chance that the tree age falls outside the range of the dating method. COFETCHA (Holmes, 1983) provided two possible correlations for the outer ring during the span of the CMC: 1792 A.D. ($r = 0.38$) and 1859 A.D. ($r = 0.32$). Both kill-dates are possible, but the older date is more likely. The younger date, which has a slightly lower correlation coefficient, would require that the glacier advance >2 km in about 30 to 35 years. Although not impossible, the slower advance rate of 20 m/yr, implied by the older date, seems more realistic. These trees were more than 200 years old, implying that forests were growing in this part of the valley since at least the last half of the 16th century.

An historical photo (Figure 3.30) of the glacier shows that the terminus advanced to a Little Ice Age maximum position 4.5 km in front of the 1995 terminus by the 1890s. The photo shows the glacier advancing into a mature forest. The 1891 Alaska Coast Pilot (United States Coast and Geodetic Survey, 1891, p.136) supported the evidence from the photograph when it stated that the glacier was "undoubtedly still advancing, as will be readily seen by the destruction of trees from the gradual encroachment of the face of the glacier". The position of the terminus in the late 19th century is further supported by the U.S. Coast and Geodetic Survey (1895) and International Boundary Commission (1952) maps (Figures 3.25 and 3.31) surveyed in 1887 and 1904/9. Throughout the valley a distinctive trimline can be traced to the 1890s ice limit. Trees growing outside of this trimline starting growing prior to 1240 ± 5 A.D. (PR-19; Table 3.2; Figure 3.28), indicating the the 1890's ice limit of Patterson Glacier marks the most extensive advance of the Little Ice Age.

Trees cored inside the maximum ice limit shown on the photograph began growing in 1898 ± 5 A.D. (PM-6), indicating that the glacier began its retreat in the late 1890's, shortly after the photograph was taken (Figure 3.28). Trees cored between the 1890s and 1965 terminus positions imply the ice front retreated at a more-or-less steady rate during that time, averaging 25 m/yr (PR-4 and PR-9; Table 3.2; Figures 3.28 and 3.33). Photographic data indicate that the average retreat increased to ca. 74 m/yr between 1965 and 1995 when Patterson Lake began to form at the terminus and the glacier lost additional ice through freshwater calving. In recent years the glacier has continued its steady retreat and also has been thinning.

BAIRD GLACIER

Early to Middle Neoglaciation

The early Neoglacial history of Baird Glacier is based on stratigraphic evidence in the outlet channel of Spurt Lake, as well as basal peat ages and ^{36}Cl surface exposure ages from Point Agassiz Peninsula and Vanderput Point (Figure 3.34). This evidence suggests that Baird Glacier expanded beyond its modern position at least once, and possibly twice, during the Holocene.

Wood fragments in glacial lacustrine sediments (TBW-2; Table 3.5 and Figure 3.34) above till in Spurt Lake Creek (Figure 3.35) provide a minimum limiting age of 2,316 (2,301, 2,237, 2,199) 2,152 years ago for at least one Holocene advance in of Baird Glacier. This age is consistent with two cosmogenic ^{36}Cl ages of 2,720 ± 529 and 2,700 ± 413 years for a boulder (VAN-1; Figure 3.36 and Table 3.6) on the terminal moraine at the northwestern margin of Thomas Bay (Vanderput Point). A second boulder from just inside the moraine south of Ruth Island and near the base of Point Agassiz Peninsula has a ^{36}Cl age of 905 ± 94 years. Basal peat obtained from a 1.6-m core collected inside the southern portion of the moraine (near cosmogenic samples TB-2; Figure 3.34) has a calibrated radiocarbon age of 1,062 (977) 939 years (PTAG-2-160). These dates, taken in conjunction, point to a period of moraine construction with a minimum age of ca. 1,000 to 900 years ago.

An additional boulder (TB-1) located near sample TB-2 had a much older ^{36}Cl age (8,980 ± 954; Table 3.6). No other studies have reported an early Holocene ice advance in southeastern Alaska; therefore, this outlying ^{36}Cl date is likely due to prior surface exposure.

Cosmogenic surface ages from the moraine support a Neoglacial advance of Baird Glacier to the mouth of Thomas Bay by 2,700 years ago. The stratigraphic evident suggests that by about 2,200 years ago the ice margin had retreated to within 6 km of the 1995 terminus position. However, two interpretations of the younger (1,000-900 yr) dates are possible: (1) they represent minimum limiting ages for the older moraine (making them irrelevant in the context of the evidence from Spurt Lake Creek), or (2) Baird Glacier readvanced by ca. 1000-1100 A.D. to nearly the same position as the earlier Neoglacial moraine, creating a compound moraine (assuming the moraines on opposite sides of the bay are correlative). The second hypothesis is supported by the agreement of cosmogenic ^{36}Cl and radiocarbon ages from the Point Agassiz Peninsula moraine (both dated at 1,000 to 900 years ago). However, there is no stratigraphic evidence for the younger advance in the Spurt Lake Creek section above the 2,200-year-old outwash, nor is there an obvious unconformaty (Figure 3.35). Therefore, further data are required to determine whether there was more than one late-Holocene advance of Baird Glacier that reached the mouth of the bay.

Late Neoglaciation: Little Ice Age

Baird Glacier appears to be at its Little Ice Age maximum position, protected from calving by a large outwash plain (Figure 3.37). This outwash plain has prograded about a kilometer into Thomas Bay since first mapped by Thomas in 1887 (ca. 10 m/yr; Figure 3.31). A trimline on the rock walls above the glacier terminus (Figure 3.38) appears to define an earlier, steeper terminus, consistent with the morphology of most tidewater-calving glaciers. This likely marks the position of the former calving margin of Baird Glacier. If the average growth rate of the outwash plain (10 m/yr) is extrapolated back in time, then the construction of the outwash apron would have began between 1650 and 1750 A.D., i.e., just before the other major calving glaciers in the area began drastic retreat. Thus, the outwash plain may have protected Baird Glacier from retreat at that time.

SUMMARY

The four glaciers included in this study all experienced two to three periods of major advance and retreat during the middle to late Holocene. Retreat followed periods of advance that culminated about 3,500-3,300, 2,700-2,200, 1,100-900, and 220-110 years ago (1780/1890 A.D.) (Figure 3.39).

OTHER NEOGLACIAL COASTAL GLACIER FLUCTUATIONS ALONG THE NORTHWESTERN MARGIN OF NORTH AMERICA[2]

STIKINE AND JUNEAU ICEFIELDS

Although there is no direct evidence for glacier advance, preliminary reconnaissance by Ryder (1987) along the southeastern (Canadian) margin of the Stikine Icefield indicates that the climate became cold and/or wet enough to lower the level of permanent snowfields after about 4,000 years ago. This date is based on the presence of 4,231-3,988-year-old (3,760 ± 70 ^{14}C year; S-2279) caribou antlers melting out of receding snowfields. The winter range of caribou currently does not extend to the altitude of the subfossil samples, indicating that shortly after they were shed snowfall increased and/or temperatures cooled, causing a drop in snowline. Snowline remained lowered until the last half of the twentieth century when the antlers were discovered. Because caribou will sometimes wander above the snowline, these dates may be meaningless. However, interpreted in conjunction with other glacial (below) and palynological (Figure 2.2; Heusser, 1995) evidence, they provide supporting evidence for cooling temperatures/increasing precipitation around 4,000 years ago.

Ryder's (1987) study also provides evidence for the Little Ice Age chronologies of the southeastern Stikine Glaciers. Dendrochronologically dated moraines and historical observations made since the mid-19th century indicate that Great Glacier retreated from it's three moraines in the early 18th century, the mid 19th century, and in the late 19th century, respectively. Although, not dated directly, Mud Glacier and Flood Glacier are bounded by at least two end moraines that appear to correlate with those of Great Glacier. *In situ* stumps overridden by the advancing Scud Glacier, now exposed 100 m above the glacier

---

[2] Figure 3.39 summarizes the timing of glacier advance in the region as discussed below.

surface, have overlapping kill-dates between 1420 and 1435 A.D., indicating that the Little Ice Age advance of Scud Glacier was underway by the early 15th century (samples S-2297 and S-2298).

Motyka and Beget (1996) discussed data for Taku Glacier and summarized what is known about the advance/retreat history of the land-based glaciers originating from the Juneau Icefield (Cross, 1968; Lawrence, 1950; Röthlisberger, 1986)[3]. Based on their interpretations and the calibration of their published ^{14}C dates, there are about four periods of Neoglacial advance in the region. Several glaciers from the Juneau Icefield and nearby British Columbia reached maxima between 3,400 and 2,200 years ago. However, evidence points to asynchrony of glacier maxima within this time period. There is good synchrony around the icefield for advances between 1,800 and 1,300 and between 1,200 and 1,050 years ago, and from 1300-1800 A.D. All of the glaciers studied in the region began their most recent retreat between 1750 and 1783 A.D. At least one land-based glacier (Mendenhall) experienced a minor readvance that culminated in the late 19th to early 20th century (many of the smaller glaciers have not been studied in as great detail). All of the land-based glaciers have continued to retreat through the 20th century; however, Taku Glacier has advanced from a retracted position since 1890 A.D. (Motyka and Beget, 1996).

GLACIER BAY AND THE ST. ELIAS MOUNTAINS:

Goodwin (1988) summarized evidence of three major ice advances of the trunk glaciers in Glacier Bay. (Sketchy evidence exists for an advance that occurred about 5,100 years ago (4,500 ^{14}C years; McKenzie and Goldthwait, 1971); however Goodwin (1988) suggests that verification of this requires further study.) The glacier occupying the West Arm of Glacier Bay advanced to dam Muir Inlet between ca. 2,600 and 1,900 years (2,500 to 2,000 ^{14}C years) ago. After a period of retreat and forest reestablishment, Muir Inlet was again blocked by an ice advance between ca. 1,600 and 800 years (1,700 to 900 ^{14}C years) ago. Glaciers in Muir Inlet were probably also advancing during this time (McKenzie and Goldthwait, 1971). After a second period of retreat, glaciers in both arms of the bay advanced, coalesced, and ultimately flowed to the mouth of the fjord. This period of

---

[3] Much of the data they cite come from a paper by Röthlisberger (1986), which was written in German and was not accessible for this study.

advance was underway by at least the 14th century, and retreat from the mouth of Glacier Bay began sometime in the early to middle 18th century.

Brady Glacier, to the west of the main Glacier Bay fjord, reached successive maxima between ca. 3,200 and 1,950 and 1,600 and 1,300 years ago, and readvanced during the Little Ice Age until 1876 A.D. when it began it's recent retreat (Derksen, 1976). Derksen (1976) attributed the asynchrony between Brady Glacier and the Glacier Bay system to the outwash apron that helped stabilize the terminus of Brady Glacier. This is very similar to the situation occurring at the terminus of Baird Glacier in Thomas Bay.

Mann and Ugolini (1985) reported that the glaciers in the Lituya Bay district were advancing between ca. 6,800 and 5,700, ca. 3,800 and 1,800, and ca. 1,400 and 400 years ago. Tidewater glaciers in Lituya Bay began to retreat in the 16th century and continue to retreat at present.

WESTERN GULF OF ALASKA

Calkin et al. (2001) summarized evidence for late-Holocene fluctuations of glaciers along the western Gulf of Alaska, including glaciers of Seward Peninsula, Kenai Peninsula, Prince William Sound, and Icy Bay, as well as large glaciers along the central coast (Bering Glacier and Hubbard Glacier). They concluded that there is general strong synchrony among the glacier variations in this region.

The earliest advance in the region is recorded at Yakutat Bay where Hubbard Glacier was expanding by 6,850 years ago. After a series of advances and retreats, most likely influenced in part by glacier surging, Hubbard Glacier reached the mouth of the bay and remained there until about 2,700 years ago (Barclay et al., 2001). The three most widespread periods of glacier extension in the region occurred 3,600 to 3,000 years ago, 1,500 to 1,300 years ago, and during the Little Ice Age. At least three major glacier systems were advancing from 3,600 to 3,000 years ago: McCarty Glacier on the Kenai Peninsula (ca. 3,600 years ago; Post, 1980; Wiles and Calkin, 1993), Icy Bay (ca. 3,480 years ago; Gloss, 1997) and Beare Glacier (Calkin et al., 2001). Calving and land-terminating glaciers of the Kenai Mountains (Wiles and Calkin, 1993), western Prince William Sound (Wiles et al., 1999a), Icy Bay (Porter, 1989), Bering (Wiles et al., 1999b), Sheredin and Beare glaciers (Calkin et al., 2001) all reached maxima between 450 and 650

A.D. Little Ice Age maxima occurred during the middle 13th, early 15th, middle 17th, and late 19th centuries.

SOUTHERN BRITISH COLUMBIA

Desloges and Ryder (1990) and Ryder and Thompson (1986) reported three major periods of glacier expansion in the central and southern Coast Mountains during the Holocene. Evidence from the Mt. Garibaldi region supports a mid-Holocene advance between 7,000 and 5,700 years (6,000 and 5,000 ^{14}C years) ago, referred to as the "Garabaldi phase" (Ryder and Thomson, 1986). Along the central British Columbia coast near Bella Coola, wood buried in a lateral moraine of Jacobsen Glacier has an age of 2,715-2,316 years ago (Desloges and Ryder, 1990; GSC-4028){ #104}, implying that the glacier was at or near a maximum position close to 2,500 years ago. To the south, glaciers were advancing in the Coast Mountains between 3,500 and 1,850 years (3,300 and 1,900 ^{14}C years) ago, and reached maxima between 2,350 and 1,850 years (2,300 and 1,900 ^{14}C years) ago (Ryder and Thomson, 1986). After a period of retreat, Little Ice Age advances began for some glaciers before the 13th century and culminated in the mid-18th to early-20th centuries. Dendrochronologically dated end moraines from the Little Ice Age maximum were deposited between 1860 and 1920 A.D. throughout the region (Desloges and Ryder, 1990).

COMPARISON OF REGIONAL GLACIAL CHRONOLOGIES

The earliest documented Holocene ice advance in northwestern North America occurred in Yakutat Bay, Lituya Bay and southern British Columbia about 7,000-6,000 years ago (Figure 3.39). These advances were underway shortly after pollen records indicate a drop in summer temperatures and rise in precipitation (Figure 2.2; Heusser, 1995). Evidence for this advance along the southern margin of the Stikine Icefield has not been found. However, because this advance was commonly less extensive than later advances, it is likely that evidence may have been eroded or remains buried.

The next well-documented advance began between about 4,000 and 3,000 years ago and is recorded throughout northwestern North America. This is also a significant time in pollen cores, represented by a rapid increase in precipitation and cooling of summer temperatures

(Heusser, 1995). Snowline was also dropping along the Stikine River about the same time (Ryder, 1987). In many cases, this period of advanced ice margins continued for the next one to two millennia, culminating in ice maxima between ca. 3,000 and 1,900 years ago. This period of advance is prominent in Thomas Bay, where the Paterson Glacier was in an advanced position after 3,200 years ago and Baird Glacier (possibly coalesced with Patterson Glacier) reached a maximum position between 2,700 and 2,200 years ago. Like the Paterson Glacier, other glaciers in northwestern North America appear to have remained relatively extensive since this time (Desloges and Ryder, 1990).

In the study region LeConte Glacier is inferred to have dammed Cabin Creek by ca. 4,300 years ago but had retreated out of the upper creek valley by ca. 3,200 years ago. The glacier terminus was in a retracted state from this time until it readvanced after 2,100 years ago. These dates imply that LeConte Glacier was not synchronous with early-to-mid Neoglacial advances in the region. This asynchrony may result from the relatively high accumulation area ratio (AAR) of LeConte Glacier, which is the result of a large accumulation area and a steep gradient at snowline. Even at its mid-fjord maximum position during the Little Ice Age, LeConte Glacier had an AAR of 0.9, similar to it's modern AAR (0.92) (Viens, 1995).

Advancing ice was also common about 1,500 to 1,100 years ago, with some areas experiencing maxima as late as ca. 900 years ago. In the study area, this advance is evident in LeConte Bay where LeConte Glacier was advancing at this time, and possible in Thomas Bay, where limited evidence suggests that Baird Glacier may have reached a maximum position ca. 900 years ago.

The Little Ice Age generally was the most-extensive Neoglacial advance throughout the coastal region of northwestern North America. Although glaciers retreated from their Neoglacial maximum somewhat asynchronously between about 1600 and 1900 A.D., there are two significant periods of retreat that characterized the region (Figure 3.39). In addition, an early mid-13th century retreat is recorded regionally in at least two areas, but not evident in the study area. During the mid-18th and late-19th centuries several glaciers in the region retreated from extensive terminal moraines or from recessional moraines. The advance/retreat history of Patterson, LeConte, and Shakes glaciers is broadly synchronous with several other glacier fluctuations in the northeastern Pacific.

There are only a few glaciers in the region that are still at their Little Ice Age maximum limit, including Baird Glacier. These glaciers are all former tidewater-calving glaciers, the termini of which are buried by a blanket of outwash. It is very likely that these glaciers will respond to 20th century warming by retreating in the next 30 years.

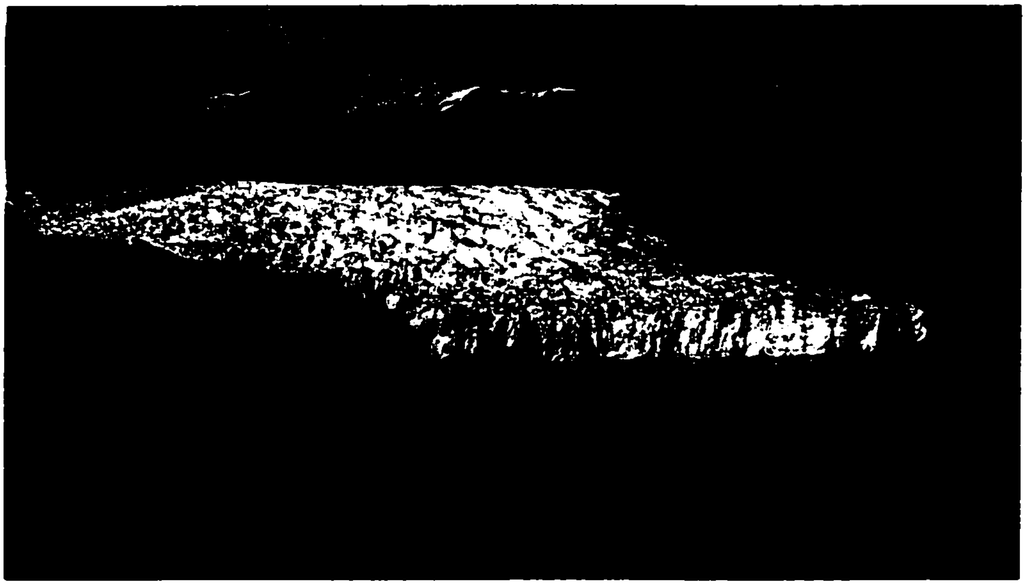

Figure 3.1 – Terminus of LeConte Glacier in 1993.

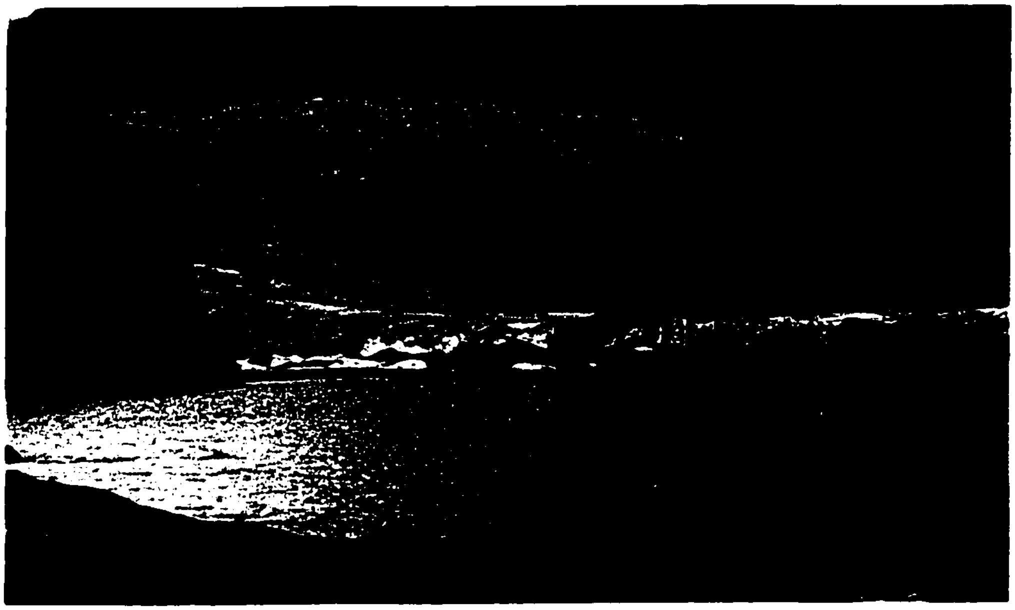

Figure 3.2 – Patterson Glacier in 1994.

Figure 3.3 – 1897 photograph of the U.S. Coast and Geodetic Survey Steamer *Patterson* in Chatham Straight, southeast Alaska (NOAA Photo Library, NOAA Central Library; NOAA Office of Coast Survey, Hydrographic Descriptive Report 2333).

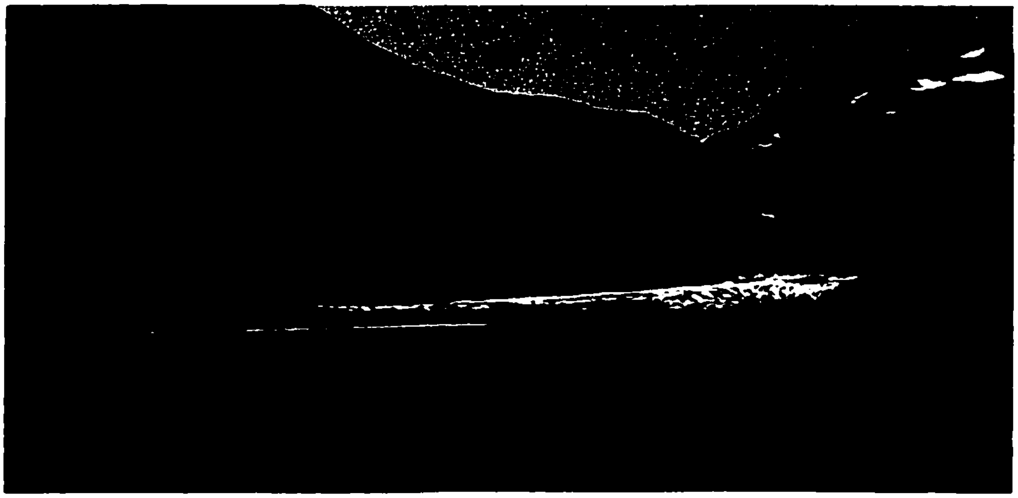

Figure 3.4 – Baird Glacier terminus in 1995.

Figure 3.5 – Shakes Glacier in 1995.

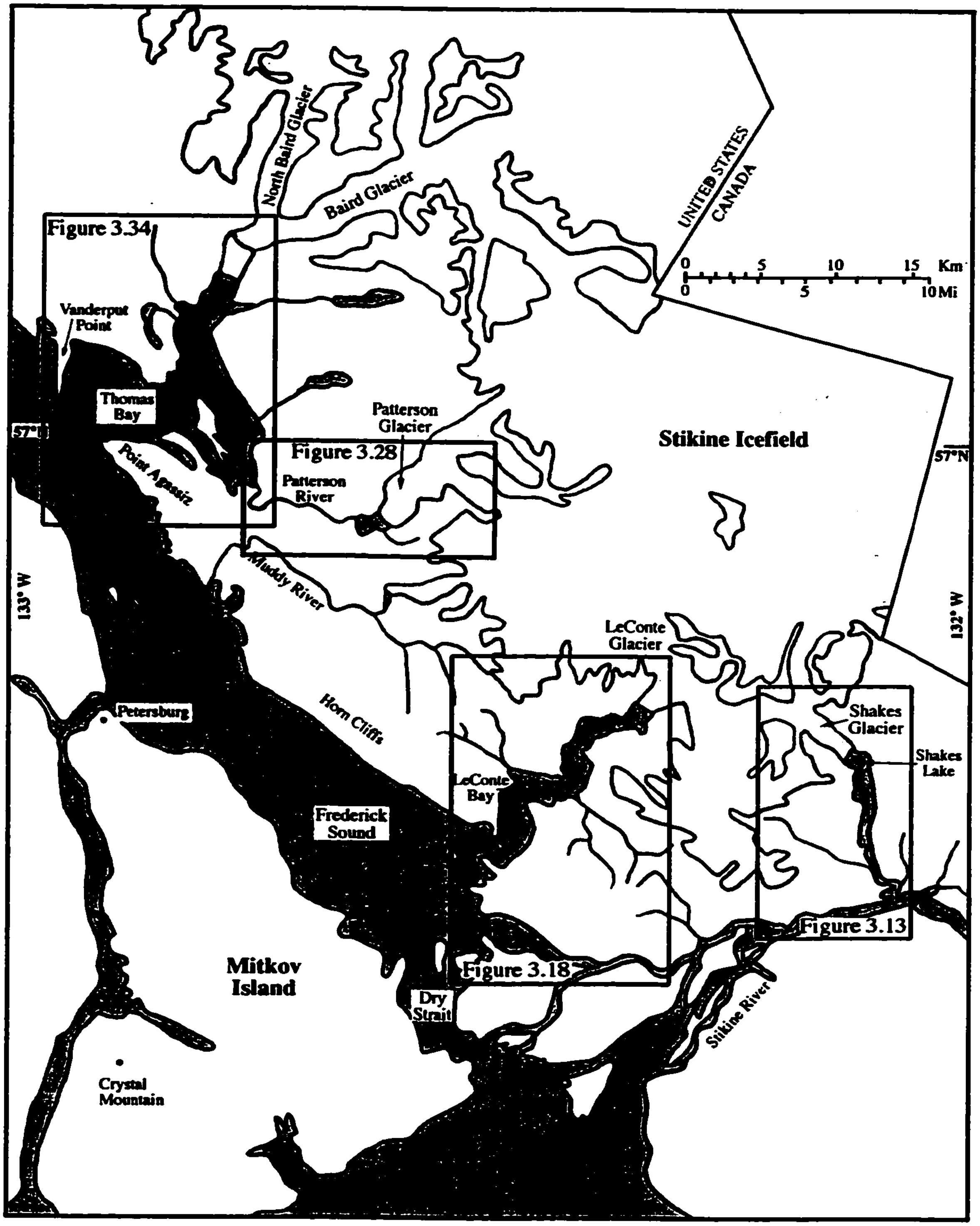

Figure 3.6 – Regional map of the southeastern part of the Stikine Icefield showing the location of regional glacier maps (Figures 3.13, 3.18, 3.28 and 3.34).

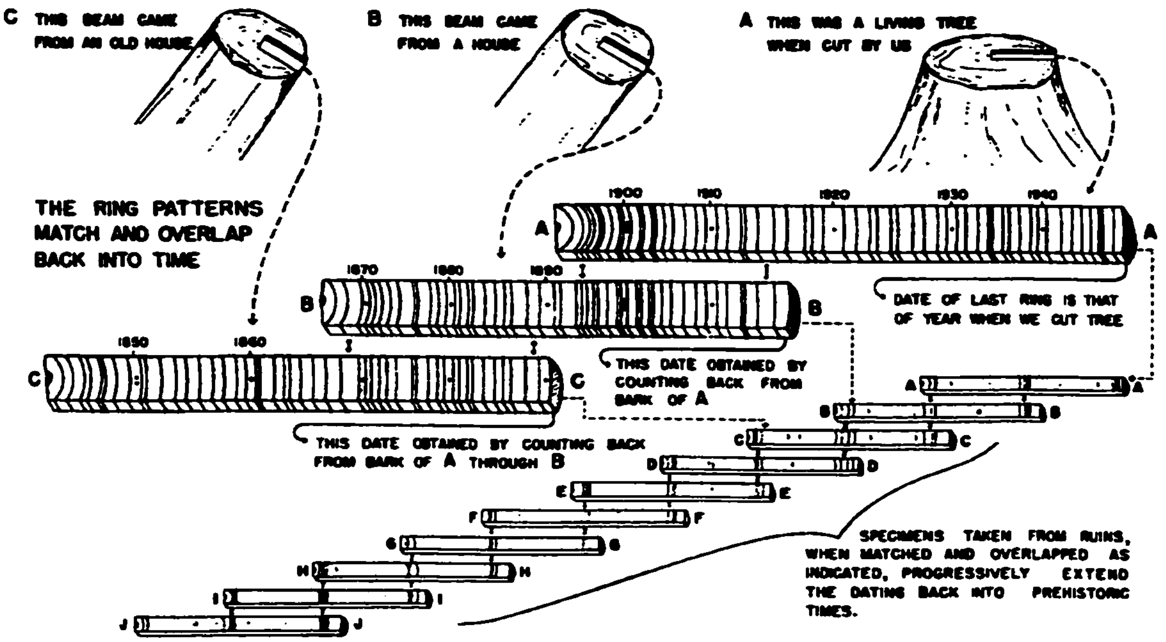

Figure 3.7 – Cross dating sub-fossil wood samples, from Stokes and Smiley (1968).

Figure 3.8 – (a) Photograph of late Pleistocene and Holocene sediments exposed in the *Scandia House* parking lot, downtown Petersburg. Terry Swanson (University of Washington) is shown for scale.

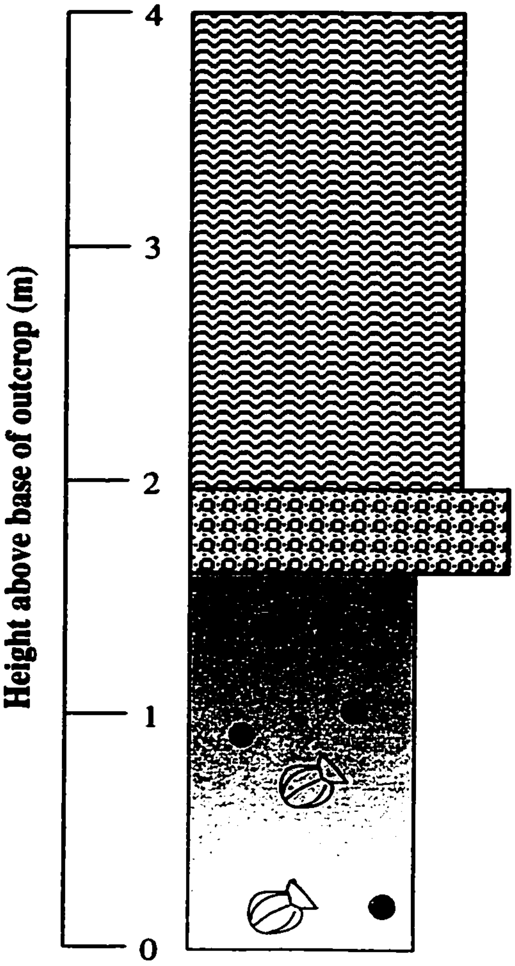

Description	Interpretation
Peat, including large wood fragments.	Late Pleistocene to Holocene muskegs.
Sandy gravel with some organics.	Beach lag formed during isostatic uplift.
Grey, clays containing a few cobbles and shells (pelycepods & gastropods). Lowest shell fragment (SCAN-3 located 30 cm from base) dated at 15,990 (15,859) 15,726 years BP.	Glacialmarine deposits formed shortly after late Pleistocene deglaciation.

Figure 3.8 (cont.) – (b) Statigraphic section of late Pleistocene and Holocene sediments exposed in the *Scandia House* parking lot, downtown Petersburg. Shows unit descriptions and interpretations as well as the location of radiocarbon-dated sample SCAN-3 (Table 3.5).

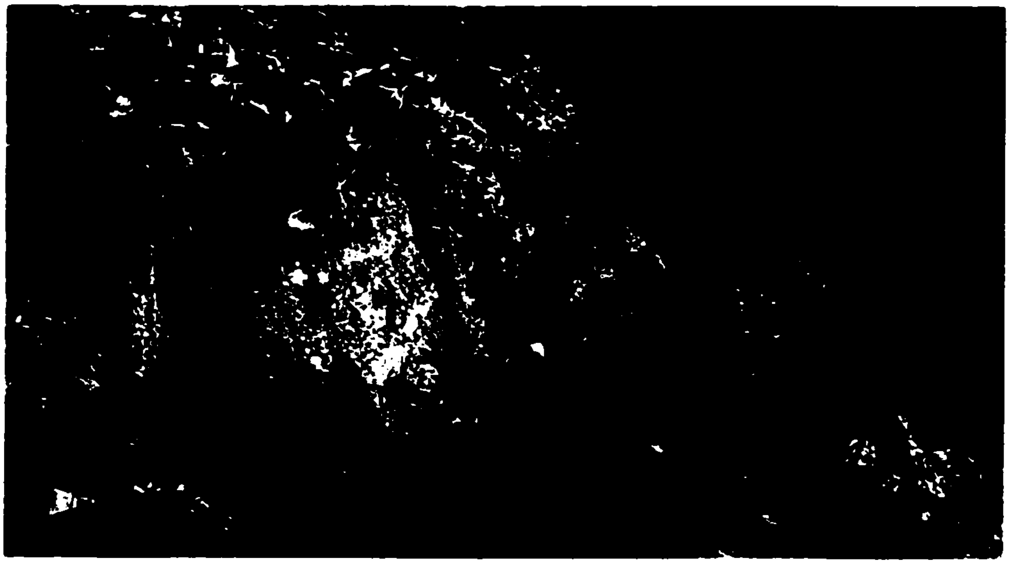

Figure 3.9 – Late Pleistocene glacialmarine drift from lower Spurt Lake Creek in Thomas Bay (Figure 3.34) where TBS-95 was collected.

Figure 3.10 – Treeline at the top of Crystal Mountain where rock samples were collected for ^{36}Cl dating and tree cores were collected for CMC (Table 3.7 and Chapter 2).

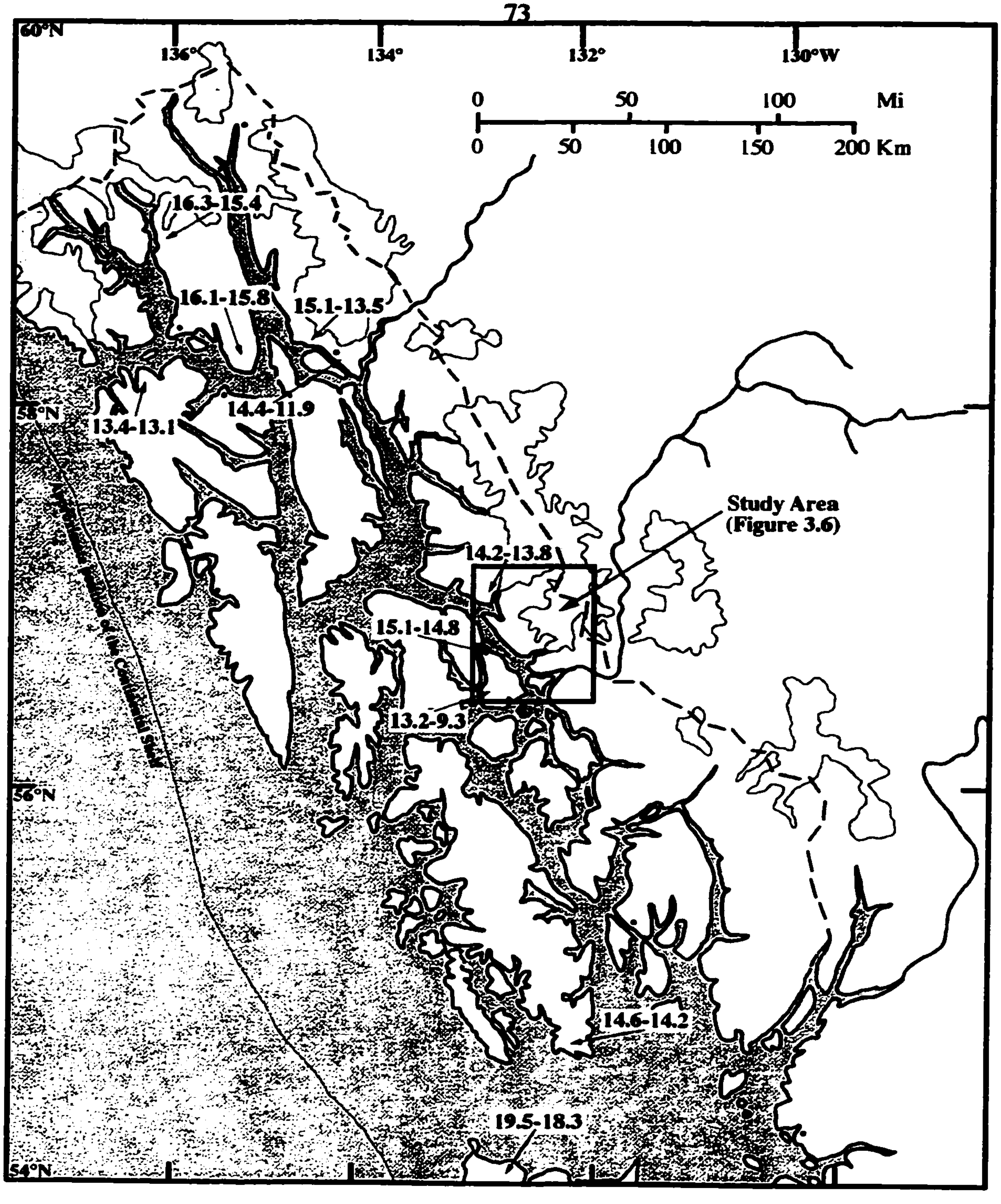

Figure 3.11 – Late Pleistocene deglaciation dates from southeastern Alaska. All dates are reported as 10^3 calibrated years B.P. and shell samples reflect a marine reservoir correction of 925 years (see text and Table 3.4 for details).

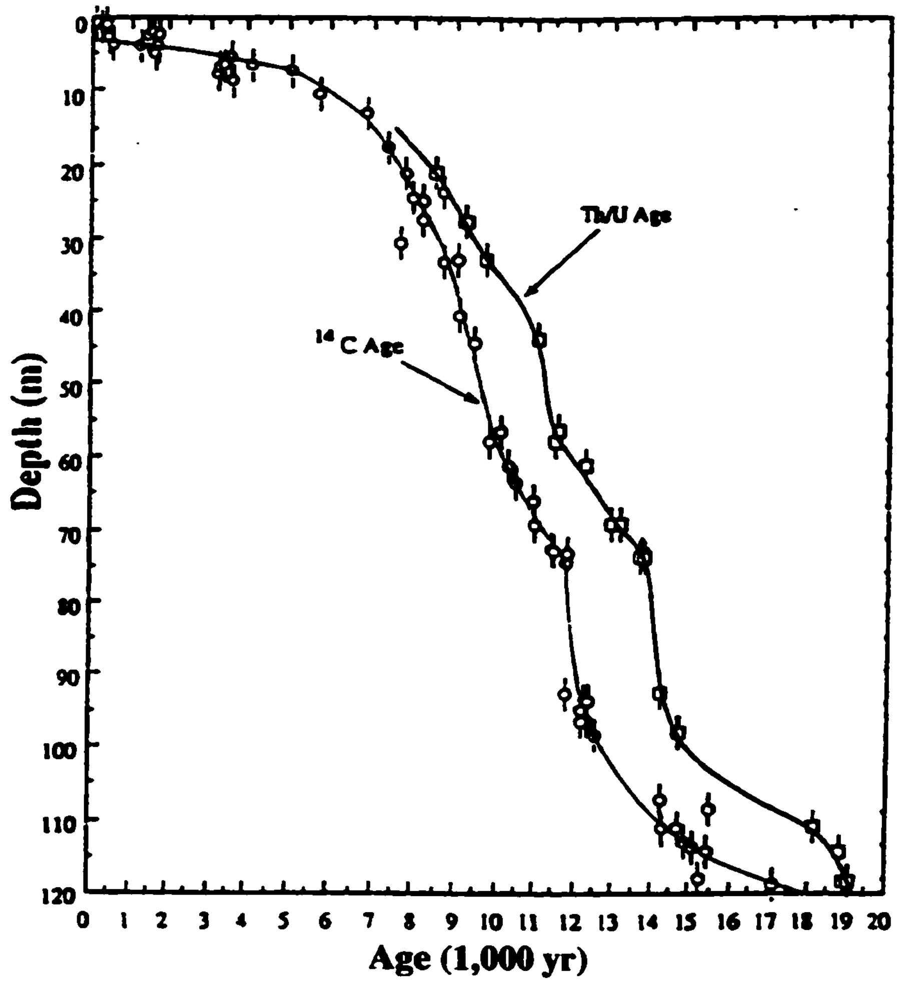

Figure 3.12 – Post glacial rise in global sea level as recorded in corals collected off the coast of Barbados (from Bard et al., 1990). Samples are thought to have grown within a few meters of sea level. Differences in radiocarbon and uranium thorium ages reflect lack of calibration of the radiocarbon dates.

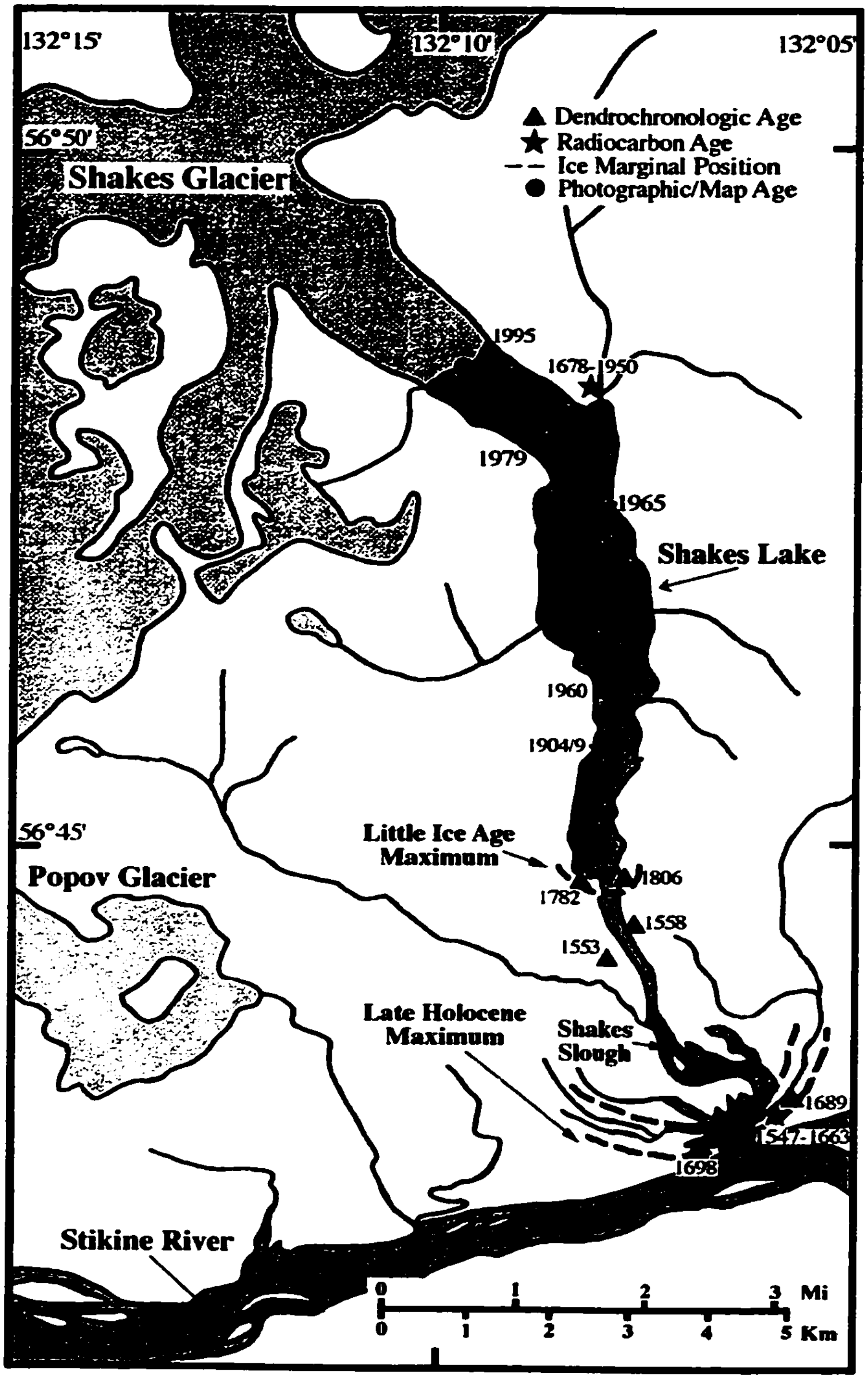

Figure 3.13 – Regional map of Shakes Glacier and vicinity showing the location of mapped and reconstructed termini positions, radiocarbon samples, and significant tree-ring ages. Radiocarbon ages are calibrated and all dates are reported in calendar years A.D. Calibrated radiocarbon ages are shown as a 1σ range and tree-ring ages are reported as the initiation of growth ±5 years.

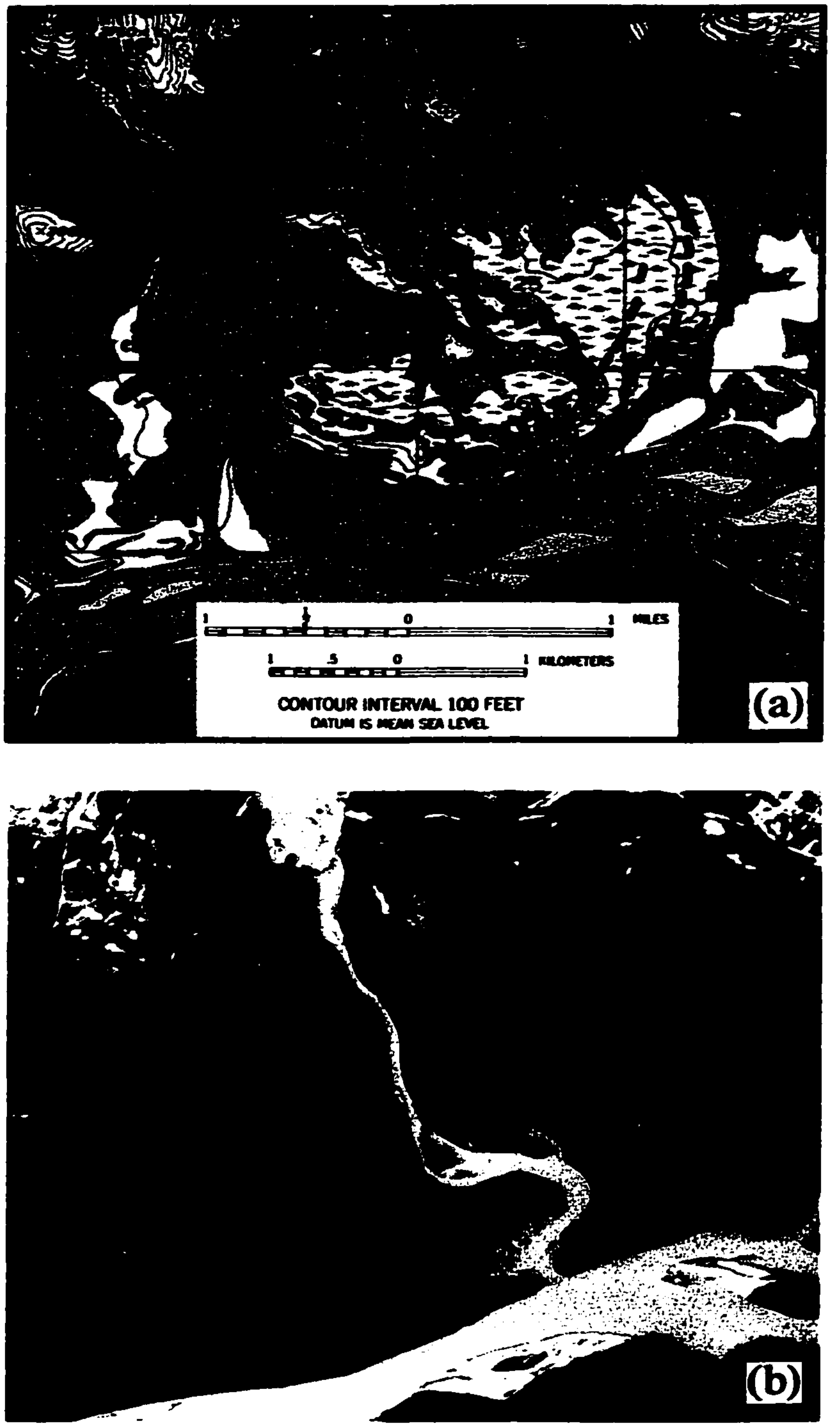

Figure 3.14 – (a) U.S. Geological Survey topographic map and (b) aerial photo (U.S. Geological Survey #6642, Aug 79) of the Shakes Glacier moraine complex at the confluence of Shakes Slough and the Stikine River. The map shows the position of an outwash channel formed by the inpoundment of a side valley.

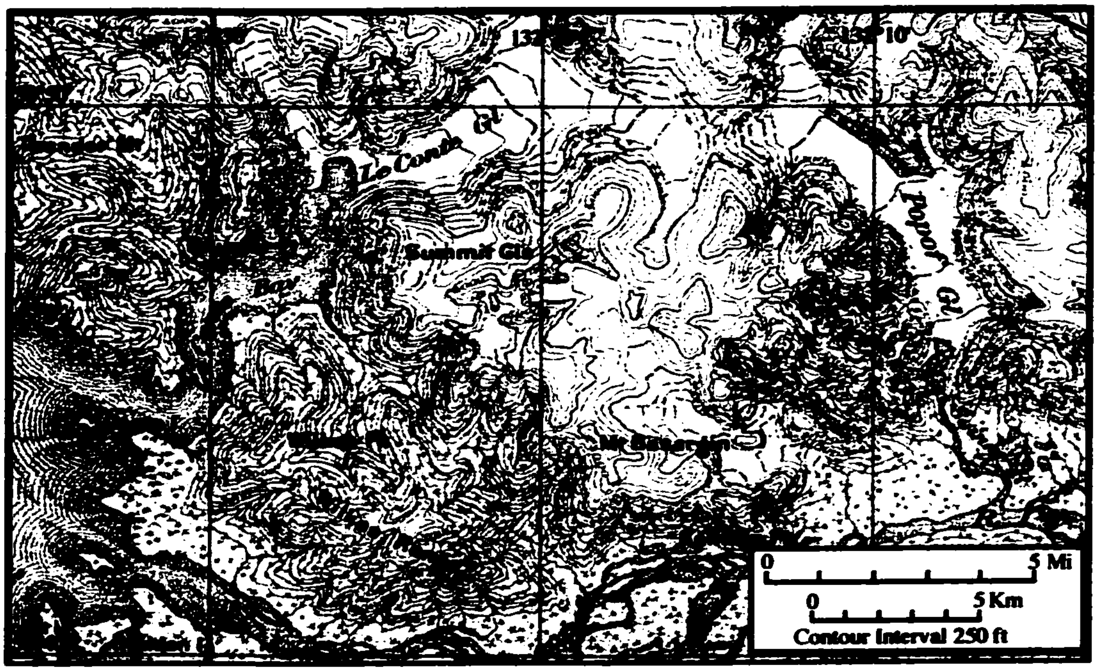

Figure 3.15 – International Boundary Commission Map (International Boundary Commission, 1952) showing the position of Shakes and LeConte glacier as surveyed between 1904 and 1909.

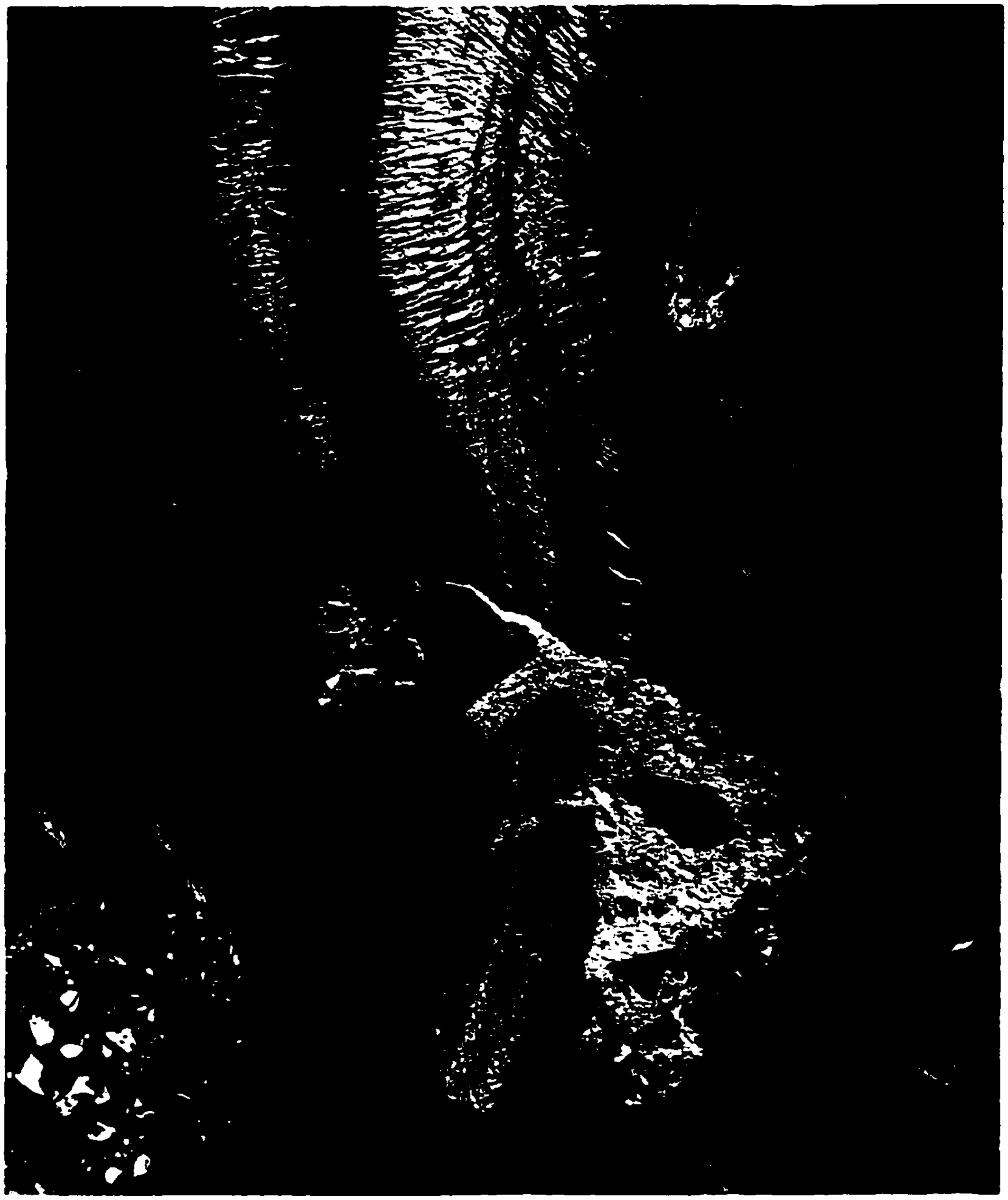

Figure 3.16 – Aerial photograph of the floating terminus of Shakes Glacier in 1977 (U.S. Geological Survey #77V2-9, 8-30-77).

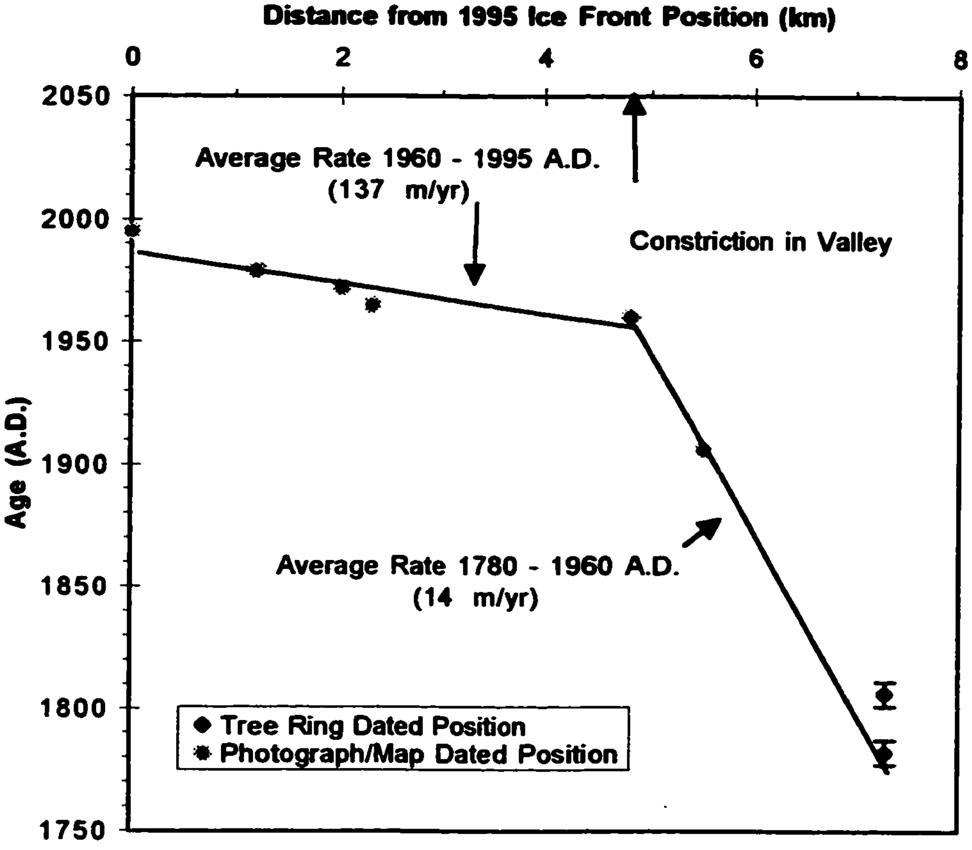

Figure 3.17 – Retreat of the Shakes Glacier terminus since the 18th century. When the terminus receded past the constriction in the valley, the retreat rate increased from 14 m/yr to 137 m/yr.

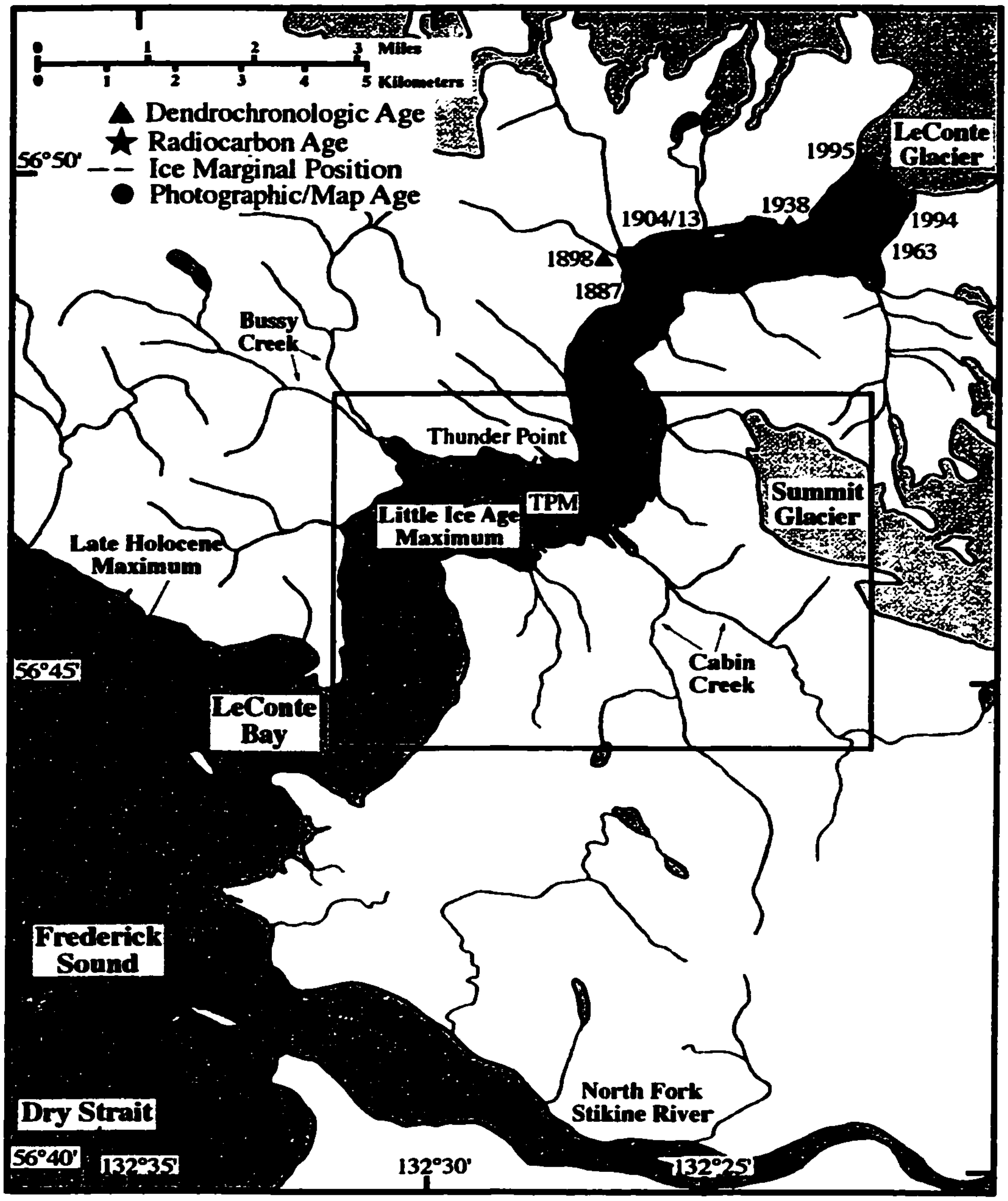

Figure 3.18 – (a) Regional map of LeConte Glacier and vicinity showing the location of mapped and reconstructed termini positions, radiocarbon samples, and significant tree-ring ages. Radiocarbon ages are calibrated and all dates younger than 1200 A.D. are reported in calendar years A.D. Radiocarbon ages older than 1200 A.D. are reported as calibrated years B.P. (refer to appropriate figures for stratigraphic relationships). Calibrated radiocarbon ages are shown as a 1σ range and tree-ring ages are reported as the initiation of growth ±5 years.

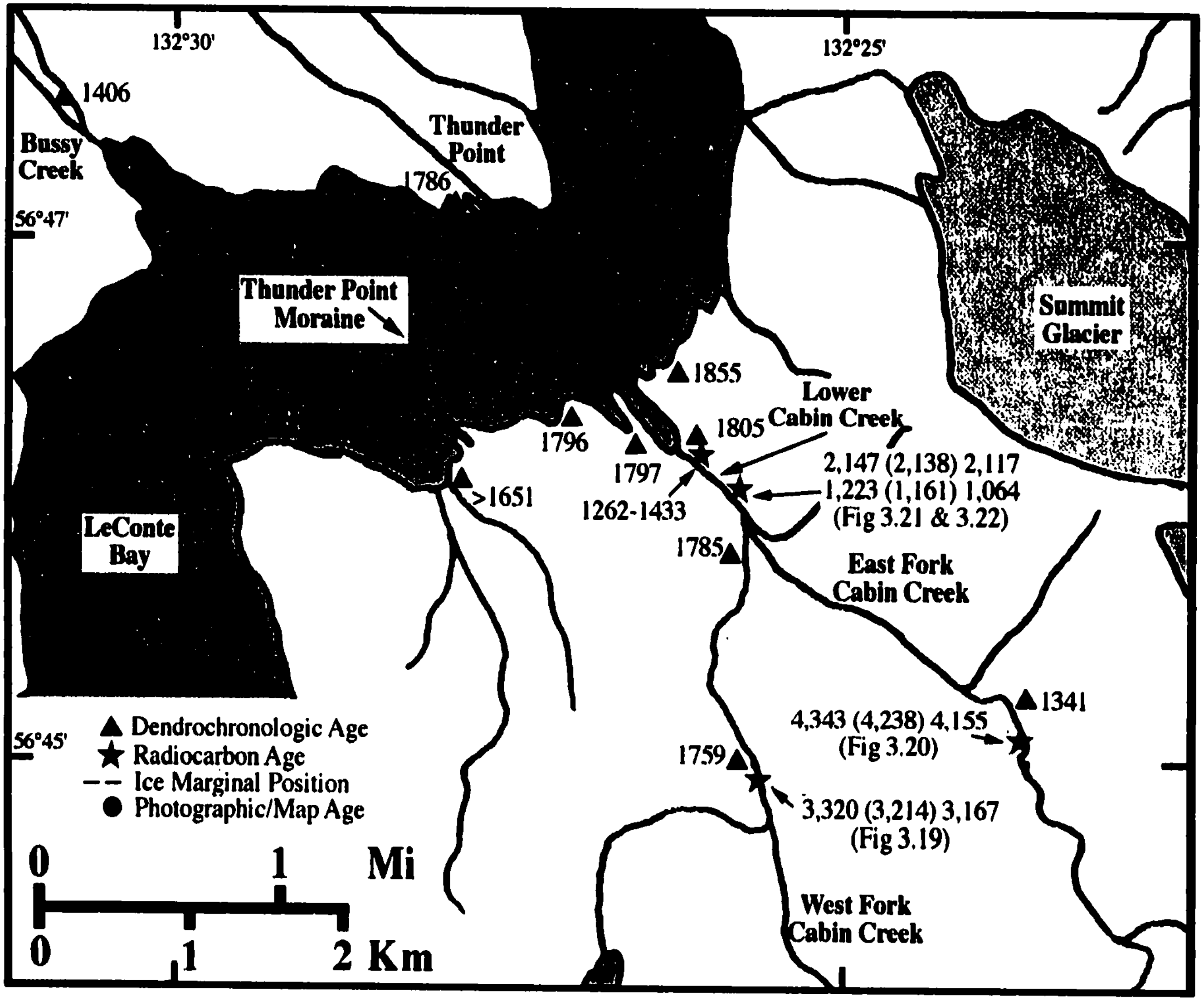

Figure 3.18 (cont.) – (b) Inset of the area around the Little Ice Age maximum. (For stratigraphic details see Figures 3.19-3.23.)

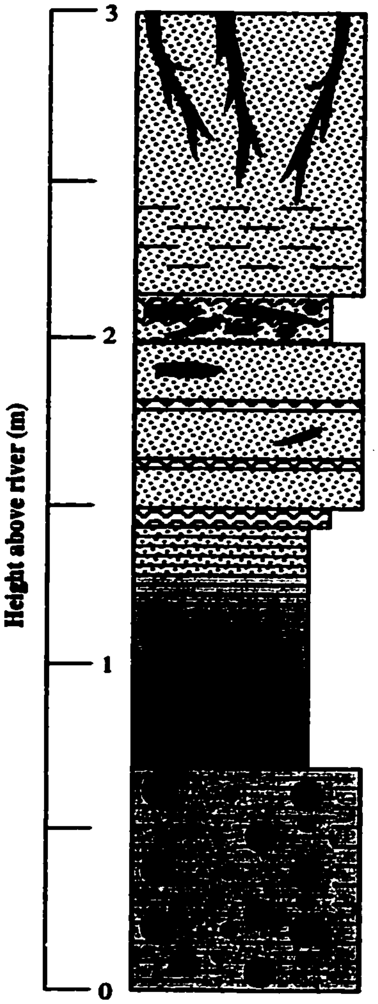

Description	Interpretation
Massive sandy silt - oxidized with a few crusty laminations. Upper part contains rootlets. Grades down into predominantly silt	Less extensive mid- to late-Neoglacial advance of LeConte impounds creek and fills with deltaic sediments.
Twigs and sticks (1-1.5 ft long) in a matrix of reddish-brown fine-grained sand. Contains sample CC4 dated at 3,320 (3,214) 3,167 years BP	Colluvium from forest floor.
Laminated fine sands (not oxidized) with some interlayers of finer silt and organic layers. Organic material is found throughout.	Deltaic sedimentation fills lake as the ice front receeds causing the impounded lake to shallow.
Grades down into... Dark grey laminated clays with occasional (0.5-2 inch) sandy-silt layers. Also contains occasional cobbles and pebbles.	Impoundment of the West Fork of Cabin Creek as LeConte Glacier receeds.
Diamicton: Silty-clay matrix with a variety of grain sizes, including striated cobbles.	Mid-Neoglacial advanceof LeConte Glacier.

Figure 3.19 – Stratigraphic section of the exposure along the west fork of Cabin Creek, showing unit descriptions and interpretations as well as the location of radiocarbon-dated sample CC-4 (Table 3.5).

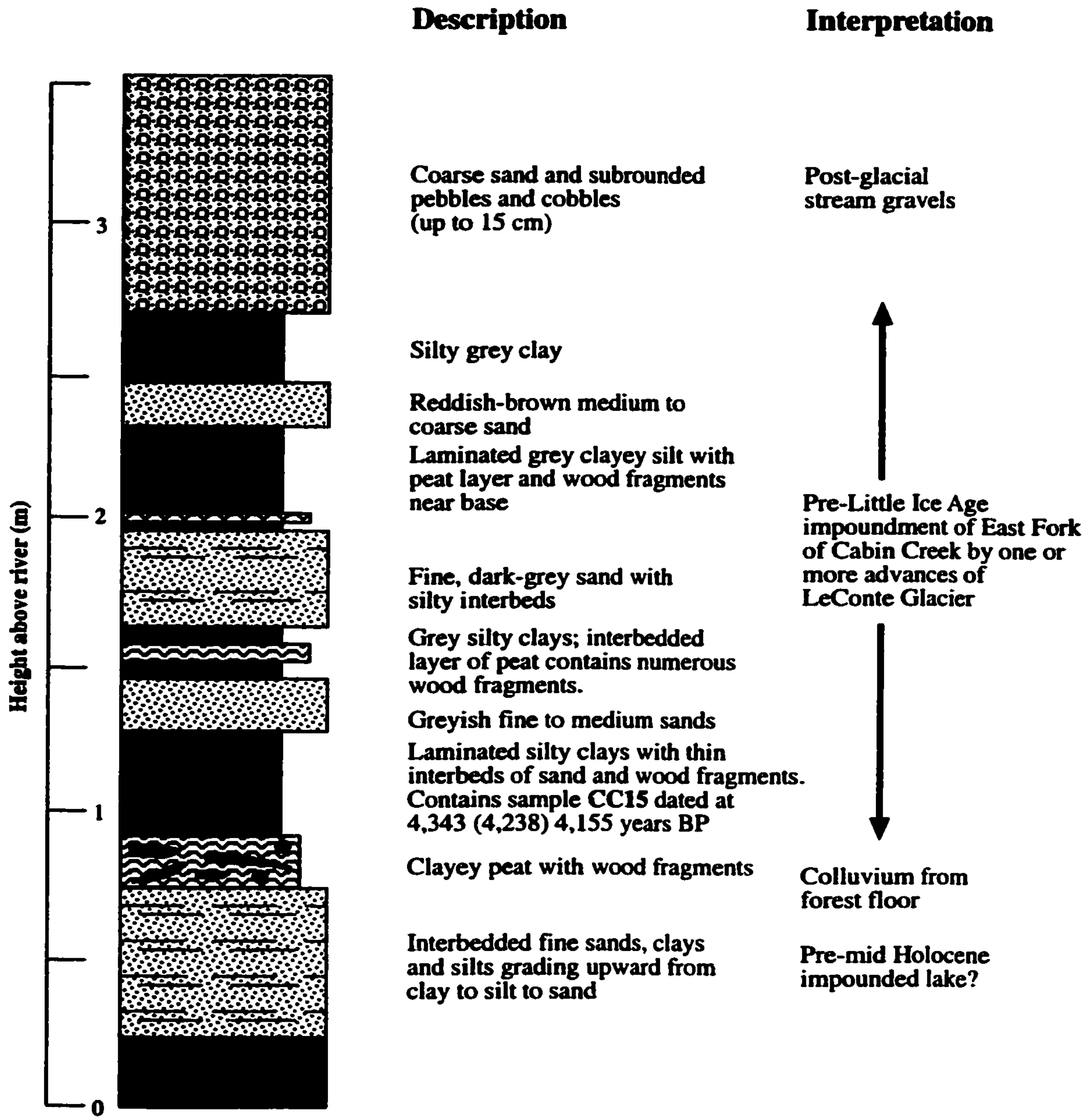

Figure 3.20 – Stratigraphic section of the exposure along the east fork of Cabin Creek, showing unit descriptions and interpretations as well as the location of radiocarbon-dated sample CC-15 (Table 3.5).

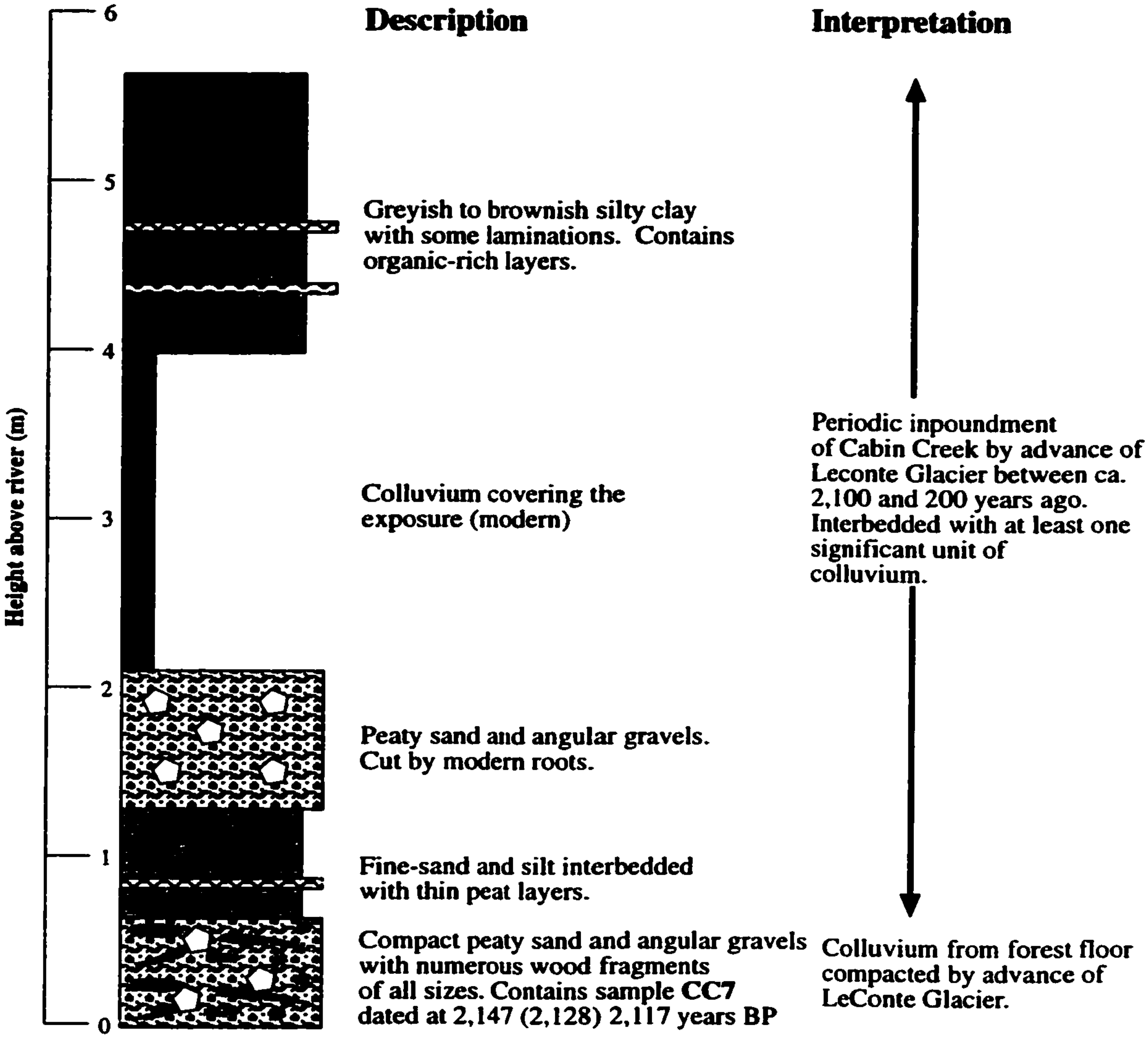

Figure 3.21 – Southern stratigraphic section of the exposure along lower Cabin Creek, showing unit descriptions and interpretations as well as the location of radiocarbon-dated sample CC-7 (Table 3.5).

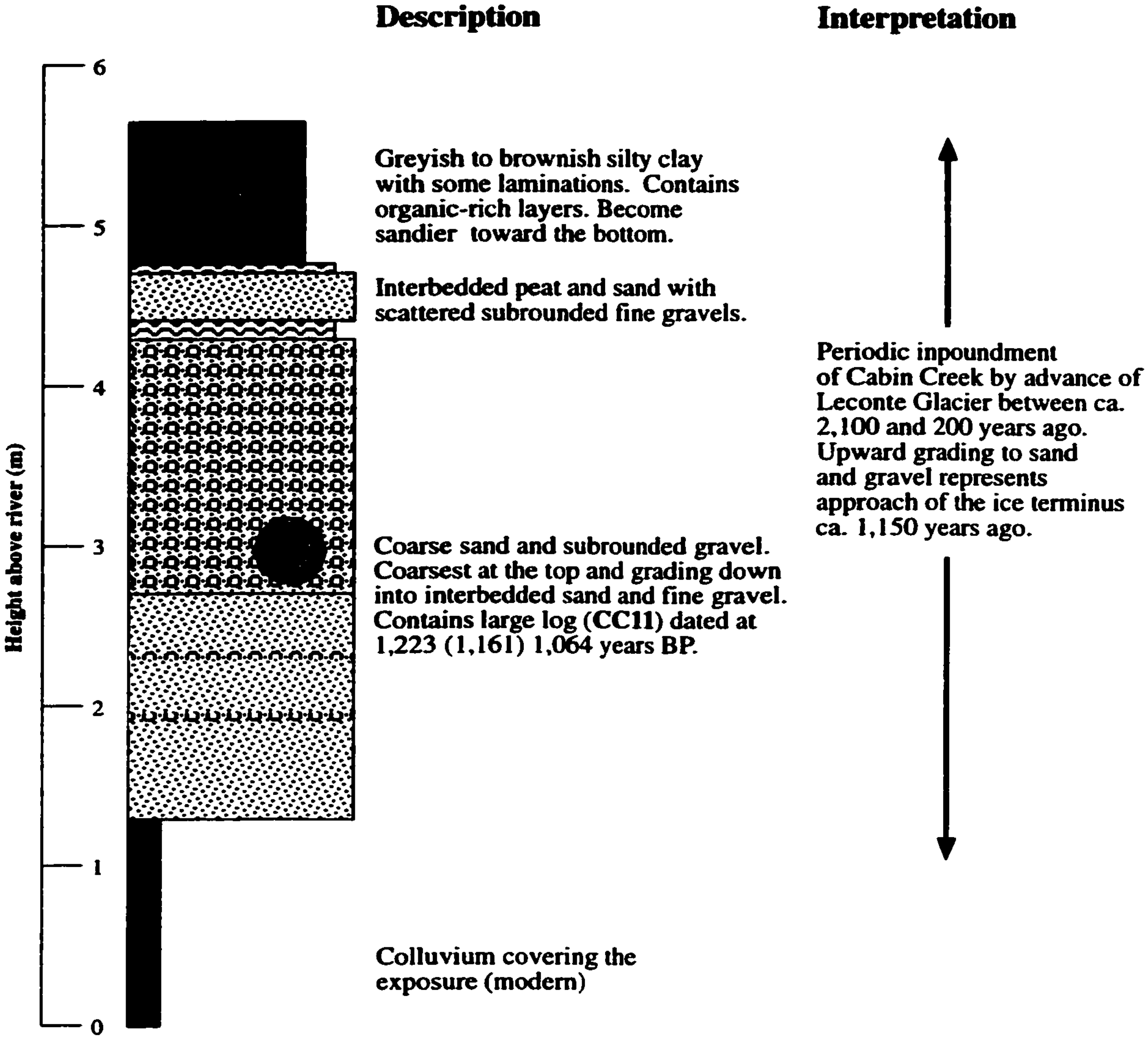

Description

Interpretation

Greyish to brownish silty clay with some laminations. Contains organic-rich layers. Become sandier toward the bottom.

Interbedded peat and sand with scattered subrounded fine gravels.

Coarse sand and subrounded gravel. Coarsest at the top and grading down into interbedded sand and fine gravel. Contains large log (CC11) dated at 1,223 (1,161) 1,064 years BP.

Colluvium covering the exposure (modern)

Periodic inpoundment of Cabin Creek by advance of Leconte Glacier between ca. 2,100 and 200 years ago. Upward grading to sand and gravel represents approach of the ice terminus ca. 1,150 years ago.

Figure 3.22 – Northern stratigraphic section of the exposure along lower Cabin Creek, showing unit descriptions and interpretations as well as the location of radiocarbon-dated sample CC-11 (Table 3.5).

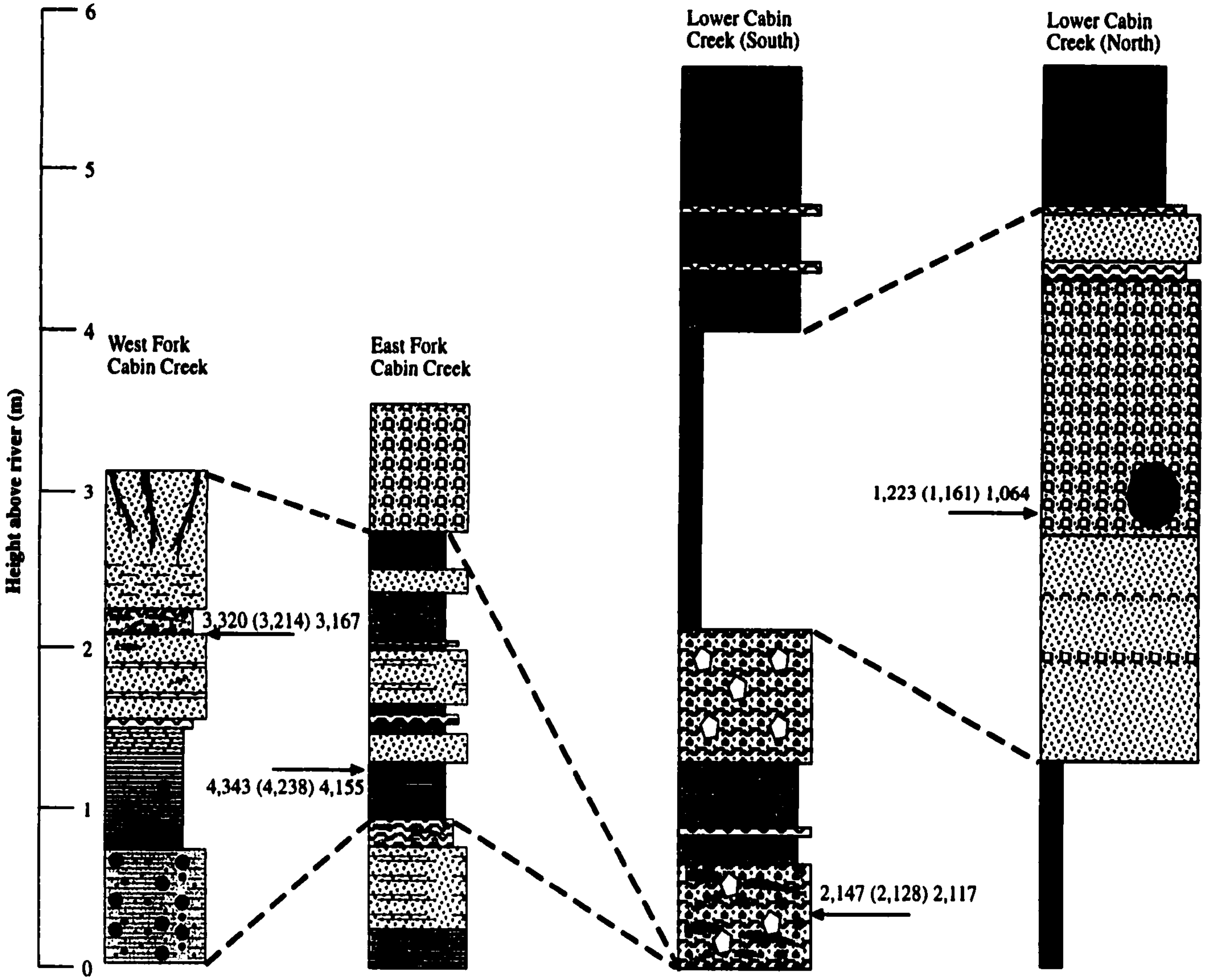

Figure 3.23 – Stratigraphic correlation between Cabin Creek sections (Figures 3.19-3.22).

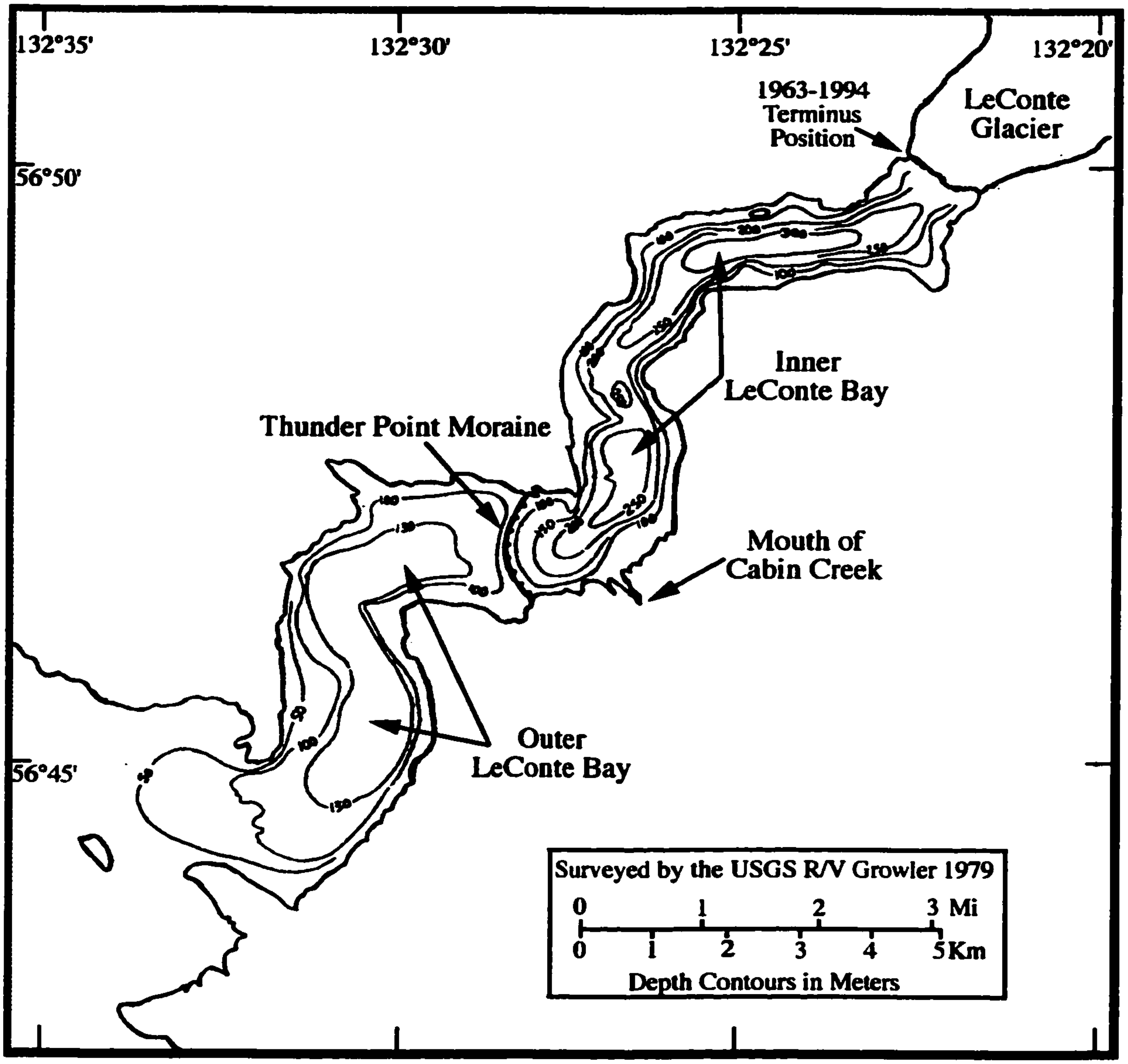

Figure 3.24 – Bathymetry of LeConte Bay (modified from Post and Motyka, 1995).

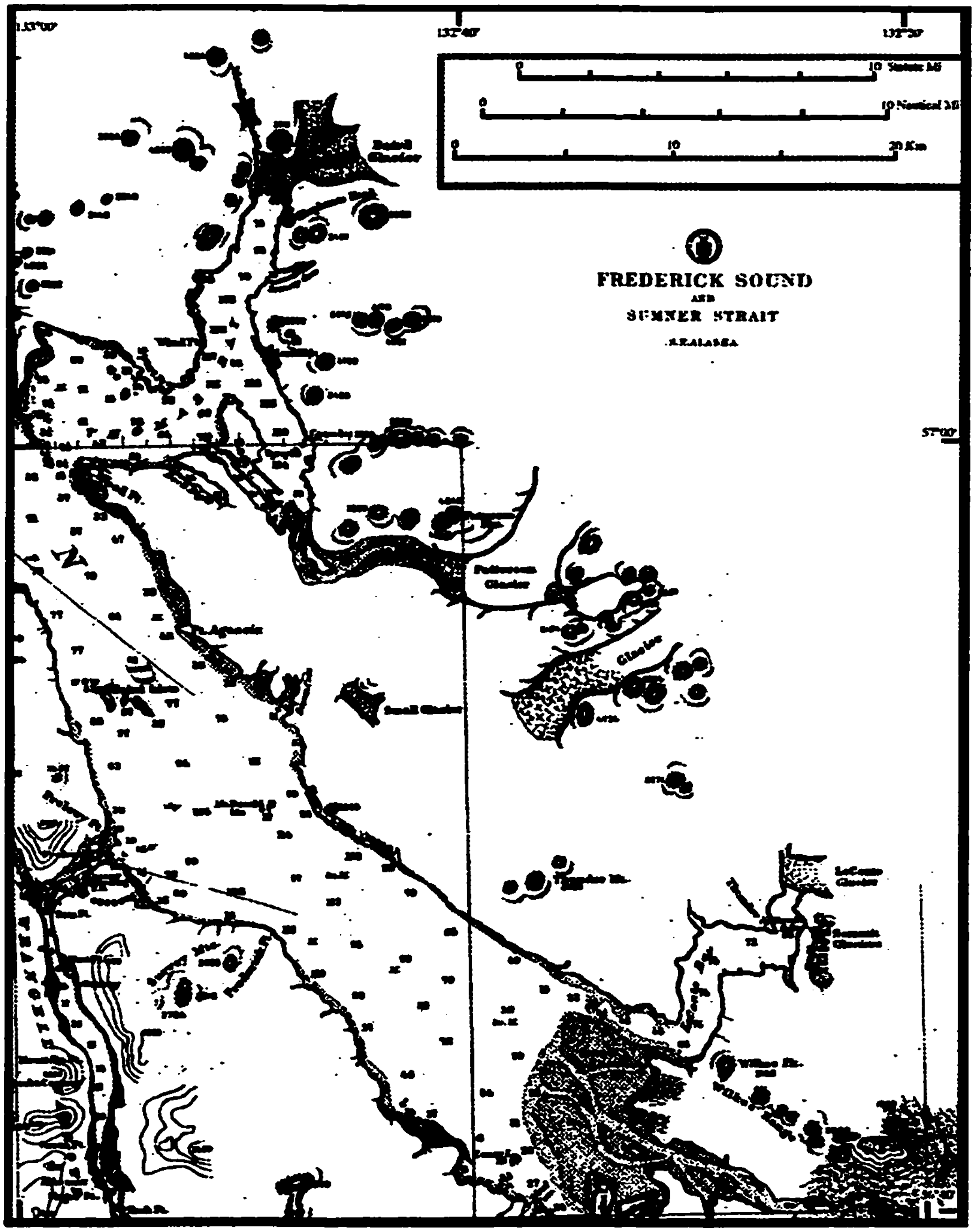

Figure 3.25 – Coast and Geodetic Survey map (U.S. Coast and Geodetic Survey, 1895) showing the position of LeConte, Patterson and Baird glaciers as surveyed in 1887.

Figure 3.26 – Photograph of the 1995 terminus of LeConte Glacier. High ice flux at the glacier terminus led to initiation of rapid retreat in 1995.

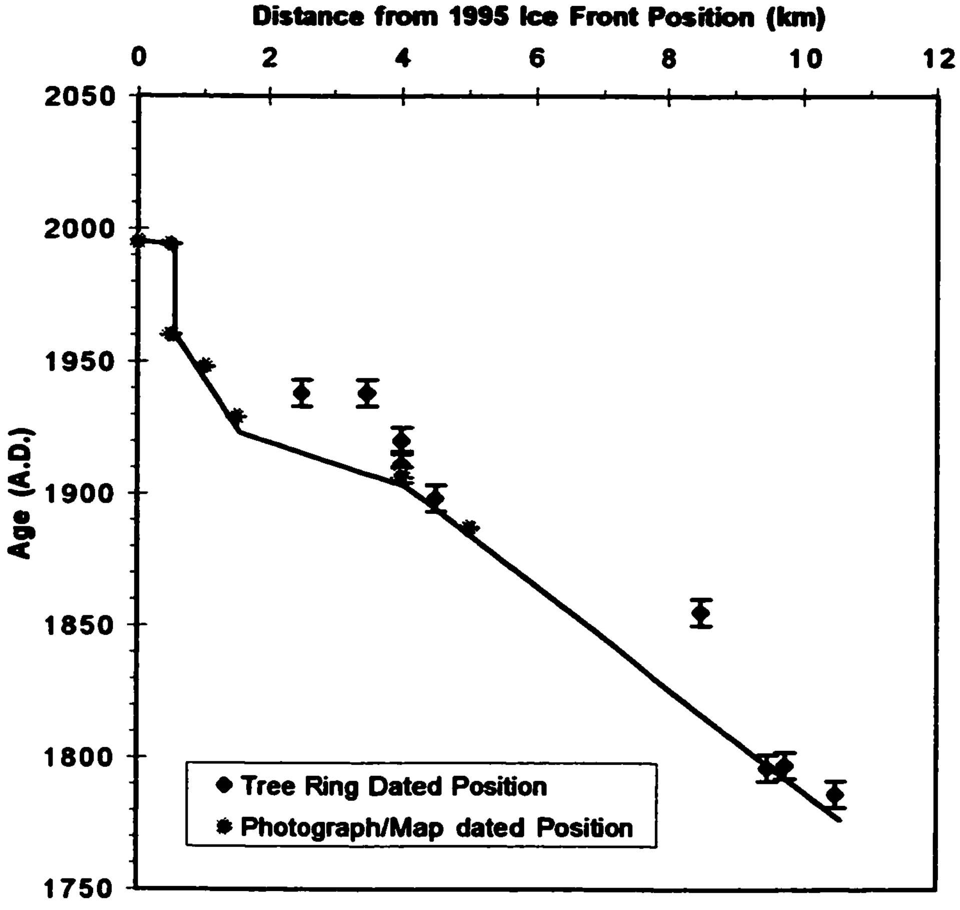

Figure 3.27 – Retreat of the LeConte Glacier terminus since the 18th century.

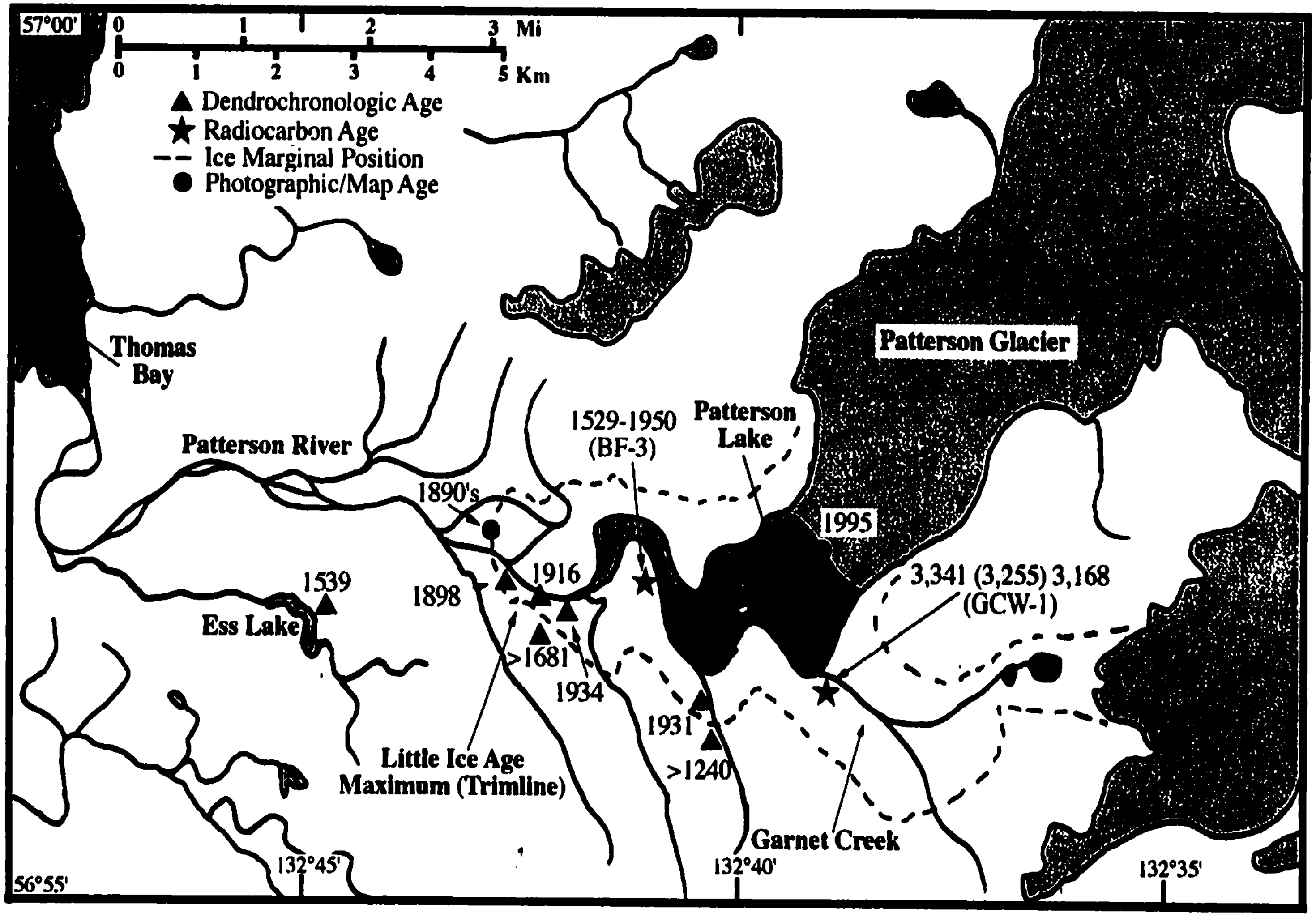

Figure 3.28 – Regional map of Patterson Glacier and vicinity showing the location of mapped and reconstructed termini positions, radiocarbon samples, and significant tree-ring ages. Radiocarbon ages are calibrated and all dates younger than 1200 A.D. are reported in calendar years A.D. Radiocarbon ages older than 1200 A.D. are reported as calibrated years B.P. Calibrated radiocarbon ages are shown as a 1σ range and tree-ring ages are reported as the initiation of growth ±5 years.

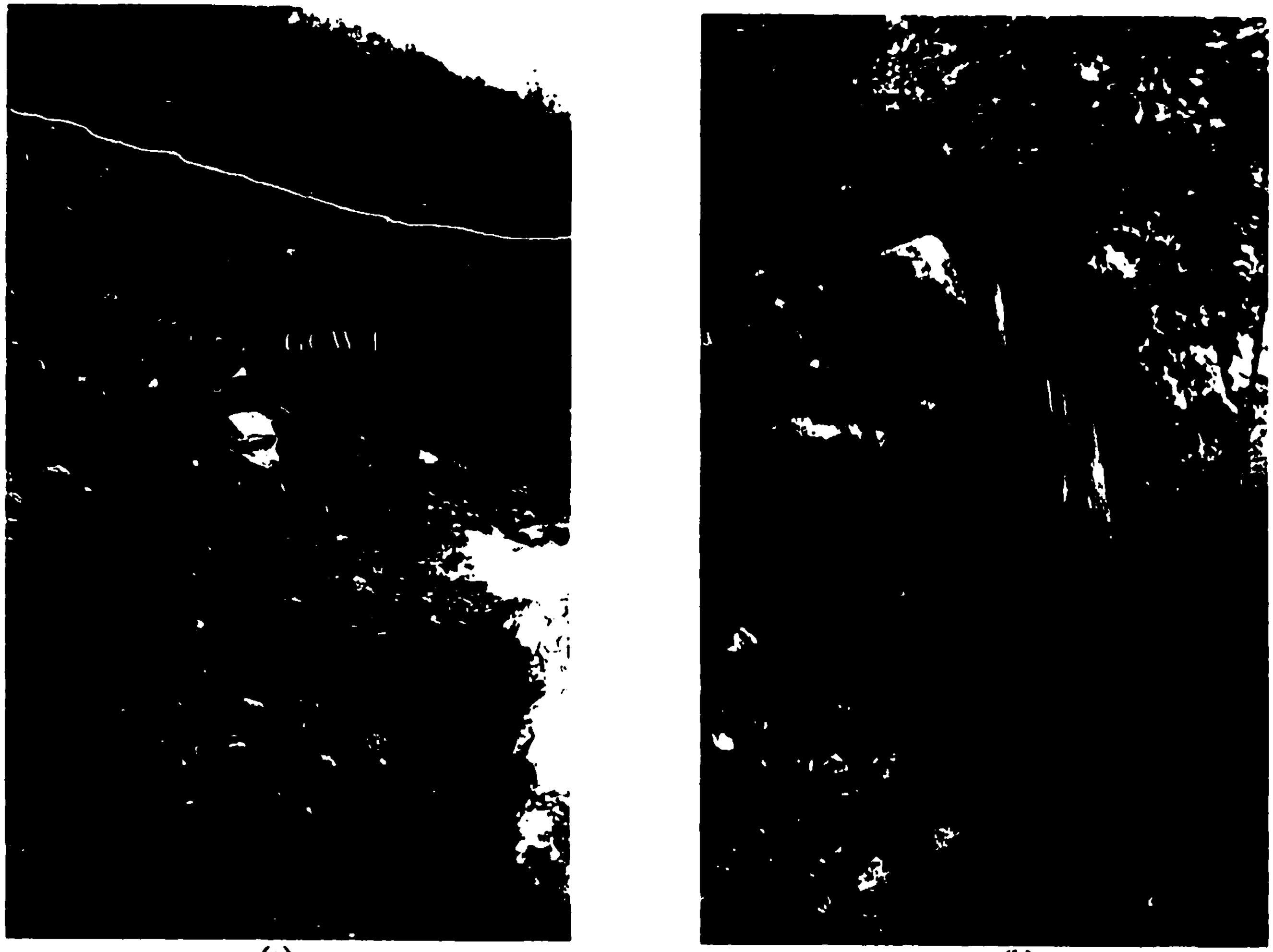

(a)

(b)

Figure 3.29 – (a) Exposure of two layers of glacial drift near the mouth of Garnet Creek and (b) Tree stumps rooted in the lower till near the mouth of Garnet Creek. The log from the lower exposure (GCW-1; Table 3.5) was dated at 3,341 (3,255) 3,168 calibrated years B.P.

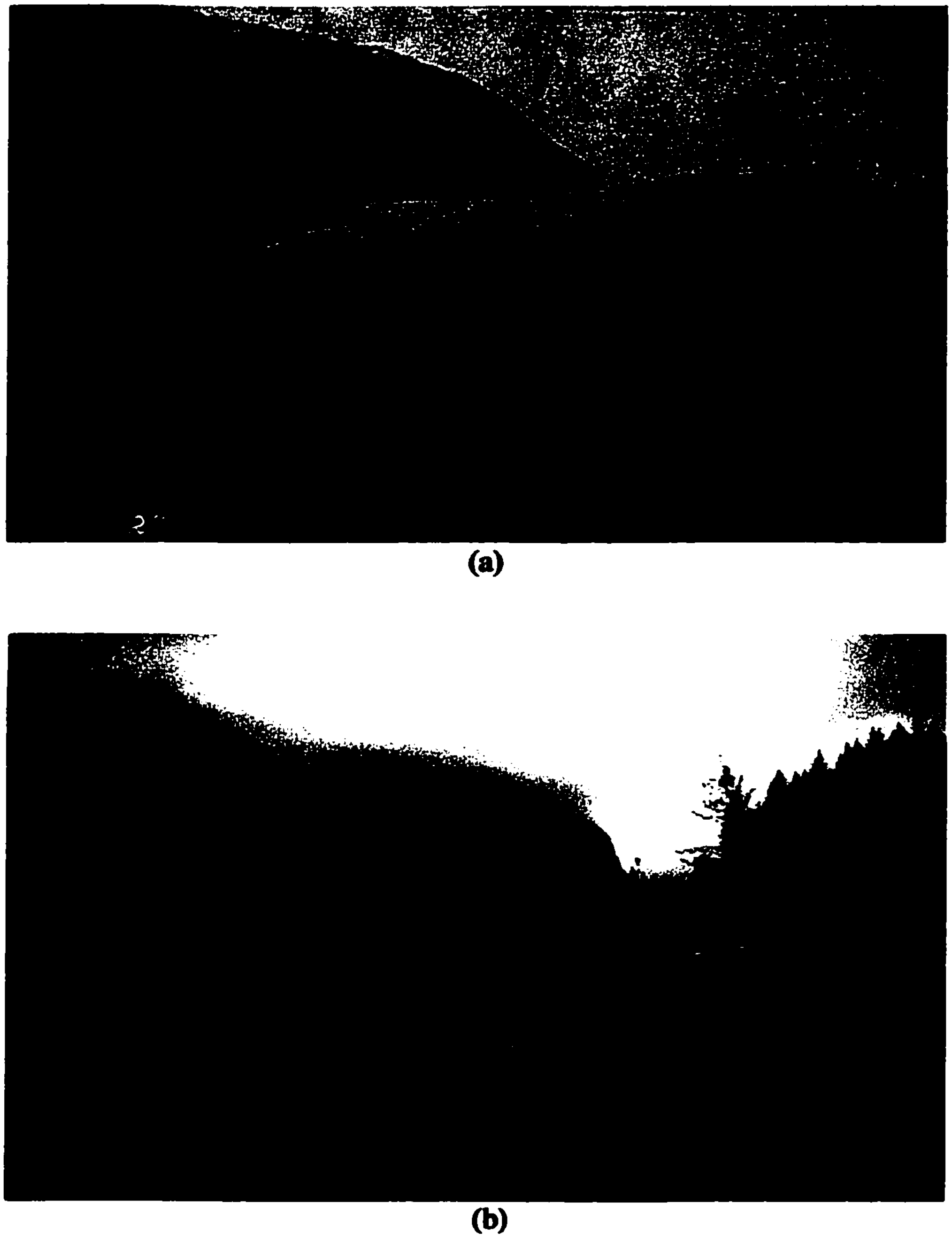

Figure 3.30 – (a) Historical photograph of the terminus of Patterson Glacier taken in the 1890's (source unknown) compared with (b) a 1995 photograph taken from the same location. These photographs show the Little Ice Age maximum position of Patterson Glacier.

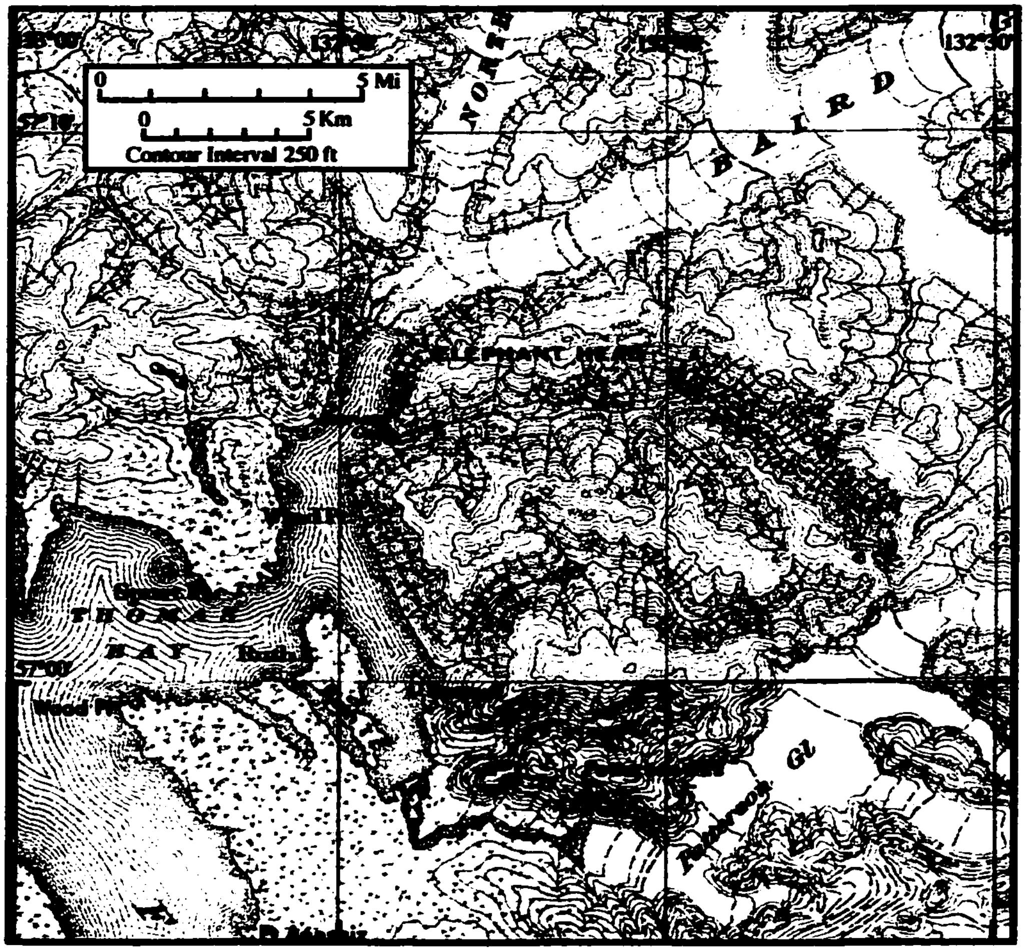

Figure 3.31 –International Boundary Commission map (International Boundary Commission, 1952) showing the position of Patterson and Baird glaciers, as surveyed between 1904 and 1909.

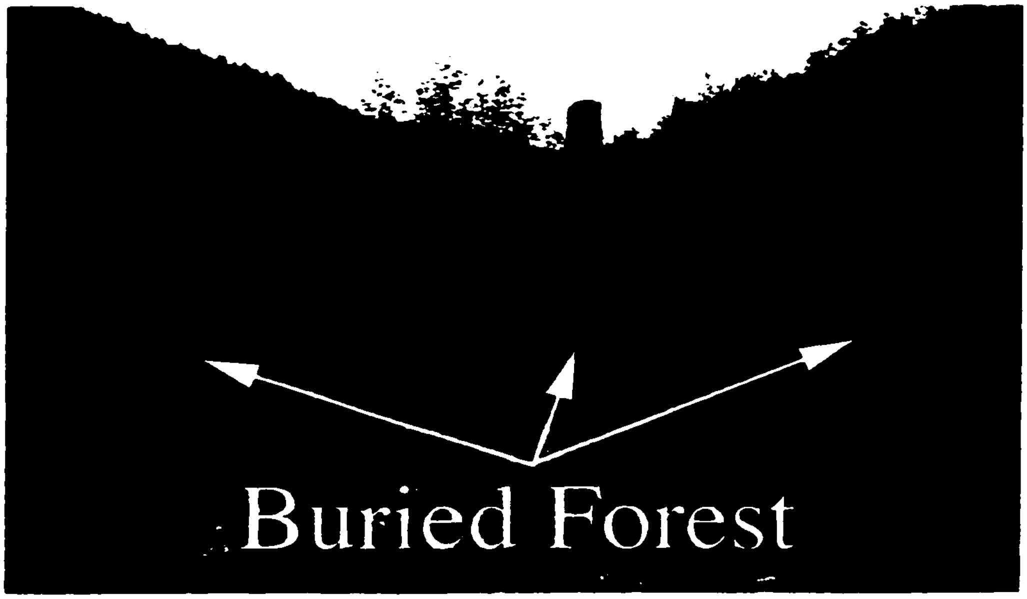

Figure 3.32 – Trees of the "buried forest" eroding out of outwash ca. 2.4 km in front of the 1995 terminus position of Patterson Glacier. Sample BF-3 (Table 3.5) from the buried forest was radiocarbon dated and cross dated with the CMC. It likely died ca. 1792 A.D. during the Little Ice Age advance of Patterson Glacier.

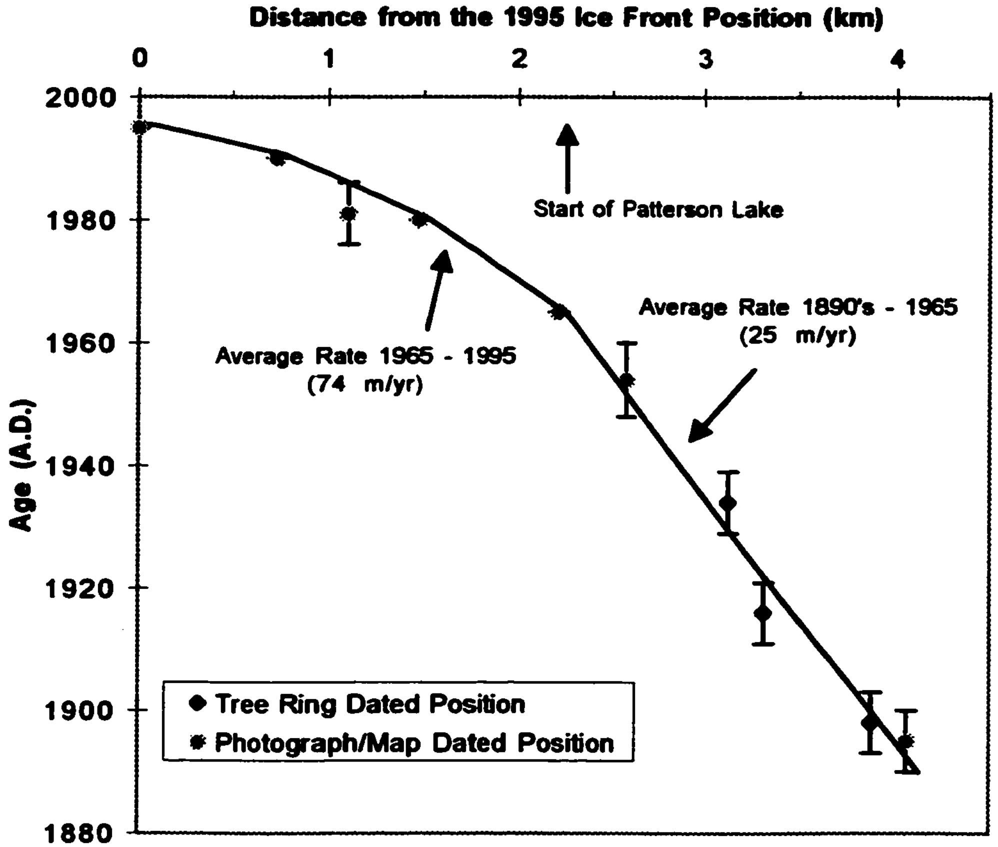

Figure 3.33 – Retreat of the Patterson Glacier terminus since the 19th century. Once the glacier formed a lake at it terminus in ca. 1965, retreat rates increased from 25 m/yr to 74 m/yr.

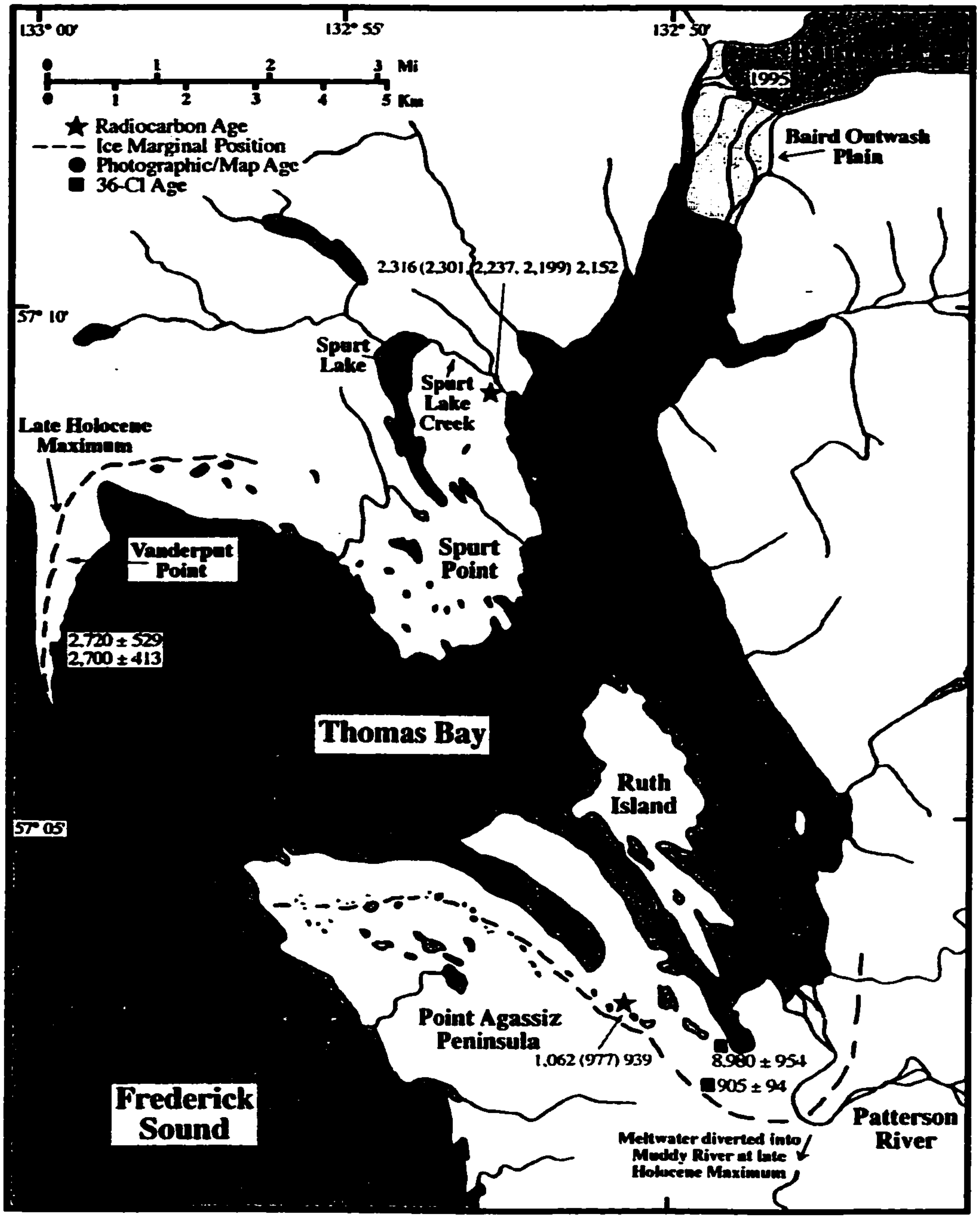

Figure 3.34 – Regional map of Baird Glacier and vicinity showing the location of mapped and reconstructed termini positions, radiocarbon samples, and ^{36}Cl samples. Radiocarbon ages are calibrated and all dates are reported as calibrated years B.P. Calibrated radiocarbon ages and ^{36}Cl exposure ages are shown as a 1σ range.

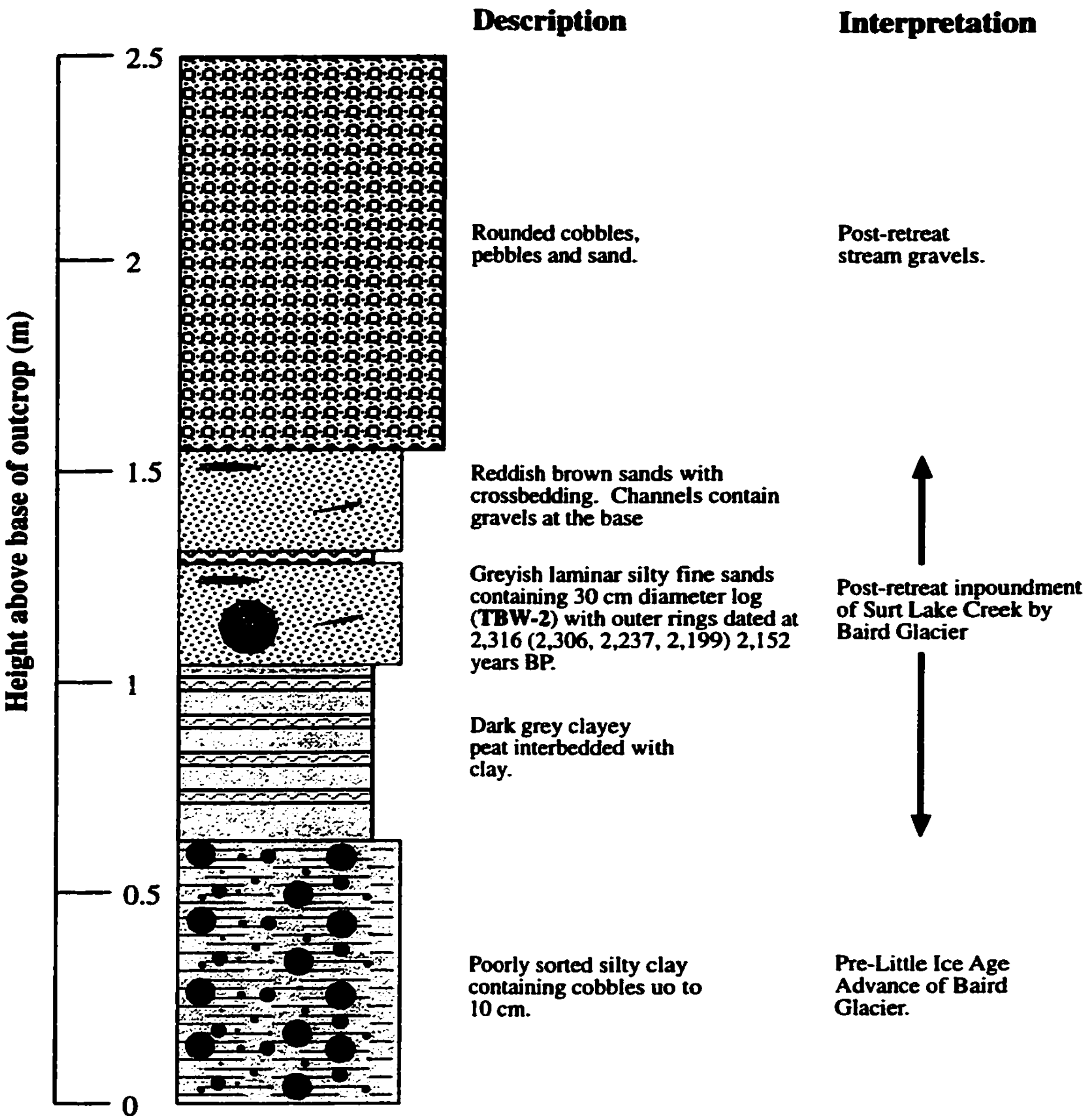

Figure 3.35 – Stratigraphic section of the exposure along Spurt Lake Creek, showing unit descriptions and interpretations as well as the location of radiocarbon-dated sample TBW-2 (Table 3.5).

Figure 3.36 – Brad Hunter (U.S. Forest Service, Petersburg) and Terry Swanson (University of Washington) sampling a granodiorite erratic (VAN-1; Table 3.7) on Vanderput Point, at the mouth of Thomas Bay.

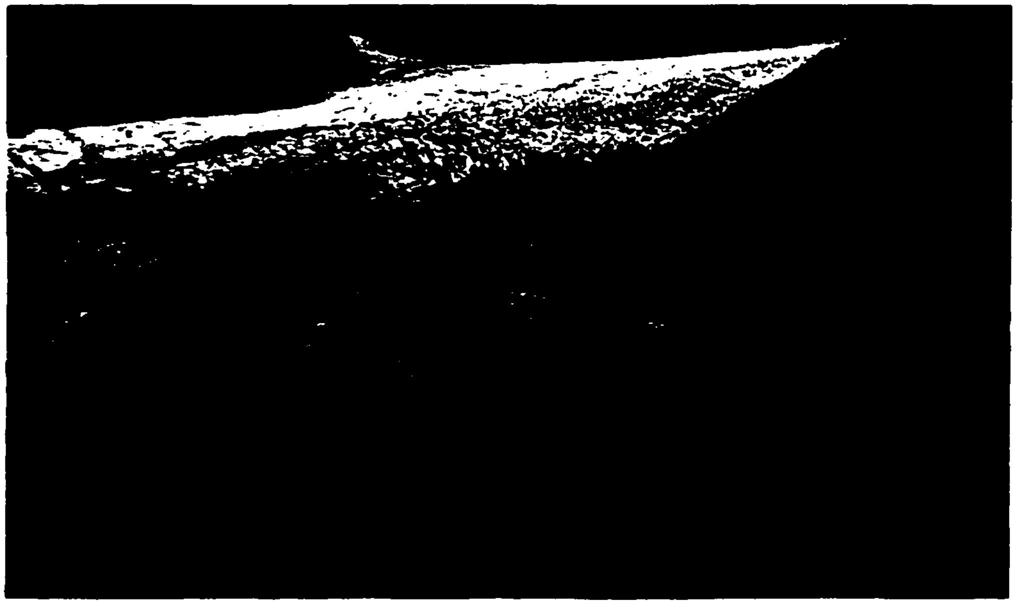

Figure 3.37 – Outwash apron in front of Baird Glacier that has been growing since at least the mid-18th century (photo from 1992).

Figure 3.38 – Trimline above the 1995 terminus of Baird Glacier that may reflect an earlier calving margin of the glacier.

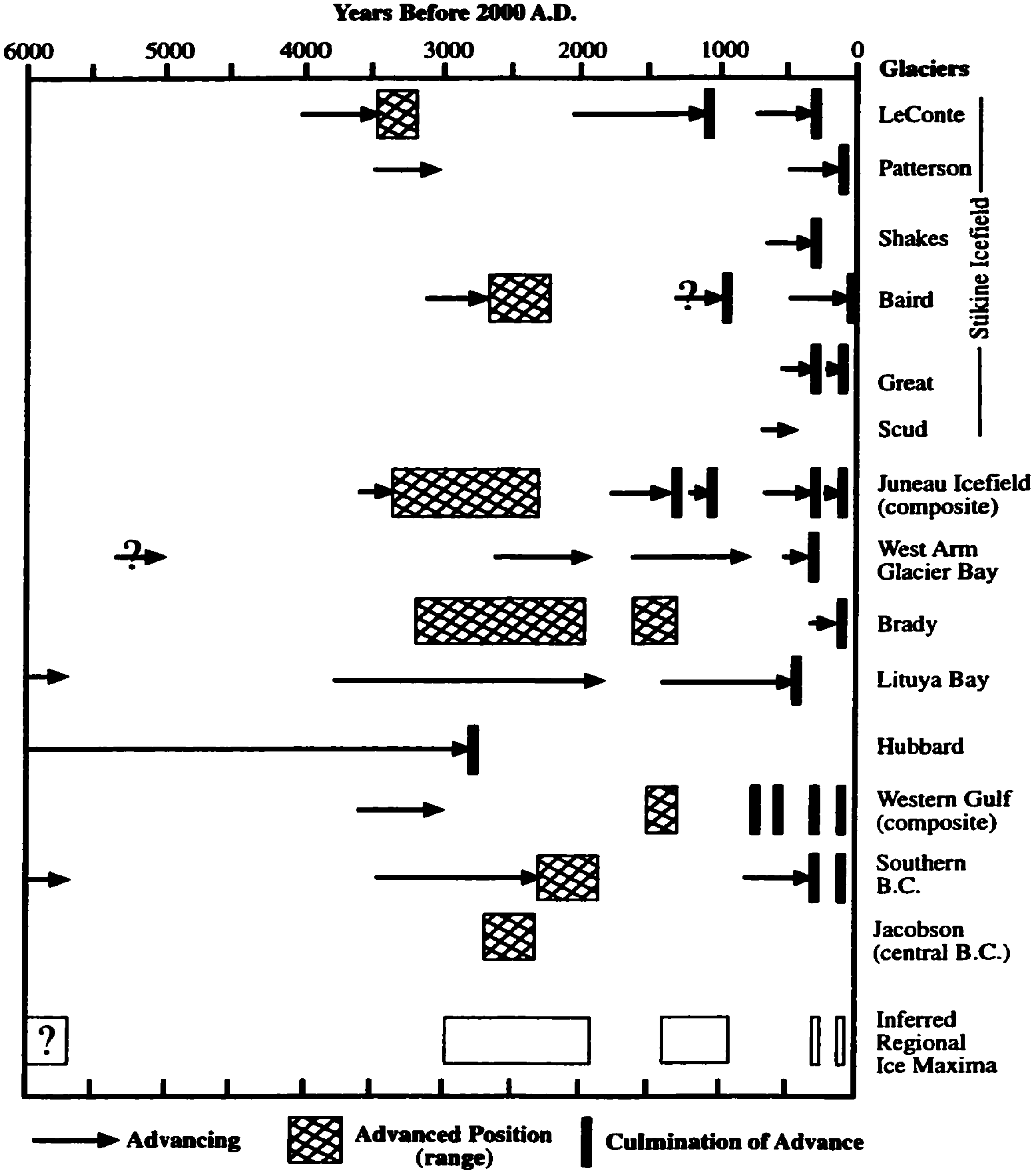

Figure 3.39 – Comparison of Neoglacial advances of glaciers along the coast of northwestern North America. Inferred regional ice maxima are times when a significant number of glaciers in northwestern North America were in advanced positions.

Table 3.1 – Basic data for glaciers included in this study (1995 statistics).

	Baird	Patterson	LeConte	Shakes
Latitude (°N)[1]	57°07'	56°57'	56°50'	56°48'
Longitude (°W)[1]	132°49'	132°39'	132°22'	132°10'
Orientation	West	West	South	South
Length (km)	50	21	36	16
Terminus condition	Stable	Retreating	Retreating	Retreating
Terminus position	Advanced	Retracted	Retracted	Retracted
Calving margin width (m)	0	0	1400	740
Water depth (m)	0	0	>80	<80
Ablation area (km^2)	257	39	34	24
Accumulation area (km^2)	527	64	438	54
Total area (km2)	784	103	472	78
ELA median (m)	1250	1190	915	975
AAR	0.67	0.62	0.93	0.69

[1] Latitute and Longitude position is for centerline of glacier at the terminus.

Table 3.2 – Significant tree cores from the study area used limit the age of deglaciated surfaces.

Glacier System	Sample ID	Species	Age of Inner Growth Ring (A.D.)	Year Growth Began ±5 (A.D.)	Diameter[1] (cm)	Altitude[2] (m)	Collected (A.D.)	Notes
Shakes	SL-1	Spruce	1797	1782	46	20	1994	
	SK-2	M. Hemlock	1821	1806	41	20	1995	
	SK-6	M. Hemlock	1568	1553	46	20	1995	
	SL-16	M. Hemlock	1573	>1558	76	20	1994	near core[3]
	SM-9	W. Hemlock	1704	1689	69	10	1994	
	SM-26	Spruce	1713	>1698	66	10	1994	near core[3]
Leconte	BC-12	W. Hemlock	1421	>1406	56	40	1993	near core[3]
	TP-5	Spruce	1801	1786	76	10	1993	
	MC-1	Spruce	1666	>>1651	117	30	1993	outer 40 cm only
	MC-13	Spruce	1812	1797	71	15	1993	
	CC-4	Spruce	1800	1785	58	30	1993	
	CC-9	W. Hemlock	1774	1759	76	120	1993	
	CC-15	Spruce	1820	1805	61	5	1993	
	CC-21	Spruce	1811	1796	87	5	1993	
	CC-26	Y. Cedar	1356	1341	84	180	1993	
	WP-4	W. Hemlock	1870	1855	61	45	1993	
	D-2	Spruce	1913	1898	51	25	1993	
	RI-4	Spruce	1953	1938	25	25	1993	
Patterson	PR-4	Spruce	1949	1934	56	65	1994	
	PR-5a	W. Hemlock	1696	>>1681	122	110	1994	outer 40 cm only
	PR-9	Spruce	1931	1916	41	65	1994	
	PR-15	Spruce	1946	1931	51	275	1994	
	PR-19	W. Hemlock	1255	>1240	61	300	1994	near core[3]
	PM-6	Spruce	1913	1898	51	65	1995	
	ESS-14	W. Hemlock	1554	1539	71	45	1994	

[1] Study used a 40-cm increment borer

[2] Appoximated using a map with a 100 ft (31 m) contour interval

[3] Increment core was within ca. 1 cm of the the true core of the tree

Table 3.3 – Radiocarbon dates (calibrated from Southon et al., 1990) used to determine an average marine reservoir effect of 925 yr.

SHELLS Sample Location and ID (RIDDL-)	^{14}C Age (^{14}C yr B.P)	Calibrated Age (cal yr B.P.)	Mean Age (cal yr B.P.)	WOOD Sample Location and ID (RIDDL-)	^{14}C Age (^{14}C yr B.P)	Calibrated Age (cal yr B.P.)	Mean Age (cal yr B.P.)	Shell-Wood Age Difference (yr)	Mean Difference (yr)
Endecko 87A-23 Core				**Endecko 87A-23 Core**					
978	10,770 ± 100	12,809 (12,699) 12,585	12,697	979	9940 ± 75	11,328 (11,071, 11,065, 11,030) 10,999	11,164	1,534	
980	10,960 ± 85	12,974 (12,879) 12,784	12,879	981	10485 ± 70	12,506 (12,402) 12,285	12,396	484	
982	11,020 ± 80	13,027 (12,935) 12,845	12,936	983	10290 ± 80	12,289 (12,135) 11,938	12,114	823	947
Cape Ball				**Cape Ball**					
1191	9,560 ± 140	10, 953(10,797, 10,755, 10,570) 10,380	10,667	1192	9090 ± 160	10,284 (10,031) 9,927	10,106	561	
Mary Point Location B				**Mary Point Location B**					
879	9,930 ± 120	11, 529 (11,008) 10,992	11,261	880	9070 ± 110	10,082 (10,020) 9,962	10,022	1,239	
881	9,710 ± 100	10,993 (10,954) 10,626	10,810	882	8930 ± 90	9,986 (9,928) 9,877	9,932	878	
883	9,790 ± 120	11,007 (10,987) 10,909	10,958	884	9070 ± 120	10,272 (10,020)9,955	10,114	845	
1193	9,780 ± 110	11,005 (10,982) 10,909	10,957	1194	9070 ± 90	10,072 (10,020) 9,972	10,022	935	
1195	9,870 ± 110	11,200 (11,000) 10,971	11,086	1196	9130 ± 120	10,284 (10,038) 9,981	10,133	953	
1205	9,850 ± 130	11,200 (10,997) 10.958	11,079	1206	9290 ± 160	10,438 (10,291, 10,248, 10,221) 10,039	10,239	841	
1207	9,690 ± 110	10,991 (10,945) 10,888	10,786	1208	8800 ± 120	9,927 (9,857, 9,699) 9,576	9,752	1,034	
1211	9,560 ± 110	10,929 (10,797, 10,755, 10,570) 10,418	10,674	1212	8850 ± 120	9,973 (9,884) 9,653	9,813	861	
1213	9,760 ± 120	11,003 (10,971) 10,888	10,946	1214	8860 ± 150	9,983 (9,890) 9,648	9,816	1,130	
1215	9,650 ± 170	10,994 (10,901) 10,474	10,734	1216	8950 ± 150	10,035 (9,959) 9,698	9,867	868	
1217	9,730 ± 100	10,996 (10,961) 10,706	10,851	1218	9030 ± 100	10,040 (9,986) 9,925	9,983	869	
1219	9,670 ± 130	10,991 (10,924) 10,548	10,770	1220	8970 ± 130	10,035 (9,971) 9,878	9,957	813	910
Mary Point Location A				**Mary Point Location A**					
977*	9,860 ± 120	11,200 (10,998) 10,964	11,082	976*	6830 ± 110	7,704 (7,622) 7,541	7,623	3,460*	
1197	7,530 ± 160	8,415 (8,325) 8,130	8,273	1198	6760 ± 120	7,654 (7,549) 7,475	7,565	960	
				1418	6200 ± 110	7,210 (7,155, 7,120, 7,087, 7,061, 7,035) 6,912	7,061		
1199	7,790 ± 110	8,646 (8,540, 8,534, 8510) 8,412	8,529	1200	6290 ± 100	7,264 (7,202)7,031	7,148	1,436	
				1419	6140 ± 90	7,167 (7,008) 6,888	7,028		
				1420	6210 ± 90	7,206 (7,159, 7,115, 7,090)7,000	7,103		
1201	762 ± 120	8,486 (8,374) 8,218	8,352	1202	6350 ± 100	7,371 (7,223) 7,172	7,272	1,081	
				1421*	7780 ± 90	8,577 (8,503) 8,415	8496*		
1203	7,390 ± 110	8,220 (8,134) 8,004	8,112	1204	6370 ± 110	7,382 (7,233) 7,176	7,279	833	
Mary Point Location C				**Mary Point Location C**					
1209	7,420 ± 90	8,319 (8,163) 8,029	8,174	1210	6560 ± 110	7,525 (7,394) 7,294	7,410	851	
				1422	6350 ± 110	7,376 (7,223) 7,099	7,238		1032*
Midden, Cohoe Creek Site				**Midden, Cohoe Creek Site**					
1228	5,715 ± 90	6,639 (6,487) 6,411	6,525	1227	4990 ± 110	5,896 (5,726) 5,605	5,751	775	775
Mary Point Location D				**Mary Point Location D**					
1434	3,190 ± 100	3,475 (3,385) 3,274	3,375	1435	2490 ± 90	2,743 (2,707, 2,628, 2,599, 2,496) 2,357	2,550	825	
1436	3,350 ± 100	3,693 (3,574) 3,465	3,579	1437	2710 ± 100	2,278 (2,781) 2,719	2,799	781	803
								Overal Average	925*

** Calculated averages reflect Southon's rejection of samples RIDDL 976, 977 and 1421*

Table 3.4 – Calibrated radiocarbon ages for deglaciation in southeastern Alaska and adjacent regions.

Location	Material[1]	^{14}C Age (^{14}C yr B.P.)	Calibrated Age (cal yr B.P.)	Age Range[2,3] (cal yr B.P.)	Source
Icy Bay (Munday Creek)	basal peat	10,820 ± 420	13,151 (12,747) 12,292	**13,151-12,292**	Heusser (1960)
Prince William Sound (Golden)	basal peat	10,015 ± 125	11,850 (11,376, 11,305, 11,211, 11,175, 11,122) 11,002	11,850-11,002	Heusser (1983)
Kenai Peninsula (Hidden Lake)	basal peat	13,730 ± 110	16,625 (16,460) 16293	**16,625-16,293**	Ager (1983)
Katalla (Copper River Delta)	shells?	14,430 ± 890	18,245 (17,291) 16,212	**17,320-15,287**	Sirkin and Tuthill (1971) from Mann (1986)
Lituya Bay	basal peat	10,520 ± 120	12,586 (12,442) 12,277	12,586-12,277	Mann (1986)
Lituya Bay	log	12,430 ± 100	14,761 (14,548) 14,353	**14,761-14,353**	Mann (1986)
Glacier Bay	peat	10,940 ± 155	13,015 (12,860) 12,705	13,015-12,705	McKenzie and Goldthait (1971)
Glacier Bay	spruce cone	11,170 ± 225	13,315 (13,078) 12,860	13,315-12,860	McKenzie and Goldthait (1971)
Glacier Bay	wood	10,400 ± 260	12,599 (12,298) 11,787	12,599-11,787	McKenzie and Goldthait (1971)
Glacier Bay	shells	10,000 ± 220	12,024 (11,204, 11179, 11,107) 10,982	11,099-10,057	McKenzie and Goldthait (1971)
Glacier Bay	shells	13,960 ± 360	17,176 (16,743) 16,285	**16,251-15,360**	McKenzie and Goldthait (1971)
Pleasant Island	basal organic sediment	12,910 ± 120	15,518 (15,292) 15,046	15,518-15,046	Hansen and Engstrom (1996)
Chilkat Peninsula	surface?	13,350 ± 100	16,127 (15,957) 15,785	**16,127-15,785**	Hamilton from Mann (1986)
Chilkat Peninsula	basal peat	10,690 ± 210	12,830 (12,621) 12,387	12,830-12,387	Cwynar (1990)
Chichagof Island	shells	12,130 ± 110	14,345 (14,152) 13,974	**13,420-13,049**	Hamilton from Mann (1986)
Emerged delta near Auke Bay (R-1)	barnacles in life position	12,730 ± 500	15,796 (15,001) 14,267	14,871-13,342	Miller (1973)
Emerged delta near Auke Bay (R-1)	mollusk shell	12,880 ± 500	16,007 (15,243) 14,464	**15,082-13,539**	Miller (1973)
Emerged delta near Auke Bay (R-1)	mollusk shell	12,300 ± 350	14,897 (14,371) 13,917	13,972-12,992	Miller (1973)
Emerged Delta (R-2)	mollusk shell	10,888 ± 340	13,132 (12,804) 12,459	12,207-11,534	Miller (1973)
Gasteneau Channel Formation	mollusk shell	11,920 ± 1,000	15,315 (13,895) 12,841	**14,390-11,916**	Miller (1973)
Gasteneau Channel Formation	mollusk shell	9,700 ± 800	12,423 (10,951) 9,912	11,498-8,987	Miller (1973)
Montana Creek	basal peat	10,300 ± 400	12,636 (12,152) 11,004	12,636-11,004	Heusser (1960)
Lemon Creek	basal peat	10,300 ± 600	12,826 (12,152) 10,952	12,826-10,952	Heusser (1960)
Thomas Bay	mollusk shell	12,670 ± 60	15,083 (14,905) 14,715	**14,158 -13,790**	This study
Petersburg	mollusk shell	13,280 ± 60	15,990 (15,859) 15, 726	**15,065-14,801**	This study
Petersburg	shells	12,400 ± 800	15,749 (14,506) 13,524	14,824-12,599	Ives et al. (1967) from Mann (1986)
Prince of Wales Island	shells	9,510 ± 280	10,989 (10,770, 10,769, 10540, 10,503, 10,486) 10,154	10,064-9,229	Swanston (1969) from Mann (1986)
Prince of Wales Island	brown bear bones	12,295 ± 120	14,586 (14,364) 14,165	**14,586-14,165**	Heaton (1996)
Queen Charlotte Islands	plant detritus	16,000 ± 570	19,525 (18,876) 18,338	**19,525-18,338**	Blaise e. al. (1990)
Port Hardy, BC	basal peat	13,630 ± 310	16,730 (16,332) 15,906	**16,730-15,906**	Hebda (1983)
Port Hardy, BC	shells	12,930 ± 160	15,601 (15,325) 15,024	14,676-14,099	Howes (1981)
Port Hardy, BC	shells	12,250 ± 220	14,642 (14,304) 14,005	13,717-13,080	Howes (1981)

[1] as reported by source

[2] minus marine reservoir effect of 925 yrs for shell samples

[3] Oldest date from each region is in bold

Table 3.5 – Calibrated radiocarbon ages from the study area.

Glacier System	Sample ID	Material	^{14}C Age	1σ	Calibrated Age (cal yr B.P.)	(A.D./B.C.)	Source
Petersburg	SCAN-3	shell	13,280	± 60	15,990 (15,859) 15,726	14,040-13,776 B.C	this study
Shakes	SM-PB-80	basal peat	300	± 70	463 (309) 287	1487-1663 A.D.	this study
	SL-3	wood	130	± 50	272 (255, 225, 134, 28, 0) 0	1678-1950 A.D.	this study
LeConte	CC-15	wood	3,850	± 30	4,343 (4,238) 4,155	2393-2205 B.C.	this study
	CC-4	wood	3,030	± 30	3,320 (3,214) 3,167	1370-1217 B.C.	this study
	CC-7	wood	2,160	± 25	2,147 (2,138) 2,117	197-167 B.C.	this study
	CC-11	wood	1,220	± 50	1,223 (1,161) 1,064	727-886 A.D.	this study
	GX-9387	wood	640	± 150	688 (643, 590, 571) 517	1262-1433 A.D.	Post & Motyka (1995)
Patterson	GCW-1	wood	3,050	± 50	3,341 (3,255) 3,186	1391-1218 B.C.	this study
	BF-3	wood	270	± 50	421 (299) 0	1529-1950 A.D.	this study
Baird	TBS-95	shell	12,670	± 60	15,083 (14,905) 14,715	13,133-12,765 B.C.	this study
	TBW-2	wood	2,230	± 25	2,316 (2,306, 2,237, 2,199) 2,152	366-202 B.C.	this study
	PTAG-2-160	basal peat	1,100	± 60	1,062 (977) 939	888-1011 A.D.	this study
Stitine River	S-2297	tree stump	455	65	530 (508) 472	1420-1478 A.D.	Ryder (1987)
	S-2298	tree stump	625	140	672 (638, 600, 562) 515	1278-1435 A.D.	Ryder (1987)
	S-2279	antlers	3,760	70	4,231 (4,127, 4,115, 4,092) 3,988	2281-2038 B.C.	Ryder (1987)

Table 3.6 – Cosmogenic 36Cl samples discussed in this study.

		Erosion Rate: 0 mm/10^3 yr			Erosion Rate: 1.0 mm/10^3 yr		
Sample ID	Rock Type	Age (yr)		Error (yr)	Age (yr)		Error (yr)
XTAL-1	granodiorite bedrock	12,200	±	327	12,050	±	323
XTAL-2	granodiorite boulder	8,470	±	339	8,390	±	336
XTAL-3	granodiorite bedrock	11,090	±	318	10,960	±	315
XTAL-4	granodiorite bedrock	11,920	±	319	11,770	±	315
XTAL-5	granodiorite bedrock	9,510	±	761	9,340	±	747
XTAL-6	granodiorite bedrock	10,800	±	512	10,650	±	504
XTAL-7	granodiorite boulder	14,790	±	479	14,510	±	470
SR-2	granodiorite bedrock	13,510	±	781	13,170	±	761
SR-3	granodiorite bedrock	11,240	±	1,236	11,010	±	1,211
			±			±	
VAN-1A	granodiorite erratic	2,750	±	535	2,720	±	529
VAN-1B	granodiorite erratic	2,720	±	416	2,700	±	413
TB-1	diorite erratic	9,190	±	976	8,980	±	954
TB-2	granodiorite erratic	910	±	95	905	±	94

CHAPTER 4: TIDEWATER GLACIERS AND CLIMATE CHANGE

BACKGROUND - CALVING THEORY

It has long been known that the steady-state position of alpine glacier termini is related to climate. Ablation-season temperatures and accumulation-season precipitation are the primary factors controlling a glacier's mass balance and the corresponding equilibrium line altitude (ELA). If a change in climate causes a shift in the ELA, the glacier terminus will respond by advancing or retreating toward a new steady-state position. The advance/retreat behavior of tidewater calving glaciers has been shown to be mainly a function of fjord geometry (Mercer, 1961), water depth at the glacier terminus (Brown et al., 1982), and sedimentation and sediment recycling at the glacier terminus (Powell, 1991). These three factors directly influence the rate of iceberg calving at the glacier terminus, which is the dominant process of ice loss in the ablation zone.

Post (1975) was one of the first to propose that water depth at the calving margin strongly affects the rate of iceberg calving. Glaciers that terminate on a morainal shoal are generally stable, but once a glacier retreats into water that deepens as the ice front recedes, calving rate increases rapidly and results in drastic retreat of the terminus. Using data collected from 13 Alaskan tidewater calving glaciers, Brown et al. (1982) derived the following relationship between calving speed and water depth:

$$V_C = C \times H_w + D$$

where V_C is the mean calving speed (m a^{-1}), C is a calving coefficient (27.1 ± 2 a^{-1}), H_w is the mean water depth at glacier front (m) and D is a constant (0 m a^{-1}). The data fit this empirical relationship with a correlation coefficient (r) of 0.95, indicating that much of the variability in average annual calving rate can be accounted for by water depth.

Calving is also an important form of ablation for glaciers that terminate in freshwater; however, the factors that control calving rate along freshwater and tidewater glacier margins apparently differ. Funk and Röthlisberger (1989) determined a relationship between calving speed and water depth based on analysis of six glaciers in Alaska, Greenland, Italy, and Switzerland that calve into lakes. They found that the same basic calving relationship developed for tidewater calving glaciers (Brown et al., 1982) was true for freshwater calving glaciers, only the calving coefficient (C) was 1.9 a^{-1} and D equals 12. Calving speed of these glaciers is about 1/10 that found for Alaskan tidewater glaciers (Brown et al., 1982). Laumann and Wold (1992) used this relationship to predict the retreat of Austdalsvatn Glacier, Norway after the terminus was flooded by rising lake level. They found that the retreat was consistent with Funk and Röthlisberger's model. Furthermore, some freshwater calving glaciers apparently have floating tongues that calve tabular icebergs. Such differences may be due to differences in water salinity, water temperature, and/or ice buoyancy.

Post (1975) hypothesized that a tidewater calving glacier can only advance down a fjord if a shallow terminal moraine shoal is built at the ice margin, thereby decreasing water depth at the terminus and lowering calving speed. By influencing water depth at the ice front, sedimentation rate at the glacier terminus determines the rate at which a tidewater glacier can advance downfjord. Aggradation at the terminus can produce a morainal shoal that develops at a rate dependent on the size of the drainage basin, the erosion rate, and the sediment dispersal pattern (Powell, 1991), and the rate of sediment recycling at the terminus (Alley, 1991). This results in relatively slow advance into a deep fjord (10's m/yr) because the advance is limited by the rate of moraine construction and migration. If the glacier retreats from the shoal into water that deepens upfjord, a progressive increase in the calving rate will result and can lead to irreversible retreat of the terminus. Rapid loss of ice causes retreat rates to be approximately an order of magnitude faster (100's m/yr) than advance rates. Retreat continues until the calving flux equals ice flux. This occurs either where the cross-sectional area of the fjord is greatly reduced or at the head of the fjord in shallow water where the glacier remains until a positive mass balance and construction of a new morainal shoal will permit it to readvance. This cycle is known as the temperate tidewater glacier advance/retreat cycle (Figure 4.1). Studies based on modern and historical evidence from Alaskan glaciers suggest that this cycle typically lasts from 1,000 to 2,000 years, with an advance phase that is an order of magnitude longer than the retreat phase (Viens, 1995). During the cycle, a tidewater calving glacier can be in one of four phases of the advance/retreat cycle: (1) advancing, (2) stable-extended, (3) drastically retreating, or (4) stable-retracted (Figure 4.1).

By using accumulation area ratio (AAR) data for Alaskan tidewater calving glaciers, Viens (1995) produced a model showing that climate acts as a first-order control on the advance/retreat cycle of calving glaciers by setting maximum limitations on glacier advance and determining where the terminus will stabilize during retreat. By placing constraints on the stable-advanced and stable-retracted positions of tidewater glacier termini, climate also affects the length of the calving cycle. Furthermore, this model also predicts that a state of quasi-equilibrium exists at the terminus between ice flux (primarily controlled by climate) and calving flux (primarily controlled by water depth and fjord geometry) throughout the advance phase of the calving cycle. During the retreat phase the glacier is often insensitive to changing climate because the calving flux is much greater than ice flux. This means that the terminus position is potentially sensitive to changing climate for 90% of the calving glacier cycle.

A rising ELA seems to have a more dramatic impact on tidewater calving glaciers than does a falling one because retreat can lead to decoupling of the glacier/climate system. A drop in ELA would cause a land-based glacier to advance, but the advance of a tidewater glacier may be offset by an increase in the calving flux as the glacier advances into water that deepens as the ice front advances. Therefore, the response of a tidewater glacier terminus to a positive climate change may be restricted by the rate of growth and migration of a terminal moraine.

Because the termini of advancing calving glaciers are in a state of quasi-equilibrium between ice flux and calving flux, a significant rise in ELA (e.g., the scale of the rise at the end of the Little Ice Age) may upset this state and trigger a general retreat of tidewater calving glacier termini, even if they are not at fully extended positions. Such a trigger would cause many of the tidewater glaciers to retreat more-or-less in phase. Eighty to ninety percent of the tidewater calving glaciers in Alaska have retreated in the last 250 years, implying a related cause (Viens, 1995). It seems likely that this cause was the global rise in ELA between ca. 1750 and 1950.

Tidewater calving glaciers that have just completed the retreat phase of the tidewater calving glacier advance/retreat cycle will be the least sensitive to climate change because once they have retreated into shallow water, many will have a much high ice flux than calving flux at the terminus. Therefore, the terminus position of glaciers that were retreating or in a retracted position at the end of the Little Ice Age may not have been affected by the changing climate, and would have begun to readvance as soon as they stabilized at the head of the fjord. This may explain why 10 to 20% of Alaska's tidewater glaciers apparently have not retreated in the last 200 years, despite the marked shift in regional climate.

RESPONSE OF STIKINE GLACIERS TO CLIMATE CHANGE

By comparing middle to late Holocene glacier histories reconstructed along the southern margin of the Stikine Icefield (Chapter 3) with summer temperature reconstructions from palynology (Figure 2.2; Heusser, 1995) and dendrochronology (Chapter 2), it may be possible to correlate changes in summer temperature with retreat of glacier termini. Neoglacial terminus fluctuations can be compared with Heusser's (1995) summer temperatures derived from the Munday Creek pollen core (Figure 2.2), which show low-frequency changes throughout the Holocene. In contrast, Little Ice Age glacier fluctuations can be compared with high-resolution tree-ring records from Crystal Mountain (Figures 2.4 and 2.5).

Early to middle Neoglaciation

Without a high-resolution regional, or even a low-resolution local, temperature proxy for the Holocene, it is difficult to draw any significant conclusions about the relationship between tidewater-calving glacier retreat and middle Holocene climate change. However, the significant regional periods of glacier recession during the Holocene (of both calving and land-based glaciers) are roughly correlative around the northeastern Pacific Ocean (Figure 3.39). These include Neoglacial events between 4,000 and 1,900, 1,600 and 900 years ago, and Little Ice Age retreats that began in the mid-18th, and late-19th centuries. The fact that these events are broadly synchronous around the region implies that glacier retreat throughout coastal southeastern Alaska and British Columbia was triggered by the same events. (Actual glacier response time may range over several decades because of differences in terminus response time.) The only variables that could affect glaciers over such a large region would be regional (or global) climate change or sea level change. Because retreat affected both land-based and calving glaciers, it is likely that climate change is the major variable affecting both calving and land-based glaciers during these time periods. Heusser's (1995) climate record further implies that significant cooling and increased precipitation occurred between ca. 5,000 and 3,000 years ago and that warming episodes and decreased precipitation occurred between ca. 2,500 and 2,000, and 1,500 and 1,000 years ago, when glaciers within the region began retreating.

Late Neoglaciation: Little Ice Age

The two major periods of glacier retreat during the Little Ice Age described in Chapter 3 occur during the span of the Crystal Mountain tree-ring chronology (CMC) – the mid-18th and late-19th century retreat phases. These retreat phases are represented in the study area by LeConte and Shakes glaciers, which began retreating in the mid to late 1700's, and Patterson Glacier, which began retreating in the 1890's. As shown in Figure 3.39, both of these periods were times of ice retreat throughout southeastern Alaska.

To smooth out annual fluctuations that may not affect glacier termini, and more easily compare high-resolution climate records with low-resolution glacier chronologies, the CMC was smoothed with a 20-year running mean. The decade retreat began from the Little Ice Age maximum position for calving (grey boxes) and land-based (white boxes) glaciers was then superimposed on top of the 20-year running mean (Figure 4.2; Table 4.1).

Prior to the 20th century, the most dramatic rise in summer temperature, as recorded by ring width, occurred during the mid-18th century from ca. 1750-1770 A.D. Starting about 1750 and lasting until about 1800 A.D., 14 land-based and calving glaciers in southeastern Alaska began retreating from their most extensive Little Ice Age limits. Three additional glaciers in the region began retreating in the late 19th and early 20th centuries, a time of gradually warming summer temperatures. These data illustrate two points – (1) calving and land-based glacier retreat has been concentrated in two time periods, implying a common trigger for retreat, and (2) the most significant period of retreat (mid-18th century) corresponds with a period of rapid warming.

The late-19th century retreat of glacier termini is not correlated with a period of rapid warming. Because glacier mass balance is a function of both summer temperatures and winter precipitation, it is possible that this period of retreat involved glaciers that were more sensitive to changes in winter precipitation. Unfortunately, reliable precipitation records from multiple weather stations do not start until the 20th century. However, general precipitation trends show that the early 20th century was drier than average. It is possible that this trend extends back into the late 19th century and may explain this period of retreat. Many land-based glaciers formed less-extensive end moraines at this time; however, calving glaciers that were already in the retreat phase would not be significantly affected by changing mass balance at that time.

There is no definitive physical characteristic that is shared among glaciers that retreated in the late 19th century compared to those that retreated in the mid-18th century. Three of the four glaciers that retreated in the late 19th century, or have not yet started to retreat (e.g., Baird Glacier) are large glacier systems with surface areas greater than ca. 800 km^2 (e.g., Icy Bay glacier system). However, Patterson Glacier, with a surface area of ca. 100 km^2 began retreating in the 1890's and several large glacier systems (e.g., Taku Glacier, Glacier Bay) already retreated in the 18th century. Along with the tidewater glaciers in Lituya Bay, which retreated out of phase in the early 17th century, Taku Glacier, Hubbard Glacier, and many of the smaller glaciers that were once part of the larger Glacier Bay system are now the only large glaciers in the region with advancing termini.

IMPLICATIONS FOR CALVING THEORY

The close association between the retreat of tidewater and freshwater calving glaciers with warming climate supports the hypothesis proposed by Viens (1995) that climate drives tidewater calving glacier advance/retreat cycles and that morainal shoals of tidewater glaciers can be used as a climate proxy. These relationships can be used to predict the response of glaciers in the study area to rising global temperatures over the next 50 years.

CALVING THEORY, RECONSTRUCTIONS, AND HEINRICH EVENTS

Although this study reconfirms Viens' (1995) model that climate is a first order control of the tidewater calving glacier advance/retreat cycle, it is not possible to separate the effects of summer temperature and winter precipitation on glacier termini response. At least one major period of glacier retreat during the Little Ice Age was shown to be related to warming summer temperatures; however, a second period may have been caused my decreasing winter precipitation. Very low correlation values ($r \leq 0.15$) between annual and summer temperatures and annual and winter precipitation in southeastern Alaska during the 20th century indicate that these two climatic variables act independently. Therefore, further precipitation proxy data are needed to understand fully the different effects on tidewater calving glacier termini.

As proposed by Viens (1995), moraines tell us something about climate at the time a glacier begins to retreat. For a typical temperate, land-based mountain glacier, it is assumed that the moraine represents a time when the glacier reached near steady-state and had an AAR of ca. 0.65 ± 0.05 (Porter, 1975). For calving glaciers the position of the submerged moraine and water depth over the moraine, taken in context with the distribution of the glacier surface area, will be representative of the overall climatic conditions just prior to the time of retreat. If the morainal shoal is broad and shallow (< 10 m) it is likely that the calving flux was negligible just prior to retreat of the terminus. Therefore, the moraine probably represents the position of a tidewater glacier in near steady-state, and the paleo-ELA can be estimated using the area-altitude method (Porter, 1975; Viens, 1995). If the moraine is deeply submerged, or if there is no fjord-bottom moraine, then one must assume that significant calving was occurring before retreat began and the AAR was greater than ca. 0.65. If the calving flux can be estimated - by determining moraine depth, fjord width, and estimated ice velocity - then the AAR can be estimated and ELA can be approximated by using the area-altitude method.

The crest of the Thunder Point Moraine in LeConte Bay is about 60 m deep. The depth of the moraine implies that calving contributed significantly to ablation and that it is unlikely that the terminus of LeConte Glacier was in a stable-extended position at the time retreat began. In fact, the most recent retreat of LeConte Glacier may have been caused by retreat off the Thunder Point Moraine during the advance stage of the tidewater calving glacier cycle, reinforcing the idea that advancing tidewater calving glaciers are sensitive to climate change. If the terminus had been advancing on a morainal shoal 60 m below sea level, then the ice flux at the terminus must have been significant to account for calving, and the AAR would have been greater than 0.65 at that time. Assuming no significant change in sea level, LeConte Glacier would have had an AAR similar to that of LeConte Glacier today (0.90; Viens, 1995).

Other factors that result in significant changes in water depth at the glacier terminus can also effect tidewater glacier stability. Therefore, the effects of local tectonics, glacial isostasy, and eustatic sea-level changes must not be overlooked when making climatic interpretations. The latter factor, for example, may have contributed significantly to the retreat of calving ice sheet margins at the end of the Pleistocene.

The role of climate on calving glacier termini at the end of the last glacial maximum is still difficult to quantify. Quantifying this effect on tidewater calving glacier cycles is in its preliminary stages; however, quantifying the role of climate change on freshwater calving glaciers is even more preliminary. This study supports Funk and Röthlisberger's (1989) model of slower rates for freshwater calving then for tidewater calving, and shows that at least in one instance (Shakes Glacier), freshwater calving glaciers are also responding to warming summer temperatures in the mid-18th century. However, it does not help quantify the relationship, nor does it necessarily reveal how large freshwater calving ice sheet margins, such as those present at the end of the Pleistocene, behave.

If ice sheets involved in Heinrich Events (Heinrich, 1988) were temperate-based, then it is likely that retreat was initiated by changing climate. After initiation of Heinrich Events , ice sheets would retreat into water that deepened as the ice front receded, and their behavior would have become decoupled from climate. At that stage, they would have had more of an influence on climate, by affecting the surface water temperature and salinity of the North Atlantic, than climate had on them.

PREDICTIONS

With a basic understanding of the role of climate change on calving glacier dynamics, it is possible to make some predictions about the future behavior of the glaciers included in this study. The initial predictions assume no change in climate in the next 50 years. However, because it is expected that temperatures will continue to rise well into the next century (Houghton et al., 2001), some further predictions are made below.

Shakes Glacier

Because Shakes Glacier is approaching both steady state and what appears to be the head of Shakes Lake, it is likely that Shakes Glacier will continue to retreat until its terminus is grounded at or above the level of the lake. At this point it is expected to stabilize, unless temperatures continue to rise, in which case Shakes will continue to retreat.

LeConte Glacier

LeConte Glacier will most likely continue its current retreat phase until the water depth at the terminus decreases. It is unlikely that it will retreat out of tidewater, because the ice flux at the terminus of LeConte Glacier is extremely high, and this should cause the glacier to stabilize in moderately deep water in the near future. When this happens, advance will be controlled by the rate of sedimentation at the glacier terminus (which is slow in the case of LeConte Glacier).

Patterson Glacier

Patterson Glacier most likely will continue to retreat until it is completely out of Patterson Lake (or in shallow water). Based on the geometry of the basin, it appears that this will occur in the next 10 to 20 years. AAR measurements indicate that the glacier is near steady-state, and should stabilize in this position, unless a major change of climate occurs.

Baird Glacier

Baird Glacier, with an AAR of only 0.65, most likely will began to retreat in the next 20 years as global temperatures rise. Once the glacier retreats off its outwash apron and into the deep basin upvalley, a freshwater lake will develop, and the glacier will begin calving. It is likely, that the retreat of Baird Glacier will continue well into the future at a pace similar to that of Shakes Glacier. Based on the geometry of the fjord, the retreat could create a lake that is more than 25 km long, extending all the way to the foot of Devil's Thumb.

FUTURE WORK

Future work should be directed at three outcomes – (1) extending and better quantifying climate records constructed from tree rings, (2) better quantifying the tidewater calving glacier advance/retreat cycle, and (3) better understanding the processes associated with temperate freshwater calving.

(1) Recent studies (Bradley, 1999; Briffa et al., 1998; D'Arrigo and Jacoby, 1993) have shown that late-wood density provides a potentially better climate proxy than ring width. Therefore, further analysis of the Crystal Mountain tree-ring chronology may provide a means of quantifying temperature changes during the last 400 years. Furthermore,

collection and analysis of other high-altitude trees from the region may provide a means of extending the climate record throughout the Little Ice Age. Despite the additional data provided by this study, the region between south-central Alaska and southern British Columbia still lacks comparable Holocene climate records.

(2) Both field data (this study) and modeling (Viens, 1995) suggest that the relationship between tidewater calving glaciers and climate change is quantifiable. Quantifying this relationship would help improve understanding of tidewater calving glacier advance/retreat cycles, the climatic significance of morainal shoals, and the role of calving in Pleistocene deglaciation episodes and during Heinrich Events.

(3) Very little work has been done to identify and quantify the processes that operate at the termini of freshwater calving glaciers. The study by Funk and Röthlisberger (1989) used only six glaciers to determine a calving law and, therefore, is extremely preliminary. As glacier termini continue to retreat during the 21st century, impounding lakes between the terminal moraine and the ice front, opportunities for studying these processes should abound.

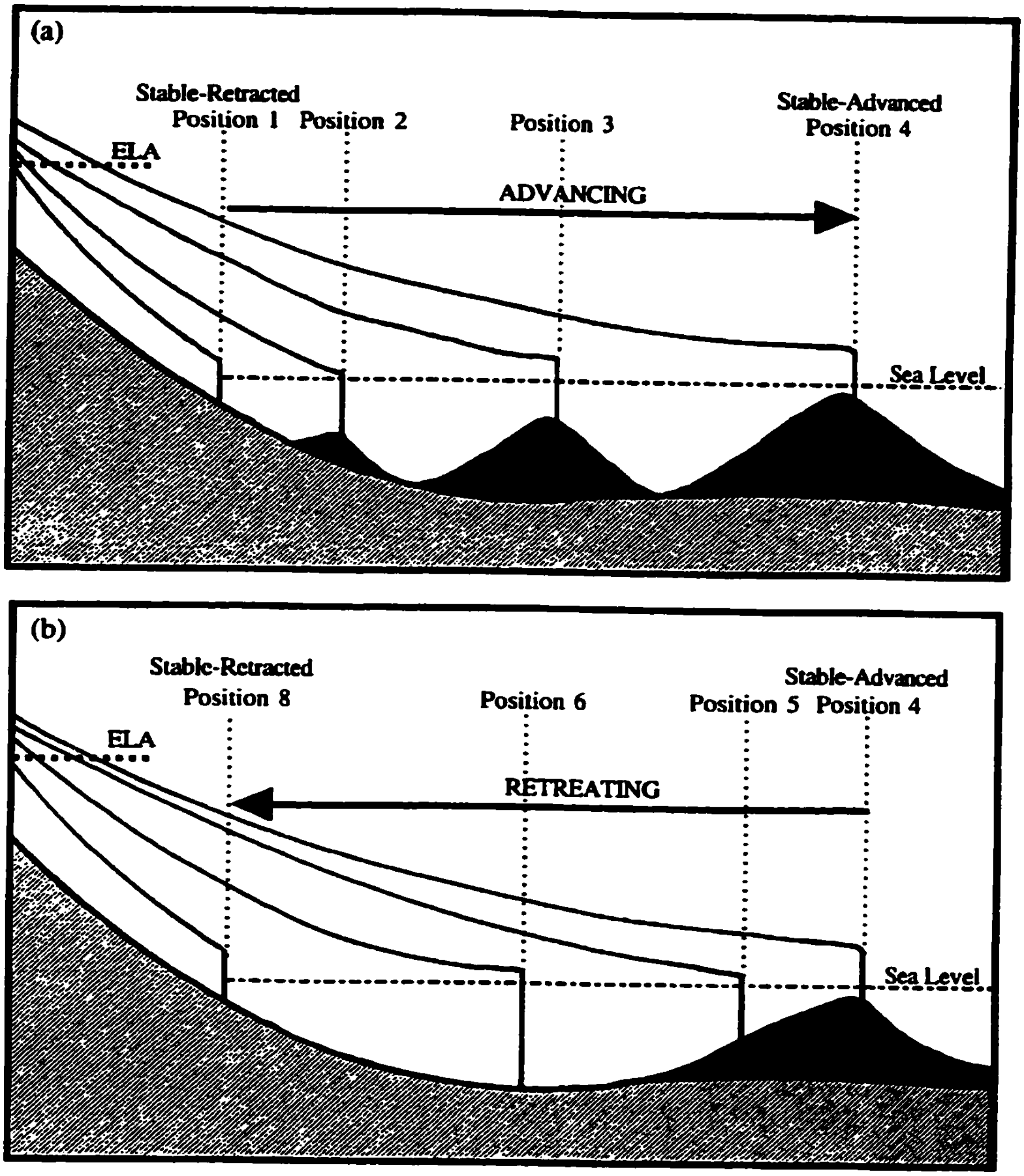

Figure 4.1 – Tidewater calving glacier cycle (from Viens, 1995).

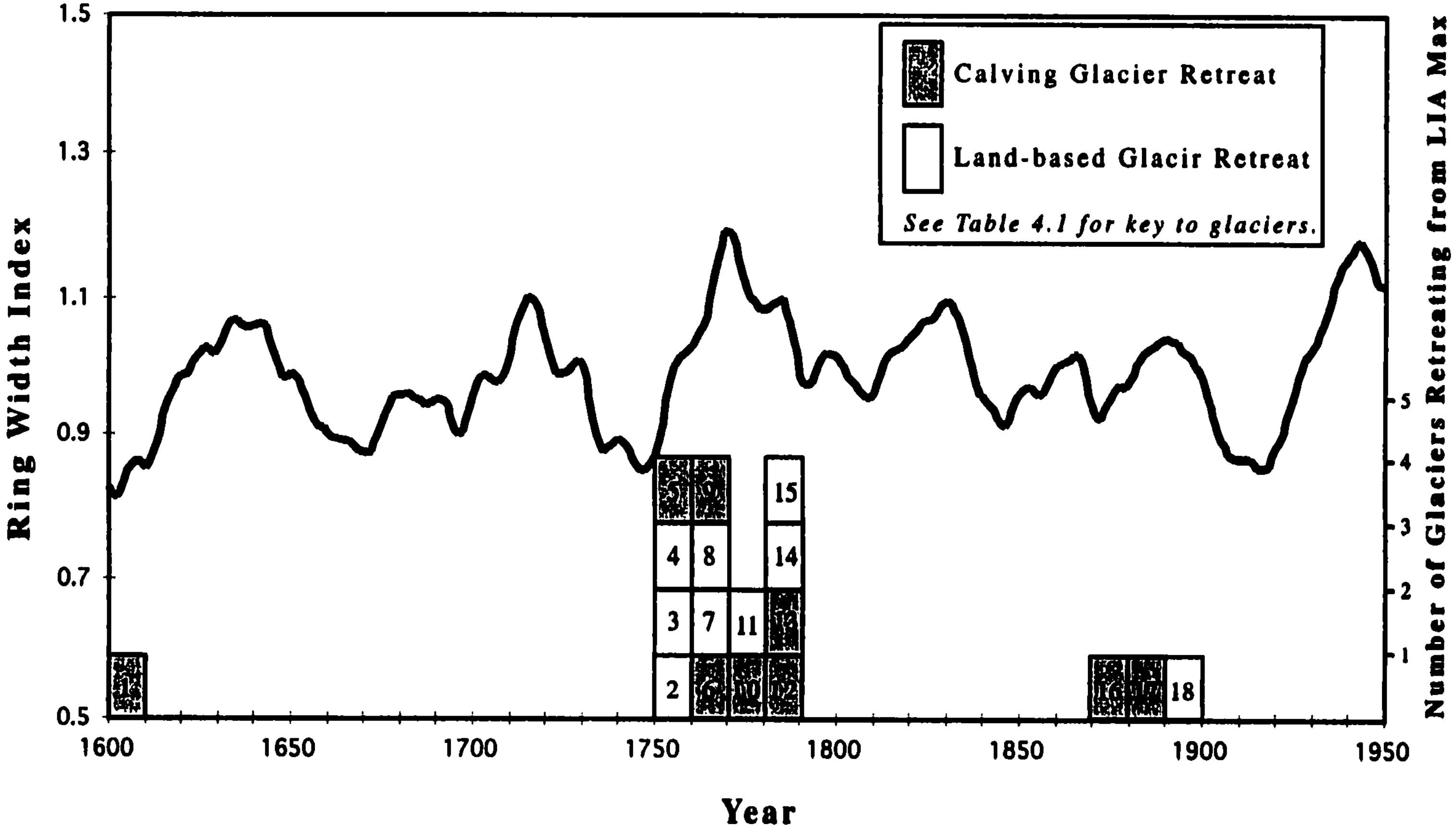

Figure 4.2 – Graph comparing 20-year running mean of summer temperature variations derived from tree rings (CMC; Figure 2.5) with the initiation of glacier retreat in southeastern Alaska. Boxes show retreat from the most extensive Little Ice Age moraine for calving glacier termini (grey) and land-based termini (white). Numbers correspond with glacier data on Table 4.1.

Table 4.1 – Glaciers from southeastern Alaska that have known ages for retreat from their most extensive Little Ice Age position.

Glacier ID[1]	Glacier Name	Year of Retreat from LIA Maximum	Terminus State[2]	Orientation	Reference
1	Lituya Bay	1600	T	S	Mann and Ugolini (1985)
2	Lemon	1750	L	W	Heusser and Marcus (1964)
3	Llewellyn	1750	L	E	Miller (1964)
4	Tulsequah	1750	L	SE	Miller (1964)
5	Taku	1750	T	SE	Motyka and Beget (1996)
6	Glacier Bay	1760[3]	T	S	Goodwin (1988)
7	Norris	1762[3]	L	E	Pierce (1954)
8	Herbert	1765	L	W	Lawrence (1950)
9	Mendenhall	1768[3]	F	SW	Lawrence (1950)
10	Bering	1775[3]	F	S	Molnia and Post (1995)
11	Twin	1776[3]	L	S	Lawrence (1950)
12	LeConte	1780	T	S	This Study
13	Shakes	1780	F	S	This Study
14	Gilkey	1783	L	W	Heusser and Marcus (1964)
15	Eagle	1783[3]	L	SW	Lawrence (1950)
16	Brady	1870	T	SE	Derksen (1976)
17	Icy Bay	1880	T	S	Porter (1989)
18	Patterson	1898	F	W	This Study
19	Baird	x	T	W	This Study

[1] Corresponds to Figure 4.2.

[2] T=Tidewater Calving, F=Freshwater Calving, and L=Land Based

[3] Average value of published age range

BIBLIOGRAPHY

Ager, T. A. (1983). Holocene vegetational history of Alaska. *In* "Late Quaternary Environments of the United States." (H. E. Wright, Jr., Ed.), pp. 128-140. Minnesota Press, Minneapolis.

Alaska Climate Research Center. (2001). Alaska Climate Research Center Online Data (http://climate.gi.alaska.edu/climatology/data.html). State of Alaska.

Alaska/U.S. Department of Commerce - Weather Bureau. (1920-1995). "Climatological data: Alaska Section." U.S. Weather Bureau, Seattle.

Alley, R. (1991). Sedimentary processes may cause fluctuations of tidewater glaciers. *Annals of Glaciology* **15**, 119-124.

Anderson, H. E. (1955). Climate in southeast Alaska in relation to tree growth. *Alaska Forest Research Center, U.S. Department of Agriculture Forest Service Station Paper* **3**, 11 p.

Aruscavage, P. J., and Campbell, E. Y. (1983). An ion-selective electrode method for determination of chlorine in geological materials. *Talanta* **30**, 745-749.

Barclay, D. J., Calkin, P. E., and Wiles, G. C. (2001). Holocene history of Hubbard Glacier in Yakutat Bay and Russell Fiord, southern Alaska. *Geological Society of America Bulletin* **113**, 388-402.

Bard, E., Hamelin, B., Fairbanks, R. G., and Zinder, A. (1990). Comparison between radiocarbon and uranium series ages on glacial age Barbados corals. *Nature* **345**, 405-409.

Barnosky, C. W., Anderson, P. M., and Bartlein, P. J. (1987). The northwestern U.S. during deglaciation: vegetational history and paleoclimate implications. *In* "North America and adjacent oceans during the last deglaciation." (W. F. Ruddiman, and H. E. Wright, Jr., Eds.), pp. 289-322. The Geology of North America. Geological Society of America, Inc., Boulder.

Blaise, B., Clague, J. J., and Mathewes, R. W. (1990). Time of maximum late Wisconsin glaciation, west coast of Canada. *Quaternary Research* **34**, 282-295.

Blake, W. P. (1868). Notes upon the geography and geology of Russian America and the Stickeen River, from observation made in 1863, pp. 1-19. House of Representatives Ex. Doc. 177, 40th Congress, 2d session, Washington D.C.

Bradley, R. S. (1999). "Paleoclimatology: reconstructing climates of the Quaternary." Harcourt/Academic Press, San Diego.

Briffa, K. R., Jones, P. D., Scheingruber, F. H., and Osborn, T. J. (1998). Influence of volcanic eruptions on Northern Hemisphere summer temperature over the past 600 years. *Nature* **393**, 450-455.

Briner, J. P., and Swanson, T. W. (2001). Late Pleistocene cosmogenic ^{36}Cl glacial chronology of southwestern Ahklun Mountains, Alaska. *Quaternary Research* **56**, 148-154.

Broecker, W. S., Bond, G., Klas, M., Clark, E., and McManus, J. (1992). Origin of the northern Atlantic's Heinrich events. *Climate Dynamics* **6**, 265-273.

Brown, C. S., Meier, M. F., and Post, A. (1982). Calving speed of Alaska tidewater glaciers, with application to Columbia Glacier. U.S. Geological Survey Professional Paper 1258-C.

Calkin, P. E., Wiles, G. C., and Barclay, D. J. (2001). Holocene coastal glaciation of Alaska. *Quaternary Science Reviews* **20**, 449-461.

Clague, J. J. (1989). Quaternary Geology of the Canadian Cordillera. *In* "Quaternary Geology of Canada and Greenland." (R. J. Fulton, Ed.). The Geology of North America v. K-1. Geological Society of America, Denver.

Cook, E. R. (1985). "A time series analysis approach to tree-ring standardization." Unpublished Ph.D. thesis, University of Arizona.

Cook, E. R., and Holmes, R. L. (1984). "User manual for ARSTAN." Laboratory of Tree Ring Research, University of Arizona, Tucson.

Cross, A. T. (1968). Mendenhall Glacier buried forest. *In* "19th Alaska Science Conference Abstracts." American Association for the Advancement of Science, Whitehorse.

Cwynar, L. C. (1990). A late Quaternary vegetation history from Lily Lake, Chilkat Peninsula, southeast Alaska. *Canadian Journal of Botany* **68**, 1106-1112.

D'Arrigo, R., and Jacoby, G. C. (1993). Dendroclimatic evidence from northern North America. *In* "Climate Since AD 1500." (R. S. Bradley, and P. D. Jones, Eds.), pp. 296-311. Routledge, London.

de Silva, S. L., and Zielinski, G. A. (1998). Global influence of the A.D. 1600 eruption of Huaynaputina, Peru. *Nature* **393**, 455-458.

Denton, G. H., and Hughes, T. J. (1981). "The last great ice sheets." Wiley, New York.

Derksen, S. J. (1976). Glacial geology of the southwestern Brady Glacier region. Institute of Polar Studies Report 60, pp. 97. Ohio State University, Columbus.

Desloges, J. R., and Ryder, J. M. (1990). Neoglacial history of the Coast Mountains near Bella Coola, British Columbia. *Canadian Journal of Earth Sciences* **27**, 281-290.

Dobry, J., and Klinka, K. (1998). Reconstructing temperature from tree rings of Pacific Silver Fir in coastal British Columbia. *Northwest Science* **72,** 81-87.

Echelmeyer, K., and Motyka, R. J. (1997). LeConte Glacier, Alaska: surface elevation changes and calving retreat. *In* "Calving Glaciers - Report of a Workshop." (C. J. van der Veen, Ed.), pp. 67-70. Byrd Polar Research Center, Columbus.

Emmons, G. T. (1991). "The Tlingit Indians." University of Washington Press, Seattle.

Field, W. O. (1975). Glaciers of the Coast Mountains: Boundary Ranges (Alaska, British Columbia, and Yukon Territory). *In* "Mountain Glaciers of the Northern Hemisphere." (W. O. Field, Ed.), pp. 299-492. Army Cold Regions Research and Engineering Laboratory, Hanover, NH.

Fritts, H. C. (1976). "Tree Rings and Climate." Academic Press, London.

Funk, and Röthlisberger, F. (1989). Forecasting the effects of a planned reservoir which will partially flood the tongue of Unteraargletscher in Switzerland. *Annals of Glaciology* **13,** 76-81.

Gehrels, G. E., and Berg, H. C. (1994). Geology of southeastern Alaska. *In* "The Geology of Alaska." (G. Plafker, and H. C. Berg, Eds.), pp. 451-468. Geology of North America (DNAG). Geological Society of America, Boulder, CO.

Gloss, J. L. (1997). "Tree-ring analysis and general chronology, Icy Bay, Alaska." Unpublished Masters thesis, State University of New York at buffalo.

Goodwin, R. G. (1988). Holocene glaciolacustrine sedimentation in Muir Inlet and ice advance in Glacier Bay, Alaska, U.S.A. *Arctic and Alpine Research* **20,** 55-69.

Hamilton, T. D. (1994). Late Cenozoic glaciation of Alaska. *In* "Geology of North America." (G. Plafker, and H. C. Berg, Eds.), pp. 813-844. Geology of North America (DNAG). Geological Society of America, Boulder, CO.

Hamilton, T. D., and Thorson, R. M. (1983). The Cordilleran ice sheet in Alaska. *In* "The late Pleistocene." (S. C. Porter, Ed.), pp. 38-52. University of Minnesotta Press, Minneapolis.

Hansen, B. C. S., and Engstrom, D. R. (1996). Vegetation history of Pleasand Island, southeastern Alaska, since 13,000 yr B.P. *Quaternary Research* **46,** 161-175.

Heaton, T. H., Talbot, S. L., and Shields, G. F. (1996). An Ice Age Refugium for Large Mammals in the Alexander Archipelago, Southern Alaska. *Quaternary Research* **46,** 186-192.

Hebda, R. J. (1983). Late-glacial and postglacial vegetation history at Bear Cove Bog, northeast Vancouver Island, British Columbia. *Canadian Journal of Botany* **61,** 3172-3192.

Heinrich, H. (1988). Origin and consequences of cyclic ice rafting in the northeast Atlantic Ocean during the past 130,000 years. *Quaternary Research* **29**, 142-152.

Heusser, C. J. (1960). Late Pleistocene environments of North Pacific North America. *American Geographical Society Special Publication* **35**.

Heusser, C. J. (1983a). Holocene vegetational history of the Prince William Sound region, south-central Alaska. *Quaternary Research* **19**, 337-355.

Heusser, C. J. (1983b). Vegetational history of the northwest United States, including Alaska. *In* "Late Quaternary environments of the United States." (S. C. Porter, Ed.), pp. 239-258. Minnesota Press, Minneapolis.

Heusser, C. J. (1985). Quaternary pollen records from the interior Pacific Northwest coast; Aleutians to Oregon-California boundary. *In* "Pollen records of the late-Quaternary North American sediments." (V. M. Bryant, and R. G. Holloway, Eds.), pp. 141-165. American Association of Stratigraphic Palynologists Foundation, Dallas.

Heusser, C. J. (1995). Late-Quaternary vegetation response to climate-glacial forcing in North Pacific America. *Physical Geography* **16**, 118-149.

Heusser, C. J., Heusser, L. E., and Peteet, D. M. (1985). Late-Quaternary climatic change on the American North Pacific coast. *Nature* **315**, 485-487.

Heusser, C. J., and Marcus, M. G. (1964). Historical variations of Lemon Creek Glacier, Alaska, and their relationship to the climate record. *Journal of Glaciology* **5**, 77-86.

Holmes, R. L. (1983). Computer assisted quality control in tree-ring dating and measurement. *Tree-Ring Bulletin* **43**, 69-75.

Houghton, J. T., Ding, Y., Griggs, D. J., Noguer, M., van der Linden, P. J., and Xiaosu, D. (2001). Climate Change 2001: The Scientific Basis (Contribution of Working Group I to the Third Assessment Report of the Intergovernmental Panel on Climate Change (IPCC)). *In* "IPCC Third Assessment Report." pp. 944. Cambridge University Press, Cambridge.

Howes, D. E. (1981). Late Quaternary sediments and geomorphic history of North-central Vancouver Island. *Canadian Journal of Earth Sciences* **18**, 1-12.

International Boundary Commision. (1927). International boundary region between Portland Canal and Stikine River, Alaska-British Columbia (Sheet 5). U.S. Geological Survey, Washington D.C.

International Boundary Commission. (1952). International boundary between United States and Canada from Cape Muzon to Mount St. Elias. International Boundary Commision, Ottowa.

Jacoby, G. C., and D'Arrigo, R. D. (1995). Tree ring width and density evidence of climatic and potential forest change in Alaska. *Global Biogeochemical Cycles* **9**, 227-234.

Klotz, O. J. (1895). Experimental application of the photo-topographical method of surveying to the Baird glacier, Alaska. *Journal of Geology* **3,** 512-518.

Laumann, T., and Wold, B. (1992). Reactions of a calving glacier to large changes in water level. *Annals of Glaciology* **16,** 158-162.

Lawrence, D. B. (1950). Glacier fluctuation for six centuries in southeastern Alaska and its relation to solar activity. *Geographical Review* **40,** 191-223.

Leonard, E. M. (1997). The relationship between glacial activity and sediment production: evidence from a 4450-year varve record of Neoglacial sedimentation in Hector Lake, Alberta, Canada. *Journal of Paleolimnology* **17,** 319-330.

Leonard, E. M., and Reasoner, M. A. (1999). A continuous Holocene glacial record inferred from proglacial lake sediments in Banff National Park, Alberta, Canada. *Quaternary Research* **51,** 1-13.

Liu, B., Phillips, F. M., Fabryka-Martin, J. T., Fowler, M. M., Biddle, R. S., and Stone, W. D. (1994). Cosmogenic ^{36}Cl accumulation in unstable landforms, I. Effects of the thermal neutron distribution. *Water Resources Research* **30,** 1071-1074.

Luckman, B. H., Briffa, K. R., Jones, P. D., and Schweingruber, F. H. (1997). Tree-ring based reconstruction of summer temperatures at the Columbia Icefield, Alberta, Canada, AD 1073-1983. *The Holocene* **7,** 375-389.

Mann, D. H. (1983). "The Quaternary history of the Lituya glacial refugium, Alaska." Unpublished Ph.D. thesis, University of Washington.

Mann, D. H. (1986a). Reliability of fjord glacier's fluctuations for paleoclimate reconstructions. *Quaternary Research* **25,** 10-24.

Mann, D. H. (1986b). Wisconsin and Holocene glaciation of southeast Alaska. *In* "Glaciation in Alaska: The Geologic Record." (T. D. Hamilton, K. M. Reed, and R. M. Thorson, Eds.), pp. 237-265. Alaska Geographical Society, Anchorage.

Mann, D. H., and Hamilton, T. D. (1995). Late Pleistocene and Holocene paleoenvironments of the north Pacific coast. *Quaternary Science Reviews* **14,** 449-471.

Mann, D. H., and Ugolini, F. C. (1985). Holocene glacial history of the Lituya district, southeast Alaska. *Canadian Journal of Earth Sciences* **22,** 913-928.

Mann, M., Bradley, R. S., and Hughes, M. K. (1998). Global scale temperature patterns and climate forcing over the past six centuries. *Nature* **392,** 779-788.

McCarthy, D. P., and Luckman, B. H. (1993). Estimating ecesis for tree-ring dating of moraines: A comparative study from the Canadian Cordillera. *Arctic and Alpine Research* **25,** 63-68.

McCelland, W. C., and Gehrels, G. E. (1987). Analysis of a major shear zone in Duncan Canal, Kupreanof Island, southeastern Alaska. *Geological Society of America Abstracts with Programs* **19,** 430.

McKenzie, G. D., and Goldthwait, R. P. (1971). Glacial history of the last eleven thousand years in Adams Inlet, southeastern Alaska. *Geological Society of America Bulletin* **82,** 1767-1782.

Mercer, J. H. (1961). The response of fjord glaciers to changes in the firn limit. *Journal of Glaciology* **3,** 850-858.

Miller, M. M. (1964). Inventory of terminal position changes in Alaskan coastal glaciers since the 1750's. *Proceedings from the American Philisophical Society* **108,** 257-273.

Miller, R. D. (1973). Gastineau Channel Formation, a composite glaciomarine deposit near Juneau, Alaska. *U.S. Geological Survey Bulletin* **1394-C,** C1-C20.

Molnia, B. F., and Post, A. (1995). Holocene history of Bering Glacier, Alaska: A prelude to the 1993-1994 surge. *Physical Geography* **16,** 87-117.

Motyka, R. J. (1997). Deep-water calving at LeConte Glacier, southeast Alaska. *In* "Calving Glaciers - Report of a Workshop." (C. J. van der Veen, Ed.), pp. 115-118. Byrd Polar Research Center, Columbus.

Motyka, R. J., and Beget, J. E. (1996). Taku Glacier, southeast Alaska, U.S.A.: Late Holocene history of a tide-water glacier. *Arctic and Alpine Research* **28,** 42-51.

Muir, J. (1893). Alaska. *The American Geologist* **6,** 287-299.

Muir, J. (1915). "Travels in Alaska." Houghton Mifflin, Boston.

National Climate Data Center (NCDC) and Environmental Research Laboratory (ERL). (1998). Radiosonde Data of North America 1990-1996 Dataset CD-ROM. National Oceanic and Atmospheric Administration (NOAA).

Olson, W. M., and Thilenius, J. F. (1993). The Alaska travel journal of Archibald Menzies, 1793-1794, pp. 247. University of Alaska Press, Fairbanks.

Peteet, D. M. (1986). Modern pollen rain and vegetational history of the Malaspina Glacier District, Alaska. *Quaternary Research* **25,** 100-120.

Phillips, F. M., and Plummer, M. A. (1996). CHLOE: A program for interpreting in-situ cosmogenic nuclide data for surface exposure dating and erosion studies. *Radiocarbon* **38,** 98.

Phillips, F. M., Zreda, M. G., Benson, L. V., Plummer, M. A., Elmore, D., and Sharma, P. (1996). Chronology for fluctuations in late Pleistocene Sierra Nevada glaciers and lakes. *Science* **274,** 749-751.

Pierce, R. L. (1954). Interpretative report on the Norris and Taku Glaciers of the 1953 Juneau Ice Field Research Project Geobotanical Program, pp. 16. Department of Botany, University of Minnesota.

Porter, S. C. (1975). Equilibrium-line altitudes of late Quaternary glaciers in the Southern Alps, New Zealand. *Quaternary Research* **5**, 27-47.

Porter, S. C. (1981). Glaciological evidence of Holocene climate change. *In* "Climate and History." (T. M. L. Wigley, M. J. Ingram, and G. Farmer, Eds.), pp. 82-110. Cambridge University Press, Cambridge.

Porter, S. C. (1989). Late Holocene fluctuations of the fiord glacier system in Icy Bay, Alaska, U.S.A. *Arctic and Alpine Research* **21**, 364-379.

Porter, S. C., and Swanson, T. W. (1998). Radiocarbon age constraints on rates of advance and retreat of Puget Lobe of the Cordilleran ice sheet during the last glaciation. *Quaternary Research* **50**, 205-213.

Post, A. (1975). Preliminary hydrography and historical terminal changes of Columbia Glacier. *U.S. Geological Survey Hydrologic Investigations Atlas* **HA-559**, 3 sheets.

Post, A. (1980). Preliminary bathymetry of McCarty Fiord and Neoglacial changes of McCarty Glacier. *U.S. Geological Survey Open-File Report* **80-424**, 4 sheets.

Post, A., and Motyka, R. J. (1995). Taku and Le Conte glaciers, Alaska: Calving-speed control of late-Holocene asynchronous advances and retreats. *Physical Geography* **16**, 59-82.

Powell, R. D. (1991). Grounding-line systems as second-order controls on fluctuations of tidewater termini of temperate glaciers. *In* "Glacial marine sedimentation: Paleoclimate significance (Geological Society of America Special Paper 261)." (J. B. Anderson, and G. M. Ashley, Eds.), pp. 74-94. Geological Society of America, Denver.

Röthlisberger, F. (1986). "10,000 Jahre Gletschergeschichte der Erde." Verlag Press, Frankfurt.

Russell, I. C. (1898). The glaciers of North America. *Geographical Journal*, 553-564.

Ryder, J. M. (1987). Neoglacial history of the Stikine-Iskut area, northern Coast Mountains, British Columbia. *Canadian Journal of Earth Sciences* **24**, 1294-1301.

Ryder, J. M., and Thomson, B. (1986). Neoglaciation in the southern Coast Mountains of British Columbia: chronology prior to the late Neoglacial maximum. *Canadian Journal of Earth Sciences* **23**, 273-438.

Schweingruber, F. H. (1996). "Tree Rings and Environment. Dendroecology." Paul Haupt Publishers, Berne.

Schweingruber, F. H., Briffa, K. R., and Nogler, P. (1993). A tree-ring densitometric transect from Alaska to Labrador. *International Journal of Biometeorology* **37**, 151-169.

Sigafoos, R. S., and Hendricks, E. L. (1969). The time interval between stabilization of alpine glacial deposits and establishment of tree seedlings. *U.S. Geological Survey Professional Paper* **650-B**, B89-B93.

Sirkin, L. A., and Tuthill, S. J. (1971). Late Pleistocene palynology and stratigraphy of Controller Bay Region, Gulf of Alaska. *In* "Etudes sur le Quaternaire dans le Monde, Vol. 1." pp. 197-208. Association Francaise pour l'Etude du Quaternaire (AFEQ), Paris.

Southon, J. R., Nelson, D. E., and Vogel, J. S. (1990). A record of past ocean-atmosphere radiocarbon differences from the northeast Pacific. *Paleooceanography* **5**, 197-206.

Stokes, M. A., and Smiley, T. L. (1968). "An introduction to tree-ring dating." University of Chicago Press, Chicago.

Stuiver, M., and Reimer, P. J. (1993). Extended ^{14}C data base and revised Calib 3.0 ^{14}C age calibration program. *Radiocarbon* **35**, 215-230.

Swanson, T. W. (1994). "Determination of 36 Cl production rates from the deglaciation history of Whidbey Island, Washington." Unpublished PhD thesis, University of Washington.

Swanson, T. W., and Caffee, M. L. (2001). Determination of ^{36}Cl production rates derived from the well-dated deglaciation surfaces of Whidbey and Fidalgo islands, Washington. *Quaternary Research* **56**, 366-382.

Tangborn, W. (1997). Using low-altitude meteorological observations to calculate the mass balance of Alaska's Columbia Glacier and relate it to calving and speed. *In* "Calving Glaciers - Report of a Workshop." (C. J. van der Veen, Ed.), pp. 141-161. Byrd Polar Research Center, Columbus.

U.S. Coast and Geodetic Survey. (1895). Frederick Sound and Sumner Straight, S.E. Alaska. U.S. Coast and Geodetic Survey, Washington D.C.

United States Coast and Geodetic Survey. (1891). Pacific Coast Pilot: Alaska. U.S. Government Publishing Office, Washington, D.C.

van der Veen, C. J. (1996). Tidewater calving. *Journal of Glaciology* **42**, 375-386.

Vancouver, G. (1798). "A voyage of Discovery to the North Pacific Ocean, and round the world." G.G. and J. Robinson, London (facsimile edition reprinted by N. Israel, Amsterdam, 1967).

Viens, R. J. (1995). "Dynamics and mass balance of tidewater calving glaciers of southern Alaska." Unpublished Masters thesis, University of Washington.

Viereck, L. A., and Little, E. L. (1972). "Alaskan trees and shrubs." U.S. Department of Agriculture Handbook 410, Washington D.C.

Warner, B. G., Mathewes, R. W., and Clague, J. J. (1982). Ice-free conditions on the Queen Charlotte Islands, British Columbia, at the height of late Wisconsin glaciation. *Science* **218,** 675-677.

White, B. M., Seifert, S. L., Hitchcock, B. W., O'Neel, S., Motyka, R. J., and Connor, C. L. (1999). 1999 Results of student field survey at LeConte tidewater glacier, southeastern Alaska. *Abstracts with Programs, Geological Society of America* **31,** 269.

Wiles, G. C., Barclay, D. J., and Calkin, P. E. (1999a). Tree-ring-dated "Little Ice Age" histories of maritime glaciers from western Prince William Sound, Alaska. *The Holocene* **9,** 163-173.

Wiles, G. C., and Calkin, P. E. (1993). Neoglacial fluctuations and sedimentation of an iceberg-calving glacier resolved with tree-rings (Kenai fjords National Park, Alaska). *Quaternary International* **18,** 35-42.

Wiles, G. C., D'Arrigo, R., and Jacoby, G. C. (1996). Temperature changes along the Gulf of Alaska and the Pacific Northwest coast modeled from coastal tree rings. *Canadian Journal of Forest Research* **26,** 474-481.

Wiles, G. C., D'Arrigo, R., and Jacoby, G. C. (1998). Gulf of Alaska atmosphere-ocean variability over recent centuries inferred from coastal tree-ring records. *Climatic Change* **38,** 289-306.

Wiles, G. C., Post, A., Muller, E. H., and Molnia, B. F. (1999b). Dendrochronology and late Holocene history of Bering piedmont glacier, Alaska. *Quaternary Research* **52,** 185-195.

Willard, R., Jr. (1995). Tlingit National Anthem (http://members.aol.com/waya94/page1.htm). Aperture Publishing and Haa -tl'atgi.

APPENDIX A: CLIMATE DATA FOR SOUTHEASTERN ALASKAN WEATHER STATIONS

Climate Data Summaries for Southeast Alaska Weather Stations

SE Alaska Composite

	Jan	Feb	Mar	Apr	May	Jun	July	Aug	Sept	Oct	Nov	Dec	Annual
Temps (°C)													
Avg	-1.5	-0.1	1.9	5.2	8.9	12.1	13.7	13.5	10.8	6.8	2.4	-0.1	6.2
St Dev	3.1	2.5	1.6	1.2	1.2	1.1	1.0	1.0	0.8	1.2	2.3	2.6	0.8
Max	5.1	4.9	6.3	7.6	11.7	15.3	16.4	15.8	13.3	9.1	6.2	4.6	7.9
Min	-10.1	-8.6	-1.7	1.5	6.4	9.6	11.1	11.5	8.1	2.4	-5.1	-8.5	4.3
Precipitation (mm)													
Avg	216	186	172	156	133	107	124	169	266	383	273	243	2440
St Dev	91	82	62	58	51	41	49	78	96	111	103	91	340
Max	521	479	406	341	298	200	375	434	648	659	685	486	3563
Min	26	5	27	31	49	24	31	38	65	52	15	40	1008
Thornthwait Index	4.6	3.4	2.6	1.9	1.3	0.9	0.9	1.3	2.5	4.6	4.3	4.6	329.3
Warmth Index				0.2	3.9	7.1	8.7	8.5	5.8	1.8			35.9
Coldness Index	-6.5	-5.1	-3.1								-2.6	-5.1	-22.2

Wrangell

	Jan	Feb	Mar	Apr	May	Jun	July	Aug	Sept	Oct	Nov	Dec	Annual
Temps (°C)													
Avg	-1.7	0.2	2.5	5.5	9.3	12.3	13.8	13.6	10.9	6.8	2.3	-0.1	6.2
St Dev	3.5	2.5	1.6	1.3	1.5	1.4	1.3	1.3	1.2	1.3	2.5	2.8	1.0
Max	6.6	4.6	6.7	8.1	12.4	15.4	17.7	16.3	13.5	10.2	6.9	5.2	8.8
Min	-10.2	-8.7	-0.9	1.8	6.3	9.3	10.5	10.0	8.5	3.8	-4.7	-9.3	4.2
Precipitation (mm)													
Avg	178	147	134	121	109	100	121	149	231	326	223	197	2033
St Dev	90	70	54	43	40	34	49	67	91	98	91	84	249
Max	430	334	271	226	216	171	266	368	463	595	615	420	2880
Min	15	0	38	20	23	25	35	35	44	132	42	48	1523
Thornthwait Index	3.8	2.6	1.9	1.4	1.0	0.8	0.9	1.2	2.1	3.9	3.4	3.7	265.8
Warmth Index				0.5	4.3	7.3	8.8	8.6	5.9	1.8			37.1
Coldness Index	-6.7	-4.8	-2.5								-2.7	-5.1	-21.8

Petersburg

	Jan	Feb	Mar	Apr	May	Jun	July	Aug	Sept	Oct	Nov	Dec	Annual
Temps (°C)													
Avg	-2.2	-0.3	1.7	4.8	8.6	11.7	13.3	12.8	10.1	6.2	1.7	-0.9	5.6
St Dev	3.7	2.5	1.6	1.3	1.2	1.2	0.9	0.9	1.0	1.1	2.5	2.9	0.8
Max	5.7	5.3	5.2	7.9	11.2	14.4	15.1	15.0	12.6	8.6	5.9	4.6	7.7
Min	-11.9	-5.3	-1.7	0.9	6.2	9.6	11.8	11.0	6.3	2.9	-5.1	-7.3	3.9
Precipitation (mm)													
Avg	251	209	189	174	153	130	135	180	290	419	306	273	2722
St Dev	116	95	74	64	72	51	59	88	116	127	128	114	353
Max	531	432	323	348	349	233	304	423	538	738	680	540	3477
Min	38	3	47	28	43	13	40	26	53	209	68	44	1811
Thornthwait Index	5.9	4.0	3.0	2.2	1.5	1.1	1.0	1.5	2.8	5.3	5.1	5.7	391.4
Warmth Index					3.6	6.7	8.3	7.8	5.1	1.2			32.7
Coldness Index	-7.2	-5.3	-3.3	-0.2							-3.3	-5.9	-25.3

Juneau

	Jan	Feb	Mar	Apr	May	Jun	July	Aug	Sept	Oct	Nov	Dec	Annual
Temps (°C)													
Avg	-2.1	-0.4	1.6	5.1	9.2	12.8	14.1	13.6	10.6	6.5	1.8	-0.7	6.0
St Dev	3.5	2.8	1.7	1.3	1.3	1.5	1.1	1.0	0.8	1.1	2.5	2.8	0.8
Max	4.2	4.9	6.0	7.8	12.3	16.7	17.1	16.4	12.9	9.1	5.9	4.4	7.6
Min	-10.3	-9.9	-2.7	1.1	6.6	9.7	11.5	10.6	7.9	2.4	-5.1	-10.6	4.2
Precipitation (mm)													
Avg	181	162	157	140	146	107	151	191	285	340	240	209	2263
St Dev	90	83	59	61	63	47	72	88	105	110	101	90	461
Max	521	412	283	289	333	292	341	476	485	678	657	470	3042
Min	12	2	14	12	40	14	6	33	30	52	15	22	1008
Thornthwait Index	4.1	3.0	2.5	1.7	1.4	0.8	1.1	1.5	2.7	4.1	3.9	4.1	309.3
Warmth Index				0.1	4.2	7.8	9.1	8.6	5.6	1.5			36.9
Coldness Index	-7.1	-5.4	-3.4								-3.2	-5.7	-24.8

Ketchican

	Jan	Feb	Mar	Apr	May	Jun	July	Aug	Sept	Oct	Nov	Dec	Annual
Temps (°C)													
Avg	1.0	2.6	3.6	6.2	9.7	12.6	14.5	14.8	12.1	8.1	4.3	2.2	7.6
St Dev	2.7	1.9	1.2	1.1	1.2	1.4	1.1	1.1	1.1	1.0	1.9	2.1	0.6
Max	6.5	6.4	6.4	8.9	12.1	16.8	17.7	17.5	14.6	10.6	8.6	6.6	9.3
Min	-7.8	-4.6	0.8	3.2	6.5	9.0	10.9	12.4	7.8	5.9	-0.8	-4.3	5.8
Precipitation (mm)													
Avg	345	320	286	289	220	186	188	260	353	582	423	393	3863
St Dev	157	149	134	146	105	87	102	152	169	188	176	154	670
Max	795	650	631	792	534	364	713	861	713	1076	1368	893	5136
Min	30	21	70	40	57	25	24	23	43	217	71	108	2520
Thornthwait Index	6.2	5.0	4.1	3.5	2.1	1.5	1.4	2.0	3.2	6.9	6.1	6.5	485.7
Warmth Index				1.2	4.7	7.6	9.5	9.8	7.1	3.1			43.0
Coldness Index	-4.0	-2.4	-1.4								-0.7	-2.8	-11.4

Haines

	Jan	Feb	Mar	Apr	May	Jun	July	Aug	Sept	Oct	Nov	Dec	Annual
Temps (°C)													
Avg	-5.1	-2.6	0.3	4.5	9.3	13.2	14.6	13.7	10.3	5.3	-0.7	-3.4	4.9
St Dev	3.7	3.2	2.0	1.6	1.5	1.3	1.0	1.1	0.9	1.2	2.9	3.3	0.8
Max	2.5	3.9	3.8	8.2	12.7	16.1	17.2	16.4	12.2	7.7	4.3	1.8	6.6
Min	-11.9	-11.9	-4.5	0.2	6.2	9.8	12.2	11.5	7.8	2.6	-7.3	-11.3	2.9
Precipitation (mm)													
Avg	137	113	99	71	52	35	42	67	151	238	167	147	1321
St Dev	75	61	67	55	37	26	28	43	80	107	84	75	261
Max	406	263	293	308	183	133	139	179	354	517	444	424	2287
Min	12	0	0	9	5	3	3	0	9	80	37	15	915
Thornthwait Index	4.4	2.5	1.6	0.8	0.4	0.2	0.3	0.5	1.4	3.0	3.2	3.8	221.1
Warmth Index					4.3	8.2	9.6	8.7	5.3	0.3			36.3
Coldness Index	-10.1	-7.6	-4.7	-0.5							-5.7	-8.4	-37.0

Sitka

	Jan	Feb	Mar	Apr	May	Jun	July	Aug	Sept	Oct	Nov	Dec	Annual
Temps (°C)													
Avg	-0.3	1.1	2.4	4.8	7.8	10.6	12.6	13.1	10.9	7.0	2.9	0.6	6.1
St Dev	3.1	2.1	1.6	1.4	1.1	1.0	0.8	1.0	1.1	1.2	2.2	2.3	0.9
Max	6.2	5.4	7.0	7.8	11.7	13.5	15.4	16.1	12.9	10.4	7.3	6.0	9.1
Min	-8.7	-3.6	-1.4	1.5	5.4	8.4	10.3	11.2	9.3	4.6	-3.1	-7.2	4.3
Precipitation (mm)													
Avg	219	177	177	140	121	91	117	175	298	372	277	246	2417
St Dev	98	91	71	60	60	50	56	86	115	131	108	92	339
Max	450	479	406	341	263	227	305	476	648	836	657	505	3563
Min	26	5	36	22	22	13	11	13	90	128	69	22	1510
Thornthwait Index	4.2	2.9	2.6	1.7	1.2	0.8	0.9	1.4	2.8	4.4	4.2	4.4	315.1
Warmth Index					2.8	5.6	7.6	8.1	5.9	2.0			32.1
Coldness Index	-5.3	-3.9	-2.6	-0.2							-2.1	-4.4	-18.4

Southeast Alaska Composite: Mean Daily Temperature (°C)

Year	Jan	Feb	Mar	Apr	May	Jun	Jul	Aug	Sep	Oct	Nov	Dec	Annual
1995	0.5	0.6	1.6	7.6	11.3	13.2	14.6	13.2	13.3	7.5	1.9	-0.8	7.4
1994	0.4	-4.0	3.9	7.2	9.6	13.0	14.6	15.8	11.3	7.4	0.7	0.6	7.4
1993	-2.3	1.4	3.0	7.4	11.6	13.6	15.4	14.8	11.8	8.6	3.9	3.5	7.9
1992	3.4	2.0	3.7	6.0	8.9	13.2	14.0	13.3	8.1	5.1	3.7	-1.9	6.9
1991	-2.5	2.8	1.5	6.0	9.5	12.7	13.5	13.7	11.4	5.9	4.0	2.4	7.0
1990	-1.0	-2.1	3.8	7.0	10.3	13.0	15.4	15.0	11.8	5.8	-1.0	-2.6	6.3
1989	-1.8	-2.0	1.1	7.1	9.8	13.1	15.3	14.5	12.2	6.5	1.8	3.6	6.8
1988	-1.4	0.9	3.9	6.0	9.5	12.2	12.9	13.4	10.3	8.0	4.0	0.9	6.6
1987	1.8	3.0	1.7	5.9	9.1	11.3	14.7	14.6	10.8	7.4	4.7	2.0	7.1
1986	2.0	-0.5	3.3	3.7	8.4	12.1	13.9	12.8	11.1	8.6	1.3	3.0	6.4
1985	3.4	-1.3	2.2	4.0	7.9	10.8	13.6	12.9	10.5	4.9	-4.7	1.2	5.4
1984	1.5	3.0	5.2	6.4	9.5	11.6	13.1	13.6	10.7	5.9	0.7	-2.8	6.4
1983	1.0	3.0	3.8	6.8	9.8	13.1	14.0	13.1	9.6	6.3	1.7	-4.1	6.0
1982	-6.1	-2.0	1.7	4.1	7.4	13.5	14.3	12.9	11.3	6.6	0.5	1.1	5.3
1981	5.1	1.9	5.0	5.0	11.4	12.2	14.3	14.5	11.3	7.2	4.4	-0.2	7.5
1980	-3.9	3.0	2.5	6.4	10.0	13.8	13.8	14.0	10.9	8.6	5.3	-3.1	6.5
1979	-3.0	-6.4	3.6	6.0	8.6	11.4	14.1	15.4	12.1	8.6	4.5	-0.5	6.2
1978	-2.1	1.8	2.6	6.6	9.0	13.0	13.2	14.3	10.8	7.9	1.0	-0.6	7.1
1977	1.7	4.9	2.6	5.9	9.0	12.4	14.2	15.4	11.0	6.7	-0.3	-5.1	6.6
1976	-0.1	-1.4	1.5	5.4	7.6	11.1	13.6	13.3	10.9	6.4	4.9	1.9	6.3
1975	-2.4	-3.1	0.8	4.1	8.4	10.4	13.6	12.9	11.1	6.3	0.3	-1.0	5.2
1974	-5.4	0.2	-0.3	5.3	8.2	10.6	12.7	13.9	11.9	6.7	3.1	2.1	5.8
1973	-2.8	-0.8	2.3	5.3	8.1	10.6	12.2	11.5	10.3	5.7	-2.9	0.2	5.0
1972	-6.4	-3.5	0.2	2.1	7.8	10.4	14.0	13.3	9.5	5.8	3.3	-1.9	4.8
1971	-5.3	0.2	0.7	4.2	6.4	11.3	14.2	13.7	9.9	5.1	1.8	-4.0	5.2
1970	-2.4	3.8	4.0	4.8	7.9	11.2	12.3	12.1	9.4	6.1	1.6	-2.7	5.7
1969	-9.8	-1.5	1.7	5.4	9.9	14.0	12.2	11.5	11.0	7.7	3.4	3.5	5.9
1968	-3.4	0.3	3.5	3.7	9.9	11.9	14.3	13.7	10.0	5.8	3.4	-3.4	5.8
1967	-1.9	1.1	-0.8	4.8	8.6	12.9	13.0	14.1	10.8	7.1	2.2	0.0	6.0
1966	-6.1	0.4	2.0	4.6	6.9	11.8	13.9	12.3	10.5	4.9	-0.1	-0.2	5.1
1965	-2.7	-1.1	2.4	5.1	7.0	10.5	13.8	13.6	11.0	6.9	0.6	0.2	5.5
1964	0.0	2.6	-0.1	4.2	7.5	12.5	12.7	12.3	10.4	6.8	1.0	-6.5	5.3
1963	-0.6	3.0	1.9	4.8	9.9	10.8	13.7	14.5	12.1	7.5	-0.6	1.6	6.6
1962	-0.6	-0.5	0.2	5.1	7.9	10.7	13.9	13.7	10.5	7.7	4.8	1.0	6.2
1961	1.6	1.3	3.0	5.5	9.7	12.0	14.3	13.7	10.3	5.9	0.8	-2.4	6.3
1960	-0.2	2.2	1.5	6.6	10.5	11.4	13.7	13.3	10.5	7.7	3.0	2.8	6.9
1959	-4.1	0.4	2.1	5.2	8.9	13.2	13.8	12.7	10.5	6.5	2.4	2.7	6.2
1958	3.2	0.7	2.5	7.1	9.9	15.1	15.4	13.4	10.0	6.3	2.1	1.2	7.5
1957	-3.5	-0.8	3.1	5.2	9.9	12.7	13.5	15.3	12.8	7.2	4.7	0.4	6.8

Year	Jan	Feb	Mar	Apr	May	Jun	Jul	Aug	Sep	Oct	Nov	Dec	Annual
1956	-2.9	-3.4	0.2	5.0	8.5	10.8	14.2	13.2	9.9	4.6	4.0	-0.7	5.6
1955	1.4	0.3	-0.3	4.3	6.9	10.8	14.0	12.1	10.2	5.5	-2.5	-4.8	4.8
1954	-4.2	-2.0	1.3	2.0	8.9	12.2	13.0	14.5	11.5	7.0	5.8	-0.4	5.8
1953	-5.4	2.2	1.4	5.9	9.9	13.5	14.8	13.9	10.8	7.6	3.0	2.0	7.0
1952	-5.7	0.5	1.4	4.0	7.9	11.4	13.9	13.7	10.7	8.5	4.3	2.1	6.1
1951	-4.2	-2.5	-1.7	4.6	8.7	11.9	15.7	14.2	11.7	5.3	2.3	-2.5	5.3
1950	-8.6	-0.3	2.2	3.9	7.3	13.6	12.9	14.1	11.0	5.5	-2.2	0.9	5.2
1949	-1.6	-4.6	3.3	4.8	8.6	10.3	12.9	12.9	11.8	6.7	6.0	-3.5	5.7
1948	1.3	-3.5	0.2	3.3	9.8	13.6	14.5	13.5	9.9	6.5	1.6	-4.5	5.5
1947	-4.1	-1.1	3.2	5.0	9.4	12.2	14.2	13.2	11.1	7.2	4.1	2.3	6.4
1946	0.9	1.1	1.7	4.2	10.3	13.9	13.1	12.8	10.9	5.7	0.6	-3.3	6.0
1945	1.9	1.1	2.5	4.0	10.3	11.1	12.3	12.8	10.3	7.0	-1.1	-0.2	6.0
1944	2.1	1.1	1.4	5.4	8.5	12.7	13.6	13.3	11.4	8.5	3.6	1.0	6.9
1943	-4.4	0.0	0.7	5.5	8.7	12.2	12.5	12.9	10.7	7.1	5.3	3.6	6.3
1942	3.6	2.6	2.3	6.1	11.7	13.1	14.5	14.0	11.8	7.2	0.1	-3.3	6.9
1941	0.1	1.1	4.7	7.6	9.9	13.6	14.5	15.5	11.0	7.3	2.5	-0.6	7.3
1940	1.1	0.5	3.0	7.4	9.4	11.9	14.8	13.1	11.7	8.6	1.8	2.0	7.4
1939	1.0	-2.2	0.9	4.0	8.1	11.9	13.4	12.3	10.2	5.6	3.7	4.2	6.1
1938	0.3	-2.7	2.4	6.0	8.3	10.6	12.8	13.6	12.6	8.7	3.4	0.6	6.8
1937	-3.1	-1.9	3.9	5.2	8.7	13.2	13.3	12.8	11.8	8.8	2.9	-1.8	6.2
1936	-1.7	-8.6	1.0	5.8	9.4	15.3	14.8	15.2	10.9	9.1	6.2	-1.0	6.3
1935	-3.1	3.4	-0.6	5.6	8.9	12.4	13.9	13.1	11.3	5.2	2.2	2.8	6.2
1934	-1.1	3.3	3.5	6.7	10.4	12.1	15.0	14.4	11.0	7.3	3.7	-0.2	7.1
1933	-3.0	-1.3	1.0	4.4	9.2	11.1	12.3	13.7	10.4	4.7	4.4	-8.5	5.3
1932	-1.8	-2.6	2.0	6.3	8.8	10.4	12.2	13.6	9.9	7.3	1.0	-2.6	5.0
1931	3.7	2.6	1.5	6.8	8.8	12.9	13.9	13.9	11.1	6.6	1.3	0.2	7.0
1930	-4.9	-0.4	0.7	5.0	8.3	11.7	13.4	14.4	10.9	5.5	3.6	4.6	6.1
1929	-0.5	-0.3	2.1	3.7	8.4	12.2	13.0	13.5	11.8	8.2	4.2	-1.4	6.3
1928	0.6	1.7	1.5	4.7	8.4	13.2	14.0	12.7	10.8	6.5	4.1	1.4	6.6
1927	-1.6	0.8	2.4	2.4	8.3	13.0	15.4	14.9	11.0	6.0	-1.7	-3.6	5.6
1926	4.6	2.0	5.1	6.8	9.5	13.6	14.3	14.6	10.3	7.8	3.3	0.6	7.8
1925	-2.8	-1.1	2.0	4.8	9.6	12.2	13.7	13.6	11.1	7.8	4.7	4.1	6.8
1924	1.4	2.3	3.8	4.2	9.2	13.2	13.4	13.6	10.2	6.8	3.6	-0.9	6.8
1923	-1.3	1.1	2.3	6.2	9.4	12.9	15.0	15.8	11.6	9.1	5.8	1.3	7.4
1922	0.6	-2.6	1.2	4.5	8.1	11.9	12.9	13.8	10.4	7.7	4.9	-1.6	6.1
1921	-1.8	0.9	0.7	5.2	8.3	12.8	12.7	12.9	11.0	7.7	2.0	1.6	6.0
1920	-3.3	2.3	1.3	3.3	6.9	11.1	14.8	12.8	10.0	5.9	3.5	1.0	5.8
1919	1.1	0.1	-0.2	5.8	7.9	10.7	13.0	13.9	11.8	6.1	0.7	-0.4	5.7
1918	0.6	-0.5	-0.2	4.0	7.9	11.8	15.1	13.3	11.7	7.1	3.8	0.6	6.3
1917	-2.8	-1.0	1.6	5.6	8.1	10.6	11.9	13.0	10.7	6.4	4.9	-5.2	5.1
1916	-6.9	1.0	0.6	6.1	8.4	11.7	13.3	13.6	10.5	7.6	3.5	-0.5	5.8

Year	Jan	Feb	Mar	Apr	May	Jun	Jul	Aug	Sep	Oct	Nov	Dec	Annual
1915	1.9	1.6	5.9	6.0	11.7	13.0	16.4	13.3	10.9	6.8	2.9	1.8	7.7
1914	-1.7	2.1	3.3	6.3	8.8	12.5	11.5	12.4	9.8	9.0	3.0	-1.3	6.3
1913	-3.3	2.0	1.8	4.3	8.4	13.1	13.6	13.6	10.1	6.2	3.9	2.6	6.4
1912	0.2	4.0	3.8	6.0	11.4	11.7	14.2	12.0	10.9	7.4	3.3	1.9	7.2
1911	-5.1	0.8	1.9	3.4	7.6	10.2	14.6	15.2	11.6	8.4	1.2	0.3	5.6
1910	0.8	-1.7	-0.1	4.2	8.5	11.3	M	12.9	12.2	7.1	3.0	1.9	M
1909	-10.1	-3.9	3.9	4.8	8.2	11.7	14.2	13.1	10.4	6.1	-1.8	-0.6	4.7
1908	2.1	1.5	1.6	4.7	8.3	11.6	13.9	11.7	8.5	4.6	2.1	-0.6	6.0
1907	-3.8	-2.1	-0.2	5.2	10.7	11.2	13.4	12.9	11.1	7.9	4.5	3.4	6.2
1906	-3.3	2.9	3.9	5.5	8.8	11.3	12.7	12.7	10.4	8.1	4.5	0.0	6.5
1905	0.6	2.9	6.3	5.7	9.7	12.8	14.5	12.9	10.4	7.0	5.4	2.9	7.6
1904	-3.1	-3.6	0.1	5.4	7.9	9.6	11.1	12.6	10.3	8.3	4.3	3.8	4.3
1903	1.0	0.3	0.2	4.2	7.3	12.3	13.4	14.0	10.4	7.3	2.4	4.3	6.4
1902	1.4	3.2	0.1	5.0	8.3	13.1	12.8	11.8	9.9	8.0	1.6	-3.6	6.0
1901	-0.4	-2.2	2.5	4.4	7.4	10.5	13.2	12.1	10.3	7.1	2.3	2.1	5.8
1900	0.6	-0.6	2.1	5.1	7.9	11.6	13.2	12.8	10.4	5.6	1.5	1.8	6.0
1899	-2.5	-3.3	-1.6	4.5	6.4	9.9	15.1	13.1	10.4	5.3	5.5	1.2	5.3
1898	M	M	M	M	M	M	M	M	M	M	M	2.1	M
1897	M	-0.6	M	M	M	M	M	M	M	M	M	M	M
1896	M	M	M	M	M	M	M	M	10.4	7.4	-1.4	1.0	M
1895	-3.1	M	M	M	M	M	13.1	11.5	M	M	M	M	M
1894	M	M	M	M	M	M	M	M	M	M	M	-2.4	M
1893	M	M	M	M	M	M	M	M	M	M	M	M	M
1892	-1.9	M	M	M	M	M	M	M	M	M	M	M	M
1891	1.7	-2.6	1.6	5.7	8.6	12.9	15.8	14.0	10.1	6.1	0.7	-2.3	6.0
1890	-8.1	-5.3	-0.3	1.5	8.9	11.8	14.1	13.1	10.3	5.7	4.0	-1.7	4.5
1889	M	M	M	M	M	M	M	M	M	M	M	-2.0	M
1888	M	M	M	M	M	M	M	M	M	M	M	M	M
1887	M	M	M	M	M	M	M	M	M	M	M	M	M
1886	M	M	M	M	M	M	M	M	M	M	M	M	M
1885	M	M	M	M	M	M	M	M	M	M	M	M	M
1884	-1.1	-4.3	1.3	6.4	7.1	11.9	13.4	12.9	8.7	2.4	M	M	M
1883	M	M	M	M	10.2	11.4	11.8	12.3	10.7	5.8	-5.1	-1.9	M
1882	M	M	M	M	M	M	M	M	M	M	M	M	M
1881	M	M	M	M	M	M	13.6	M	M	5.2	1.8	M	M
Avg	-1.5	-0.1	1.9	5.2	8.9	12.1	13.7	13.5	10.8	6.8	2.4	-0.1	6.2
St Dev	3.1	2.5	1.6	1.2	1.2	1.1	1.0	1.0	0.8	1.2	2.3	2.6	0.8
Max	5.1	4.9	6.3	7.6	11.7	15.3	16.4	15.8	13.3	9.1	6.2	4.6	7.9
Min	-10.1	-8.6	-1.7	1.5	6.4	9.6	11.1	11.5	8.1	2.4	-5.1	-8.5	4.3

Number of Weather Stations with Temperature Data (6 total)

Year	Jan	Feb	Mar	Apr	May	Jun	Jul	Aug	Sep	Oct	Nov	Dec	Annual
1996	5	5	5	5	5	4	3	4	4	4	3	2	0
1995	5	5	5	4	5	5	5	5	5	4	5	6	4
1994	6	5	5	4	5	5	5	5	5	5	5	5	4
1993	6	6	6	6	6	6	6	6	6	6	5	6	5
1992	6	6	6	6	6	6	6	5	6	6	6	6	5
1991	5	6	6	5	6	6	6	6	6	6	6	6	4
1990	6	6	6	6	6	6	5	6	6	6	6	6	5
1989	6	6	6	6	5	6	6	6	6	6	6	5	4
1988	5	5	5	6	6	6	6	6	6	6	6	6	5
1987	6	6	4	6	6	6	6	6	6	6	6	6	4
1986	5	5	4	5	5	5	5	5	6	5	6	6	3
1985	5	5	5	5	5	5	6	6	6	5	5	5	5
1984	6	6	6	5	6	5	6	6	6	6	5	6	5
1983	6	6	6	6	6	6	4	6	6	5	5	5	3
1982	6	6	5	6	5	6	6	5	6	6	6	6	5
1981	6	5	5	5	5	6	6	6	6	6	6	6	5
1980	5	5	5	5	5	5	4	5	5	5	6	6	4
1979	5	5	5	5	5	5	5	5	5	5	5	5	5
1978	6	6	6	5	5	4	5	5	5	4	5	5	2
1977	6	6	6	6	6	5	6	6	6	6	6	6	5
1976	5	6	5	6	6	6	6	6	6	6	6	6	5
1975	5	5	5	5	5	4	5	5	5	5	4	5	3
1974	5	5	5	5	5	5	5	5	5	5	5	5	5
1973	5	5	5	5	6	5	5	5	5	5	5	5	5
1972	5	5	5	5	6	6	5	5	5	4	5	5	4
1971	5	6	6	6	5	6	6	5	5	4	5	5	3
1970	6	6	5	6	6	6	6	6	6	6	5	5	5
1969	6	6	6	6	6	6	6	6	6	5	6	6	5
1968	6	6	6	6	6	6	6	6	6	6	6	6	6
1967	6	6	6	6	6	6	6	6	6	6	6	6	6
1966	6	6	6	6	6	6	6	6	6	6	6	6	6
1965	6	6	6	6	6	6	5	6	6	5	6	6	5
1964	6	6	6	6	6	6	6	6	6	6	6	6	6
1963	6	6	6	6	6	6	6	6	6	6	6	6	6
1962	6	6	6	6	6	5	6	6	6	6	6	6	5
1961	5	6	6	6	6	6	6	6	6	6	6	6	5
1960	6	6	6	6	6	6	6	6	6	6	6	6	6
1959	6	6	6	6	6	6	5	6	6	6	6	6	5
1958	5	6	6	6	6	6	6	6	6	6	5	6	4

Year	Jan	Feb	Mar	Apr	May	Jun	Jul	Aug	Sep	Oct	Nov	Dec	Annual
1957	5	5	5	5	5	5	5	5	6	6	6	6	5
1956	6	6	6	6	6	5	4	5	5	5	5	5	4
1955	6	6	6	6	6	6	6	6	6	6	6	6	6
1954	6	6	6	6	6	6	6	6	6	6	6	6	6
1953	6	6	6	5	6	6	6	6	5	6	6	6	4
1952	6	6	6	6	6	6	6	6	6	6	6	6	6
1951	6	6	6	6	6	6	6	6	6	6	6	6	6
1950	6	5	6	6	6	6	6	6	6	6	6	6	5
1949	6	6	6	6	6	6	6	6	6	6	6	6	6
1948	6	6	6	6	6	6	6	6	6	6	6	6	6
1947	6	6	6	6	6	6	6	6	6	6	6	6	6
1946	6	6	6	6	6	6	6	6	6	6	6	6	6
1945	6	6	6	6	6	6	6	6	6	6	6	6	6
1944	6	6	6	6	6	6	6	6	6	6	6	6	6
1943	6	6	6	6	6	6	6	6	6	6	6	6	6
1942	6	6	6	6	5	6	6	6	6	6	6	6	5
1941	6	6	6	6	6	6	6	6	6	6	6	6	6
1940	6	6	6	6	6	6	6	6	6	5	6	6	5
1939	6	6	6	6	6	6	6	6	6	6	6	6	6
1938	6	6	6	5	6	6	6	6	6	6	6	6	5
1937	6	6	6	6	6	6	6	6	6	6	6	6	6
1936	5	4	5	5	5	5	5	5	5	5	5	6	4
1935	5	5	4	5	5	5	5	5	5	5	5	5	4
1934	5	5	5	5	5	5	5	5	5	4	5	5	4
1933	6	6	6	6	6	6	6	5	4	5	5	5	4
1932	6	6	6	6	6	4	5	5	5	5	6	6	4
1931	6	6	6	6	6	6	6	6	6	6	6	6	6
1930	6	6	6	6	6	6	6	6	6	6	6	6	6
1929	5	5	5	5	5	5	5	5	5	5	6	6	5
1928	5	5	5	5	5	5	5	5	5	5	5	5	5
1927	6	6	6	6	6	6	6	6	6	6	5	5	4
1926	5	5	5	5	5	5	5	6	5	5	5	5	4
1925	4	4	4	4	5	5	5	5	5	5	5	5	4
1924	3	3	3	3	3	3	3	3	4	4	4	4	3
1923	4	4	4	4	4	3	3	3	3	3	3	3	3
1922	3	3	3	3	3	3	3	3	3	3	4	4	3
1921	4	4	4	4	4	4	3	2	3	3	3	3	2
1920	4	4	4	4	4	4	4	4	4	4	4	4	4
1919	4	4	4	4	4	4	4	4	4	4	4	3	3
1918	4	4	4	4	3	3	4	4	4	4	4	4	3
1917	3	3	3	3	2	3	3	3	3	3	4	4	2

Year	Jan	Feb	Mar	Apr	May	Jun	Jul	Aug	Sep	Oct	Nov	Dec	Annual
1916	3	3	3	3	3	3	3	3	3	3	3	3	3
1915	3	3	3	3	3	3	3	3	3	3	3	3	3
1914	3	3	3	3	3	3	3	3	3	3	3	3	3
1913	3	3	3	2	3	3	3	3	3	3	3	3	2
1912	2	2	2	2	3	3	3	3	3	3	3	3	2
1911	3	3	3	3	3	3	2	2	2	2	2	1	1
1910	2	2	1	1	1	1	0	1	3	2	3	3	0
1909	1	1	1	1	2	2	2	2	2	2	2	2	1
1908	2	2	2	2	2	2	1	1	1	1	1	1	1
1907	2	2	2	2	2	2	2	2	2	2	2	2	2
1906	1	1	1	1	1	1	1	1	1	1	1	1	1
1905	2	1	2	2	2	2	2	2	2	2	2	2	2
1904	2	1	1	2	2	2	2	2	2	2	2	2	1
1903	1	2	2	2	2	2	2	2	2	1	1	1	1
1902	2	2	2	2	2	2	2	2	2	2	2	2	2
1901	2	2	2	2	2	2	2	2	2	2	2	2	2
1900	2	2	2	2	2	2	2	2	2	2	2	2	2
1899	1	1	1	1	2	2	2	2	2	2	2	2	1
1898	0	0	0	0	0	0	0	0	0	0	0	1	0
1897	0	1	0	0	0	0	0	0	0	0	0	0	0
1896	0	0	0	0	0	0	0	0	1	1	1	1	0
1895	1	0	0	0	0	0	1	1	0	0	0	0	0
1894	0	0	0	0	0	0	0	0	0	0	0	1	0
1893	0	0	0	0	0	0	0	0	0	0	0	0	0
1892	1	0	0	0	0	0	0	0	0	0	0	0	0
1891	1	1	1	1	1	1	1	1	1	1	1	1	1
1890	1	1	1	1	1	1	1	1	1	1	1	1	1
1889	0	0	0	0	0	0	0	0	0	0	0	1	0
1888	0	0	0	0	0	0	0	0	0	0	0	0	0
1887	0	0	0	0	0	0	0	0	0	0	0	0	0
1886	0	0	0	0	0	0	0	0	0	0	0	0	0
1885	0	0	0	0	0	0	0	0	0	0	0	0	0
1884	1	1	1	1	1	1	1	1	1	1	0	0	0
1883	0	0	0	0	1	1	1	1	1	1	1	1	0
1882	0	0	0	0	0	0	0	0	0	0	0	0	0
1881	0	0	0	0	0	0	1	0	0	1	1	0	0
Avg	4.825	4.825	4.773	4.784	4.856	4.814	4.773	4.814	4.866	4.753	4.845	4.876	4.13402

SE Alaska Composite: Monthly Precipitation (mm)

Year	Jan	Feb	Mar	Apr	May	Jun	Jul	Aug	Sep	Oct	Nov	Dec	Annual
1995	49	107	129	84	66	83	96	117	139	319	208	217	1485
1994	201	86	231	148	156	85	79	81	412	372	303	171	2575
1993	243	287	134	69	96	67	74	62	179	356	325	292	2402
1992	333	192	175	139	218	73	93	116	369	221	275	151	2355
1991	167	286	130	134	142	80	127	237	345	298	355	382	3074
1990	169	190	168	88	49	105	81	172	286	334	209	275	2124
1989	347	5	70	39	105	53	76	68	231	312	326	338	1931
1988	134	267	240	138	133	98	190	167	258	412	416	212	2649
1987	284	186	126	251	168	189	78	94	429	447	466	269	2867
1986	257	143	207	152	113	112	84	177	134	567	325	293	2645
1985	405	263	166	196	142	150	73	144	179	270	87	270	2308
1984	343	240	212	82	99	160	149	221	159	273	185	225	2348
1983	293	140	55	132	179	107	124	329	226	357	88	40	1902
1982	145	62	124	171	178	25	88	127	197	369	149	108	1610
1981	217	153	192	165	71	131	103	220	437	276	372	121	2457
1980	125	130	174	271	101	80	153	175	250	474	404	233	2523
1979	127	80	172	46	159	121	133	49	237	356	272	326	2078
1978	84	98	151	128	123	81	92	144	145	654	227	200	1923
1977	191	288	204	198	61	146	93	59	191	471	240	131	2273
1976	361	196	200	122	203	92	149	166	303	327	310	310	2739
1975	237	190	138	123	102	124	153	103	240	227	217	298	2153
1974	144	330	47	137	160	146	102	87	179	659	395	399	2786
1973	231	194	192	155	200	120	163	180	276	349	75	198	2357
1972	189	177	227	165	124	127	107	252	240	382	213	203	2446
1971	203	203	175	167	160	79	48	194	216	322	253	153	2173
1970	179	217	183	207	184	156	166	213	359	310	125	213	2513
1969	76	65	141	165	95	82	252	236	173	195	546	299	2322
1968	208	184	199	253	63	76	114	125	435	319	319	108	2404
1967	228	283	62	66	141	85	193	247	399	371	218	193	2486
1966	157	175	262	95	291	61	86	209	339	465	196	191	2528
1965	313	235	83	153	160	136	50	113	65	512	145	245	2233
1964	257	354	220	201	159	91	160	196	149	391	252	232	2663
1963	289	271	131	142	93	200	112	44	378	425	254	304	2642
1962	383	29	228	192	80	164	89	158	377	308	298	339	2645
1961	219	241	179	217	98	147	162	346	210	548	299	239	2903
1960	227	119	239	171	79	130	179	171	284	533	234	335	2700
1959	106	209	294	143	121	70	225	206	218	344	370	470	2775
1958	267	114	70	152	183	49	128	245	221	488	255	298	2470
1957	66	177	102	205	113	108	126	102	194	224	375	241	2113

Year	Jan	Feb	Mar	Apr	May	Jun	Jul	Aug	Sep	Oct	Nov	Dec	Annual
1956	88	177	194	152	229	114	93	393	169	372	420	398	2849
1955	280	212	249	137	206	117	57	273	242	396	159	108	2435
1954	165	375	127	138	99	90	99	38	204	352	336	421	2445
1953	122	324	253	168	137	72	91	195	308	509	246	374	3014
1952	267	185	165	244	182	108	145	202	396	445	302	195	2836
1951	186	141	215	205	98	160	89	110	151	223	216	181	1974
1950	34	190	105	162	174	45	237	220	315	195	143	208	2165
1949	355	121	134	309	128	177	118	156	325	503	389	135	2851
1948	348	102	138	31	95	83	150	172	440	515	428	217	2719
1947	284	135	300	209	120	124	86	235	400	314	271	285	2761
1946	224	141	187	186	49	35	189	199	267	373	294	230	2374
1945	214	213	270	137	72	166	225	63	302	480	141	145	2428
1944	296	93	269	122	186	95	98	181	153	542	277	220	2532
1943	285	213	82	204	114	39	216	237	366	374	461	434	3025
1942	313	139	223	142	68	76	91	120	181	439	221	226	2300
1941	200	52	170	124	120	121	141	42	181	446	365	147	2109
1940	118	82	254	132	163	137	78	329	251	281	268	184	2422
1939	314	193	165	185	138	94	147	298	335	529	413	327	3138
1938	292	200	143	217	176	179	129	77	339	354	293	348	2901
1937	115	138	175	155	119	125	158	196	241	437	162	217	2280
1936	127	58	223	159	131	39	164	97	265	420	596	291	2464
1935	213	236	91	121	154	136	137	224	209	183	285	347	2406
1934	347	177	168	172	79	113	73	113	139	312	181	199	2095
1933	175	162	134	169	91	122	132	255	153	363	442	46	2217
1932	294	270	109	79	136	198	172	99	385	279	294	157	2491
1931	277	271	143	197	204	109	112	240	200	438	171	173	2534
1930	34	288	214	130	98	123	128	133	276	434	421	486	2765
1929	229	158	223	75	92	93	149	206	85	493	469	176	2432
1928	355	184	251	122	199	35	124	133	212	302	272	289	2478
1927	143	167	274	129	98	51	56	130	303	359	135	214	2061
1926	411	261	232	222	148	118	110	78	79	410	133	399	2615
1925	216	121	243	189	122	127	193	143	139	238	356	412	2635
1924	299	261	171	287	189	24	176	214	470	367	332	131	3078
1923	169	369	299	195	131	50	74	230	368	277	482	441	3150
1922	299	92	221	272	160	46	75	188	340	287	413	126	2559
1921	179	334	132	117	144	111	140	183	270	487	250	386	2836
1920	348	221	148	134	166	107	35	434	264	345	202	207	2611
1919	332	122	154	172	141	77	109	155	235	270	271	241	2280
1918	261	185	164	184	165	102	107	344	198	463	412	307	3042
1917	253	170	133	92	109	160	224	374	301	532	685	229	3302
1916	26	179	175	193	135	153	172	170	353	398	314	214	2480

Year	Jan	Feb	Mar	Apr	May	Jun	Jul	Aug	Sep	Oct	Nov	Dec	Annual
1915	277	127	275	304	64	132	56	300	253	419	429	339	2974
1914	156	285	240	198	154	51	375	224	333	279	257	164	2714
1913	272	165	195	124	164	55	212	248	348	414	337	275	2132
1912	49	175	105	69	128	133	110	173	290	489	308	460	2160
1911	125	139	160	169	60	64	49	58	103	229	188	203	1008
1910	175	86	127	151	135	79	174	62	142	347	175	300	1550
1909	27	79	299	116	129	131	163	235	421	212	100	108	2020
1908	117	133	134	196	110	49	79	144	417	248	115	171	1670
1907	36	158	57	66	104	78	102	247	363	292	223	73	1799
1906	147	44	27	174	80	59	140	100	120	350	354	112	1707
1905	84	100	130	160	51	66	60	193	197	251	340	273	1907
1904	157	11	77	143	138	187	179	90	349	300	296	225	1892
1903	228	203	72	101	132	30	65	119	162	369	165	380	1910
1902	313	55	140	118	128	54	190	344	351	188	172	129	2184
1901	240	161	204	195	106	43	31	306	270	408	123	299	2384
1900	219	96	72	298	121	68	114	184	237	275	277	184	2145
1899	100	89	38	109	110	135	42	168	224	276	200	194	1663
1898	M	M	M	M	M	M	M	M	M	M	M	206	M
1897	M	129	M	M	M	M	M	M	M	M	M	M	M
1896	M	M	M	M	M	M	M	M	358	246	15	269	M
1895	147	M	M	M	M	M	82	195	191	M	M	M	M
1894	M	M	M	M	M	M	M	M	M	M	M	183	M
1893	M	M	M	M	M	M	M	M	M	M	M	M	M
1892	347	M	M	M	M	M	M	M	M	M	M	M	M
1891	521	68	144	161	102	56	60	330	262	284	265	179	2432
1890	82	166	150	125	123	162	140	56	435	287	469	174	2369
1889	M	M	M	M	M	M	M	M	M	M	207	137	M
1888	M	M	M	M	M	M	83	160	114	52	59	64	M
1887	199	125	187	169	185	127	194	238	268	M	M	M	M
1886	187	479	256	195	93	115	83	272	648	630	521	83	3563
1885	265	250	307	341	90	60	98	102	212	344	245	297	2611
1884	316	147	263	92	298	99	141	190	337	370	414	180	2818
1883	119	176	406	121	142	166	201	259	210	280	244	338	2600
1882	301	253	103	71	55	90	145	117	246	245	291	344	2597
1881	M	M	M	107	79	62	140	64	214	154	379	280	M
Avg	216	186	172	156	133	107	124	169	266	383	273	243	2440
St Dev	91	82	62	58	51	41	49	78	96	111	103	91	340
Max	521	479	406	341	298	200	375	434	648	659	685	486	3563
Min	26	5	27	31	49	24	31	38	65	52	15	40	1008

Number of Weather Stations with Precipitation Data (6 total)

Year	Jan	Feb	Mar	Apr	May	Jun	Jul	Aug	Sep	Oct	Nov	Dec	Annual
1995	5	5	5	4	5	5	5	5	5	5	5	5	5
1994	6	5	5	4	5	5	5	5	5	5	5	5	4
1993	6	6	6	6	6	5	6	6	6	6	6	6	5
1992	6	6	6	6	6	6	6	6	6	6	6	6	6
1991	5	6	6	5	6	6	6	6	6	6	6	6	4
1990	6	6	6	6	6	6	5	6	6	6	6	6	5
1989	6	6	6	6	5	6	6	6	6	6	6	5	4
1988	5	5	5	6	6	6	6	6	6	6	5	6	4
1987	6	6	4	6	6	6	6	6	6	5	5	6	4
1986	5	5	4	5	5	5	5	5	6	5	5	6	2
1985	5	5	5	5	5	5	6	6	6	5	5	5	5
1984	6	6	6	6	6	6	6	6	6	6	6	6	6
1983	6	6	6	6	6	6	6	6	6	6	5	5	5
1982	6	5	5	6	5	5	5	5	6	6	6	5	4
1981	6	6	6	6	6	6	6	6	6	6	6	6	6
1980	5	5	5	5	5	5	5	5	5	5	6	6	5
1979	5	5	5	5	5	5	5	5	5	5	5	5	5
1978	6	6	6	6	5	5	5	5	4	5	5	5	4
1977	6	6	6	6	6	6	6	6	6	6	6	6	6
1976	6	6	6	6	6	6	6	6	6	6	6	6	6
1975	5	5	5	5	5	5	5	5	5	5	5	5	5
1974	5	5	5	5	5	5	5	5	5	5	5	5	5
1973	6	6	5	5	5	5	5	5	5	5	5	5	5
1972	6	6	5	6	6	6	5	6	5	5	5	6	5
1971	6	6	6	6	6	6	6	6	6	6	6	6	6
1970	6	6	6	6	6	6	6	6	6	6	6	6	6
1969	6	6	6	6	6	6	6	6	6	6	6	6	6
1968	6	6	6	6	6	6	6	6	6	6	6	6	6
1967	6	6	6	6	6	6	6	6	6	6	6	6	6
1966	6	6	6	6	6	6	6	6	6	6	6	6	6
1965	6	6	6	6	6	6	5	6	6	5	6	6	5
1964	6	6	6	6	6	6	6	6	6	6	6	6	6
1963	6	6	6	6	6	6	6	6	6	6	6	6	6
1962	6	6	6	6	6	6	6	6	6	6	6	6	6
1961	6	6	6	6	6	6	6	6	6	6	6	6	6
1960	6	6	6	6	6	6	6	6	6	6	6	6	6
1959	6	6	6	6	6	6	6	6	6	6	6	6	6
1958	6	6	6	6	6	6	6	6	6	6	6	6	6
1957	5	5	5	5	5	5	5	5	6	6	6	6	5

Year	Jan	Feb	Mar	Apr	May	Jun	Jul	Aug	Sep	Oct	Nov	Dec	Annual
1956	6	6	6	6	6	5	5	5	5	5	5	5	5
1955	6	6	6	6	6	6	6	6	6	6	6	6	6
1954	6	6	6	6	6	6	6	6	6	6	6	6	6
1953	6	6	6	6	6	6	6	6	5	6	6	6	5
1952	6	6	6	6	6	6	6	6	6	6	6	6	6
1951	6	6	6	6	6	6	6	6	6	6	6	6	6
1950	6	5	6	6	6	6	6	6	6	6	6	6	5
1949	6	6	6	6	6	6	6	6	6	6	6	6	6
1948	6	6	6	6	6	6	6	6	6	6	6	6	6
1947	6	6	6	6	6	6	6	6	6	6	6	6	6
1946	6	6	6	6	6	6	6	6	6	6	6	6	6
1945	6	6	6	6	6	6	6	6	6	6	6	6	6
1944	6	6	6	6	6	6	6	6	6	6	6	6	6
1943	6	6	6	6	6	6	6	6	6	6	6	6	6
1942	6	6	6	6	5	5	5	5	5	5	6	6	5
1941	6	6	6	6	6	6	6	6	6	6	6	6	6
1940	6	6	6	6	6	6	6	6	6	5	6	6	5
1939	6	6	6	6	6	6	6	6	6	6	6	6	6
1938	6	6	6	5	6	6	6	6	6	6	6	6	5
1937	6	6	6	6	6	6	6	6	6	6	6	6	6
1936	5	4	5	5	5	5	5	5	5	5	5	6	4
1935	4	4	4	5	5	5	4	5	5	5	5	5	4
1934	5	5	5	5	5	5	5	5	5	4	5	5	4
1933	6	6	6	6	6	6	6	5	5	5	5	5	5
1932	6	6	6	6	6	5	5	5	5	5	6	6	5
1931	6	6	6	6	6	6	6	6	6	6	6	6	6
1930	6	6	6	6	6	6	6	6	6	6	6	6	6
1929	5	5	5	5	5	5	5	5	5	5	6	6	5
1928	5	5	5	5	5	5	5	5	5	5	5	5	5
1927	5	6	6	6	6	6	6	6	6	6	5	5	4
1926	5	5	5	5	5	5	5	6	5	5	5	5	4
1925	4	4	4	4	4	5	5	5	5	6	5	5	4
1924	3	3	3	3	4	4	4	4	4	5	5	4	3
1923	4	4	4	4	4	3	3	3	3	3	3	3	3
1922	3	3	3	3	3	3	3	3	3	3	4	4	3
1921	4	4	4	4	4	4	4	4	3	3	3	3	3
1920	4	4	4	4	4	4	4	4	4	4	4	4	4
1919	4	4	4	4	4	4	4	4	4	4	4	4	4
1918	4	4	4	4	3	3	3	4	4	4	4	4	3
1917	3	3	3	3	3	3	3	3	3	3	4	4	3
1916	3	3	3	3	3	3	3	3	3	3	3	3	3

Year	Jan	Feb	Mar	Apr	May	Jun	Jul	Aug	Sep	Oct	Nov	Dec	Annual
1915	3	3	3	3	3	3	3	3	3	3	3	3	3
1914	3	3	3	3	3	3	3	3	3	3	3	3	3
1913	3	3	3	2	3	3	3	3	3	3	3	3	2
1912	2	2	2	2	3	3	3	3	3	3	3	3	2
1911	3	3	3	3	3	2	2	2	2	2	2	1	1
1910	2	2	2	2	2	2	2	2	3	3	3	3	2
1909	2	2	2	2	2	2	2	2	2	2	2	2	2
1908	2	2	2	2	2	2	2	2	2	2	2	1	1
1907	2	2	2	2	2	2	2	2	2	2	2	2	2
1906	2	2	2	2	2	2	2	2	2	2	2	2	2
1905	2	2	2	2	2	2	2	2	2	2	2	2	2
1904	2	1	1	2	2	2	2	3	3	3	3	2	1
1903	2	2	2	2	2	2	2	2	2	1	1	1	1
1902	2	2	2	2	2	2	2	2	2	2	2	2	2
1901	2	2	2	2	2	2	2	2	2	2	2	2	2
1900	2	2	2	2	2	2	2	2	2	2	2	2	2
1899	1	1	1	1	2	2	2	2	2	2	2	2	1
1898	0	0	0	0	0	0	0	0	0	0	0	1	0
1897	0	1	0	0	0	0	0	0	0	0	0	0	0
1896	0	0	0	0	0	0	0	0	1	1	1	1	0
1895	1	0	0	0	0	0	1	1	1	0	0	0	0
1894	0	0	0	0	0	0	0	0	0	0	0	1	0
1893	0	0	0	0	0	0	0	0	0	0	0	0	0
1892	1	0	0	0	0	0	0	0	0	0	0	0	0
1891	1	1	1	1	1	1	1	1	1	1	1	1	1
1890	1	1	1	1	1	1	1	1	1	1	1	1	1
1889	0	0	0	0	0	0	0	0	0	0	1	1	0
1888	0	0	0	0	0	0	1	1	1	1	1	1	0
1887	1	1	1	1	1	1	1	1	1	0	0	0	0
1886	1	1	1	1	1	1	1	1	1	1	1	1	1
1885	1	1	1	1	1	1	1	1	1	1	1	1	1
1884	2	2	2	2	2	2	2	2	2	1	1	1	1
1883	1	1	1	1	2	2	2	2	2	2	2	2	1
1882	2	3	3	2	2	2	2	2	1	1	1	1	1
1881	0	0	0	1	1	2	2	2	3	3	3	2	0
Avg	4.235	4.209	4.174	4.2	4.235	4.217	4.217	4.27	4.27	4.217	4.27	4.27	3.82609

APPENDIX B: TREE RING DATA

Raw ring width data for Crystal Mountain tree cores collected August 1995.

Year	Raw Ring Width Measurement for Core:													
	CR1E	CR2E	CR3N	CR4S	CR5N	CR6N	CR7E	CR7N	CR8E	CR9E	CR9N	CR11N	CR12N	CR13N
1554												63		
1555												54		
1556												81		
1557												108		
1558												136		
1559												126		
1560												145		
1561												86		
1562												121		
1563												174		
1564												147		
1565												162		
1566												140		
1567												118		
1568												133		
1569												77		
1570												114		
1571												30		
1572												38		
1573												69		
1574												127		
1575												138		
1576												67		
1577												35		
1578												69		
1579												62		
1580												48		
1581												86		
1582												70		
1583												90		
1584												62		
1585												26		
1586												44		
1587												80		
1588												83		
1589												116		
1590												94		
1591												67		
1592												20		
1593												41		
1594												57		
1595												27		
1596												37		
1597												55		
1598												63		
1599												42		
1600												39		

Year	Raw Ring Width Measurement for Core:													
	CR1E	CR2E	CR3N	CR4S	CR5N	CR6N	CR7E	CR7N	CR8E	CR9E	CR9N	CR11N	CR12N	CR13N
1601												32		
1602												26		
1603												5		
1604												26		
1605												27		
1606												34		
1607												21		
1608												42		
1609												26		
1610												43		
1611		104										47		
1612		135										37		78
1613	29	81					43					44		48
1614	44	87					55					43		43
1615	83	87					72					13		64
1616	115	112					126					23		104
1617	77	91					114					31		120
1618	24	64					44					26		52
1619	94	112					115					32		153
1620	39	68					81					19		112
1621	47	78					70					20		105
1622	30	65					61					6		84
1623	47	147					87					19		104
1624	34	118					95					19		122
1625	66	113					105					16		90
1626	50	98					104					10		101
1627	84	105					121					14		156
1628	48	58					75					23		127
1629	77	54					81					32		140
1630	30	71					80					33		202
1631	42	35					128					12		136
1632	59	67					211					16		179
1633	33	43					153					7		68
1634	86	112					161					19		117
1635	78	116					96					16		117
1636	61	77					122					23		101
1637	40	93					168					18		71
1638	44	101					149					20		65
1639	9	33					133					8		46
1640	45	86					172					20		71
1641	15	102					125					26		76
1642	74	140					100					32		118
1643	43	76					34					25		89
1644	29	78					45					28		81
1645	36	83					60					28		97
1646	56	144					57					30		82
1647	55	211					54					42		86

Year	Raw Ring Width Measurement for Core:													
	CR1E	CR2E	CR3N	CR4S	CR5N	CR6N	CR7E	CR7N	CR8E	CR9E	CR9N	CR11N	CR12N	CR13N
1648	31	126					29					34		55
1649	36	139					78					54		67
1650	37	99					67					32		73
1651	97	143					88					70		88
1652	35	79					27					46		58
1653	22	66					38					21		48
1654	14	45					59					34		59
1655	39	51					65					16		61
1656	22	40					51					23		76
1657	16	41					57					27		72
1658	42	38					48					30		59
1659	23	41					54					40		76
1660	73	41					51					38		67
1661	108	60					41					49		100
1662	62	61					58					55		104
1663	30	38					35					23		70
1664	5	18					20					35		43
1665	25	37					32					44		64
1666	11	32					36					29		45
1667	12	53					48					37		66
1668	13	39					43					33		69
1669	41	49					48					40		53
1670	45	53					16					34		72
1671	61	57					52					34		85
1672	43	39					26					30		65
1673	23	46					45					47		78
1674	19	63					49				174	58		86
1675	29	55					36				88	44		52
1676	4	30					11				59	27		24
1677	23	111					25				89	28		54
1678	22	71					32				56	41		60
1679	8	55			32		12				44	21		41
1680	30	89			40		33				52	14		52
1681	55	121			41		46				75	26		48
1682	100	112			50		38				66	29		59
1683	121	88			48		44			111	91	37		64
1684	76	90			31		30			105	106	35		55
1685	52	102			45		55			101	111	62		71
1686	38	103			40		75			75	74	37		86
1687	38	79			25		67			70	71	24		89
1688	26	79			30		61			104	98	15		79
1689	17	37			23		62			55	68	26		24
1690	44	49		16	48		79			91	98	26		79
1691	22	42		34	40		24			90	70	27		72
1692	25	35		33	55		24			112	108	18		56
1693	35	27		20	40		31			98	104	27		61
1694	59	33		16	76		45			133	99	27		70

Year	Raw Ring Width Measurement for Core:													
	CR1E	CR2E	CR3N	CR4S	CR5N	CR6N	CR7E	CR7N	CR8E	CR9E	CR9N	CR11N	CR12N	CR13N
1695	27	40		6	64		23			91	77	37		71
1696	24	33		22	54		14			84	83	12		33
1697	22	35		6	25		11			49	55	20		50
1698	19	35		15	32		14			54	67	9		29
1699	22	47		14	32		12			54	56	18		54
1700	23	31		24	63		19			94	95	7		34
1701	32	40		21	58		30			76	92	20	39	40
1702	25	48		14	85		30			69	87	22	48	55
1703	25	36		11	71		15			50	66	17	56	57
1704	48	46		6	65		29			71	87	20	50	44
1705	46	33		9	53		27			80	101	16	79	24
1706	9	12		7	20		10			63	64	20	78	12
1707	28	43		10	63		82			136	118	30	61	34
1708	23	85		8	100		75			133	151	0	162	72
1709	57	113		13	104		78			93	115	18	140	94
1710	58	135		17	112	199	84			92	114	27	129	83
1711	45	82		22	79	147	28			72	96	15	114	72
1712	53	73		12	101	127	57			96	154	22	144	92
1713	72	49		4	88	121	37			75	115	25	100	79
1714	58	43		15	57	72	10			53	90	15	47	62
1715	26	39		19	92	93	15			59	105	20	26	65
1716	33	60		10	68	110	26			59	83	34	88	54
1717	6	24		12	43	69	4			26	50	16	20	32
1718	17	53		14	78	133	12			51	77	25	60	31
1719	15	66		16	104	134	14			70	83	33	51	40
1720	23	99		30	125	132	40			50	81	32	44	45
1721	38	83		39	129	132	59	156		82	107	42	72	38
1722	55	89		28	160	177	56	158		115	137	42	88	62
1723	83	62		32	160	262	85	200		117	137	44	97	56
1724	83	30		15	99	152	22	98		77	97	25	40	33
1725	68	11		12	73	117	10	57		62	93	9	44	25
1726	57	22		13	103	135	14	114		45	60	22	47	42
1727	29	23		25	94	149	29	124		46	74	24	52	48
1728	53	12		13	57	118	9	75		47	98	20	43	31
1729	58	30		19	78	151	36	132		75	96	28	58	62
1730	39	27		12	50	100	14	85	43	58	88	14	20	39
1731	31	48		27	41	85	11	86	41	60	104	14	43	51
1732	44	55		28	66	117	35	130	54	86	94	24	53	70
1733	42	48		36	62	123	44	135	52	83	102	31	59	75
1734	43	28		25	41	76	12	83	39	63	76	21	41	48
1735	54	35		31	62	100	28	91	28	57	72	23	13	67
1736	49	32		35	66	60	20	60	39	58	92	20	15	51
1737	63	32		39	78	104	55	126	48	66	81	21	0	39
1738	19	11		30	34	50	34	76	34	65	71	20	14	41
1739	24	14		45	36	68	29	85	36	57	80	32	51	60
1740	22	19		41	50	58	13	48	29	44	78	29	56	55
1741	36	18		42	46	79	13	46	27	38	67	21	69	58

Year	Raw Ring Width Measurement for Core:													
	CR1E	CR2E	CR3N	CR4S	CR5N	CR6N	CR7E	CR7N	CR8E	CR9E	CR9N	CR11N	CR12N	CR13N
1742	32	18		28	35	79	13	65	29	43	53	24	51	38
1743	26	24		18	50	74	18	62	25	41	65	14	52	31
1744	17	14		14	18	60	5	19	8	35	43	14	8	15
1745	52	48		35	58	140	27	93	41	86	94	27	65	58
1746	38	34		24	38	126	12	46	21	85	79	18	63	44
1747	30	44		37	53	158	45	107	39	70	90	29	74	43
1748	37	31		25	46	141	23	88	24	77	78	29	46	48
1749	28	29		22	39	118	29	105	28	78	75	31	39	56
1750	41	35		20	37	152	41	106	56	67	68	19	59	60
1751	19	28		22	28	97	23	73	59	73	65	37	32	62
1752	25	51		44	35	104	31	83	52	72	55	30	50	71
1753	16	35		26	19	75	12	41	35	47	56	15	13	48
1754	20	35		20	19	99	16	62	34	56	54	15	35	32
1755	6	31		30	17	76	9	38	35	43	48	23	22	36
1756	22	52		46	47	130	17	64	39	112	112	39	55	45
1757	14	40		54	45	105	25	70	37	84	97	22	70	39
1758	20	43		53	40	111	19	52	28	82	90	34	72	42
1759	13	37		55	30	99	9	36	26	113	104	56	50	31
1760	27	63		62	21	90	12	52	39	116	81	39	64	33
1761	53	67		101	42	131	39	121	57	127	114	59	156	65
1762	15	61		85	28	104	23	80	44	134	94	34	121	70
1763	18	75		124	51	174	54	152	88	202	155	52	213	103
1764	5	45		50	23	117	12	46	34	127	96	37	138	78
1765	19	86		66	50	149	44	98	59	131	101	53	143	76
1766	17	43		64	32	126	16	58	63	104	78	15	109	71
1767	15	77		42	37	93	14	65	46	106	43	44	71	67
1768	12	62		39	25	67	16	56	43	97	60	34	62	58
1769	18	59		49	40	107	25	78	42	100	84	30	81	45
1770	15	64		69	40	124	42	115	50	114	106	60	98	57
1771	13	64		70	54	133	56	89	49	111	89	29	105	51
1772	8	50		52	40	95	30	53	35	86	72	51	57	58
1773	15	49		50	38	79	22	44	38	120	84	41	43	54
1774	0	68		60	57	136	27	56	38	124	127	60	86	87
1775	9	43		63	53	117	30	67	29	114	91	49	114	63
1776	10	42		72	62	159	38	130	40	168	126	66	164	71
1777	12	56		102	74	202	41	184	45	235	180	104	140	94
1778	11	67		65	64	142	36	121	47	145	119	116	100	89
1779	6	44		60	21	110	16	61	41	102	94	56	56	76
1780	14	67		45	62	148	65	136	54	148	153	87	116	96
1781	8	42		31	22	95	24	72	20	79	70	90	57	63
1782	9	48		25	25	93	16	53	32	139	98	99	70	49
1783	7	35		32	25	74	33	70	21	114	98	82	67	62
1784	13	41		57	29	74	16	64	40	106	81	59	61	51
1785	24	56		72	39	95	31	88	35	119	89	60	60	54
1786	23	45		34	15	54	9	19	18	95	69	49	19	32
1787	46	57	64	45	23	64	10	39	22	158	106	25	48	46
1788	26	60	82	58	59	77	23	43	30	153	145	55	41	40

Year	Raw Ring Width Measurement for Core:													
	CR1E	CR2E	CR3N	CR4S	CR5N	CR6N	CR7E	CR7N	CR8E	CR9E	CR9N	CR11N	CR12N	CR13N
1789	20	48	49	39	42	38	9	25	20	142	124	45	22	42
1790	22	42	60	46	29	53	18	56	35	91	87	46	32	39
1791	22	48	58	53	46	67	32	61	31	104	101	54	50	54
1792	31	47	81	99	46	120	58	86	40	130	132	79	83	82
1793	43	50	88	58	73	115	50	87	44	145	127	66	103	61
1794	29	38	59	42	55	68	25	50	17	99	91	54	59	42
1795	33	64	58	63	62	104	26	52	22	142	133	64	51	68
1796	7	45	55	60	47	70	9	16	20	137	104	55	26	49
1797	25	67	75	85	35	72	37	75	39	110	103	53	41	62
1798	21	62	65	65	41	66	18	30	27	64	77	36	26	66
1799	19	61	42	70	34	48	23	50	29	60	76	48	42	51
1800	7	34	26	29	25	34	4	9	12	50	66	54	21	50
1801	10	33	32	32	21	27	9	38	23	48	47	55	50	62
1802	6	35	64	52	26	36	15	50	24	78	70	54	58	46
1803	25	64	99	67	62	71	39	69	35	123	113	70	68	60
1804	44	60	133	79	68	110	78	94	39	141	137	81	88	63
1805	40	30	157	43	59	67	41	54	25	118	145	65	76	61
1806	29	46	151	56	37	54	20	40	39	125	142	30	86	53
1807	31	37	152	71	42	53	23	37	54	141	150	52	71	58
1808	13	32	120	36	27	37	10	28	33	139	152	46	55	41
1809	14	31	65	41	41	39	13	36	34	124	123	37	47	36
1810	5	27	32	14	16	9	6	8	16	93	94	30	28	17
1811	16	34	74	42	50	48	23	29	32	91	84	36	68	40
1812	14	41	97	68	52	48	43	65	29	51	74	54	67	60
1813	7	40	119	90	60	52	46	48	29	52	66	46	56	58
1814	7	36	87	56	43	36	38	40	16	79	100	43	33	50
1815	13	38	78	54	27	27	38	41	34	86	85	35	50	48
1816	17	59	121	83	44	38	59	72	50	144	179	70	65	54
1817	13	42	86	51	17	22	22	28	16	114	121	45	35	33
1818	6	40	69	31	20	16	10	21	8	81	114	98	9	39
1819	11	62	41	30	27	28	19	31	12	84	111	82	27	39
1820	14	71	59	29	30	32	13	40	26	88	112	73	33	27
1821	21	72	74	45	57	54	27	95	30	81	122	78	43	48
1822	10	82	122	48	54	56	16	83	34	104	139	74	53	71
1823	11	56	129	28	48	63	19	119	23	99	129	65	79	59
1824	12	40	196	49	58	74	23	91	33	123	138	69	117	41
1825	25	73	254	91	69	136	51	125	59	126	148	73	119	58
1826	23	41	133	103	42	89	20	67	39	98	104	52	72	25
1827	13	44	91	78	50	80	15	28	34	86	94	65	60	25
1828	19	54	76	105	43	97	18	69	37	98	125	77	69	43
1829	9	54	57	97	47	115	15	34	32	87	91	86	57	57
1830	11	47	32	73	26	63	13	48	26	72	79	81	72	46
1831	7	50	20	49	37	38	6	22	7	66	58	56	61	20
1832	16	64	40	59	50	61	20	65	37	53	62	70	104	39
1833	19	51	44	61	62	52	20	81	38	61	72	93	70	45
1834	15	43	59	73	43	75	24	50	43	101	59	69	76	44
1835	11	34	71	75	52	74	29	65	57	94	72	61	96	46

Year	Raw Ring Width Measurement for Core:													
	CR1E	CR2E	CR3N	CR4S	CR5N	CR6N	CR7E	CR7N	CR8E	CR9E	CR9N	CR11N	CR12N	CR13N
1836	12	43	56	57	34	47	18	34	39	73	45	57	50	26
1837	16	66	71	88	53	62	21	39	55	112	64	64	78	67
1838	14	57	51	72	33	49	18	48	56	127	70	59	70	63
1839	20	52	62	77	46	42	32	51	50	88	71	68	69	66
1840	17	36	40	70	34	42	18	30	34	67	60	40	56	58
1841	10	44	37	57	23	33	16	32	25	48	68	37	65	39
1842	8	40	39	63	22	26	12	30	25	56	52	48	63	34
1843	10	41	52	52	28	27	14	26	22	79	66	49	48	46
1844	17	60	63	123	36	33	17	59	36	93	75	74	67	56
1845	18	62	68	105	30	52	14	52	37	111	82	59	47	56
1846	12	44	56	90	24	42	11	35	35	81	62	27	50	45
1847	6	33	39	54	16	24	8	24	16	47	21	38	39	48
1848	14	36	70	58	25	36	12	33	21	96	60	92	94	50
1849	7	13	40	21	6	16	9	12	0	54	44	17	31	27
1850	12	42	55	40	32	39	12	29	18	68	65	63	62	58
1851	20	48	73	67	42	62	25	46	30	93	85	64	75	54
1852	17	49	77	74	36	73	35	66	32	72	68	47	83	49
1853	6	32	31	28	22	32	9	20	14	42	39	29	26	20
1854	5	32	26	17	8	16	5	10	4	28	13	28	16	11
1855	16	38	52	44	37	41	22	41	43	65	45	18	70	35
1856	13	43	62	53	50	42	26	37	44	73	57	34	80	49
1857	20	46	75	49	54	68	32	84	64	80	69	36	108	56
1858	22	61	87	67	51	81	32	84	75	93	72	55	114	44
1859	29	59	90	61	52	90	38	72	62	87	70	63	124	48
1860	36	48	62	59	53	84	33	60	55	67	48	65	98	50
1861	32	41	56	41	39	65	32	55	30	68	49	32	78	56
1862	22	32	39	47	20	59	12	33	19	56	35	53	92	51
1863	13	20	26	15	16	41	9	26	13	50	50	37	85	48
1864	14	27	47	21	28	43	20	34	31	61	63	58	87	62
1865	8	14	33	21	21	38	12	19	21	51	66	30	70	63
1866	10	21	36	31	26	38	16	34	24	52	59	25	64	68
1867	18	34	52	29	33	47	20	44	37	72	72	36	81	76
1868	21	37	77	35	36	67	24	57	62	89	100	62	93	92
1869	23	36	80	47	40	89	33	51	33	94	103	49	97	87
1870	11	19	46	24	26	51	10	22	26	68	55	44	54	64
1871	5	13	25	19	10	39	3	9	7	64	60	20	15	56
1872	11	29	43	40	31	67	28	48	30	59	65	37	61	82
1873	24	29	49	50	16	73	14	34	37	61	71	39	59	79
1874	21	27	65	39	30	68	25	46	51	67	86	45	71	99
1875	11	22	52	23	23	60	12	31	31	53	66	34	63	66
1876	11	15	35	10	21	52	6	13	13	35	49	15	39	56
1877	18	22	36	22	22	70	20	38	27	57	48	27	34	86
1878	12	16	32	19	23	73	17	38	22	62	61	22	33	90
1879	16	27	43	22	20	64	22	41	27	69	63	26	42	72
1880	11	27	27	33	16	34	8	16	19	48	47	21	21	46
1881	35	36	53	39	38	85	30	48	46	77	84	40	56	93
1882	22	36	31	27	18	89	20	33	39	74	111	46	60	84

Year	Raw Ring Width Measurement for Core:													
	CR1E	CR2E	CR3N	CR4S	CR5N	CR6N	CR7E	CR7N	CR8E	CR9E	CR9N	CR11N	CR12N	CR13N
1883	12	30	20	26	19	56	7	20	17	66	73	29	33	77
1884	15	32	33	34	26	93	18	35	41	94	124	64	46	104
1885	24	50	59	55	38	114	45	83	51	117	98	64	75	100
1886	9	26	38	26	21	65	13	24	15	109	77	15	49	78
1887	14	23	32	18	41	54	13	37	16	82	82	17	63	64
1888	25	30	47	39	37	58	24	39	34	78	84	28	79	76
1889	27	24	33	30	45	86	22	39	30	78	116	32	83	105
1890	18	21	46	30	39	73	14	37	38	78	112	31	77	89
1891	32	33	54	44	57	98	24	52	34	101	150	44	74	89
1892	43	31	58	40	40	62	18	35	39	149	117	31	83	93
1893	51	34	32	23	33	53	9	22	38	107	78	35	88	63
1894	42	33	38	33	30	49	12	34	44	94	36	54	95	70
1895	28	33	35	19	39	49	9	37	43	80	77	53	90	69
1896	26	36	51	22	28	47	14	41	33	82	75	45	64	69
1897	26	29	42	35	37	51	19	85	43	64	46	30	57	37
1898	23	37	32	29.	29	65	11	65	48	60	58	28	70	43
1899	14	21	20	11	23	52	10	38	24	85	71	23	30	35
1900	18	28	27	21	20	35	11	58	38	53	84	32	81	55
1901	8	26	23	20	17	58	7	40	42	78	70	27	75	36
1902	24	37	37	29	37	71	29	43	49	96	87	57	101	53
1903	13	23	23	16	19	59	14	30	30	68	76	50	64	63
1904	18	18	30	14	27	48	15	27	28	60	61	28	59	63
1905	22	29	43	32	30	68	42	48	34	78	79	29	96	75
1906	17	30	34	38	30	58	21	29	27	59	60	23	86	62
1907	21	32	30	30	17	53	16	29	36	59	73	24	86	57
1908	9	36	32	27	21	62	23	30	33	70	88	35	71	58
1909	9	35	31	22	19	51	18	34	35	56	60	34	70	54
1910	10	27	16	11	13	29	6	15	21	51	43	35	46	34
1911	9	26	20	20	12	24	11	17	35	58	47	28	84	36
1912	19	19	37	38	23	29	28	41	46	55	44	30	95	47
1913	4	16	20	19	14	20	9	14	12	57	38	21	64	40
1914	21	21	34	27	20	30	17	39	40	64	65	35	101	58
1915	17	11	24	27	16	26	12	27	19	54	46	18	80	40
1916	17	19	25	25	21	31	10	12	58	45	51	31	116	38
1917	17	15	30	19	17	35	8	6	63	47	40	22	119	37
1918	48	23	34	21	27	55	21	25	60	56	71	28	146	55
1919	19	17	20	14	22	45	15	17	18	44	45	15	123	59
1920	27	26	24	23	26	56	19	40	19	57	71	35	125	54
1921	29	27	20	25	18	48	18	40	14	31	56	28	86	35
1922	43	25	16	30	24	51	15	39	24	37	57	30	71	49
1923	28	37	24	26	23	55	21	52	34	63	83	26	98	60
1924	17	24	23	22	25	44	20	38	19	52	76	28	93	46
1925	8	28	23	12	18	36	13	29	19	52	49	21	58	49
1926	11	23	26	13	26	45	21	35	18	60	51	22	75	67
1927	21	30	25	23	36	50	26	42	31	72	43	31	91	63
1928	34	22	36	15	36	59	18	42	34	70	43	36	92	72
1929	33	37	32	19	38	59	21	29	29	73	68	40	95	89

Year	Raw Ring Width Measurement for Core:													
	CR1E	CR2E	CR3N	CR4S	CR5N	CR6N	CR7E	CR7N	CR8E	CR9E	CR9N	CR11N	CR12N	CR13N
1930	60	42	36	19	36	73	21	57	36	76	63	49	116	97
1931	46	35	24	10	40	65	29	62	37	67	67	37	124	91
1932	38	26	20	10	21	46	11	36	7	60	52	48	73	60
1933	29	21	20	8	22	54	11	18	26	62	49	38	59	52
1934	66	58	50	29	42	62	31	69	34	82	62	70	98	62
1935	61	56	43	30	42	84	39	66	29	74	77	68	122	60
1936	62	41	39	30	51	78	41	65	26	68	57	48	146	70
1937	48	18	30	28	33	42	24	57	18	65	49	38	128	67
1938	45	30	20	29	27	48	21	42	17	72	52	48	108	68
1939	47	23	19	33	27	48	27	47	16	59	64	45	117	63
1940	47	19	18	20	28	38	26	48	11	53	57	25	112	51
1941	66	28	22	34	27	42	33	47	25	68	66	30	134	47
1942	74	37	28	40	37	58	37	59	25	87	66	46	144	59
1943	72	43	26	30	41	57	47	49	36	98	62	43	157	52
1944	88	28	17	33	24	43	28	37	25	81	66	46	157	50
1945	86	30	26	20	47	38	21	39	25	88	61	63	127	61
1946	122	53	34	55	65	53	26	59	40	127	102	90	169	86
1947	94	39	17	40	33	46	29	58	17	89	73	63	148	82
1948	77	42	33	62	47	36	22	64	26	94	67	66	99	67
1949	49	19	20	18	17	38	6	27	14	47	56	47	58	51
1950	72	40	30	48	43	53	23	90	37	85	87	64	110	80
1951	77	44	24	49	51	54	28	114	28	101	120	69	152	82
1952	76	32	13	25	32	50	18	83	18	107	90	55	117	70
1953	72	41	16	42	52	70	25	116	27	119	87	68	113	77
1954	55	17	12	9	36	50	20	66	17	74	61	41	79	31
1955	33	18	13	15	24	24	9	50	18	88	80	31	75	25
1956	23	22	18	15	21	24	8	61	25	68	52	40	74	15
1957	44	26	35	18	35	40	21	76	26	71	75	39	71	49
1958	27	31	36	29	40	38	29	82	33	54	71	44	78	56
1959	27	21	23	16	46	38	18	33	21	55	76	35	73	57
1960	18	17	12	10	48	31	12	21	15	44	19	30	87	60
1961	21	26	18	23	46	42	23	48	20	52	69	35	108	53
1962	36	30	16	22	29	45	25	53	17	49	78	36	90	57
1963	69	31	24	22	32	46	55	79	18	62	93	29	97	80
1964	52	30	14	29	18	46	34	78	15	58	92	20	97	91
1965	70	64	30	29	31	42	24	88	19	76	109	47	130	117
1966	63	44	28	32	32	42	30	86	20	67	127	37	147	153
1967	47	36	17	21	24	38	24	62	21	60	112	45	139	114
1968	59	42	26	21	26	38	24	83	23	75	79	50	154	129
1969	40	33	17	17	21	25	17	68	12	68	79	38	96	107
1970	14	8	8	11	15	23	13	34	13	34	56	15	67	108
1971	27	28	19	15	6	35	11	45	16	55	64	22	93	73
1972	13	27	18	21	5	16	11	26	16	50	67	11	84	109
1973	7	10	9	9	7	16	8	20	12	33	41	12	61	62
1974	8	26	9	7	12	22	10	33	10	45	52	11	49	54
1975	19	26	17	25	24	22	34	64	21	64	74	27	105	72
1976	6	25	16	17	13	18	9	40	9	55	65	22	80	70

Year	Raw Ring Width Measurement for Core:													
	CR1E	CR2E	CR3N	CR4S	CR5N	CR6N	CR7E	CR7N	CR8E	CR9E	CR9N	CR11N	CR12N	CR13N
1977	26	37	33	46	37	33	37	80	28	95	117	44	139	113
1978	50	39	43	45	29	32	42	61	38	69	101	40	133	103
1979	58	43	39	25	19	38	21	43	28	80	48	40	133	142
1980	70	44	43	34	36	54	41	93	36	95	112	41	208	134
1981	49	28	31	23	22	47	27	59	18	71	101	30	184	121
1982	44	34	24	32	29	41	31	50	20	69	80	36	132	84
1983	36	33	24	28	20	32	34	64	10	62	70	25	138	156
1984	27	21	17	15	14	29	21	47	12	51	73	20	112	136
1985	25	42	19	10	15	33	18	40	21	74	89	20	117	77
1986	35	35	24	22	27	25	16	37	21	55	93	20	130	61
1987	23	28	10	15	20	25	14	34	22	55	65	18	132	66
1988	15	16	21	16	17	25	16	41	16	44	59	23	102	57
1989	14	27	21	23	15	20	14	34	16	49	72	19	119	58
1990	28	23	19	18	23	30	20	64	21	69	71	24	130	82
1991	25	23	13	12	22	45	18	49	23	72	90	14	124	80
1992	25	10	12	14	17	43	20	60	27	63	88	9	103	77
1993	25	12	17	16	19	27	21	49	55	68	75	17	76	75
1994	24	18	14	18	29	42	25	89	48	94	105	26	110	94
1995	17	21	27	32	31	38	32	94	153	75	96	33	122	78

VITA

Robert Joseph Viens

University of Washington

2001

Education

Ph.D. in Geological Sciences — March 1995–Dec 2001
University of Washington (Seattle, Washington)

M.S. in Geological Sciences — Sept 1991–March 1995
University of Washington

B.A. in Geological Sciences (minor in physics/astronomy) — August 1986–May 1990
Cornell University (Ithaca, New York)

Professional Experience

Geology/Environmental Instructor — Sept 1999-Present
Bellevue Community College
Develop and teach classes for Geology and Environmental Science Programs, including Introductory Geology, Ecology and the Biosphere, History of the Earth and Geology of the Pacific Northwest. Advise students and student clubs, participate in science division and college governance, and conduct outreach programs.

Outreach Instructor — July 1998–Present
Seattle City Schools
Design and teach biannual five-day training course (funded by the National Science Foundation) to prepare third grade teachers for the state's new *Rocks and Minerals* curriculum.

Webmaster and CD-ROM designer — Aug 1996–March 2000
Houghton-Mifflin (Boston, Mass)
Created, designed, and maintained the award-winning web page *Geologylink*, an interactive collection of geological news and information for students and teachers (www.geologylink.com). This web page is a supplement for Chernicoff's textbook *Geology*. Currently writing and designing a CD-ROM companion for the book and website.

Instructor and Webmaster — Sept 1995–Sept 1999
Woodland Park Zoo
Taught weekend natural history classes for children aged 5 to 12. Class topics include: rocks and minerals, primates, deserts, and arthropods. Between September 1998 and September 1999 I also maintained the zoo's web site (www.zoo.org).

Part-time Instructor — Sept 1997–Aug 1999
Bellevue, Edmonds, Everett, and Seattle Central community colleges
Designed curriculum and exercises for, and instructed Physical Geology and Environmental Science for 30 to 75 students each quarter.

Instructor Sept 1994–Sept 1998
University of Washington
Proposed, designed, and taught General Studies 101, Geology Teaching Seminar 590, and Glaciers and Volcanoes class. General Studies was a class for at-risk student athletes, that was linked to Introductory Geology. Geology Teaching Seminar was a class for incoming graduate students on teaching geology. As part of that seminar I also recruited and assigned undergraduate assistants to help new graduate students in the lab.

Teaching Assistant *Lead Teaching Assistant (Sept 1992 - June 1997)* Sept 1991–Dec 1998
University of Washington
Designed the lab curriculum for and teach Introductory Geology, Geology of the Pacific Northwest, Great Ice Ages, and Earthscapes (Geomorphology). Also taught lab sections for Geomorphology and Remote Sensing (classes for majors). Typically responsible for teaching and grading 50 to 100 students and leading 1 to 8 field trips each academic quarter. As Lead TA I coordinated, mentored, and helped train new graduate teaching assistants, and organized curriculum, materials, and TA's for large laboratory classes.

Graduate Research Sept 1991–Aug 1999
University of Washington
Proposed, obtained funding for, and conducted field research on the glacial geology of southeast Alaska. Field work was followed up with lab studies, scientific talks, and written publications.

Student Assistants Chairman Jan 1994–Dec 1994
Geological Society of America (Denver, Colorado)
Recruited, organized, trained, and supervised over 200 student volunteers from all over the U.S. for the 1994 Geological Society of America Annual Meeting.

Research Assistant/Science Writer June 1992–June 1994
U.S. Geological Survey (Denver, Colorado)
Organized data collected by Austin Post of the U.S.G.S. and wrote scientific reports on glaciers in southeast Alaska.

Lab Instructor Aug 1989–Aug 1991
Cornell University
Designed and taught lab exercises for Introductory Geology, Environmental Geology, Sedimentology and Stratigraphy, and Structural Geology. Assisted in the instruction of a four-week summer Field Geology course. Organized lecture slide collection on a computer database.

Research Assistant Jan 1987–May 1990
Cornell University Geology and Astronomy departments
Organized field samples, and prepared and analyzed fossil coral samples from Papua New Guinea. Constructed the electronic, mechanical, and circuit-board components of a charged coupling device camera for a twenty-four inch reflecting telescope. Machined and wired equipment for research and maintained the astronomical observatory.

Volunteer Experience

Wetland Restoration March 2001–Present
Organize and participate in wetland restoration projects with the city of Bellevue.

NAGT Meeting Organizer July 2000–July 2001
Organized and hosted the 2001 Northwest Sectional Meeting of the National Association of Geology Teachers at Bellevue Community College.

Woodland Park Zoo March 1995–Present

- **Education Aide** –Write program cirriculum and conservation materials for teachers, docents and classes. Some examples of work include; regular Conservation Corner column in *Zoo Edition*, background section in *Forest Explorers* Program, and Tropical Asia self-guided tour. Present teacher training lectures on a variety of topics.
- **Keeper Aide** – Helped care for orangutans and lemurs, 1995–96.
- **Docent** – Led educational tours, staffed Discovery Carts, and trained new docents, 1995-1998.

Geology Outreach Instructor Sept 1989–Present

Involved in promoting and conducting geology and environmental science outreach programs to local schools (K–12), museums and nature centers (including BCC's Summer Science Camp in 2000). Also involved in training K–12 educators and natural history tour operators.

Research Assistant Jan 1997–Feb 1997

Helped set up logistics for fieldwork in Kenya and conducted geologic research on Mt. Kenya and in the Rift Valley.

Researcher and Interpreter June 1993–Aug 1995

Conducted tree-ring studies in the Tongass National Forest and gave public talks on regional glacial history.

Radio Producer, WVBR (Ithaca, New York) Jan 1988–May 1990

Produced and hosted a two-hour, live comedy show, broadcast weekly.

Awards Received

Harry Wheeler Scholarship for Excellence in Teaching, University of Washington, 1995, 1996
J. Hoover Mackin Grant, Geological Society of America Quaternary Division, 1994
Harry Wheeler Scholarship, University of Washington, 1994
Geological Society of America Grants in Aid of Research, 1993–94
Sigma Xi Grants in Aid of Research, 1993–94
Richard E. Fuller Scholarship, University of Washington, 1993
Livingston Wernecke Scholarship, University of Washington, 1992
Chester Buchanan Memorial Scholarship, Cornell University, 1990
Dean's List, Cornell University, 1987–1990

Affiliations

Geologic Society of America, Northwest Geological Society, National Association of Geology Teachers, Environmental Educators of Washington, and Northwest Biological Society